

TR 71-24

AD 746666

..... contributing to man's  
understanding of the environment World



**TECHNICAL REPORT NO. 71-24**

**FINAL REPORT,  
PROJECT VT/0703**

**SPONSORED BY**

**ADVANCED RESEARCH PROJECTS AGENCY**

**ARPA ORDERS 624 AND 1714**



**APPROVED FOR PUBLIC RELEASE  
DISTRIBUTION UNLIMITED**

NATIONAL TECHNICAL  
INFORMATION SERVICE

 **TELEDYNE  
GEOTECH**

## DOCUMENT CONTROL DATA - R &amp; D

(Security classification of title, body of abstract and indexing annotation must be entered when the overall report is classified)

## 1. ORIGINATING ACTIVITY (Corporate author)

Teledyne Geotech  
3401 Shiloh Road  
Garland, Texas 75041

## 2a. REPORT SECURITY CLASSIFICATION

Unclassified

## 2b. GROUP

## 3. REPORT TITLE

Final Report, Project VT/0703  
January 1970 through October 1971

## 4. DESCRIPTIVE NOTES (Type of report and inclusive dates)

## 5. AUTHOR(S) (First name, middle initial, last name)

LRSM Staff

## 6. REPORT DATE

23 May 1972

## 7a. TOTAL NO. OF PAGES

216

## 7b. NO. OF REFS

8

## 8a. CONTRACT OR GRANT NO.

F33657-70-C-0646

## b. PROJECT NO.

VELA T/0703

## c.

ARPA Order Nos. 624 and 1714

## d. ARPA Code No. 8F10

## 9a. ORIGINATOR'S REPORT NUMBER(S)

TR 71-24

## 9b. OTHER REPORT NO(S) (Any other numbers that may be assigned this report)

## 10. DISTRIBUTION STATEMENT

Approved for Public Release  
Distribution Unlimited

## 11. SUPPLEMENTARY NOTES

## 12. SPONSORING MILITARY ACTIVITY

Advanced Research Projects Agency  
Nuclear Monitoring Research Office  
1400 Wilson Blvd., Arlington, Va., 22209

## 13. ABSTRACT

The progress of the Long-Range Seismic Measurements (LRSM) Program during the period 1 January 1970 through 31 October 1971 is described.

At the beginning of this report period, there were seven mobile observatories and eleven portable seismograph systems in the LRSM program. These seismograph systems participated in related programs and experiments such as MIRACLE PLAY - HUMID WATER, HANDLEY, and CANNIKIN. Six portable strain systems were operated at the Nevada Test Site. Several special studies were conducted - deep hole, long-period instrumentation evaluation; long-period noise study at Fairbanks, Alaska; atmospherically-generated seismic noise study at Grand Saline, Texas, and Wills Point, Texas.

TECHNICAL REPORT NO. 71-24

FINAL REPORT, PROJECT VT/0703  
January 1970 through October 1971

by

LRSB Staff

Sponsored by

Advanced Research Projects Agency  
Nuclear Test Detection Office  
ARPA Order Nos. 624 and 1714

This research was supported by the Advanced Research Projects Agency of the Department of Defense and was monitored by HQ USAF (AFTAC/VELA Seismological Center), Alexandria VA 22313, under Contract No. F33-657-70-C-0646.

Approved for Public Release  
Distribution Unlimited

TELEDYNE GEOTECH  
3401 Shiloh Road  
Garland, Texas

23 May 1972

IDENTIFICATION

AFTAC Project No:	VELA T/0703
Project Title:	Long-Range Seismic Measurements
ARPA Order Nos:	624 and 1714
ARPA Code No:	8F10
Contractor:	Teledyne Geotech
Contract No:	F33657-70-C-0646
Project Manager	R. G. Reakes (214) 271-2561 Garland, Texas 75041

The views and conclusions contained in this document are those of the authors and should not be interpreted as necessarily representing the official policies, either express or implied, of the Advanced Research Projects Agency, the Air Force Technical Applications Center, or the US Government.

## CONTENTS

	<u>Page</u>
GLOSSARY OF TERMS	xii
ABSTRACT	
1. INTRODUCTION	1
2. SUMMARY	2
3. FIELD OPERATIONS	3
3.1 General	3
3.2 Mobile observatory operations	3
3.2.1 General	3
3.2.2 Red Lake, Ontario (RK-ON), van operations	4
3.2.3 Wills Point, Texas (WP-TX), van operations	4
3.2.4 Pahute Mesa, Nevada (PH3NV and PH4NV), van operations	14
3.2.5 Mould Bay, NWT, Canada (NP-NT) van operations	14
3.2.6 Las Cruces, New Mexico (LC-NM), van operations	17
3.2.7 Prince George, British Columbia (PG2BC), van operations	17
3.2.8 Rawhide Mountain, Nevada (RH-NV), van operations	17
3.2.9 Houlton, Maine (HN-ME), van operations	21
3.2.10 Fairbanks, Alaska (FB2AK), van operations	28
3.3 Operation of portable systems	28
3.3.1 Project MIRACLE PLAY	28
4. INSTRUMENTATION	31
4.1 General	31
4.2 Portable system modifications	31
4.2.1 Battery power supply modifications	31
4.2.2 Modification of Battery Charger, Model 21160A	31
4.2.3 Replacement of Model 25540 $\pm 9$ Vdc regulator	31
4.2.4 Three-channel filter-amplifier units	31
4.2.5 Replacement of silver-cadmium batteries with lead-acid batteries	32
5. EVALUATION OF SUPPORT EQUIPMENT	33
5.1 General	33
5.2 Vans and instrumentation shelters	33
5.3 Vehicles	33
5.3.1 1/2-ton pickup trucks	35
5.3.2 Heavy-duty 3/4-ton pickup trucks	35
5.3.3 2-1/2-ton trucks	35
5.3.4 Snow vehicles	36
5.3.5 Utility trailers	36
5.4 Generators	36

## CONTENTS, Continued

	<u>Page</u>
6. SPECIAL PROJECTS	38
6.1 Project MIRACLE PLAY - HUMID WATER	38
6.2 HANDLEY accelerometer operation	38
6.3 Portable strainmeter systems	38
6.4 Intermediate period (IP) vertical strain system at IN-ME	41
6.4.1 Introduction	41
6.4.2 Instrumentation	42
6.4.3 Suppression of microseisms	53
6.4.4 Signal enhancement	61
6.4.5 Conclusions and recommendations	61
6.5 Deep-hole, long-period project	68
6.5.1 Introduction	68
6.5.2 Instrumentation	68
6.5.3 Field measurements	69
6.5.4 Installation and operation	69
6.5.5 Potential magnification	69
6.5.6 Construction and testing	69
6.5.7 PI2WY data, May 1971	89
6.5.8 Problems encountered in installation and operation	107
6.5.9 Deep-hole, long-period capability	115
6.5.10 Summary	120
6.6 Long-period studies at Fairbanks, Alaska	121
6.6.1 Objective	121
6.6.2 Site Selection and preparation	121
6.6.3 Operations and tests	123
6.6.4 Results	135
6.7 Atmospherically-generated seismic noise project	136
6.7.1 Wills Point, Texas, LP triaxial station	136
6.7.2 Long-period noise experiment at the Morton Salt Company Mine near Grand Saline, Texas (GA2TX)	147
6.8 Study, test and modification of the long-period triaxial seismometer	174
6.8.1 General	174
6.8.2 Work progress	179
7. REFERENCES	188

APPENDIX 1 - Deformation of the lower flanges in the triaxial  
seismometer

APPENDIX 2 - Tilt sensitivity of horizontal transducers

## ILLUSTRATIONS

<u>Figure</u>		<u>Page</u>
1	Map of site locations	7
2	HANDLEY accelerometer locations	8
3	HUMID WATER site locations	9
4	Location of portable strainmeter sites	10
5	Map locations of van operations	11
6	LRSM mobile observatory	12
7	Typical LRSM system field setup	13
8	View south toward camp buildings from snow patch between NP-NT array stations Z-1 and Z-2, Mould Bay, NWT, Canada, July 1966	15
9	North Pole, Northwest Territory array	16
10	Lay-out of Site RH-NV, Nye County, Nevada	18
11	Frequency response of the short-period seismograph system	19
12	Frequency response of accelerometer system at RH-NV	20
13	Standard LP frequency response	22
14	System frequency response of LP vertical with 40-second filter	23
15	System frequency response of the LP vertical with 60-second filter	24
16	System frequency response of LP horizontal with 100-second filter	25
17	Block diagram of seismograph system at RH-NV	26
18	Frequency response of accelerometer system for HANDLEY	39

## ILLUSTRATIONS, Continued

<u>Figure</u>		<u>Page</u>
19	Block diagram of IP strain seismograph system at HN-ME	43
20	Amplitude response to ground displacement of the vertical strain and the vertical inertial short-period and intermediate-period seismographs at HN-ME showing close matching of the strain and inertial outputs in the designed range of the 90-degree phase compensators	44
21	Relative power spectral density of microseisms recorded at Houlton, Maine, on 4 September 1970 by the intermediate-period vertical inertial and vertical strain seismographs	45
22	Coherence and phase lead of the IP vertical strain over the IP inertial seismograph recordings of a six-minute sample of microseismic noise recorded on 4 September 1970. Parzen smoothing, 10 samples/sec, 7 percent lags	46
23	Amplitude response to ground displacement of the vertical strain and the vertical inertial intermediate period seismographs, at HN-ME, showing resulting amplitude-response match following improvement of the phase-response match effected on 11 November 1970	49
24	Tape playback of SP, IP, and LP seismic data recorded at Houlton, Maine, on 01 December 1970. The initial arrival from an earthquake in the Adreanof Island region ( $\Delta = 64^\circ$ , $m_b = 5.6$ ) is recorded on the summation trace at a higher signal to noise ratio than on the LPZ trace. O.T. = 21:09:37.2Z, $51.4^\circ$ N, $175.3^\circ$ W, $\Delta = 64^\circ$ , $m_b = 5.6$ , depth = 36 km.	50
25	Tape playback of the Adreanof Island earthquake recorded at Houlton, Maine, on 01 December 1970	51
26	Phase response of the intermediate-period vertical (IPZ) strain and IPZ inertial seismographs in response to the calibrator equivalent of constant prograde elliptical earth displacement	52

## ILLUSTRATIONS, Continued

<u>Figure</u>		<u>Page</u>
27	Power spectral density of a 12-minute sample of seismic noise recorded by the intermediate-period vertical inertial, vertical strain, and summation seismographs at HN-ME at 0100Z on 25 November 1970. The power spectral density of system noise and tape recorder noise for the summation channel are included	54
28	Coherence and phase difference between the strain and inertial channels	55
29	Playouts from magnetic tape of the system noise and seismic noise samples from which the power spectral density data of figure 27 were computed	56
30	Ratio of power spectral density of microseismic noise for the IPZ inertial seismograph to that of the IPZ summation, showing the pattern of change in suppression of microseisms with increasing back-ground level	58
31	Power spectral density of inertial, strain, and summation recordings corresponding to curves 1 and 4 of figure 43, showing that poor suppression of seismic noise at frequencies below 0.1 Hz is prevented by an increase in the power level of microseisms recorded on the IPZ strain trace.	59
32	Coherence and phase difference between the strain and inertial channels	60
33	P arrival from an earthquake in Northern Chile showing how, on the average, the IP strain system contributes little to increasing the signal-to-noise ratio when compared with recordings from the SPZ and LP components. Origin 11:08:42.5Z, 20.9S, 69.8W, Mb = 6.0, h = 33 km	62
34	Magnetic-tape recording of SPZ, IP strain system, and LP components showing a factor-of-four improvements in signal-to-noise ratio for the P wave on the IPZ summation recording compared with the SPZ. Origin 14:16:18.0Z, 13 November 1970, LEYTE, 11.9N, 124.0E, $\Delta = 127^\circ$ , Mb = 5.4 h = 15 km	63

## ILLUSTRATIONS, Continued

<u>Figure</u>		<u>Page</u>
35	P-wave from an earthquake in the Ascension Island region ( $\Delta = 75^\circ$ ) showing the varied character of the P-wave on the IPZ summation trace. Origin 16:01:18.7Z, 11.7S, 14.1W, Mb = 5.3, h = 33 km	64
36	Tape playback of an earthquake recorded at Houlton, Maine, on 05 September 1970 showing improved resolution of closely spaced body phases on the IPZ summation trace compared with the SPZ and LPZ traces. Origin 07 52 27.4Z, 52N 15.4E, Sea of Okhotsk, $\Delta = 76.5^\circ$ , M = 5.7, h = 580 km	65
37	Earthquake from the Sea of Okhotsk showing change in character of the IPZ summation trace and potential discrimination of S phases arriving at closely spaced intervals	66
38	Smoothed amplitude spectrum of vertical background at Las Cruces, New Mexico, and estimated system threshold in terms of equivalent displacement spectrum for the modified deep-hole, long-period sensors	73
39	Block diagram, downhole amplifier systems - DHA1 and DHA2	75
40	Block diagram, 23900 (3-1/2 sec)/Phototube Amplifier (PTA) System	76
41	Frequency response of experimental deep-hole, long-period velocity systems	80
42	Comparison of background and system noise for down-hole amplifier system DHA1	81
43	Comparison of background and system noise for down-hole amplifier system DHA2	82
44	Comparison of background and system noise difference for downhole amplifier systems DHA1 and DHA2	83
45	Block diagram, LP systems and filter channels	84
46	Block diagram, test amplifier assemblies "A," "B," "C"	85

## ILLUSTRATIONS, Continued

<u>Figure</u>		<u>Page</u>
47	Configurations, three-channel filter assemblies	86
48	Comparison of system noise for downhole amplifier systems DHA1, DHA2	88
49	Response curves for PTA system (2980-30/5240) channels Z25, Z40, and Z44.	90
50	Response curves for amplifier "A" system channels Z25A, Z40A, and Z90A	91
51	Response curves for amplifier "B" system channels Z25B, Z40B, and Z90B	92
52	Response curves for amplifier "C" system channels Z25C, Z40C, Z90C, and downhole amplifier systems DHA1 and DHA2	93
53	System noise spectra for the PTA system, channels Z25, Z40, Z44	94
54	System noise spectra for the "conventional pre-amplifier" system, channels Z25A, Z40A, Z90A	95
55	System noise for the "low-noise" preamplifier B-system, direct coupled	96
56	System noise for the "low-noise" preamplifier C-system direct coupled with feedback (limited at shorter periods by recording system, see response figure 65)	97
57	System response, surface vertical LZ - wide-band, LZK - high gain, notched response	99
58	System response, surface north-south LN - wide-band LNK - high gain, notched response	100
59	System response, surface east-west LE - wide-band LEK - high gain, notched response	101
60	System response, deep-hole systems DHA1 - 130 feet depth, DHA2 - 8000 feet depth	102

## ILLUSTRATIONS, Continued

<u>Figure</u>		<u>Page</u>
61	System response, DHA1 wide-band, 130 feet depth	103
62	System response, DHA2 wide-band, 8000 feet depth	104
63	System response, LZK/SSA - LZK channel with special solid-state amplifier replacing PTA	105
64	System response for the low-frequency microbarograph used at PI2WY (estimated)	106
65	Power density spectra of long-period channels during strong barometric activity, low seismic background	108
66	Coherence of long-period channels with respect to microbarograph during strong barometric activity	109
67	Coherence of vertical channels with respect to microbarograph during strong barometric activity	110
68	A section of the time series for processed data shown in figures 78, 79, 80 showing effects of atmospheric pressure variation	111
69	Power density spectra of system noise equivalent mean square displacement density	112
70	Comparison of backgrounds and system noise observed at mine installations QC-AZ, LC-NM, and OGD	116
71	Block diagram of seismograph system at FB2AK	122
72	Fairbanks, Alaska (FB2AK) site layout	124
73	FB2AK long-period frequency response	126
74	Spectra of the long-period seismograph background noise. Wind velocity 0-5 miles/hour. Not corrected for seismograph response	127
75	Spectra of the vertical long-period seismograph background noise. Wind velocity 15-20 miles/hour. Not corrected for seismograph response	128

## ILLUSTRATIONS, Continued

<u>Figure</u>		<u>Page</u>
76	Coherences between long-period vertical seismographs at the surface and at 60 feet: a. wind velocity 15-20 miles/hr; b. wind velocity 0-5 miles/hr.	129
77	Typical instrumentation and response, atmospherically-generated noise project, Grand Saline, Texas	137
78	Sketch of location and layout at WP-TX	139
79	Drilled section with interval velocities	140
80	Block diagram of seismograph system at WP-TX	143
81	Vertical and horizontal distances between systems	149
82	Average frequency response of microbarographs and seismographs	150
83	Power spectral density	151
84	Noise recorded during a calm period	153
85	Ratio of earth to system noise for the vertical seismograph located in the mine at Grand Saline	154
86	Noise recorded during a windy period	156
87	Noise recorded during the passage of acoustic waves	157
88	Comparison of observed responses with calculated buoyant responses	164
89	Velocity model of earth structure at the Grand Saline salt dome	166
90	Velocity model of the earth structure surrounding the Grand Saline salt dome	167
91	Comparison of the observed and predicted surface vertical displacement responses for windy period data	169

ILLUSTRATIONS, Continued

<u>Figure</u>		<u>Page</u>
92	Comparison of observed and predicted vertical displacement responses for acoustic wave data	170
93	Comparison of the observed Grand Saline vertical displacement response with those predicted for a granitic half space and a thin low velocity layer overlying a granitic half space	172
94	Triaxial Transducer, Model 31300	176
95	Transducer Module, Model 26310	177
96	Modified flange with retained metal webbing	181
97	Modified flange with recessed stanchion sockets	182
98	Completed vault installation in Kleer mine, Grand Saline, Texas (GA3TX)	183
99	Frequency response of triaxial seismograph channels tested at Grand Saline	184

## TABLES

<u>Table</u>		<u>Page</u>
1	List of sites occupied during this report period	5
2	RH-NV channel assignments	27
3	Project MIRACLE PLAY site locations	29
4	Available vans, generators, and vehicles; 31 October 1971	34
5	Portable strainmeter site locations	40
6	Smoothed phase lag of strain output relative to inertial output	48
7	Comparative values of $f_s$ for various seismometers	71
8	PI2WY channel designations	98
9	Seismometer dimensions corresponding to various suspension heights and parameters of a simple brass pendulum that occupies the total available volume	119
10	The buoyant response of a vertical seismograph	159
11	Estimated frequency response, windy period data	162
12	Estimated frequency response, acoustic wave data	163
13	Parameters used in the calculation of displacement responses	171
14	Pressure sensitivities of triaxial modules measured under various test conditions in salt mine at Grand Saline, Texas. The TR1 module has a standard flange, the TR2 module has webbed flange, and the TR3 module has recessed stanchion sockets.	185

## GLOSSARY OF TERMS

AFTAC	Air Force Technical Applications Center
Anemometer	An instrument for measuring or indicating the speed or force of the wind
ARPA	Advanced Research Projects Agency
BCD	Binary Coded Decimal
dB	Decibels
EDP	Electronic Data Processing
LASA	Large Aperture Seismic Array
LP	Long Period
LPH	Long Period Horizontal
LRL	Lawrence Radiation Laboratory
LRSM	Long-Range Seismic Measurements
$\mu$ bar	Microbar
Microbarograph	An instrument designed to detect and record very small variations in atmospheric pressure
mm	Millimicron
NTS	Nevada Test Site
PTA	Phototube Amplifier
SDCS	Special Data Collection System
SDL	Seismic Data Laboratory
SP	Short Period
TFSO	Tonto Forest Seismological Observatory
Triax	Applies to a description of instrumentation that interests itself in three axes that intersect at a common point. Two horizontals oriented $90^\circ$ from one another and a vertical seismometer is a triaxial device. Three symmetrical triaxial seismometer modules all oriented to detect motions in an axis $55^\circ$ from vertical and $120^\circ$ from one another is also a triaxial device.
USC&GS	United States Coast and Geodetic Survey
VELA-Uniform	The research and development program for the improvement of detection of underground nuclear explosions.

# ABSTRACT

The progress of the Long-Range Seismic Measurements (LRSM) Program during the period 1 January 1970 through 31 October 1971 is described.

At the beginning of this report period, there were seven mobile observatories and eleven portable seismograph systems in the LRSM program. These seismograph systems participated in related programs and experiments such as MIRACLE PLAY - HUMID WATER, HANDLEY, and CANNIKIN. Six portable strain systems were operated at the Nevada Test Site. Several special studies were conducted - deep hole, long-period instrumentation evaluation; long-period noise study at Fairbanks, Alaska; atmospherically-generated seismic noise study at Grand Saline, Texas, and Wills Point, Texas.

FINAL REPORT, PROJECT VT/0703  
January 1970 through October 1971

1. INTRODUCTION

The Long-Range Seismic Measurements Program (LRSM), a VELA-Uniform project, was initiated on 1 June 1960. The VELA-Uniform research project is directed towards creating major advances in all areas of seismic detection, identification, and location techniques, to the end that a better understanding of the detection and identification of underground nuclear explosions will be achieved.

The LRSM program has provided a majority of the detection and recording systems in support of the VELA-Uniform objectives. A vast amount of data is presently available on a nonclassified basis for use in arriving at a technical assessment of the effectiveness of a test-ban control system. In addition, these data are available to others in the scientific community for use in many varied studies.

Seven technical reports have been written covering the work performed in the LRSM program previous to the time period covered by this report:

a. TR 61-3, Final Report on Phases I, II, and III, Long-Range Seismic Measurements Program, covers work performed from 1 June 1960 through 31 December 1960.

b. TR 62-22, Interim Report on Operating Procedures, Project VT/0704, records the LRSM activities from 1 September 1961 through 31 December 1962.

c. TR 66-78, Interim Report No. 2, Project VT/4051, for the period 1 January 1963 through 30 June 1964.

d. TR 66-92, Interim Report No. 3, Project VT/4051, for the period 1 July 1964 through 31 March 1966;

e. TR 68-19, Final Report, Project VT/6703, for the period April 1966 through March 1968;

f. TR 69-7, Final Report, Project VT/8703, for the period January 1968 through December 1968.

g. TR 70-4, Final Report, Project VT/8703, for the period January 1969 through December 1969.

This report describes the progress of the LRSM program during the period 1 January 1970 through October 1971. The research was supported by the Advanced Research Projects Agency, Nuclear Test Detection Office, under Project VELA-Uniform and accomplished under the technical direction of the Air Force Technical Applications Center under Contract F33657-70-C-0646.

## 2. SUMMARY

A detailed review of all work performed by the LRSM program from January 1970 through October 1971 is contained in this report.

At the beginning of the report period, there were seven mobile observatories (vans) in the LRSM program. Four of the vans were in operation, two were in storage at the Nevada Test Site, and one was on standby status at Fairbanks, Alaska (FB-AK).

The Red Lake, Ontario, Canada (RK-ON) operation was terminated in August 1970, and the van was returned to Garland. It was later moved to Wills Point, Texas, (WP-TX), to be used during special long-period seismograph tests. The two vans in storage at the Nevada Test Site were reactivated in February 1970 for the HANDLEY event and were placed back in storage at NTS in March 1970. The two vans were transferred to the University of California on 25 August 1971.

The Mould Bay, Canada (NP-NT) operation was terminated on 10 July 1970, and the van was transferred to the Canadian Transportation Agency on 22 July 1970. The Las Cruces, New Mexico, van (which had been transferred to Air Force Weapons Laboratory [AFWL] but left on site) was reactivated from 13 March 1970 to 26 March 1970 for a special event; no equipment transfer was involved at this time. The Prince George, British Columbia (PG-BC) operation was terminated on 17 August 1970, and the van was moved to Rawhide Mountain, Nevada (RH-NV).

The Rawhide, Nevada, station became operational on 21 April 1971, and operations were terminated on 2 August 1971. The van was moved to Garland where it is presently on standby. Operations at Houlton, Maine (HN-ME), were terminated on 4 February 1971, and the van was moved to Garland. It was transferred to Develco, Inc., Mountain View, Calif., on 23 August 1971 for use on an AFOSR contract. Operations at the Fairbanks, Alaska (FB2AK), site began on 9 June 1970, and were terminated on 14 July 1971. The van was left on standby status at the site.

Special projects supported during this report period were:

- a. Intermediate period vertical strain system at Houlton, Maine (HN-ME);
- b. Acquisition of accelerometer data at NTS from the HANDLEY event;
- c. Operation of portable strainmeter systems in Nevada;
- d. Investigation, construction, and testing of deep-hole long-period instrumentation.
- e. Long-period noise studies at Fairbanks, Alaska (FB2AK);
- f. Atmospherically-generated seismic noise studies;
- g. Study, test, and modification of the long-period triaxial seismometer.

### 3. FIELD OPERATIONS

#### 3.1 GENERAL

The LRSM mobile observatories and portable systems continued to record seismic signals from earthquakes and underground explosions in support of the VELA-Uniform Program. These field teams also continued to be active participants in related programs and special studies.

A listing of all sites occupied during this report period (January 1970-October 1971) is presented in table 1. Figure 1 shows the location of the sites listed in table 1. Figure 2 shows site locations of accelerometer systems for the HANDLEY event. Figure 3 shows the site locations of the portable systems for the HUMID WATER event. Figure 4 shows the site locations of the portable strainmeter systems.

#### 3.2 MOBILE OBSERVATORY OPERATIONS

##### 3.2.1 General

Operational durations and transport information for the eight mobile observatory vans utilized from January 1970 through October 1971 is summarized in the following tabulation:

<u>Van</u>	<u>Team</u>	<u>Site location</u>	<u>Designator</u>	<u>Date</u>	
				<u>Operational</u>	<u>Closed</u>
208	03	Red Lake, Ontario	RK-ON	17 July 63	17 Aug 70
208	03	Garland, Texas	(standby)	-	-
208	03	Wills Point, Texas	WP-TX	18 Mar 71	-
232	08	Pahute Mesa, Nevada	PH4NV	18 Mar 70	07 Apr 70
232	08	Nevada Test Site (standby, transferred to Univ. of Calif., 25 Aug 71)			
213	13	Mould Bay, Canada	NP-NT	23 Aug 63	10 July 70
213	13	Mould Bay, Canada (van transferred to Canadian Trans. Agcy. 22 July 70)			
229	15	Las Cruces, New Mexico	LC-NM (AF Weap. Lab)	13 Mar 70	26 Mar 70
206	28	Prince George, B.C.	PG2BC	05 Oct 68	17 Aug 70
206	28	Rawhide Mtn., Nev. (standby)	RH-NV	-	-

Van	Team	Site location	Designator	Date	
				Operational	Closed
206	28	Rawhide Mtn., Nevada	RH-NV	21 Apr 71	02 Aug 71
206	28	Garland, Texas	(standby)	-	-
223	30	Houlton, Maine	HN-ME	25 Oct 66	04 Feb 71
223	30	Garland, Texas (standby, transferred to Develco 23 Aug 71)			
210	35	Pahute Mesa, Nevada	PH3NV	18 Mar 70	07 Apr 70
210	35	Nevada Test Site (standby, transferred to Univ. of Calif. 25 Aug 71)			
219	36	Fairbanks, Alaska	FB2AK	09 June 70	14 June 71
219	36	Fairbanks, Alaska (standby)	FB2AK	-	-

Map locations for these van operations are presented in figure 5. These mobile observatories recorded signals from earthquakes and underground explosions in support of the VELA-Uniform program, and provided data collection for special test projects. Figure 6 is a photograph of a mobile observatory and associated equipment. Figure 7 is a sketch of a typical mobile observatory installation. Brief descriptions of the van operations at each site will be given in the following paragraphs. Other sections of this report deal in detail with special operations involving vans at various sites.

### 3.2.2 Red Lake, Ontario (RK-ON), Van Operations

After approximately 7 years of collecting high-quality short-period and long-period seismic data, operations were terminated at station RK-ON on 17 August 1970. The bunker-type seismometer vault housing and storage facilities previously constructed at the site were left intact and arrangements were made for possible future site utilization. The recording van, associated instrumentation, and power generator crossed into the United States on 27 August and arrived in Garland, Texas, on 31 August 1970. This van, No. 208, was modified and transported to the Wills Point, Texas (WP-TX), site on 08 January 1971.

### 3.2.3 Wills Point, Texas (WP-TX), Van Operations

An abandoned petroleum prospect hole, the Pan American No. 1 J. T. Edwards Gas Unit in Van Zandt County, Texas, was selected, acquired, reentered, and plugged back. The depth/size of the well casing at this location is unusual for the region, allowing a 1001-1/2 foot working depth in 13-3/8 inch o.d. surface pipe. Operation of surface long-period and downhole triaxial long-period seismographs was started at site WP-TX on 18 March 1971. Collection of routine and special test data continues past 31 October 1971. A detailed account of the experiment is presented in section 6.7.1 of this report.

Table 1. List of sites occupied during this report period (Jan 1970-Oct 1971)

Mobile Observatories

<u>Team</u>	<u>Site location</u>	<u>Designator</u>	<u>Date</u>	
			<u>Operational</u>	<u>Closed</u>
03	Red Lake, Ontario	RK-ON	17 July 63	17 Aug 70
03	Garland, Texas	(standby)	-	-
03	Wills Point, Texas	WP-TX	18 Mar 71	-
08	Pahute Mesa, Nevada	PH4NV	18 Mar 70	07 Apr 70
08	Nevada Test Site (standby, transferred to Univ. of Calif. 25 Aug 71)			
13	Mould Bay, Canada	NP-NT	23 Aug 63	10 July 70
13	Mould Bay, Canada (van transferred to Canadian Trans. Agy. 22 July 70)			
15	Las Cruces, New Mexico	LC-NM	13 Mar 70	26 Mar 70
28	Prince George, B. C.	PG2BC	05 Oct 68	17 Aug 70
28	Rawhide Mtn., Nev. (standby)	RH-NV	-	-
28	Rawhide Mtn., Nevada	RH-NV	21 Apr 71	02 Aug 71
28	Garland, Texas	(standby)	-	-
30	Houlton, Maine	HN-ME	25 Oct 66	04 Feb 71
30	Garland, Texas (standby, transferred to Develco 23 Aug 71)			
35	Pahute Mesa, Nevada	PH3NV	18 Mar 70	07 Apr 70
35	Nevada Test Site (standby, transferred to Univ. of Calif. 25 Aug 71)			
36	Fairbanks, Alaska	FB2AK	09 June 70	14 June 71
36	Fairbanks, Alaska (standby)	FB2AK	-	-

Portable System Teams and Other Equipment

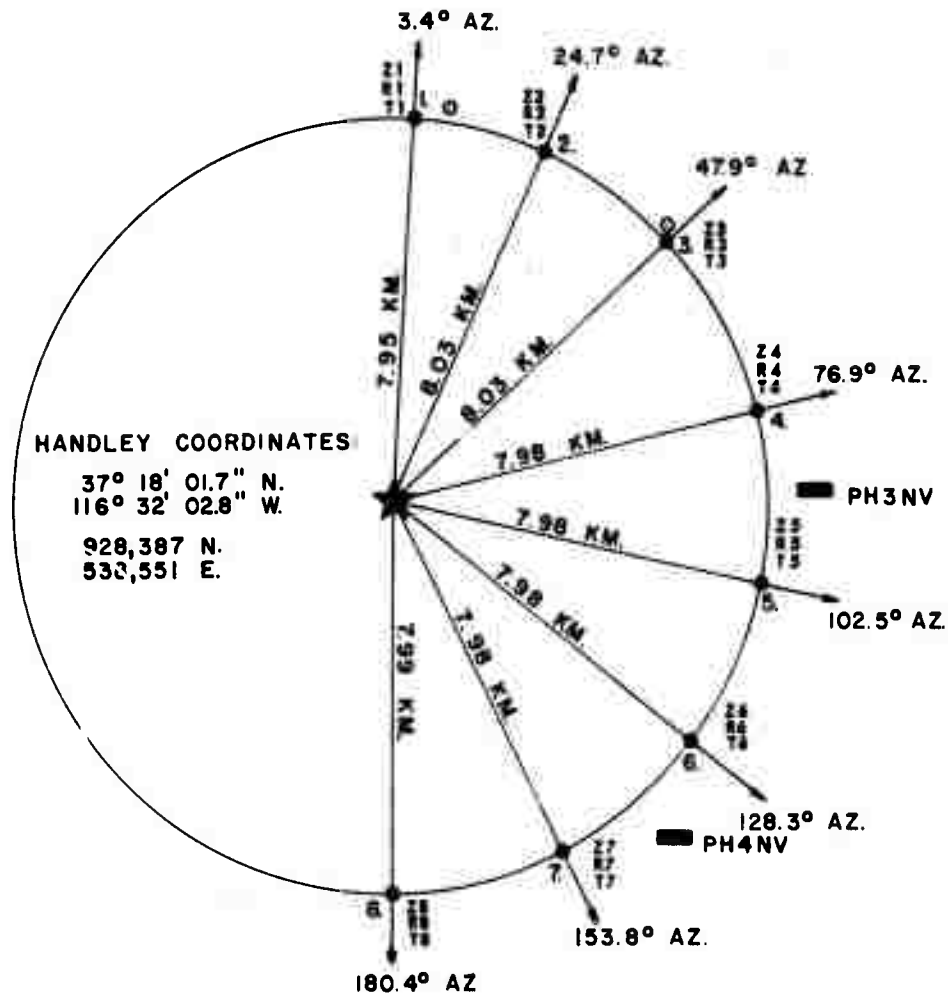
50	Richton, Mississippi	RI-MS	16 Apr 70	22 Apr 70
51	Lucedale, Mississippi	LD-MS	11 Apr 70	22 Apr 70
52	Picayune, Mississippi	PC-MS	10 Apr 70	22 Apr 70
53	Lumberton, Mississippi	LU-MS	07 Apr 70	22 Apr 70
54	Laurel, Mississippi	LL-MS	12 Apr 70	22 Apr 70
55	Lucedale, Mississippi	LD3MS	09 Apr 70	22 Apr 70
56	McComb, Mississippi	MB-MS	10 Apr 70	22 Apr 70
58	Lucedale, Mississippi	LD2MS	14 Apr 70	22 Apr 70
59	Las Cruces, New Mexico	LC-NM	17 Mar 70	26 Mar 70
60	Grand Saline, Texas	GA-TX	23 Mar 70	11 Aug 70
60	Grand Saline, Texas	GA2TX	23 Mar 70	11 Aug 70

Table 1 (Continued)

Portable System Teams and Other Equipment, Continued

<u>Team</u>	<u>Site location</u>	<u>Designator</u>	<u>Date</u>	
			<u>Operational</u>	<u>Closed</u>
Strain-meter	Rawhide Mtn., Nevada	RH-NV	29 Dec 69	01 May 70
	Rawhide Mtn., Nevada	RH-NV	31 Aug 70	17 Aug 71
	Rawhide Mtn., Nevada (transferred to Univ. of Nev. 21 Aug 71)			
Strain-meter	Kawich Peak, Nevada	KP-NV	23 Jan 70	24 Apr 70
	Kawich Peak, Nevada	KP-NV	29 Aug 70	09 Aug 71
	Kawich Peak, Nevada (transferred to Univ. of Nev. 21 Aug 71)			
Strain-meter	Quartzite Mtn., Nevada	QM-NV	25 Jan 70	24 Apr 70
	Quartzite Mtn., Nevada	QM-NV	30 Aug 70	08 Aug 71
	Quartzite Mtn., Nevada (transferred to Univ. of Nev. 21 Aug 71)			
Strain-meter	Tolicha Peak, Nevada	TI-NV	07 Jan 70	24 Apr 70
	Tolicha Peak, Nevada	TI-NV	27 Aug 70	10 Aug 71
	Tolicha Peak, Nevada (transferred to Univ. of Nev. 21 Aug 71)			
Strain-meter	Yucca Mtn., Nevada	YM-NV	20 Jan 70	24 Apr 70
	Yucca Mtn., Nevada	YM-NV	26 Aug 70	11 Aug 71
	Yucca Mtn., Nevada (transferred to Univ. of Nev. 21 Aug 71)			
Strain-meter	Oak Spr. Butte, Nev.	OB-NV	27 Feb 70	05 May 70
	Oak Spr. Butte, Nev.	OB-NV	25 Aug 70	16 Aug 71
	Oak Spr. Butte, Nev. (transferred to Univ. of Nev. 21 Aug 71)			
Triax test	Grand Saline, Texas	GA3TX	22 Sept 71	-
LP deep-hole test	Pinedale, Wyoming	PI2WY	16 Apr 71	24 Aug 71





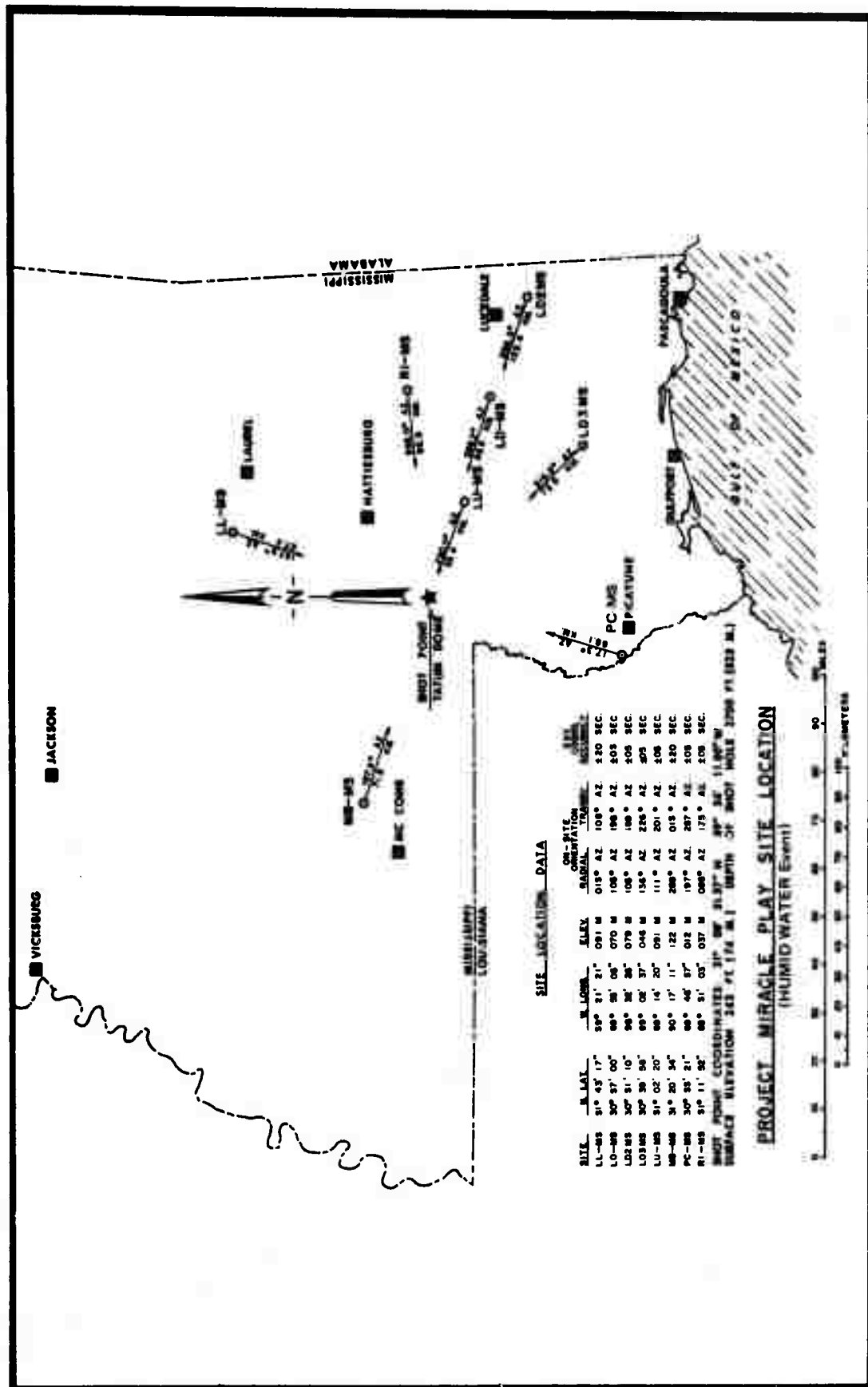
- Mobile observatory  
 ○ Magnetic-tape recorders

NOTE: CORRECTED LOCATION DATA, 9 MARCH 1970

#### SITE COORDINATES

NO.	GEOGRAPHIC		NEVADA GRID		ELEVATION	
	NORTH	WEST	NORTH	EAST	FEET	METER
1.	37° 22' 21"	116° 31' 43"	954,510	540,140	5260	1603
2.	37° 22' 00"	116° 29' 44"	952,350	549,700	5440	1658
3.	37° 20' 56"	116° 27' 59"	946,060	558,210	5560	1695
4.	37° 18' 59"	116° 26' 46"	934,230	564,130	6200	1890
5.	37° 17' 04"	116° 26' 46"	922,560	564,130	6400	1951
6.	37° 15' 20"	116° 27' 49"	912,070	559,100	6290	1917
7.	37° 14' 09"	116° 29' 40"	904,810	550,090	6210	1893
8.	37° 13' 42"	116° 32' 03"	902,150	538,590	6040	1841

Figure 2. HANDLEY accelerometer locations



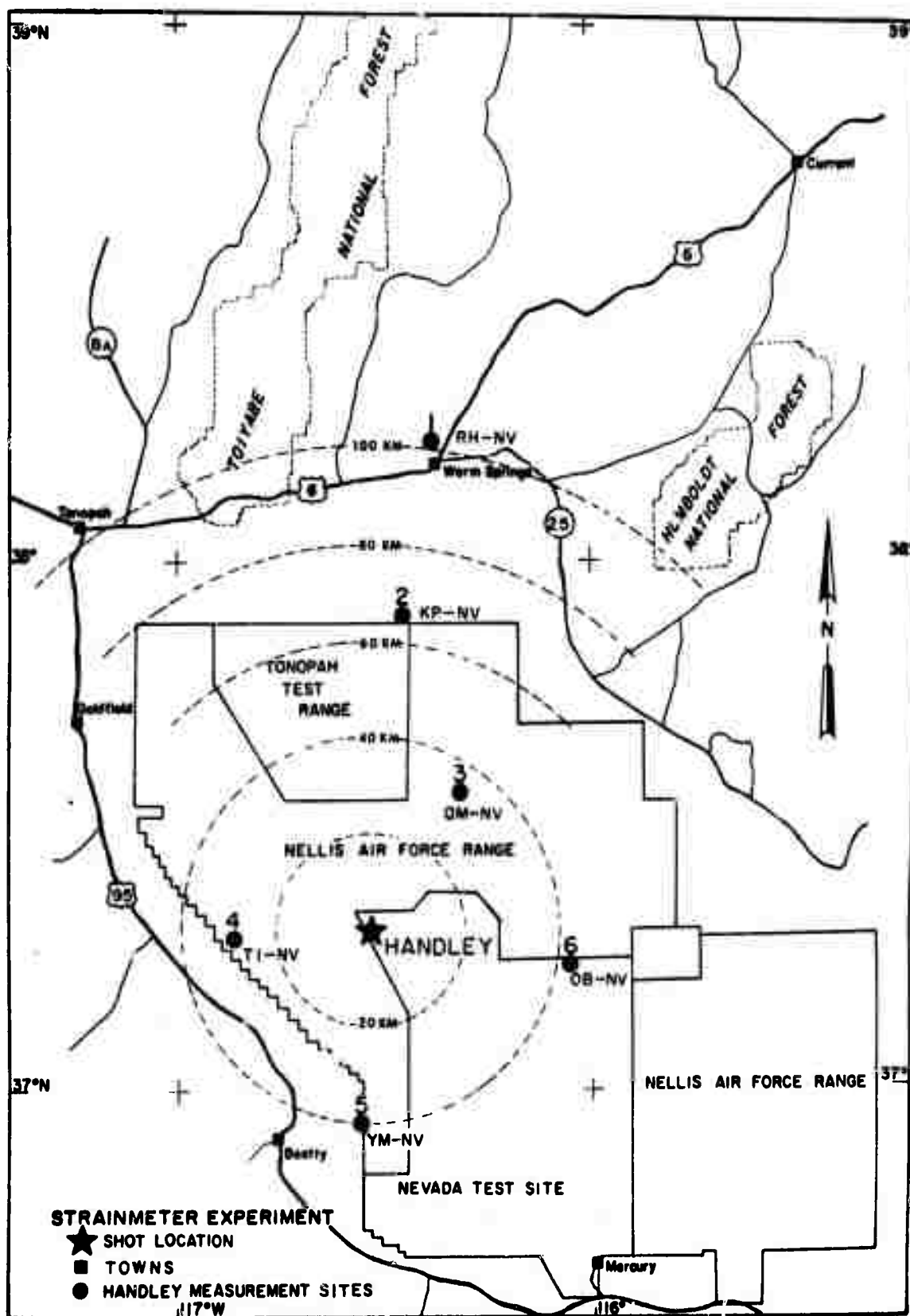


Figure 4. Location of portable strainmeter sites

G 5783



Figure 5. Map locations of van operations



Figure 6. LRS mobile observatory.

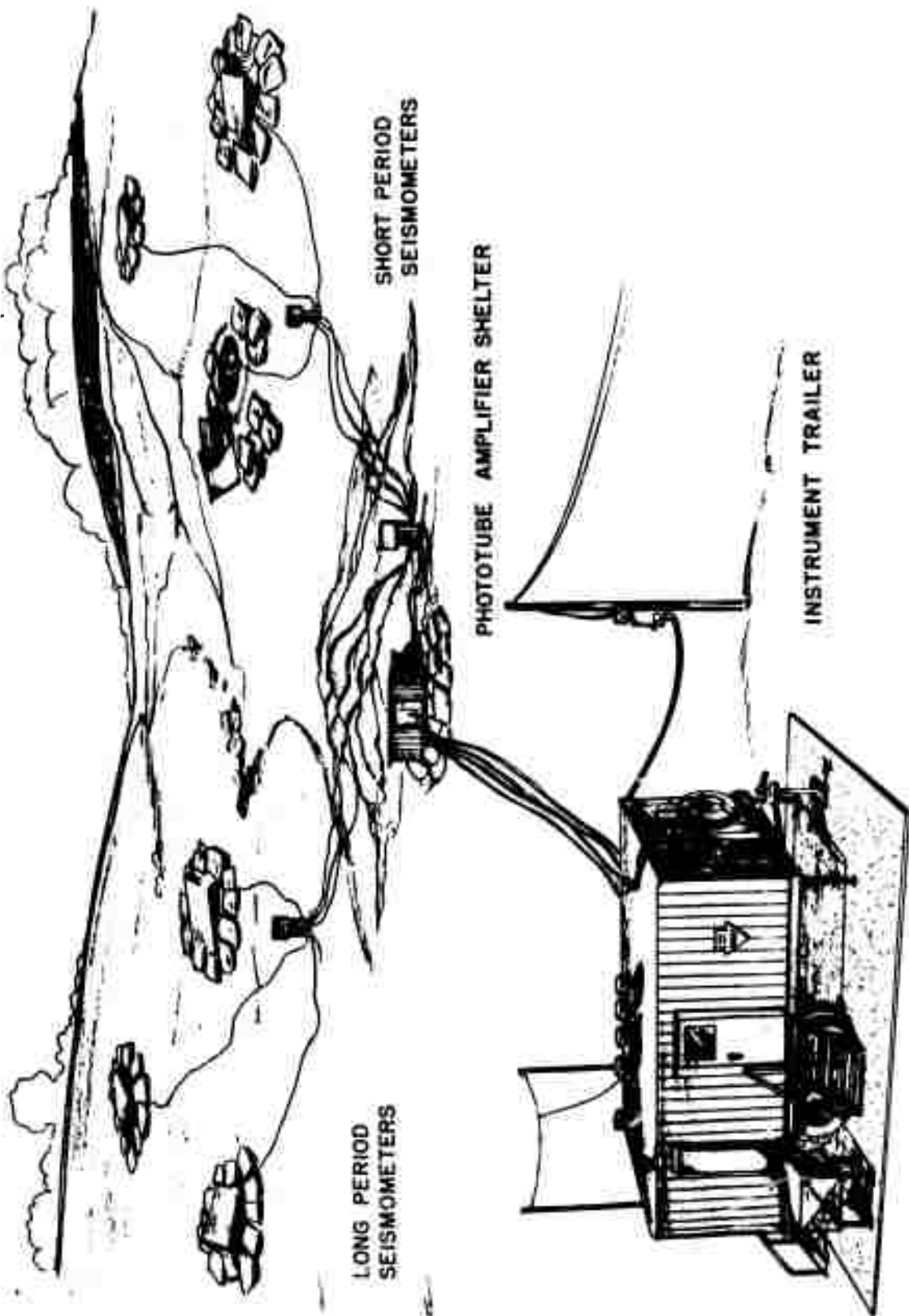


Figure 7. Typical LRSM system field setup

G 4159

### 3.2.4 Pahute Mesa, Nevada (PH3NV and PH4NV), Van Operations

The two vans for use in recording accelerometer data from the HANDLEY event were transported to sites PH3NV and PH4NV on 27 February 1970. These vans had been on standby status in the Department of Defense compound at the Nevada Test Site (NTS), after participating in a similar experiment for the JORUM event. Routine recording by the vans was delayed until 18 March 1970, because of problems with the NTS power generator at site PH4NV, which failed during the HANDLEY event. Recording of accelerometer data at van sites PH3NV and PH4NV terminated on 07 April 1970, and vans, Nos. 210 and 232, were returned to standby status. A detailed account of the experiment is presented in section 6.2 of this report.

### 3.2.5 Mould Bay, NWT, Canada (NP-NT) Van Operations

The Mould Bay location is on the southeast side of Prince Patrick Island, in the Arctic Archipelago. The array was positioned just north of the meteorological station jointly operated by Canada and the United States. Teledyne Geotech personnel operating the NP-NT station were housed at and were dependent upon the meteorological station for support. Figure 8 is a July 1966 view of the permafrost-underlain terrain from within the southern array area towards the camp buildings, and figure 9 shows a map sketch of the array.

Operation of the seven-element short-period seismograph array and the three-component long-period seismograph system in this remote locality presented somewhat unusual requirements for personnel. In addition to maintaining electronic recording systems with generator power in a hostile environment, difficulties were experienced relative to installation, supply, communications, etc. Technical Report No. 64-9, Summary Report on Array Team No. 13, Mould Bay, Canada, by The Geotechnical Corporation, February 1964, describes the initial period of installation and operation at the NP-NT station.

Station equipment and personnel arrived at Mould Bay on 26 June 1963, and operations thereafter through 1969 have been described in previous project final reports. Routine recording of the array instrumentation was continued in January 1970, with the exception of 35-mm film recording of short-period data. The detainment of a normal supply shipment and the delay of mail flights caused short supply of 35-mm film until 14 February 1970. Short-period film recording was maintained on the Develocorder during this period. A change-over of assistant team leaders was accomplished on 13 February 1970, by a charter flight for special resupply of materials. A change-over of team leaders was completed on 18 April 1970.

During the Spring resupply flights of 1970, packing materials were shipped to the NP-NT site in preparation for station equipment removal. Station operations were terminated at NP-NT on 10 July 1970. Team personnel departed the site on 22 July and arrived in Garland, Texas, on 25 July 1970. The van, generator, and array instrumentation remained on-site for disposal by the Canadian Transportation Agency. The major portion of the internal van equipment, including Develocorders and calibration components, was retained by



Figure 8. View south towards camp buildings from snow patch between NP-NT array stations Z-1 and Z-2, Mould Bay, NWT, Canada, July 1966

(1) SP HORIZONTAL INSTRUMENTS LOCATED AT ARRAY STATION Z1. LP INSTRUMENTS ARE LOCATED 190 M. SE OF ARRAY STATION Z1.

**MAK WARRREN, SEOTECH  
(TRANSIT SURVEY)**

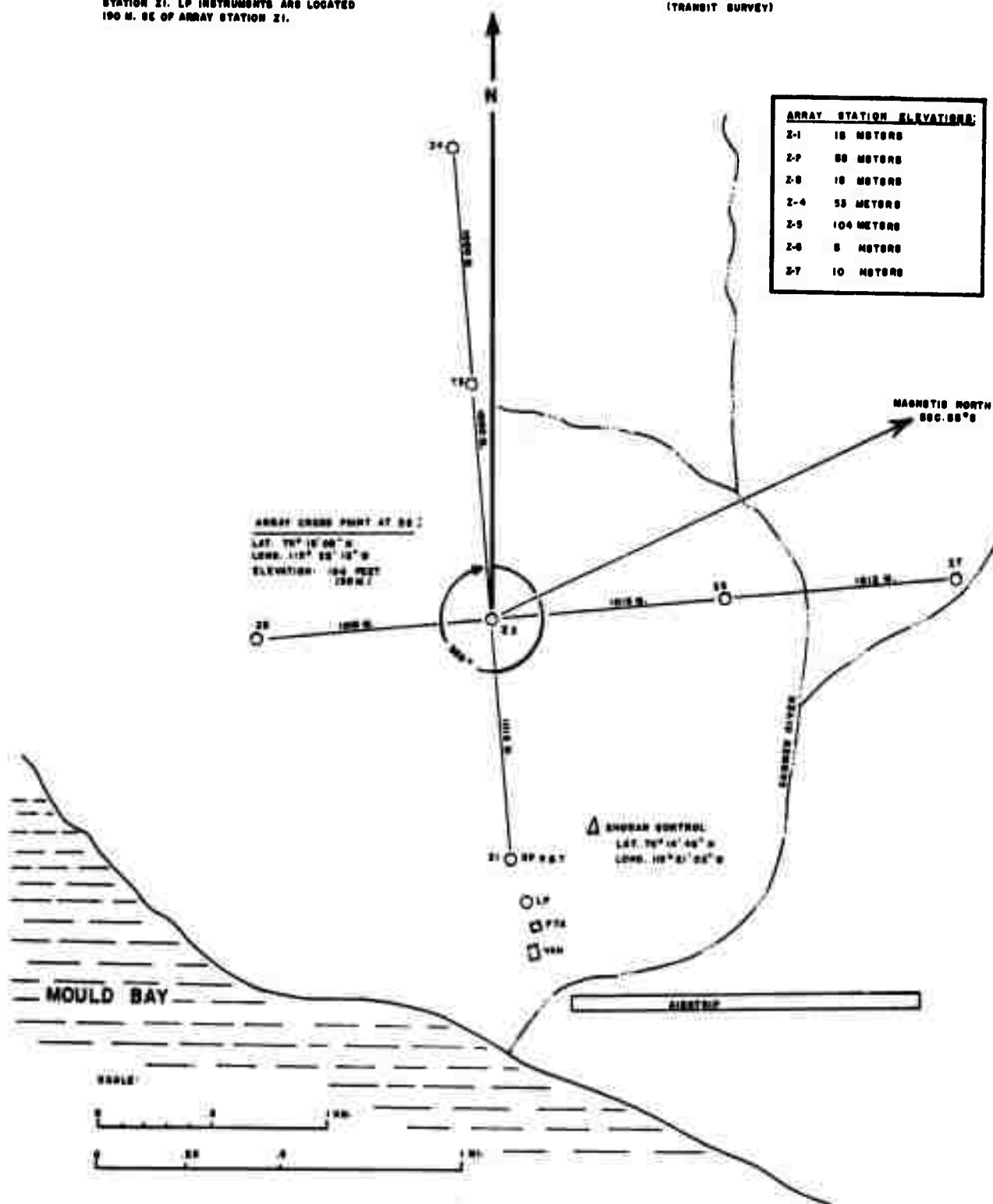


Figure 9. North Pole, Northwest Territory array

Project VT/0703, and was shipped back to the Geotech facility at Garland, Texas. The NP-NT station had furnished near-continuous seismic data for almost 7 years.

### 3.2.6 Las Cruces, New Mexico (LC-NM), Van Operations

Clearance to reoccupy and operate the recording van left on standby status at site LC-NM was obtained from the Civil Engineering Branch of the Air Force Weapons Laboratory, Sandia Base, Albuquerque, New Mexico. The standard mobile observatory short-period and long-period seismographs were operated from 13 through 26 March 1970, for the HANDLEY event. A portable system was also operated at site LC-NM from 17 through 26 March 1970, to increase signal recording capability for the HANDLEY event.

### 3.2.7 Prince George, British Columbia (PG2BC), Van Operations

Van No. 206 was used for short-period and long-period seismic data recording at PG2BC from 05 October 1968 until station termination on 17 August 1970. Seismometers and amplifiers at this site were housed in a bunker-type concrete enclosure. The bunker was left intact and arrangements were made with the landowners for possible future site utilization. Intermittent seismic monitoring operations in the Prince George, British Columbia, area (site PG-BC), had been performed by Geotech since 21 November 1962. The van from PG2BC was transported by a commercial carrier and crossed into the United States on 29 August 1970. This van arrived at the Rawhide Mountain, Nevada site (RH-NV), on 31 August 1970, for use in support of the portable strainmeter system project.

### 3.2.8 Rawhide Mountain, Nevada (RH-NV), Van Operations

Emplacements involving four surface vaults, phototube amplifier pier foundation, and generator slab were completed adjacent to the RH-NV strainmeter site on 12 November 1970. Figure 10 is a sketch of the site layout. The mobile observatory (van No. 206) had previously been transported to the location, and was to supply complementary seismic, accelerometer, and microbarograph data to the strainmeter station recordings.

Team operators arrived at site RH-NV on 09 February 1970. Difficulties were experienced with the power generator, prohibitive repair costs were estimated, and a 15 kW rental generator was obtained in Las Vegas, Nevada.

At the end of February 1971, the short-period and long-period seismometers were installed in the vaults, all outside cabling was completed, and a three-component accelerometer package was emplaced near the short-period seismometer vault. Figure 11 shows the SP system frequency response curve. Figure 12 shows the frequency response curve of the accelerometer system.

VAULTS EMPLACED TO DEPTH AND PTA IN GRAY, WEATHERING TO BROWN, ANDESITE PORPHYRY. WHITE PHENOCRYSTS OF PLAGIOCLASE GIVE THIS ROCK A SPOTTED APPEARANCE. LESSER AMOUNTS OF BLACK AUGITE PHENOCRYSTS ARE ALSO PRESENT IN THE DARK GRAY MATRIX. AGE OF THIS EXTENSIVE, MASSIVE, VOLCANIC FLOW/SILL IS TERTIARY.

PACED DISTANCES SHOWN

SP → LPE = 27 1/2 FT.

LPE → LPN = 8 FT.

LPN → LPE = 8 FT.

STRAIN TUNNEL → VAULT AREA ≈ 400 FT.

PREPARATION AS OF 12 NOV. '70

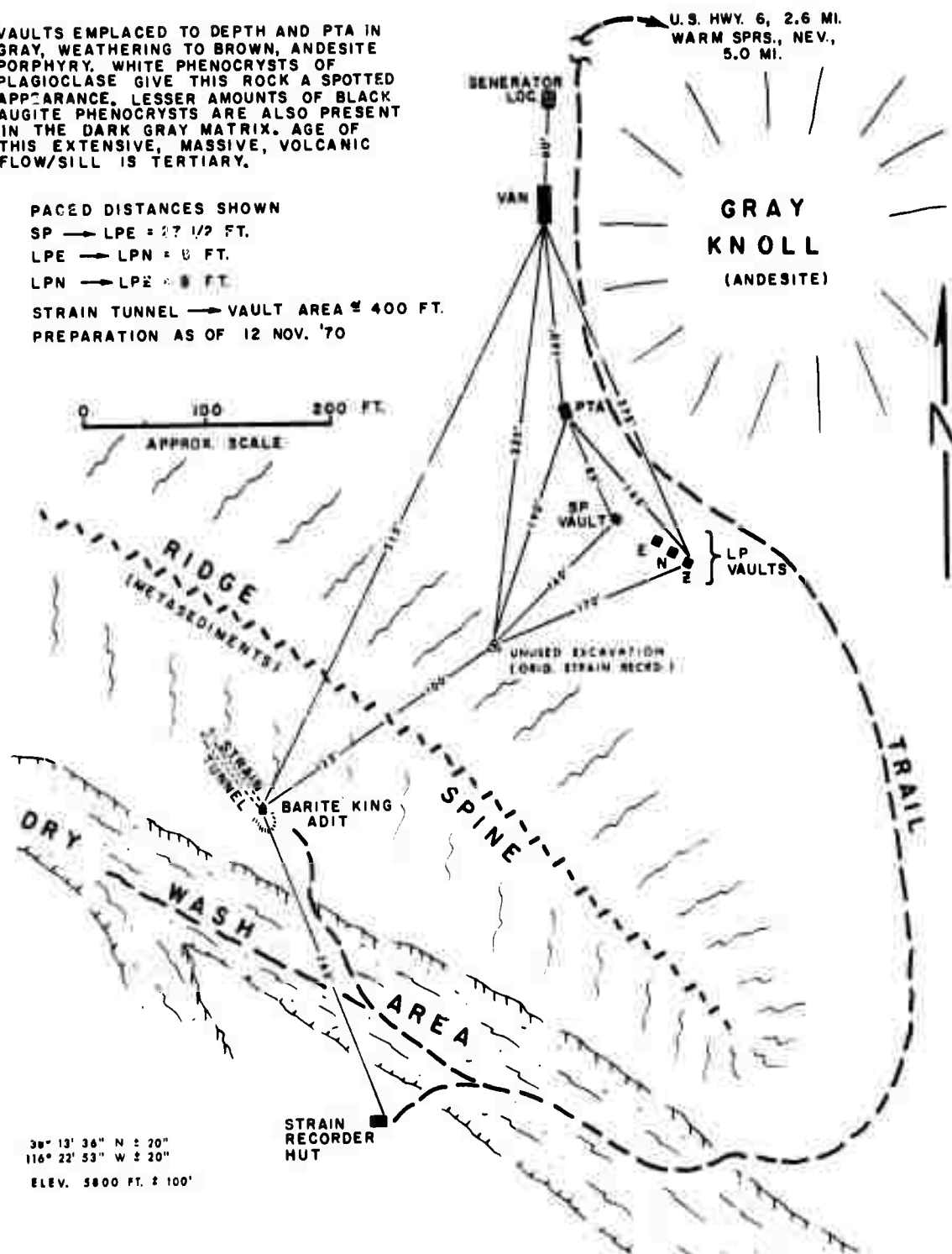


Figure 10. Lay-out of Site RH-NV, Nye County, Nevada

G 6217

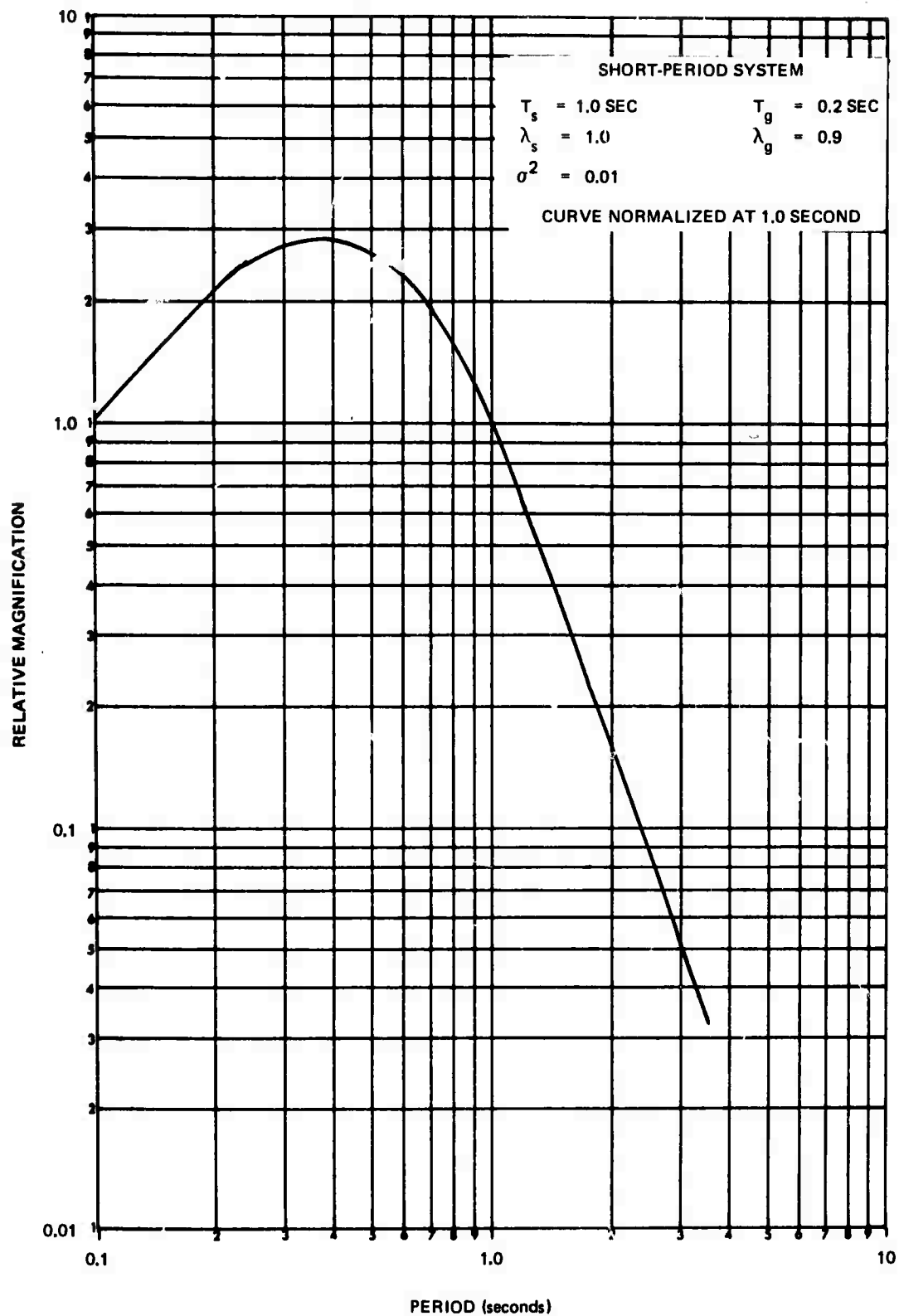


Figure 11. Frequency response of the short-period seismograph system

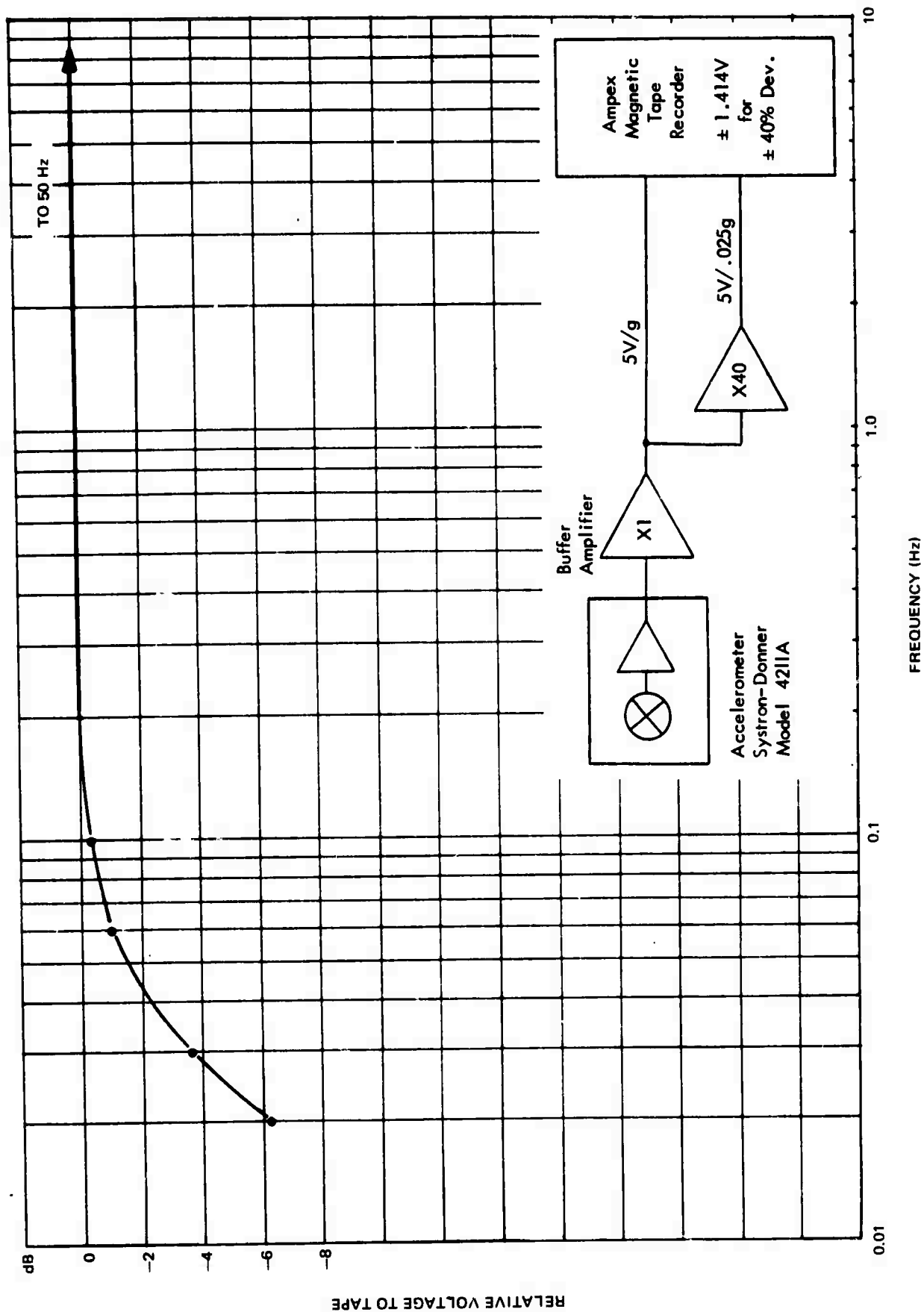


Figure 12. Frequency response of accelerometer system at RH-NV

During March 1971, the long-period seismograph amplifiers were installed, and the calibrations and tests of the long-period seismographs were in progress. Figure 13 shows the standard long-period system frequency response curve. Figures 14 and 15 show the frequency response curves of the LP vertical instrument using the 40- and 60-second filters. Intermittent power generator problems with the diesel rental unit were experienced, and the transfer of two 6.5 kW gasoline generators to the contract from nearby Government storage was initiated. On April 13, 1971, these two generators were transported to the site, and one 6.5 kW unit was utilized as a primary power source for the recording van. Routine operation of the van station at RH-NV began on 21 April 1971, with the exception of the anemometer and microbarograph data channels.

In May 1971, the microbarograph, anemometer, and an additional long-period seismograph data channel were made operational. The additional channel was a long-period, east-oriented, horizontal seismograph (LPE), with a frequency response peaking at a period of 70 seconds as shown in figure 16. Binary coded decimal (BCD) time from the RH-NV recording van was supplied to the magnetic-tape recorder of the portable strainmeter installation. Figure 17 is a block diagram of the seismograph system at station RH-NV. Also in May 1971, the rental diesel generator was returned to Las Vegas for repair and station power was provided by the two 6.5 kW gasoline generators.

In June 1971, the rental diesel generator was repaired and returned to service. Filter electronics to provide frequency responses peaking at 40 and 70 seconds were installed on the long-period, horizontal, north-oriented seismograph (LPN) and the long-period vertical seismograph (LPZ). Channel assignments for the recording instruments, as of 30 June 1971, are shown in table 2. The low-gain LPZ 40-second response data were replaced on channel 10 of the 0.03 ips magnetic-tape recorder by the LPN 70-second response data on 12 July 1971. When necessary, team members continued to support operations of the six portable strainmeter stations in the southern Nevada area (RH-NV, KP-NV, QM-NV, TI-NV, YM-NV, OB-NV).

Van operations at RH-NV were terminated on 02 August 1971. The vault excavations were backfilled and all field cable was retrieved. A commercial carrier picked up the "5th-wheel" type van on 13 August 1971 and delivered it to the Geotech facility at Garland, Texas, on 17 August 1971. Team members remained in Nevada during August to assist in the retrieval and disposition of the six portable strainmeter systems and the two vans that were previously utilized for accelerometer experiments at the Nevada Test Site (NTS).

### 3.2.9 Houlton, Maine (HN-ME), Van Operations

Recording of data from a vertical strain seismograph and an inertial seismograph installed in shallow-cased boreholes continued at site HN-ME, in addition to the normal surface short-period and long-period seismograph systems. The magnetic-tape recorder and long-period seismograph systems required extensive maintenance in January 1970. In June 1970, an amplifier pier was installed to increase the stability of the short-period strain and inertial systems. Some intermittent high-frequency noise had been present on those systems which may have been related to a shifting amplifier pier.

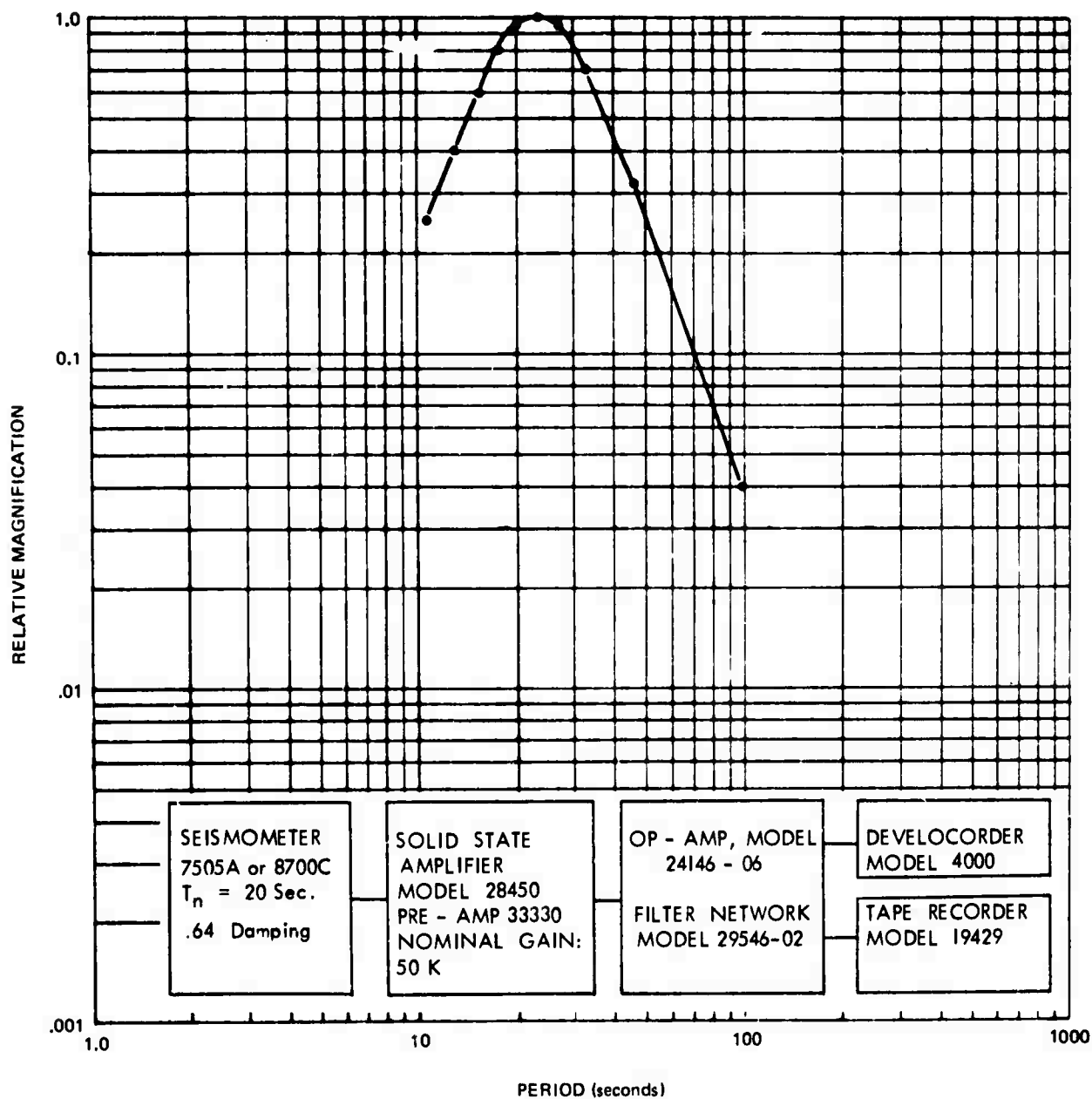


Figure 13. Standard LP frequency response

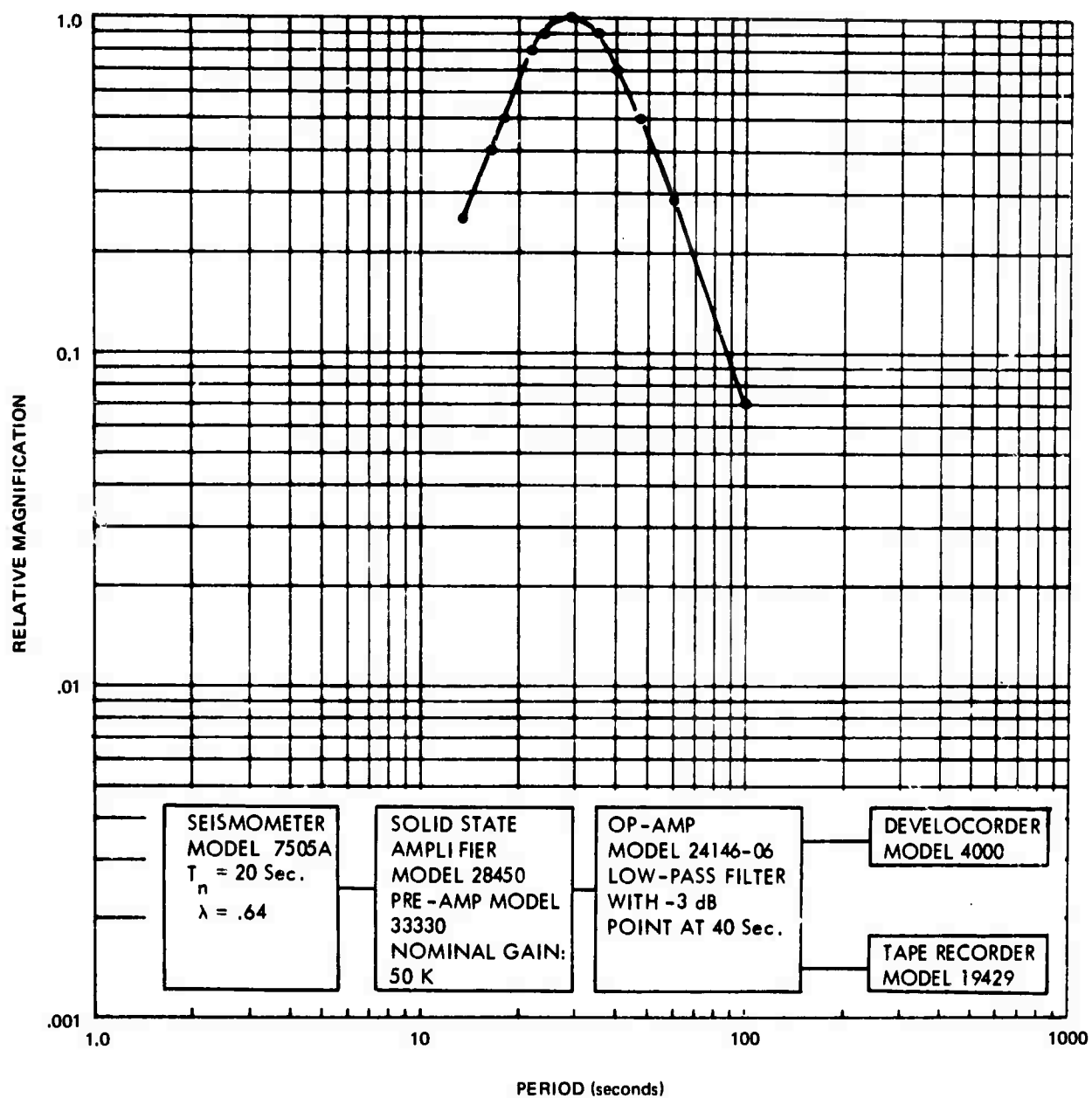


Figure 14. System frequency response of LP vertical with 40-second filter

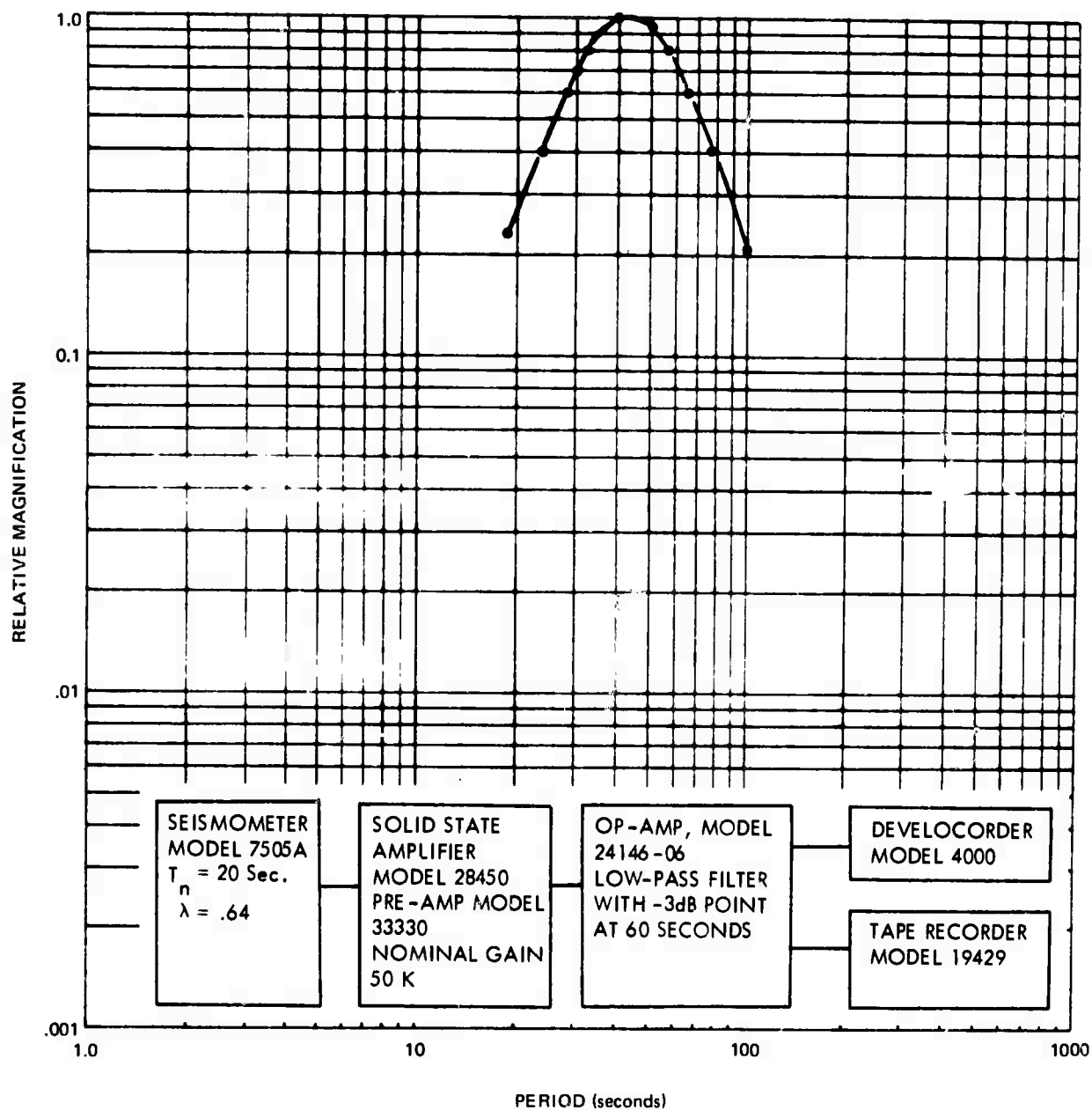


Figure 15. System frequency response of the LP vertical with 60-second filter

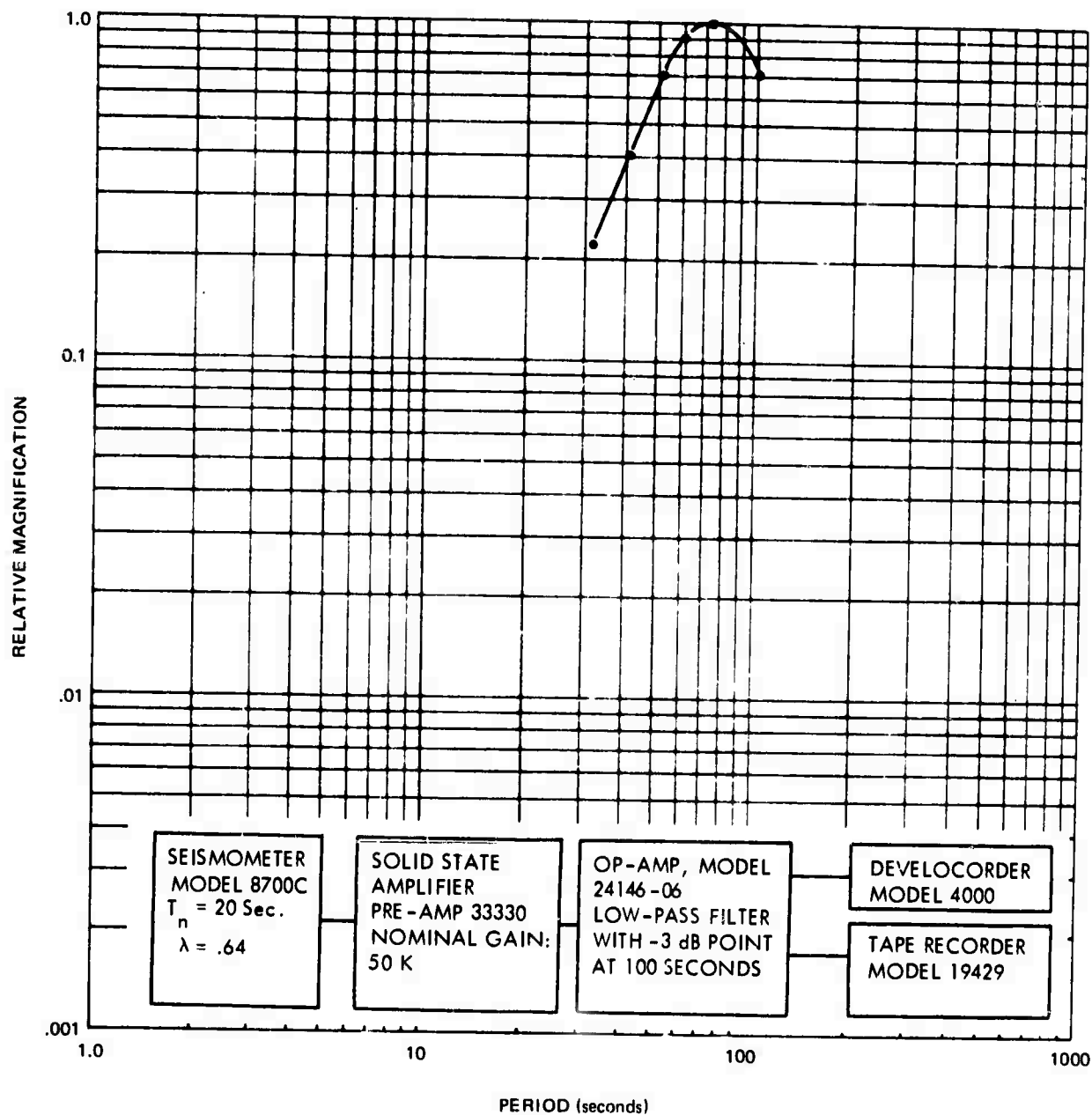


Figure 16. System frequency response of LP horizontal with 100-second filter

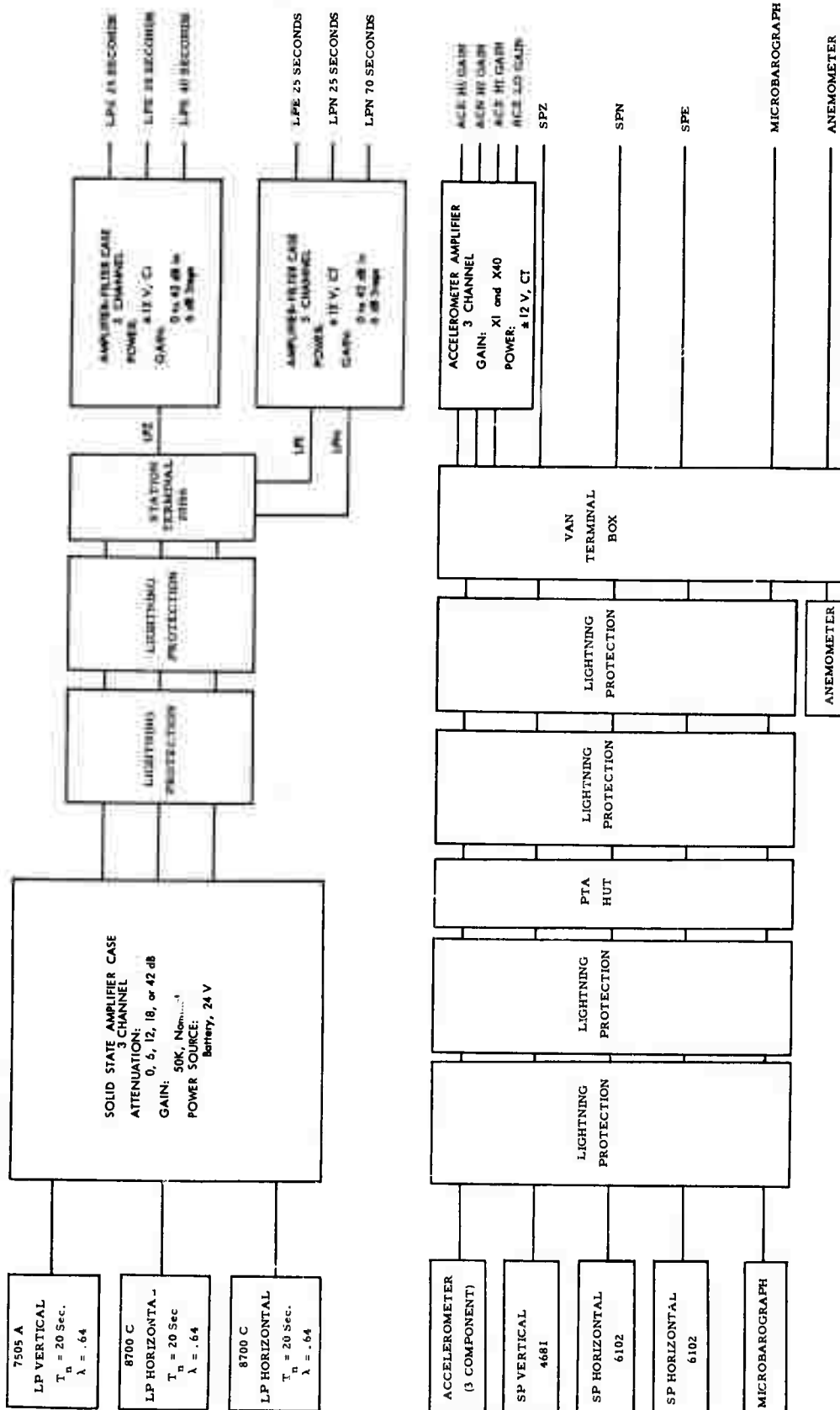


Figure 17. Block diagram of seismogram system at RH-NV

Table 2. RH-NV channel assignments

<u>Channel</u>	<u>0.3 ips Recorder #1</u>	<u>0.03 ips Recorder #2</u>	<u>Develocorder</u>
1	BCD	WWV, Time	SPZ-Hi
2	SPZ	LPZ - 25 sec - Hi	LPZ - 25 sec - Hi
3	SPN	LPZ - 30 sec - Hi	LPZ - 25 sec - Lo
4	SPE	LPZ - 40 sec - Hi	LPZ - 30 sec - Hi
5	ACZ	LPN - 25 sec - Hi	LPZ - 30 sec - Lo
6	ACN	LPE - 25 sec - Hi	LPZ - 40 sec - Hi
7	Compensation	Compensation	LPZ - 40 sec - Lo
8	ACE	LPZ - 25 sec - Lo	LPN - 25 sec - Hi
9	SPZ Lo	LPZ - 30 sec - Lo	LPN - 25 sec - Lo
10	SPN Lo	LPZ - 40 sec - Lo	LPN - 70 sec - Hi
11	SPE Lo	LPN - 25 sec - Lo	LPE - 25 sec - Hi
12	ACZ Lo	LPE - 25 sec - Lo	LPE - 25 sec - Lo
13	Anemometer	Microbarograph	Microbarograph
14	WWV, Time	BCD	Anemometer

In August and September 1970, the original vertical strain and vertical inertial systems were converted to an intermediate-period (IP) vertical strain-inertial system. Details concerning the installation, analysis, and results of the IP test are contained in section 6.4 of this report.

Data continued to be recorded at HN-ME from September through December 1970. Various phase response calibrations and special system noise tests with emphasis on the IP strain-inertial system were performed. On 17 and 18 January 1971, a rigorous series of amplitude and phase measurements were performed on the IP strain and inertial channels and on individual system components. These test data are available as a guide for possible future retrofit or alteration of component responses to improve phase matching.

Station operations at HN-ME were discontinued on 04 February 1971. Operators departed the site on 10 February 1971, and arrived in Garland, Texas, on 17 February 1971. Instrumentation vaults, boreholes, and foundations were left intact for possible occupation by a portable system at a later date. The recording van was returned to the Geotech facility at Garland, Texas. The Houlton, Maine, site had been occupied by a mobile observatory station for approximately 8-1/2 years since August 1962.

### 3.2.10 Fairbanks, Alaska (FB2AK), Van Operations

Operation of both surface long-period and downhole triaxial long-period seismographs was started at site FB2AK on 09 June 1970. This station was collocated with the Alaskan Long-Period Array site 3-3. Collection of routine and special test data at this site was performed until operations were terminated on 14 June 1971. The van was left on standby status at the site. A detailed account of the experiment is presented in section 6.6 of this report.

## 3.3 OPERATION OF PORTABLE SYSTEMS

### 3.3.1 Project MIRACLE PLAY

#### 3.3.1.1 General

A site repermit and inspection trip was made to southern Mississippi in March 1970 in preparation for the HUMID WATER gas explosion, the second of a series of experiments identified as Project MIRACLE PLAY. HUMID WATER was detonated on 19 April 1970. The eight portable system sites occupied for the DIODE TUBE event were reoccupied for the HUMID WATER event. Table 3 shows the station designator, location, and operational dates of each site. The locations of the eight portable system sites are shown in figure 3. All teams completed their recording at the end of the run on 22 April 1970, and returned to Garland, Texas.

Table 3. Project MIRACLE PLAY site locations

<u>Station designator</u>	<u>Location</u>	<u>Operational dates</u>	
		<u>SP</u>	<u>LP</u>
PC-MS	Picayune, Mississippi	10 April 70	10 April 70
MB-MS	McComb, Mississippi	9 April 70	10 April 70
LL-MS	Laurel, Mississippi	9 April 70	12 April 70
LD-MS	Lucedale, Mississippi	11 April 70	11 April 70
LD2MS	Lucedale, Mississippi	14 April 70	11 April 70
LD3MS	Lucedale, Mississippi	9 April 70	9 April 70
LU-MS	Lumberton, Mississippi	7 April 70	7 April 70
RI-MS	Richton, Mississippi	16 April 70	16 April 70

3.3.1.2 A report, Preliminary Analysis of Signals Recorded from the HUMID WATER Event by Long-Range Seismic Measurements Portable System Teams, was prepared in April 1970, and copies were sent to the Project Officer and Lt. Col. Walt Davis of the Defense Atomic Support Agency, Sandia Base, Albuquerque, New Mexico.

3.3.1.3 Technical Report 70-16, Preliminary Report on Long-Range Seismic Measurements Participation in Project MIRACLE PLAY-HUMID WATER, was published during the report period. This report gives a summary of the data collected from Project STERLING, a nuclear device detonated on 3 December 1966, and Project MIRACLE PLAY.

3.3.1.4 Power spectra of microseismic noise samples were computed from data recorded immediately preceding the STERLING, DIODE TUBE, and HUMID WATER explosion. Power spectra of a 25-second signal sample, including the segment during which the surface group peaked on the radial trace, were computed.

All analysis was done using data from LD-MS, the site with the largest signal-to-noise ratio. It must be noted that this site is anomalous in its high signal-to-noise ratio as compared with other sites at approximately the same distance.

Examination of the spectra clearly indicates the low amplitude levels recorded from DIODE TUBE. Only on the radial trace was the power level of the signal appreciably above the background noise level. The largest amplitude in the surface wave train recorded on the radial channel from the DIODE TUBE event is 4.4 times smaller than that from HUMID WATER and 2.6 times smaller than

that from STERLING. In the frequency range of appreciable power (1.0-3.0 Hz), the power ratio shows that DIODE TUBE is smaller than HUMID WATER by a factor of approximately 100 and smaller than STERLING by a factor of approximately 20. On the short-period vertical channel, the spectra indicate that the signal power does not exceed the confidence level ( $\pm 4$  dB) of the noise, i.e., no measurable signal power was detected over the whole signal range although the surface wave train can be detected visually.

A comparison of the surface wave spectra and the preceding noise shows that STERLING has little energy in the 1.0-2.0 Hz frequency range, while HUMID WATER has appreciable energy in this frequency range. Because travel path and sensor location are identical, the difference must be caused by the source mechanism.

In an attempt to improve the signal-to-noise ratio of the first arrival, the P wave, a prediction error filter, was designed.<sup>1</sup> The prediction filter uses the statistics of the preceding noise to predict the noise at the time of signal arrival and subtracts it from the record, leaving the signal unaffected. No appreciable improvement of the first arrival was obtained, probably because of the almost flat spectrum of the noise.

---

<sup>1</sup>Peacock, K. L., and Treitel, S., 1969: Predictive deconvolution; theory and practice: Geophysics, vol. 34, p. 155-169

## 4. INSTRUMENTATION

### 4.1 GENERAL

This section describes the evaluation and modification of existing equipment and the characteristics of new equipment - the objective being to improve the capability and reliability of the various systems.

### 4.2 PORTABLE SYSTEM MODIFICATIONS

#### 4.2.1 Battery Power Supply Modifications

Under the previous contract, one portable seismograph system was modified to permit the use of the main battery power supply as a power source for the Control Monitor Unit, Model 19823. The main batteries provide greater capacity and eliminate the requirement for separate battery packs for the control monitor. The modification was evaluated and subsequently performed on the 10 additional portable seismograph systems.

#### 4.2.2 Modification of Battery Charger, Model 21160A

Following the replacement of the silver-cadmium batteries by lead-acid batteries for use as system power supplies for the portable systems, it was necessary to modify the Battery Charger, Model 21160A, so that it would provide a suitable charge rate for the lead-acid batteries. Each portable system is equipped with 2 chargers, for a total of 22 for the 11 teams. The 22 chargers were modified during this report period.

#### 4.2.3 Replacement of Model 25540 $\pm 9$ Vdc Regulator

The Model 25540  $\pm 9$  Vdc regulator is no longer practical to use in small quantities because of a minimum order requirement by the vendor of one component and the length of delivery time. Another regulator, Mil Electronics Model SD49, was tested and found to be an acceptable replacement. Ten of these regulators were purchased, 5 to be used with new filter-amplifier units and 5 to be used as spares for the portable systems.

#### 4.2.4 Three-Channel Filter-Amplifier Units

Five, 3-channel, filter-amplifier units were fabricated to provide additional response shaping for the long-period seismographs. Each unit contains plug-in filter networks (3rd order Butterworth) which are interchangeable physically with standard filters. Each unit also contains one Mil Electronics Model SD49  $\pm 9$  Vdc regulator and three Model 24146 operational amplifiers. The filter channels may be connected in parallel to provide up to three different frequency responses from one seismometer.

#### 4.2.5 Replacement of Silver-Cadmium Batteries with Lead-Acid Batteries

Because of the high cost per unit time of operation of the silver-cadmium batteries used in the portable systems, they were replaced with lead-acid batteries.

The silver-cadmium batteries were retained until normal deterioration had made them unserviceable. During this report period, lead-acid batteries were placed in service on all 11 portable systems. The silver-cadmium batteries were disposed of through formal surplus declaration procedures.

## 5. EVALUATION OF SUPPORT EQUIPMENT

### 5.1 GENERAL

The support equipment includes the mobile observatory vans, instrumentation shelters, generators, trailers, and vehicles utilized during field operations. When conditions warranted, this equipment was reconfigured or augmented by the utilization of locally-constructed shelters and/or rented equipment. Table 4 lists the vans, generators, and vehicles remaining available at the end of the report period.

### 5.2 VANS AND INSTRUMENTATION SHELTERS

The recording vans, phototube amplifier shelters, and seismometer vaults continued to provide adequate service. At the beginning of this report period (01 Jan 1970), 7 of the original 40 vans remained in the program. These seven vans were Nos. 206, 208, 210, 213, 219, 223, and 232. The four vans Nos. 210, 213, 223, and 232 were transferred to other organizations/programs during this report period.

With the usage of solid-state amplifiers mounted in the vans, the phototube amplifier shelters provided other functions such as housing recorders and calibration equipment for the six portable strainmeter system stations in Nevada (RH-NV, KP-NV, QM-NV, TI-NV, YM-NV, and OB-NV). In addition to normal use as short-period seismometer vaults at various van sites, the half-shell vault cylinders were horizontally emplaced as sealed portals for the four Nevada strainmeter mine sites.

The heavy-duty, Melton-type, domed/cylindrical tank vaults constructed of 1/8-inch thick steel continued to provide housing for the long-period seismometers. One of these Melton-type vaults was modified and installed over the subsurface wellhead at Alaska Long-Period Array site 2-3.

In August 1971, a special hemispherical/cylindrical 1/4-inch thick steel vault at the Lamont-Doherty design was installed for evaluation at site WP-TX.

### 5.3 VEHICLES

The various vehicles utilized in the program included 1/2-ton and 3/4-ton pickup trucks, 2-1/2 ton trucks, snow vehicles, and utility trailers. The units all generally performed well, but some were disposed of because of reduced field requirements or increased maintenance costs. Rental units were occasionally utilized when economically advantageous.

Table 4. Available vans, generators, and vehicles; 31 October 1971

Description	Identification	Meter reading	Location	Remarks
Van, ball-hitch (Model 8513)	No. -208	-	Site WP-TX	In use
Van, ball-hitch (Model 8513)	No. -219	-	Site FB2AK	Standby
Van, 5th-wheel (Model 7700)	No. -206	-	Geotech/Garland	Standby
Generator, 3 kW Kohler	320841	-	Geotech/Garland	Standby
Generator, 6.5 kW Kohler	277809	700 hours	Geotech/Garland	Standby
Generator, 6.5 kW Kohler	277810	3700 hours	Geotech/Garland	Standby
Generator, 15 kW U.S. Mtrs.	332553-1	4900 hours	Geotech/Garland	Standby
Generator, 15 kW U.S. Mtrs.	332553-2	4000 hours	Site FB2AK	Standby
Generator, 15 kW U.S. Mtrs.	332553-3	6200 hours	Geotech/Garland	Standby
Utility trailer, Krueger	235-015	-	Geotech/Garland	Standby
Pickup truck, 3/4 ton GMC	212-010	81400 miles	Geotech/Garland	Standby (flatbed)
Pickup truck, 3/4 ton GMC	212-014	83500 miles	Site WP-TX	In use (4-wh hoist)
Pickup truck, 1/2 ton Ford	212-088	82800 miles	Geotech/Garland	Standby
Pickup truck, 1/2 ton Ford	212-097	99700 miles	Site WP-TX	In use
Prime mover, 2-1/2 ton Ford	212-086	105000 miles	Geotech/Garland	Standby
Prime mover, 2-1/2 ton Ford	212-098	54900 miles	Geotech/Garland	Standby
Pickup truck, 3/4 ton Chev.	212-099	79500 miles	Geotech/Garland	Standby
Pickup truck, 3/4 ton Chev.	212-100	56900 miles	Geotech/Garland	Standby
Pickup truck, 3/4 ton Chev.	212-101	70400 miles	Site CR2NB	In use
Pickup truck, 3/4 ton Chev.	212-102	54900 miles	Site BE-FL	In use
Pickup truck, 3/4 ton Chev.	212-103	51800 miles	Site LC-NM	In use
Pickup truck, 3/4 ton Chev.	212-104	57200 miles	Site HN-ME	In use
Pickup truck, 3/4 ton Chev.	212-105	93700 miles	Site SJ-TX	In use
Pickup truck, 3/4 ton Chev.	212-106	62600 miles	Site GA3TX	In use
Pickup truck, 3/4 ton Chev.	212-107	44100 miles	Site KN-U7	In use
Pickup truck, 3/4 ton Chev.	212-108	54300 miles	Site RK-ON	In use
Pickup truck, 3/4 ton Chev.	212-109	40300 miles	Site PG2BC	In use
Pickup truck, 3/4 ton Chev.			Site WH2YK	In use

### 5.3.1 1/2-Ton Pickup Trucks

In August 1965, ten 1/2-ton Ford pickup trucks were acquired for use in the LRSM program. Three of these units remained in service at the beginning of this report period; the others having been previously transferred or sold. An additional unit was also sold during the report period. One of the two remaining units was being used at the end of the report period and the other was on standby status. On 31 October 1971, the two remaining 1/2-ton Ford pickup trucks had an average of about 91,250 miles, most of which was accumulated on unpaved roads.

### 5.3.2 Heavy-duty 3/4-Ton Pickup Trucks

In 1961, forty 3/4-ton GMC four-wheel drive pickup trucks were acquired for use in the LRSM program. Five of these units remained in service at the beginning of this report period; the others having been previously transferred or sold. Three additional units were also transferred or sold during this report period. One of the two remaining units, because of its four-wheel drive, mounted hoist, and van hauling capability, continued to be used. The other unit had been modified to a flat-bed configuration and was placed on standby status. On 31 October 1971, these two remaining 3/4-ton GMC pickup trucks had an average of about 82,450 miles on their odometers.

The six 1967, and five 1968, 3/4-ton Chevrolet two-wheel drive pickup trucks used primarily for portable system operations continued to perform satisfactorily throughout the report period. These units have the capacity to transport all portable system instrumentation and associated support equipment within the enclosed bed of the vehicle. The enclosure protects the instrumentation while in transit, and provides shelter during station servicing operations. Two of these vehicles were extensively used in off-highway portable strainmeter operations in Nevada. On 31 October 1971, these eleven 3/4-ton Chevrolet pickup trucks had an average of about 60,520 miles on their odometers.

One 1969, 3/4-ton, Ford four-wheel drive pickup truck was borrowed from the Alaska Long-Period Array (ALPA) project for use at the FB2AK (ALPA 3-3) van site. This winch and radio-equipped vehicle was augmented with a four-wheel drive rental unit during periods of intense activity in the site area. The vehicle provided service during adverse conditions and was returned to the ALPA operation upon project termination.

### 5.3.3 2-1/2-Ton Trucks

Two 2-1/2-ton Ford trucks were utilized to transport the recording vans. The first unit was obtained in October 1964, and has been driven about 105,000 miles. A second unit was obtained in March 1966, and has been driven about 54,900 miles. Both vehicles have provided satisfactory service and have required a minimum of major repairs. These units were driven a total of about 17,450 miles during the report period hauling vans, generators, cable, etc.

#### 5.3.4 Snow Vehicles

A Kristi snow vehicle, Model KT-3, was purchased in October 1962, to provide a reliable means of off-road, short-distance transportation to those sites subject to heavy snow conditions. This vehicle was effectively utilized at several mobile observatory sites during the course of the LRSM program. When the Red Lake, Ontario (RK-ON), site was deactivated in August 1970, requirements for the unit were eliminated and the vehicle was sold at that location.

A small, modified, Bombardier snow vehicle was borrowed from the ALPA program and utilized for several winter months at the FB2AK (ALPA 3-3) site. This vehicle provided site access and was returned to the ALPA operation when the FB2AK station was placed on standby status in June 1971.

#### 5.3.5 Utility Trailers

One of the two Krueger utility trailers in use at the start of the report period was sold. These units were used extensively during past portable systems operations prior to this report period and to the acquisition of the 3/4-ton Chevrolet pickup trucks. Lease charges on the remaining utility trailer are low (\$0.95/month). This trailer was used for equipment transportation between the Geotech facility at Garland, Texas, and Pinedale, Wyoming (site PI2WY). At the end of the report period, this unit was on standby status.

### 5.4 GENERATORS

At the close of the report period, only three reliable generators were available. One was a small 3 kW Kohler utility generator for the operation of power tools, etc., during site preparation activities. The other two units are 6.5 kW Kohler generators obtained through the Atomic Energy Commission for use at the Rawhide Mountain, Nevada site (RH-NV), in April 1971. Both of the 6.5 kW units are trailer-mounted, gasoline-fueled, and were on standby status at the Geotech facility in Garland, Texas, on 31 October 1971. The two 6.5 kW generators have an average of about 2200 hours of operation per unit.

Three, 15 kW, U. S. Motors gasoline/propane fueled generators remained in the program at the end of this report period. Two of these units were awaiting disposition at the Geotech facility at Garland, Texas. The third 15 kW U. S. Motors unit was on standby status at site FB2AK. These three generators are no longer reliable for continuous operation, and have had an average of about 5030 hours of operation since being refurbished.

The two 25 kW Caterpillar diesel generators in use at the start of the report period were transferred or sold during the report period. One of these units was left on location (transferred) at the Mould Bay, Northwest Territories, Canada, site (NP-NT) when that array station was deactivated in July 1970. The other 25 kW Caterpillar unit was sold at Las Vegas, Nevada, after difficulties were experienced with the unit maintaining continuous power for the RH-NV mobile observatory station.

The Government-furnished 20 kW International-Fermount generator (S/N 771005) obtained for use at site FB2AK was unreliable. This unit was returned to Fort Wainwright, Alaska, when the FB2AK mobile observatory station was placed in standby status in June 1971.

Generators were rented to provide station power at various times during the report period at sites RH-NV and FB2AK. Generators obtained from the Nevada Test Site were used to furnish power at the Pahute Mesa, Nevada, accelerometer sites (PH3NV and PH4NV).

## 6. SPECIAL PROJECTS

### 6.1 PROJECT MIRACLE PLAY - HUMID WATER

The HUMID WATER gas explosion, the second of a series of experiments called Project MIRACLE PLAY, was monitored by eight LRSM portable system teams. The teams occupied the same sites that were occupied for the DIODE TUBE explosion. Visual analysis of the seismograms shows that the STERLING, DIODE TUBE, and HUMID WATER signals were recorded at Lucedale, Mississippi, (LD-MS). Spectra of the signals at LD-MS show that the power level of HUMID WATER was greater than that of STERLING. Refer to Technical Report No. 70-16, "Preliminary Report on Long-Range Seismic Measurements Participation in Project MIRACLE PLAY-HUMID WATER."

### 6.2 HANDLEY ACCELEROMETER OPERATION

Recording facilities and operational assistance were provided to the University of California for the acquisition of accelerometer data from the HANDLEY event.

The locations of eight sets of three-component accelerometers are shown in figure 2. A portable tape recorder, provided by Dr. Tom McEvilly of the University of California, was located at site 1 and recorded data from sites 1 and 2. This recorder was installed and maintained by Geotech personnel. At site 3, equipment service, and maintenance was performed by personnel of the U. S. Geological Survey. Two mobile observatories were provided by LRSM. One was located between sites 4 and 5 and recorded data from the two sites; a second was located between sites 6 and 7 and recorded data from sites 6, 7, and 8. Each recording van was equipped with two 1-inch, 0.3 ips, FM magnetic-tape recorders, one calibrated to provide full-scale recording for a 0.5 g signal and the other to provide full-scale recording for a 0.0125 g signal.

A block diagram of a typical data channel and the system frequency response is given in figure 18.

### 6.3 PORTABLE STRAINMETER SYSTEMS

Six portable strainmeter systems were designed, built, and tested under Project VT/8703. The installation and operation of the systems were begun under Project VT/8703, which was extended through February 1970. Additional operations after February 1970 were performed under Project VT/0703.

Work authorized under Project VT/8703 included bringing to an operational status the six portable strainmeters at the six sites selected for the HANDLEY event (figure 4 and table 5) and evaluating the systems. The six strainmeters were operated during the HANDLEY event and for a 30-day period following the event. The results are reported in Technical Report No. 70-10, Special Report, Project VT/8703, Evaluation of Field Operational Characteristics of the Portable Strainmeter System, dated 31 July 1970.

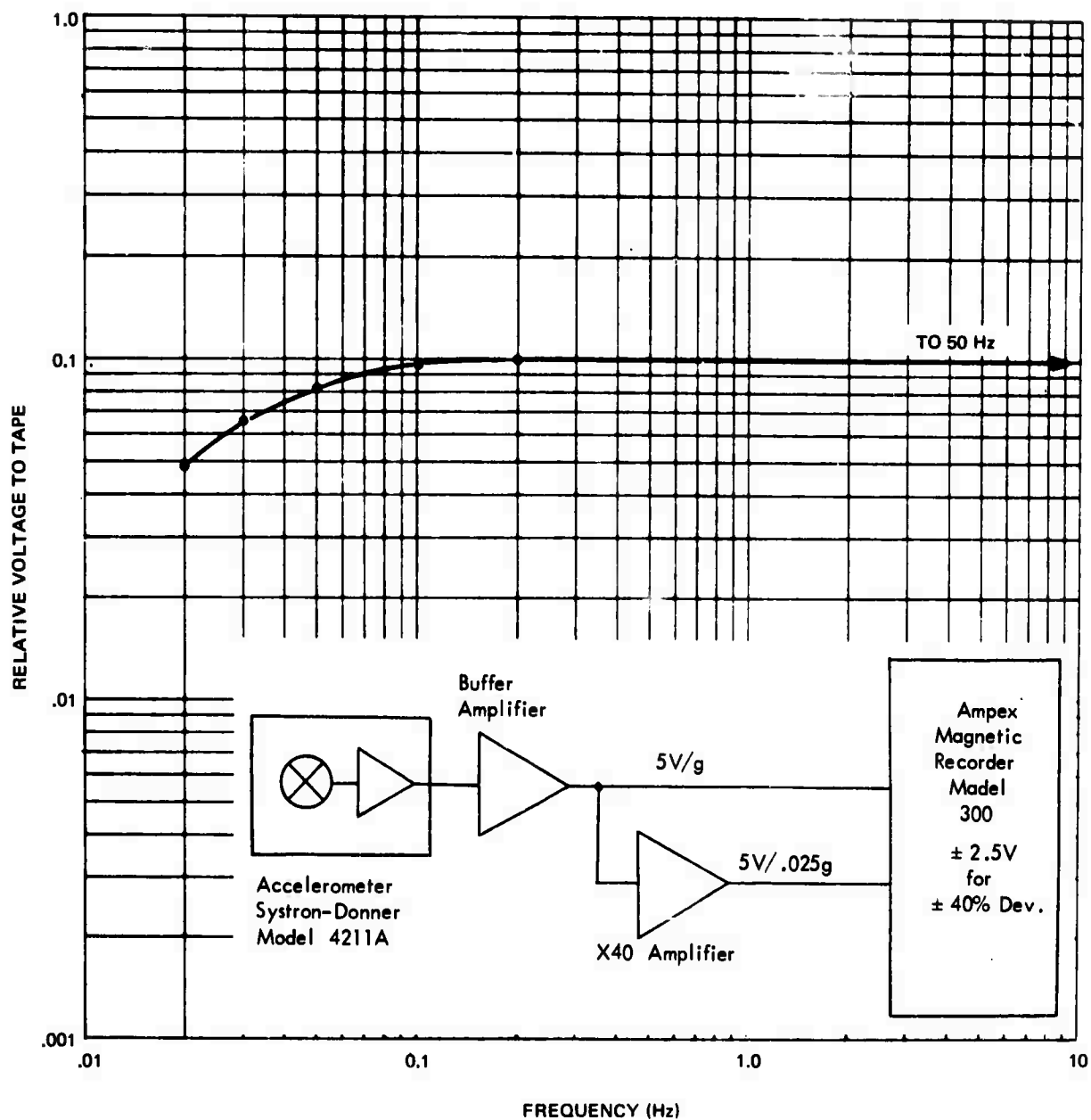


Figure 18. Frequency response of accelerometer system for HANDLEY

Table 5. Portable strainmeter site locations

Site No.	Site name	Site designator	Geographic coordinates		Elevation		Approximate azimuthal orientation of strainmeter thru site	Distance from HANDLEY (km)	Approximate deviation of strainmeter from HANDLEY radial	Type of site
			N. Lat.	W. Long.	Feet	Meters				
1	Rawhide Mtn., Nevada	RH-NV	38°13'36"	116°22'53"	5800	1768	325°	103.6	43°	Tunnel
2	Kawich Peak, Nevada	KP-NV	37°53'51"	116°27'33"	7000	2134	356°	066.5	10°	Tunnel
3	Quartzite Mtn., Nevada	QM-NV	37°33'47"	116°19'04"	6160	1878	020°	034.8	13°	Tunnel
4	Tolicha Peak, Nevada	TI-NV	37°17'07"	116°52'01"	5000	1524	266.5°	029.6	0°	Trench
5	Yucca Mtn., Nevada	YM-NV	36°55'53"	116°33'15"	4400	1341	182.5°	041.1	0°	Trench
6	Oak Spring Butte, Nevada	OB-NV	37°14'09"	116°03'09"	5680	1731	081°	043.3	19°	Tunnel

The six systems were placed in storage in a government warehouse at Mercury, Nevada, in late April and early May 1970. The strainmeters were left in place in order to preserve temperature stability in the tunnels and trenches.

The six systems were reactivated in the period 22-31 August 1970, and were operated through July 1971. The documentation and/or analysis of explosion and earthquake data in the period March 1970 through July 1971 includes the following:

a. Documentation of the NTS events HANDLEY and MINTLEAF, discussed in an earlier section of this report and reported in detail in Technical Report No. 70-10;

b. A comparison of the explosions CYATHUS and BANE BERRY, requested by the Project Officer;

c. A report on the San Joaquin Valley earthquake, requested by the Project Office;

d. A case study of the NTS explosion MINIATA, demonstrating examination of a single event recorded at six sites;

e. A comparison of the character of the strain step of a near earthquake and a near explosion at the NTS;

f. A study of the relation between direction of the strain step and changes in regional strain conditions.

Complete documentation and/or analysis is given in Technical Report No. 71-20, Special Report, VT/0703, Analysis of Data from Six Portable Strainmeters in Southern Nevada, dated 31 October 1971.

All systems were picked up, the sites were restored, and the systems were placed in storage in Reno, Nevada, during August 1971. All systems were transferred to the University of Nevada during October 1971.

#### 6.4 INTERMEDIATE PERIOD (IP) VERTICAL STRAIN SYSTEM AT HN-ME

##### 6.4.1 Introduction

The response of the short-period (SP) vertical strain system at Houlton, Maine (HN-ME) was converted to an intermediate-period (IP) response for the cancellation of 6-second microseisms as required by the Project Officer on 20 July 1970. Cancellation of Rayleigh waves was accomplished by the use of a phase compensator which provided a matched response for the vertical strain and the vertical inertial systems over the frequency range of 0.07 to 0.8 Hz.

The principal objectives of the investigation were to obtain improved detection of long-period P waves and to determine the degree of suppression of seismic noise as related to changes in the character of the noise.

#### 6.4.2 Instrumentation

Design, procurement, and installation work was done in August 1970. System checks were completed on 3 September 1970. A block diagram of the IP system is shown in figure 19. The original SP strain system at HN-ME was converted to an IP system by making the following changes:

- a. The SP Model 4300 PTA's in both the strain and inertial circuits were replaced by an LP Model 5240 PTA with a 30-second Galvanometer, Model 2980-30.
- b. A Model 8979A control module was inserted between the seismometer and PTA.
- c. The data coil in the Model 20171 shallow-hole seismometer was changed to a -9 series coil with  $R_c = 4248$  ohms, CDR = 5150 ohms.
- d. The Model 15123 phase compensator was replaced by a new Filter, Model 3516, designed to provide 90-degree phase compensation between strain and inertial channels in the frequency range 0.07 to 0.8 Hz. Voltage divider networks were added to the inputs of the new phase compensator to protect the unit against voltages exceeding 10 V p-p.

Amplitude response curves for both the SP and IP systems are shown in figure 20. Calibration at frequencies higher than 0.5 Hz in the IP system was not attempted because of the low calibration signal-to-seismic noise ratio. The IP system has a greater predicted sensitivity than the SP system at frequencies lower than about 0.5 Hz and less sensitivity at higher frequencies.

Collection of operational data began on 4 September 1970. From visual inspection of Develocorder records, an average cancellation of approximately 18 dB was estimated for the predominant 5-second microseisms recorded on 4 September. Less cancellation was observed for other days in the first week of operation. A 6-minute sample of microseismic background recorded by the IP vertical inertial and vertical strain seismographs on 4 September were digitized and computer processed. The capability of the strain-inertial combination to cancel microseisms is reflected in the plots of power spectra, coherence, and phase (figures 21 and 22). Power and phase between the strain and inertial outputs become mismatched at frequencies below 0.1 Hz and above 0.5 Hz. The average deviation from a condition of matched phase between 0.1 and 0.5 Hz was approximately 7.7 degrees.

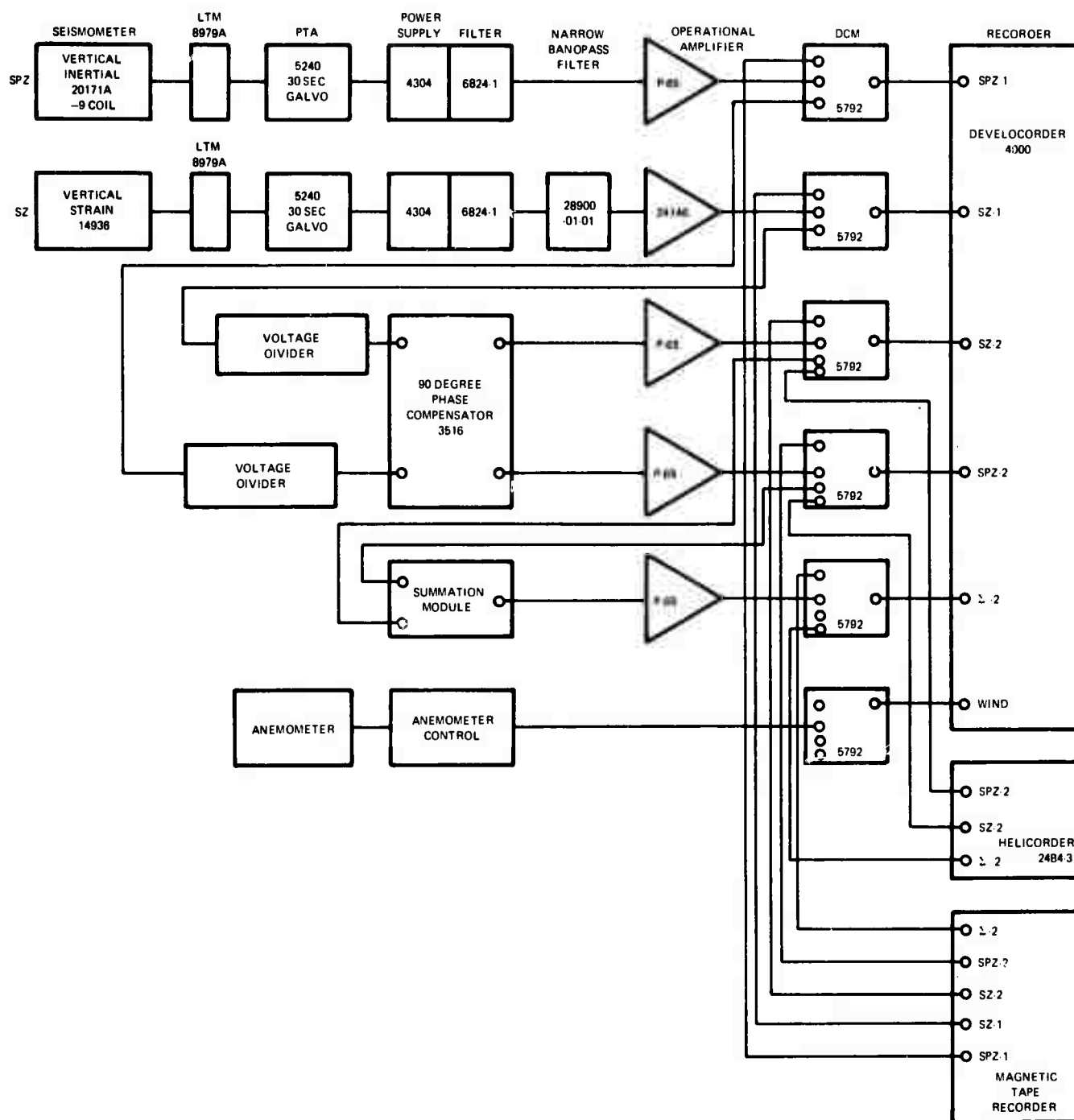


Figure 19. Block diagram of IP strain seismograph system at HNME

G 6057

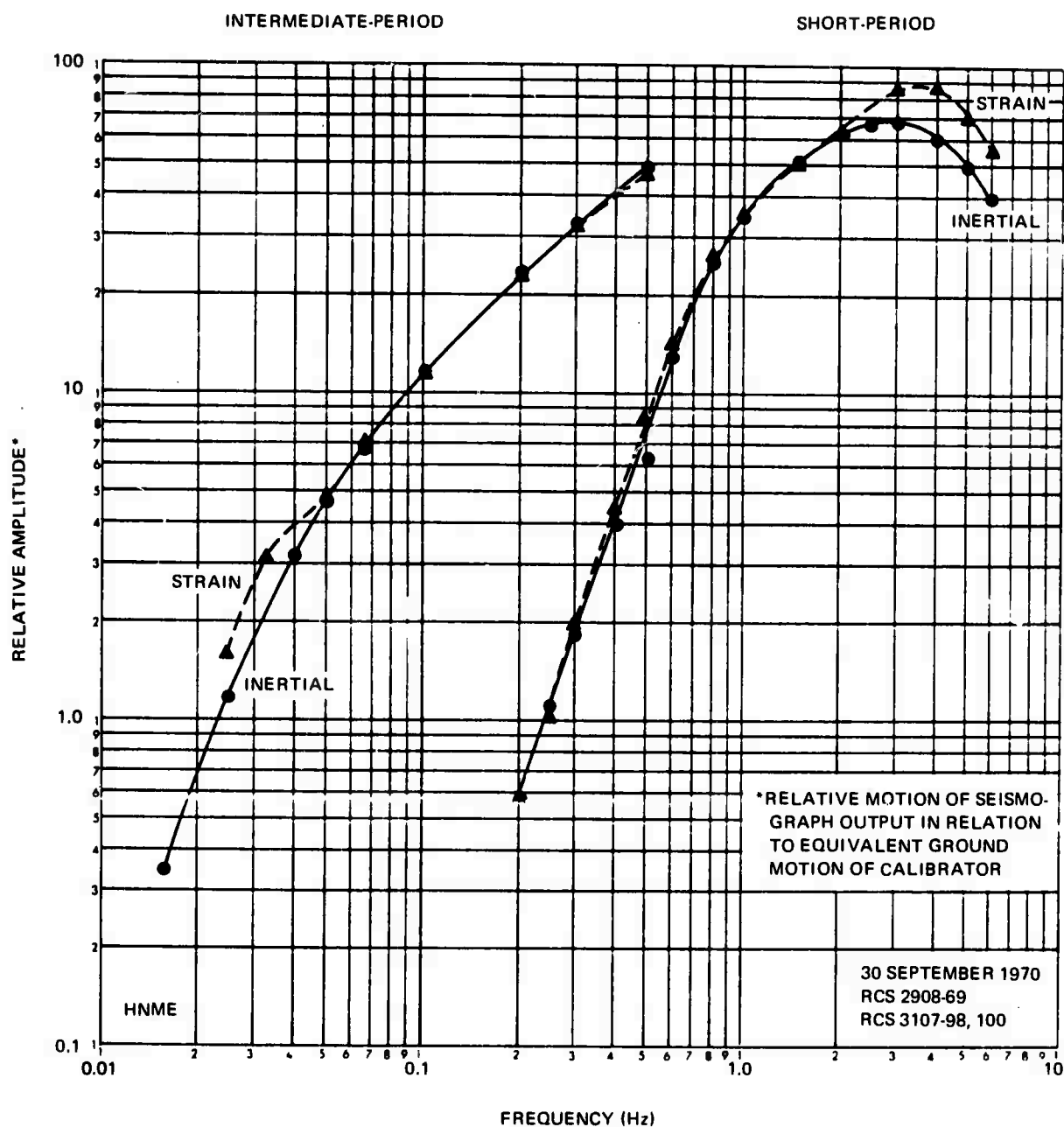


Figure 20. Amplitude response to ground displacement of the vertical strain and the vertical inertial short-period and intermediate-period seismographs at HN-ME showing close matching of the strain and inertial outputs in the designed range of the 90-degree phase compensators

G 6058

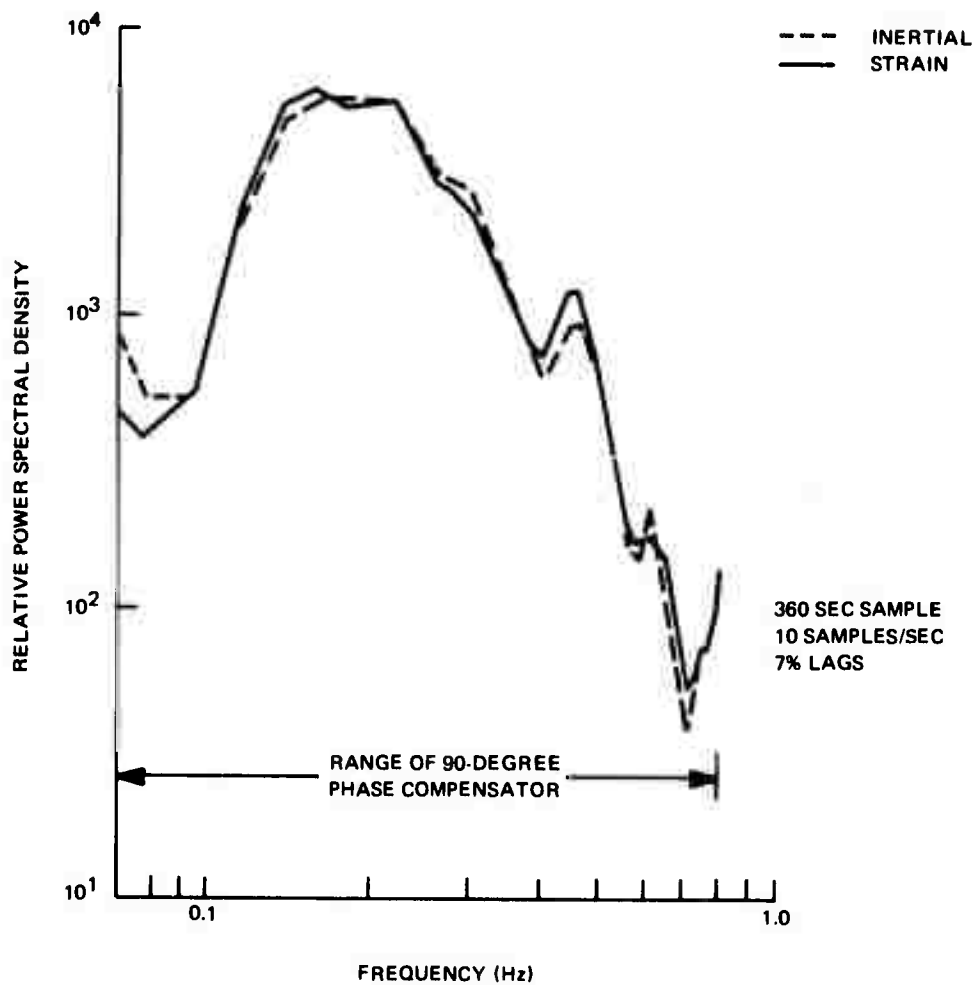


Figure 21. Relative power spectral density of microseisms recorded at Houlton, Maine, on 4 September 1970 by the intermediate-period vertical inertial and vertical strain seismographs

G 6059

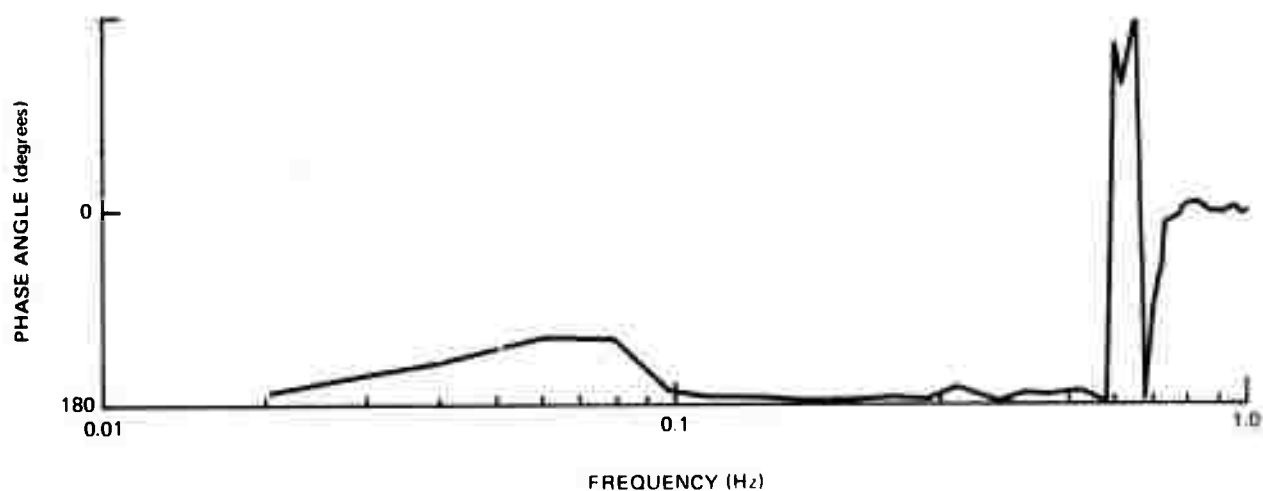
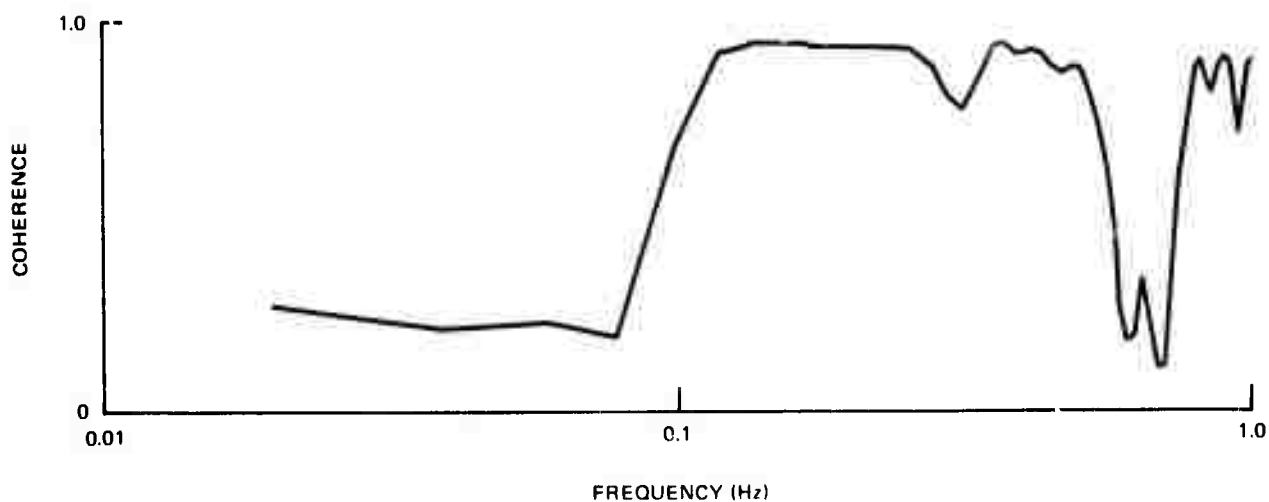


Figure 22. Coherence and phase lead of the IP vertical strain over the IP inertial seismograph recordings of a six-minute sample of microseismic noise recorded on 4 September 1970. Parzen smoothing, 10 samples/sec, 7 percent lags

G 6060

Effective cancellation was limited to a frequency range of approximately 0.1 to 0.6 Hz. It was limited at the high frequency end by system noise and at the lower end by galvanometer noise.

The phase match of the strain and inertial outputs for microseisms deteriorated rapidly at and below a frequency of about 0.1 Hz. The point of deterioration depended upon the amount of galvanometer noise at the time. The phase at low frequencies was matched within 3 degrees at 0.1 Hz, within 30 degrees at 0.067 Hz, and within 45 degrees down to a frequency of 0.025 Hz. The 90-degree phase compensator provided a matched response ( $\pm 2^\circ$ ) down to a frequency of 0.07 Hz.

By equalizing the galvanometer damping ratios in the strain and inertial channels on 11 November 1970, the phase response was substantially improved. The phase difference between the strain and inertial channels, as measured with a variable-phase function generator on 19 November, is shown in table 6. Matching within 8 degrees is obtained in the period range 1 to 20 seconds. Amplitude responses taken on the same date are shown in figure 23. Close matching of responses below 0.07 Hz and above 0.8 Hz is limited by the 90-degree phase compensator. Some mismatch in amplitude response occurs between 0.07 and 0.8 Hz.

Evaluation of the system was limited by low magnification of the background noise level. On 13 November, an additional operational amplifier was inserted in the summation channel to raise the level of the data an additional 12 dB above tape noise. On 19 November, the same increase in signal level was made available to the individual strain and inertial channels at the output of the 90-degree phase compensator. The mean level of the seismic background on the summation channel was raised to a level 20 dB above the mean level of the tape recorder noise. Measurements were taken from data recorded during a period of normal microseismic activity. A tape playback of seismic data recorded on 1 December 1970 (figure 24) shows microseisms recorded on the IPZ summation trace at a level approximately 20 dB above tape noise. The microseisms are cancelled 12 dB to 18 dB on the IPZ summation trace. Also shown is the initial arrival of a teleseism from the Adreanof Islands ( $\Delta=64^\circ$ ,  $M_b=5.6$ ) appearing on the IPZ summation trace at a higher signal-to-noise ratio than on the LPZ trace. The Rayleigh surface waves from the same event are shown in figure 25. It is noted that the waves at a period of 18 seconds are canceled nearly 36 dB. The longer periods, which are outside the most useful range of the 90-degree phase compensator, are not canceled, as well.

A rigorous series of amplitude and phase measurements was run on the IP strain and inertial channels and on individual system components on 17 and 18 January 1971. The phase response of the IPZ strain and the IPZ inertial seismographs in response to the calibrator equivalent of constant prograde elliptical earth displacement is shown as figure 26. The phase responses are well-matched in the frequency range 0.033 to 1.0 Hz.

Table 6. Smoothed phase lag of strain output relative to inertial output

<u>Frequency (Hz)</u>	<u>Phase lag (degrees)</u>
1.0	07
0.8	06
0.6	05
0.5	04
0.4	03
0.3	02
0.2	01
0.1	01
0.08	02
0.067	02
0.05	08
0.04	15
0.033	20
0.025	40
0.020	55
0.016	60
0.011	65

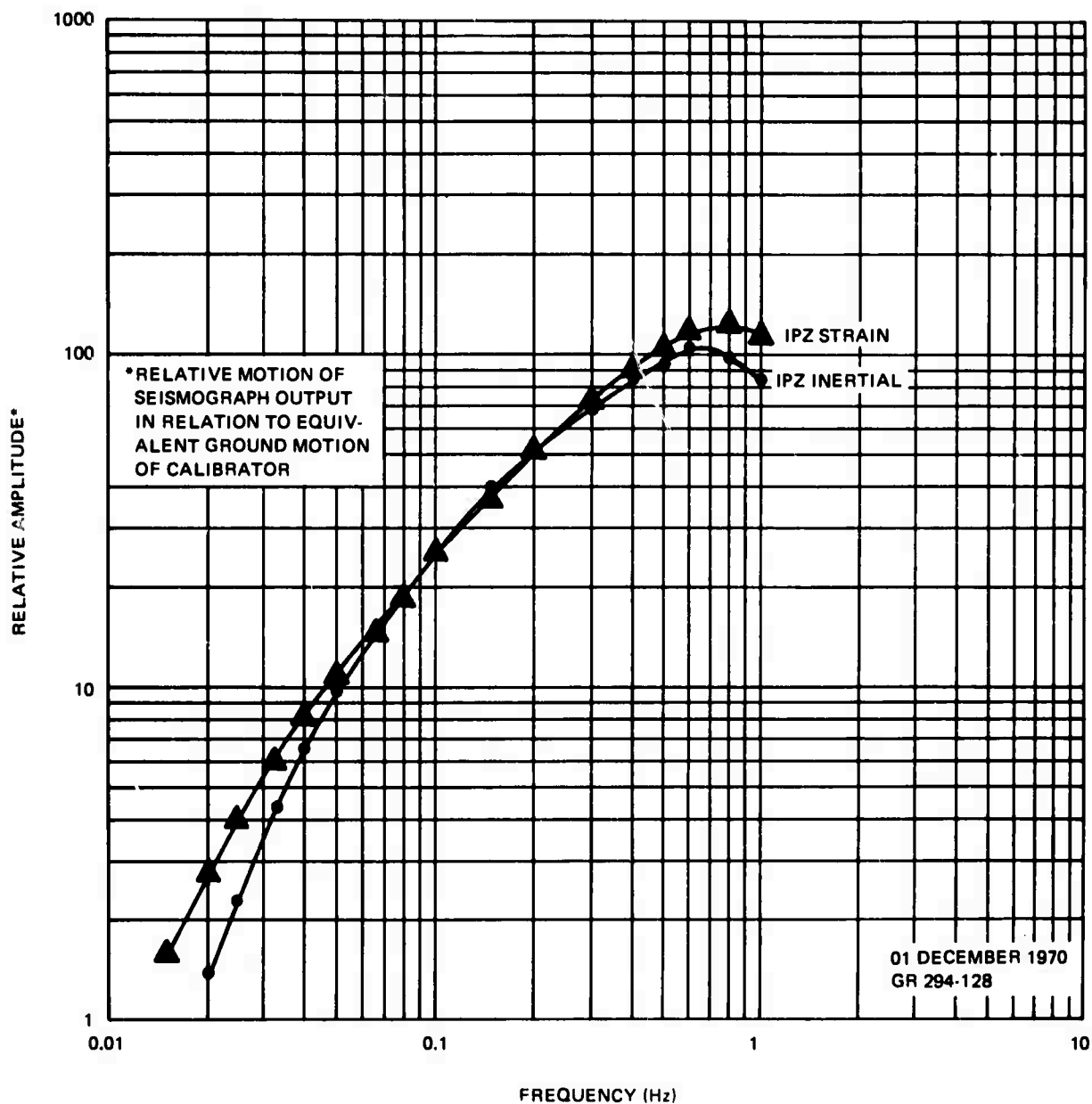


Figure 23. Amplitude response to ground displacement of the vertical strain and the vertical inertial intermediate period seismographs, at HN-ME, showing resulting amplitude-response match following improvement of the phase-response match effected on 11 November 1970

SPZ = SHORT-PERIOD VERTICAL  
 TPZ = INTERMEDIATE-PERIOD VERTICAL  
 LPZ = LONG-PERIOD VERTICAL

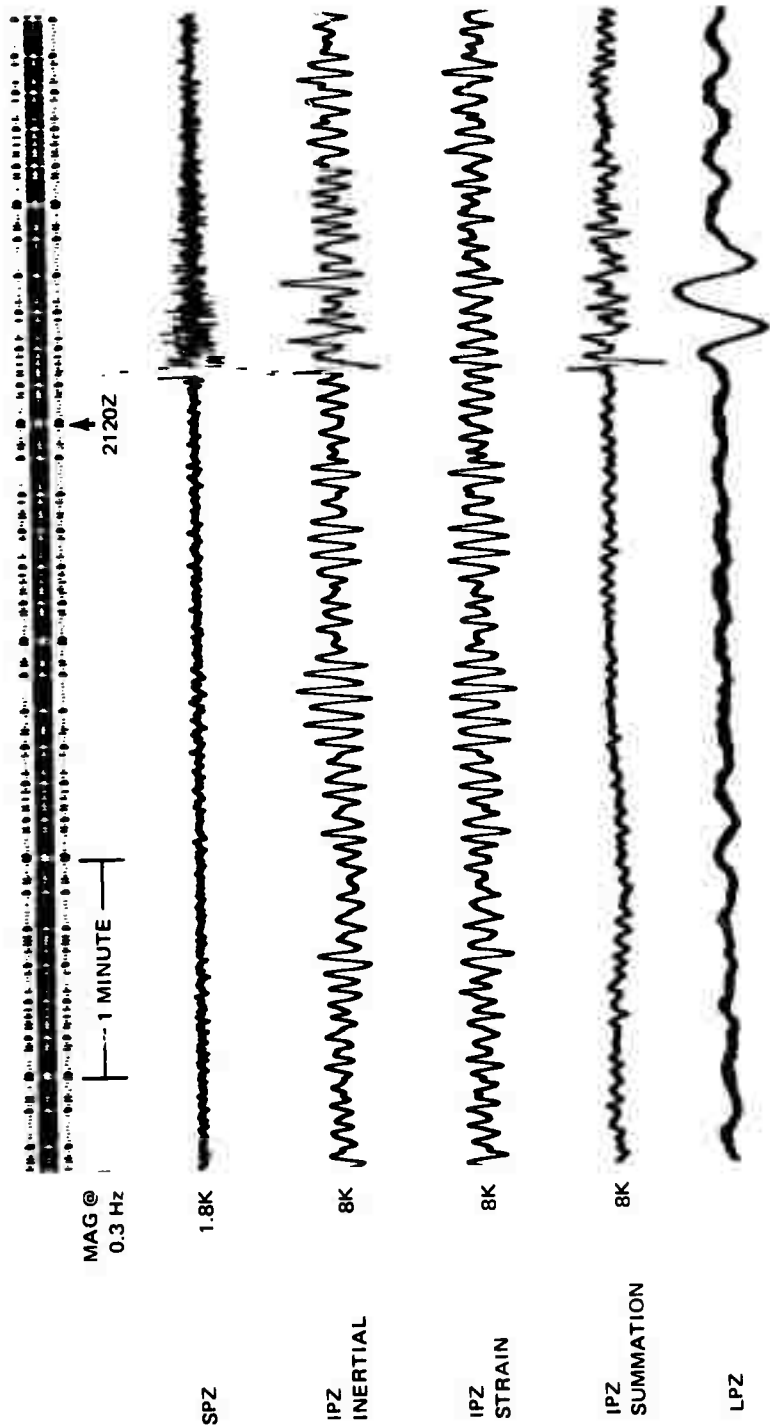


Figure 24. Tape playback of SP, IP, and LP seismic data recorded at Houlton, Maine on 01 December 1970. Microseisms on the IPZ sum trace are approximately 20 dB above tape noise. Microseisms are canceled 12 to 18 dB on the LPZ summation trace. The initial arrival from an earthquake in the Adrenof Island region ( $\Delta = 64^\circ$ ,  $m_b = 5.6$ ) is recorded on the LPZ summation trace at a higher signal to noise ratio than on the LPZ trace. O.T. = 21:09:37.22,  $51.4^\circ$  N,  $175.3^\circ$  W,  $\Delta = 6.4^\circ$ ,  $m_b = 5.6$ , depth = 36 km.

HNME  
 RUN 335  
 01 DEC 1970

G 6222

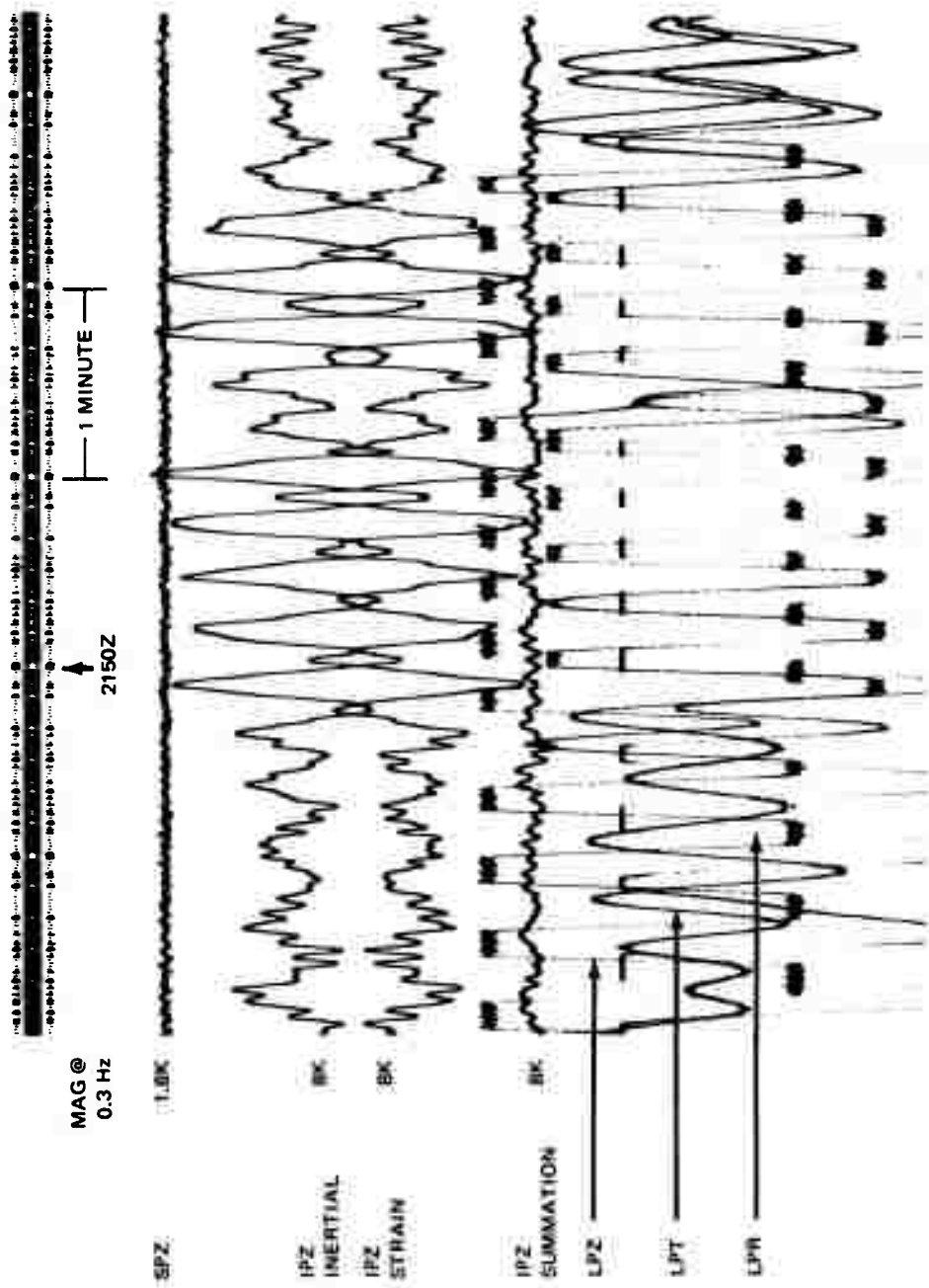


Figure 25. Tape playback of the Adreanof Island earthquake recorded at Houlton, Maine on 01 December 1970 showing approximately 36 dB cancellation of Rayleigh waves

HNME  
RUN 335  
01 DEC 1970

G 6223

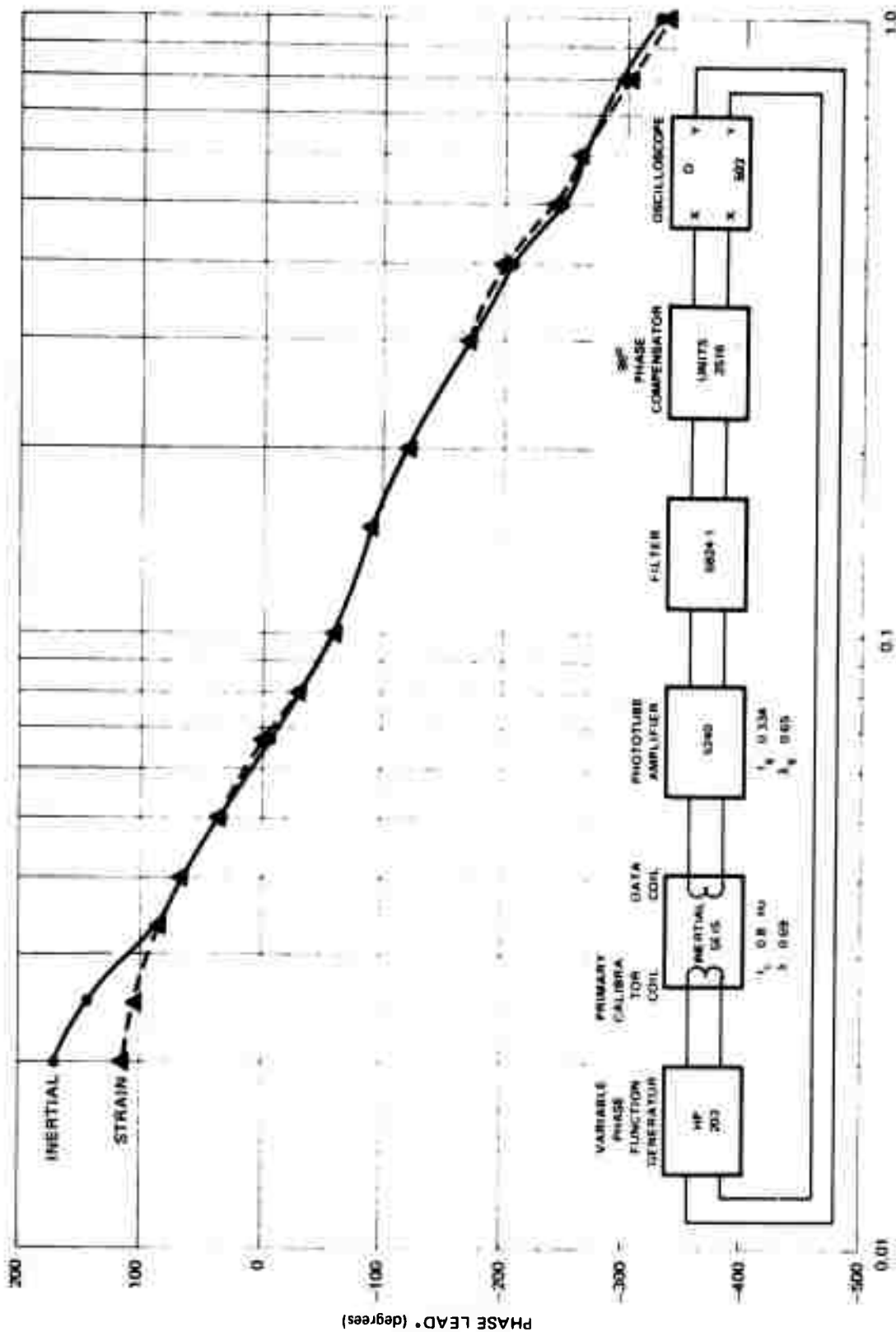


Figure 26. Phase response at the Intermediate-Period Vertical (IPZ) strain and IPZ inertial seismographs in response to the calibrator equivalent of constant prograde elliptical earth displacement

The degree of suppression of seismic noise with the IPZ inertial and IPZ strain seismographs at HN-ME and the limitations of the strain-inertial combination are reflected in figure 27, which shows plots of power spectral density of seismic noise for the strain, the inertial, and the summation channels, as well as system noise and tape noise for the summation channel. Coherence and phase difference between the strain and inertial channels are shown in figure 28. Corresponding time-domain playouts of the noise samples are shown in figure 29. The latter demonstrates a noise reduction of approximately 12 dB. At present, effective cancellation is limited to a frequency range of approximately 0.1 to 0.7 Hz. It is limited at the high frequency end by system noise and at the lower end by noise that often appears to be related to the amplitude of the storm microseisms, but at times has been over-ridden by noise attributed to the condition of the galvanometers and electrical grounding problems.

An investigation of 2 Hz noise, which is discernible on the strain output approximately 5 percent of the time and appears occasionally on the inertial trace, is caused by bow-stringing of the 30-second galvanometers. The 2 Hz noise is particularly noticeable during maintenance work in the vicinity of the galvanometers.

Another undesirable characteristic of the 30-second galvanometers is their tendency to drift off center with time, introducing a change in sensitivity of the phototube amplifier. This problem is particularly critical in systems involving a strain-inertial combination in which the system sensitivity of the individual outputs must be closely matched for proper suppression of microseisms. The problem can be avoided by substituting solid-state components for the galvanometer and phototube amplifier.

Site operations at HN-ME were discontinued at the end of the run on 4 February 1971. Instrumentation vaults, boreholes, and foundations were left intact for possible occupation by a portable system at a later date. A partial site restoration was accomplished and the site was vacated on 10 February 1971.

#### 6.4.3 Suppression of Microseisms

A study was undertaken to determine the degree of suppression of microseisms by the IP strain-inertial combination as a function of change in character of the microseisms. Most of the data samples were taken from recordings made after 1 November 1970, when the addition of another operational amplifier in each channel allowed the signal to be recorded on magnetic-tape at an increased signal-to-noise ratio. Samples from September and October have been included in order to include seasonal effects.

Power spectral density of IPZ inertial and IPZ strain outputs along with coherence and phase were computed for 18 background samples, each of 12-minute duration, in the period 4 September to 5 December 1970. The power spectral density of a typical sample of seismic background noise recorded by the inertial, strain, and strain-inertial sum is shown in figure 27. The predominant microseisms appearing in the frequency range 0.16 to 0.4 Hz (2.5 to 6 seconds) are

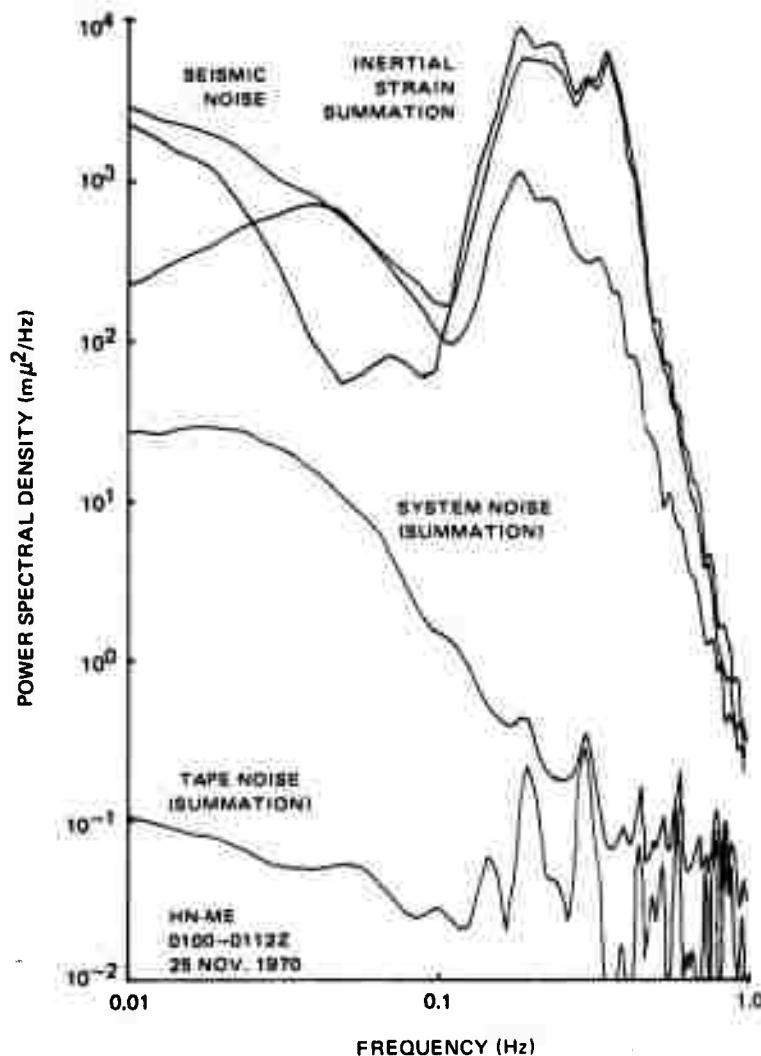


Figure 27. Power spectral density of a 12-minute sample of seismic noise recorded by the intermediate-period vertical inertial, vertical-strain, and summation seismographs at HN-ME at 0100Z on 25 Nov 1970. The power spectral density of system noise and tape recorder noise for the summation channel are included. Coherence and phase lead of the IP vertical strain over the IP inertial seismograph recordings are shown in figure 28. Parzen smoothing, 5 samples/sec, 7 percent lags

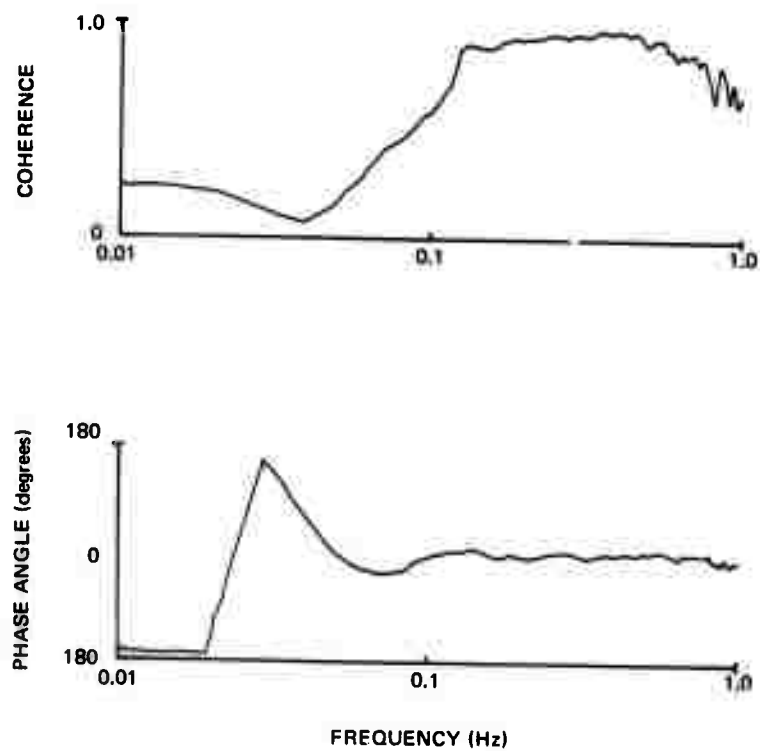


Figure 28. Coherence and phase difference between the strain and inertial channels

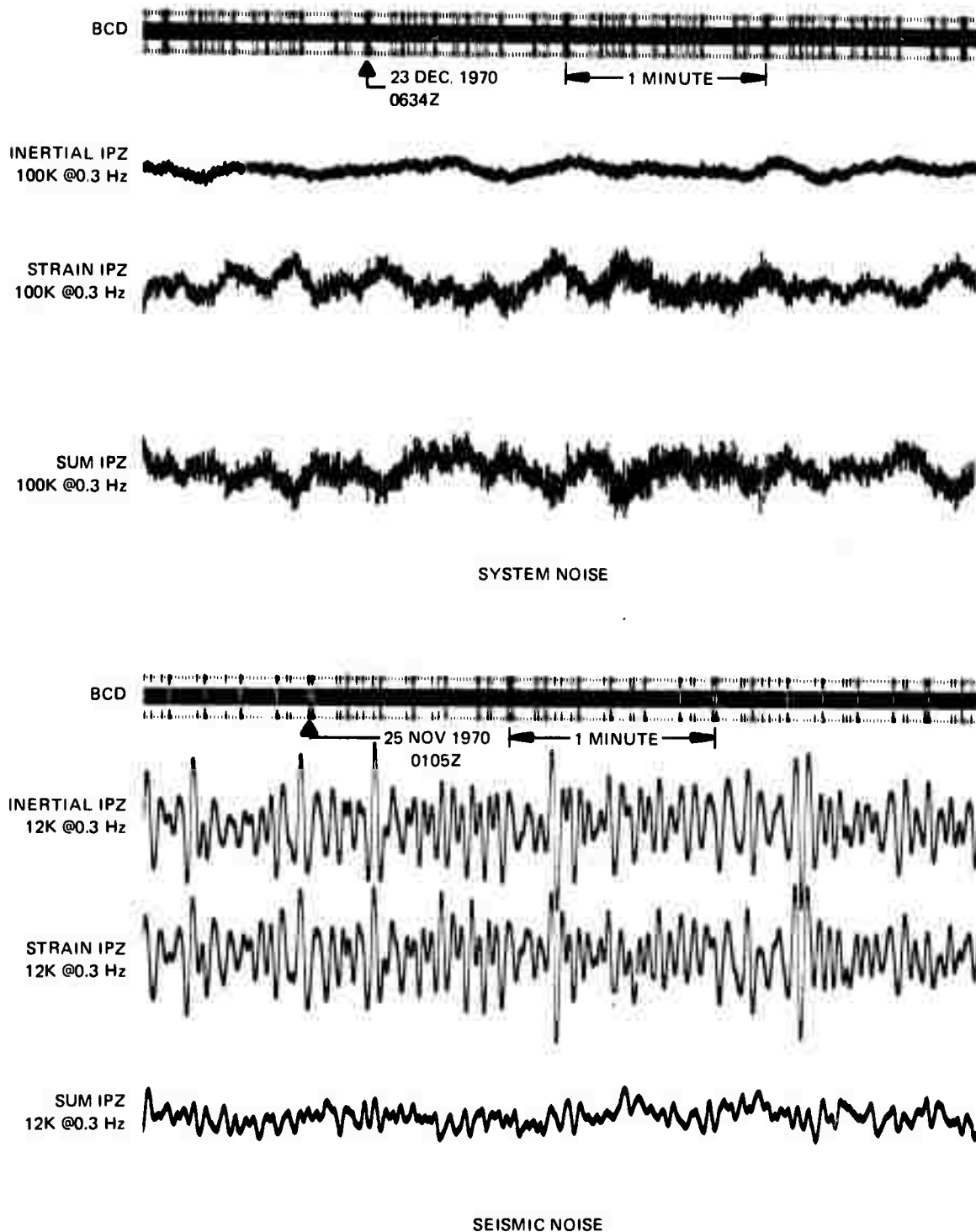


Figure 29. Playouts from magnetic tape of the system noise and seismic noise samples from which the power spectral density data of figure 27 were computed.

suppressed approximately 10 dB. The power, coherence, and phase of the data show a rapidly deteriorating match between strain and inertial recordings at frequencies below 0.1 Hz and above 0.7 Hz.

To compare extremes in noise level, four background samples were selected during the decay of a microseismic storm. The power spectral density, coherence, and phase of the IPZ inertial data showed the following tendencies: The power spectra were broader for the samples of higher power; maximum power occurred at the higher frequencies; and the lowest coherence occurred at frequencies below approximately 0.1 Hz. To determine the significance of the differences in power levels of the storm data, the power spectral density was computed for five 12-minute samples closely spaced in time. Curves computed from three adjacent samples, showed little variation between each other at coherence values exceeding approximately 0.5. Curves computed from samples with time separations of 30 and 60 minutes, respectively, show slightly larger deviations from the mean.

To determine the degree of suppression of microseisms as a function of change in their character, the power-spectral-density ratio of the IPZ inertial to the IPZ summation for the four storm samples were compared, as shown in figure 30. Line A in figure 30 is the "break even" point. Above line A, signals are enhanced; below line A, the summation output is noisier than the inertial alone. Two general tendencies are noted. First, the suppression of microseisms decreased as the storm subsided. Secondly, at frequencies below approximately 0.1 Hz, the summation data degrades the signal. Furthermore, the samples taken from the height of the storm have the lowest coherence below 0.1 Hz and cause the maximum degradation of the system below 0.1 Hz.

The data used in figure 30 were examined in detail by means of figures 31 and 32, which contain power, coherence, and phase data for the individual strain, inertial, and summation recordings for the maximum and minimum storm activity. From figure 31, it is seen that poor suppression of microseisms below a given frequency is caused by an increase in the power level of the strain output. Observed daily variations in the level of strain system noise at frequencies less than 0.1 Hz could account for part of the apparent high strain output.

Another series of seismic-noise samples, starting with the lull in the storm on 23 November 1970 and ending at the peak in the storm on 5 December 1970, were examined. The ratio of power spectral density of the inertial output to the strain output showed a distinct pattern of suppression of microseisms at a frequency near 1.5 Hz that appears not to be directly related to either the buildup of microseismic amplitude or the passage of time. However, it was observed that the noise samples that had the highest suppression in the frequency range 0.2 to 0.5 Hz had the lowest suppression of microseisms at frequencies below 0.2 Hz.

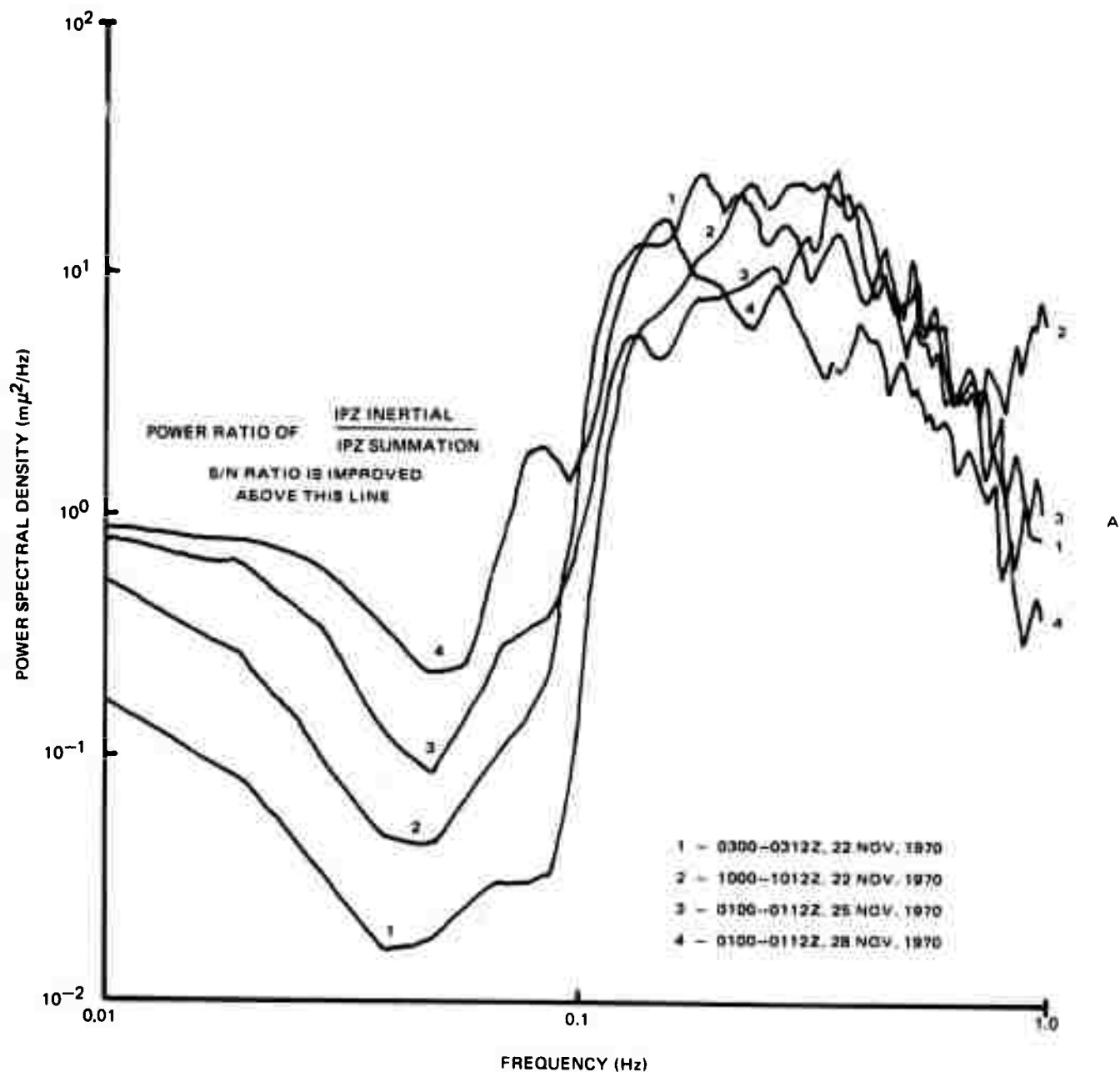


Figure 30. Ratio of power spectral density of microseismic noise for the IPZ inertial seismograph to that of the IPZ summation, showing the pattern of change in suppression of microseisms with increasing background level. Line A is the 'break even' point. Above line A, signals are enhanced. Below line A, the summation output is more noisy than the inertial alone

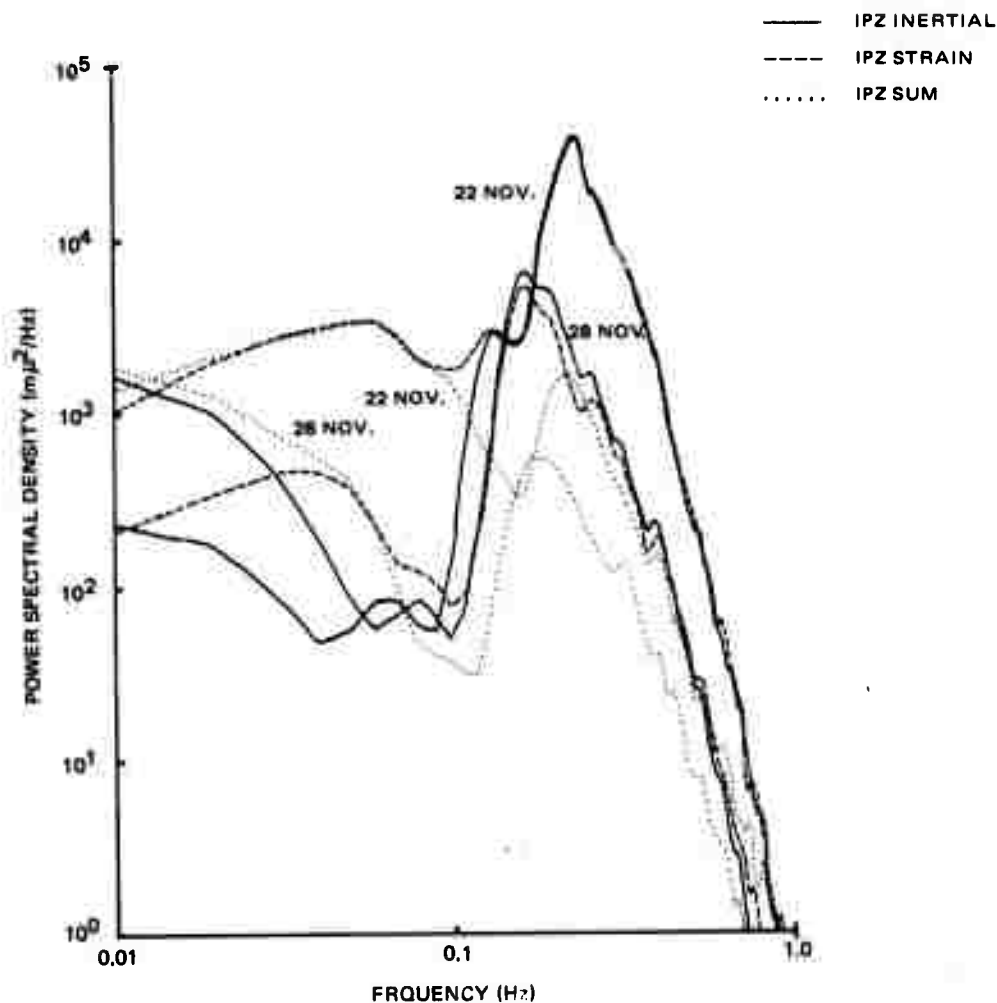


Figure 31. Power spectral density of inertial, strain, and summation recordings corresponding to curves 1 and 4 of figure 43, showing that poor suppression of seismic noise at frequencies below 0.1 Hz is prevented by an increase in the power level of microseisms recorded on the IPZ strain trace. Coherence and phase are shown in figure 32

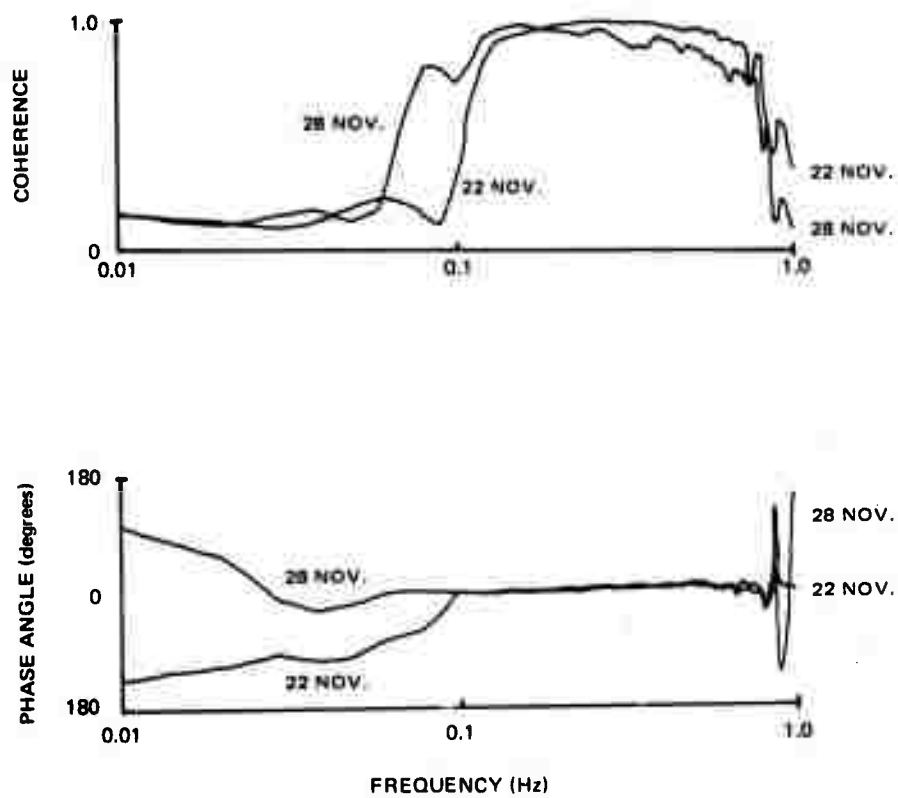


Figure 32. Coherence and phase difference between the strain and inertial channels

#### 6.4.4 Signal Enhancement

It has been shown that only for a limited number of earthquakes is the IP strain system superior to either the SP system or the LP system for the detection of the P phase. In a survey of the signal-to-noise ratio (S/N) for the P phase of 19 earthquakes, in 7 cases, the S/N on the IPZ strain summation (IPZ $\Sigma$ ) was superior to the S/N on LPZ. The improvement in S/N was less than 6 dB in 4 of the 7 cases.

A comparison of IPZ $\Sigma$  with SPZ showed 11 of 19 P waves recorded on IPZ $\Sigma$  with an improved S/N, the average improvement being about 6 dB. Recalling from Technical Report No. 69-20, Supplement to Final Report, Project VT/8704, Short-Period Multicomponent Strain System, dated 30 May 1969, that the SP strain system was shown to suppress seismic noise an average of 10 dB over the SPZ alone, it is possible to conclude by inference that the S/N ratio of IPZ $\Sigma$  for the initial P phase would be about 6 dB less than that of the SPZ $\Sigma$  for the 11 cases.

On the average, the IP strain system contributes very little to increasing the S/N ratio for the P phase. In the case shown in figure 33, the S/N ratios for the SPZ, IPZ $\Sigma$ , and LPZ for the initial P ( $\Delta=67^\circ$ ,  $M_b=6.0$ ) are approximately 9/1, 6/1, and 2/1, respectively. Only when the P wave exceeds a period of 1.0 to 1.5 seconds does the IP strain system become competitive with the SPZ, as shown in figure 34 ( $\Delta=127^\circ$ ,  $M_b=5.4$ ). In this case, the S/N ratios for the SPZ, IPZ $\Sigma$ , and LPZ are 1/1, 4.5/1, and 7/1, respectively. The first motion is evident on IPZ $\Sigma$ , whereas, it is indefinite on LPZ.

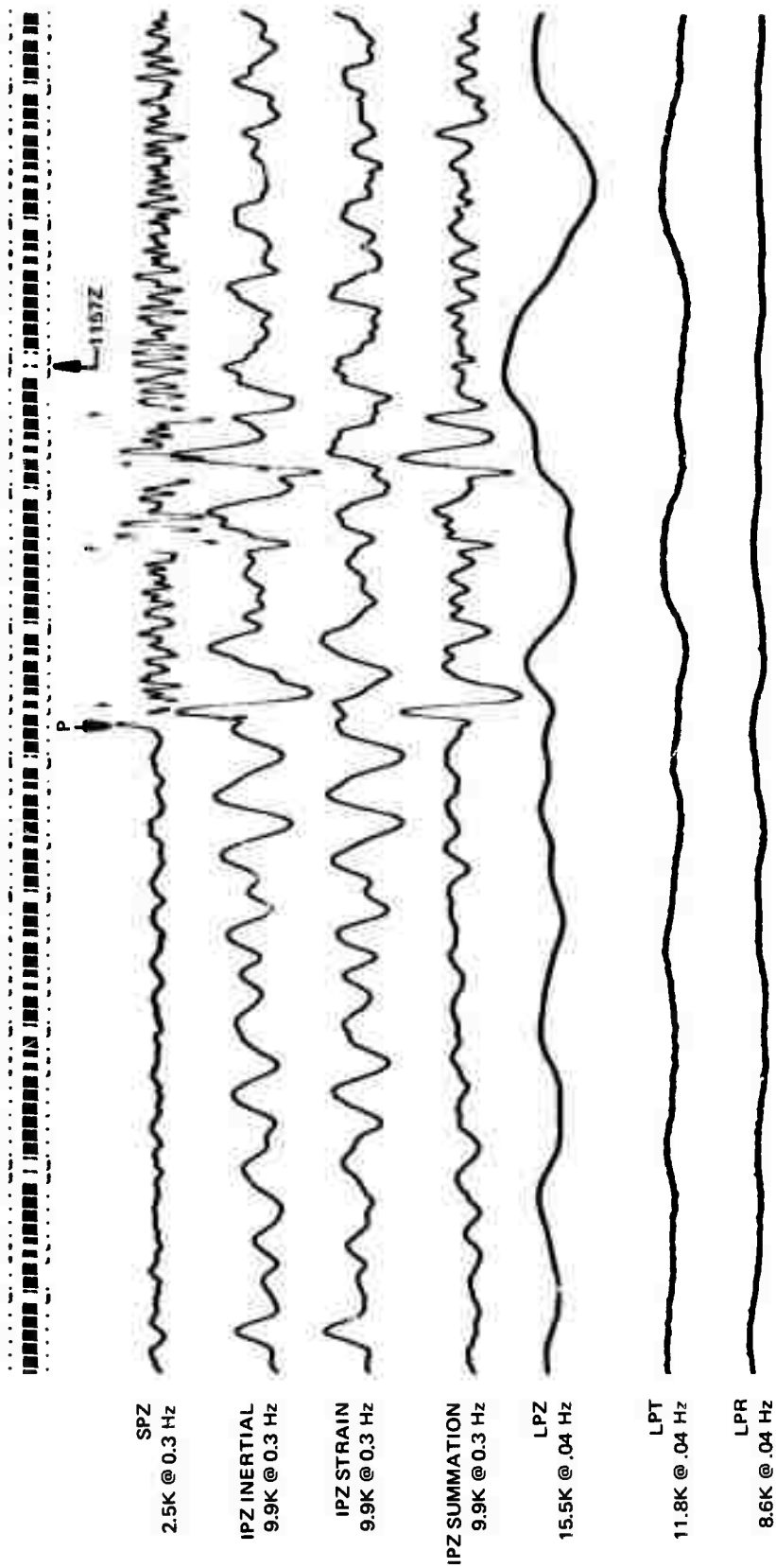
One advantage of the IP strain system is that the recordings have a more varied character than either the SP or LP. Thus, it lends itself well to the discrimination among closely spaced body phases. In figure 35, which shows the initial P for an earthquake from the Ascension Island region ( $\Delta=75^\circ$ ,  $M_b=5.3$ ), the varied character of the P wave on the IPZ $\Sigma$  trace is quite marked. Note also the particularly effective suppression of the burst of background noise occurring about 10 seconds before P.

Improved resolution of closely spaced body phases by the IPZ recording is shown in figures 36 and 37 for events from the Ascension Island region ( $\Delta=75^\circ$ ,  $M_b=5.3$ ) and the Sea of Okhotsk ( $\Delta=76.5^\circ$ ,  $M=5.7$ ), respectively. Unidentified arrivals recorded a few seconds before P and pP are sharply discriminated by the IPZ $\Sigma$  trace.

#### 6.4.5 Conclusions and Recommendations

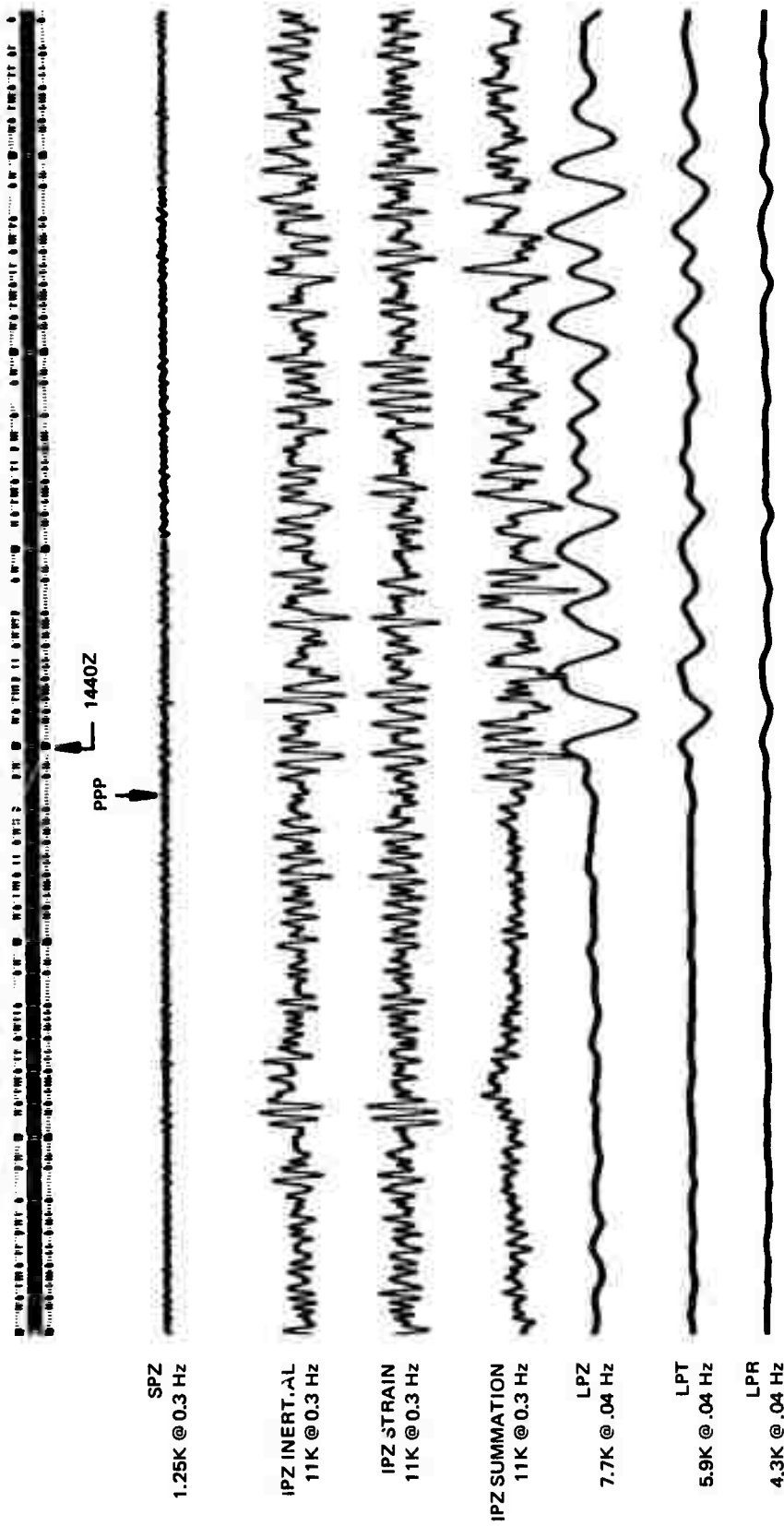
Although a limited effort for evaluation precludes a sufficiently complete evaluation of several aspects of the IP strain system and the recorded data, only a limited investigation of the data is necessary in order to conclude the following:

- a. The system is susceptible to noise in the period range 10 to 100 seconds.



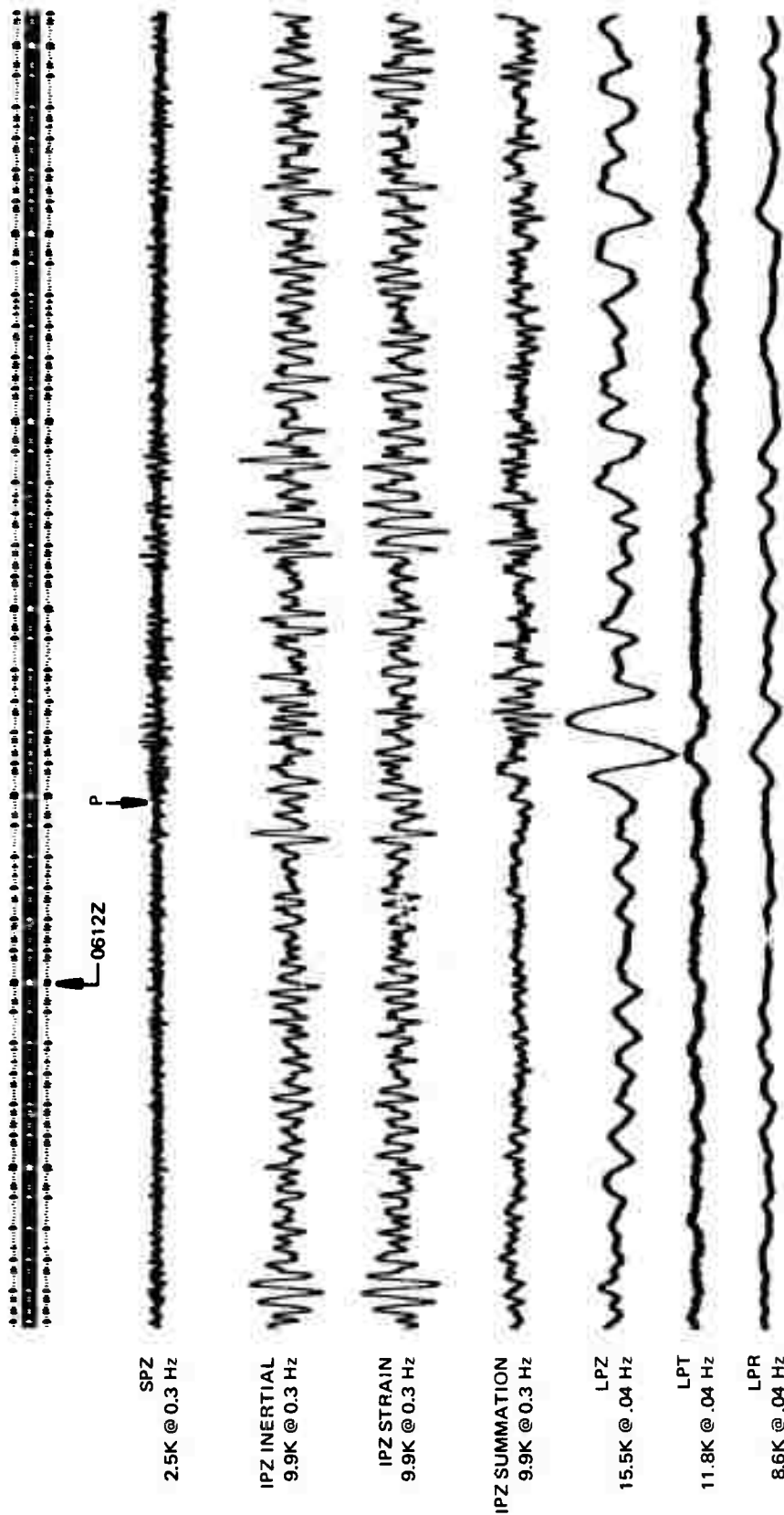
HN-ME  
28 NOV 1970

Figure 33. P arrival from an earthquake in Northern Chile showing how, on the average, the IP strain system contributes little to increasing the signal-to-noise ratio when compared with recordings from the SPZ and LP components. Origin 11:08:42.5Z, 20.9S, 69.8W, Mb = 6.0, h = 33 km.



HN-ME  
13 NOV 1970

Figure 34. Magnetic tape recording of SPZ, IP strain system, and LP components showing a factor-of-four improvement in signal-to-noise ratio for the P wave on the IPZ summation recording compared with the SPZ. Origin 14:16:18.0Z, 13 Nov 70, Leyte, 11.9N, 124.0E,  $\Delta = 127^\circ$ ,  $M_b = 5.4$ ,  $h = 15$  km



HN-ME  
29 NOV 1970

Figure 35. P-wave from an earthquake in the Ascension Island region ( $\Delta = 75^\circ$ ) showing the varied character of the P-wave on the IPZ summation trace. Origin 16:01:18.7Z, 11.7S, 14.1W, Mb = 5.3, h = 33 km

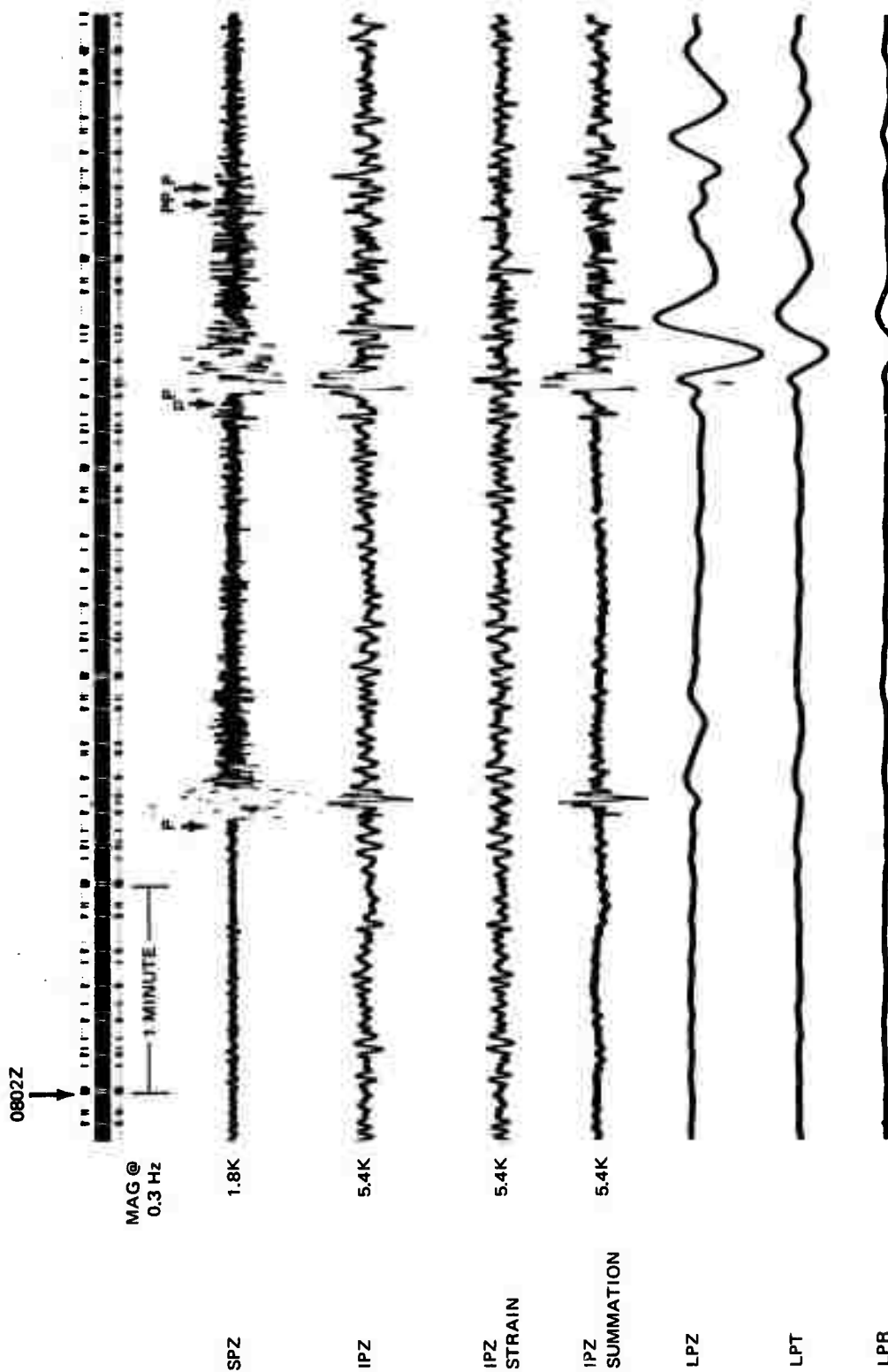
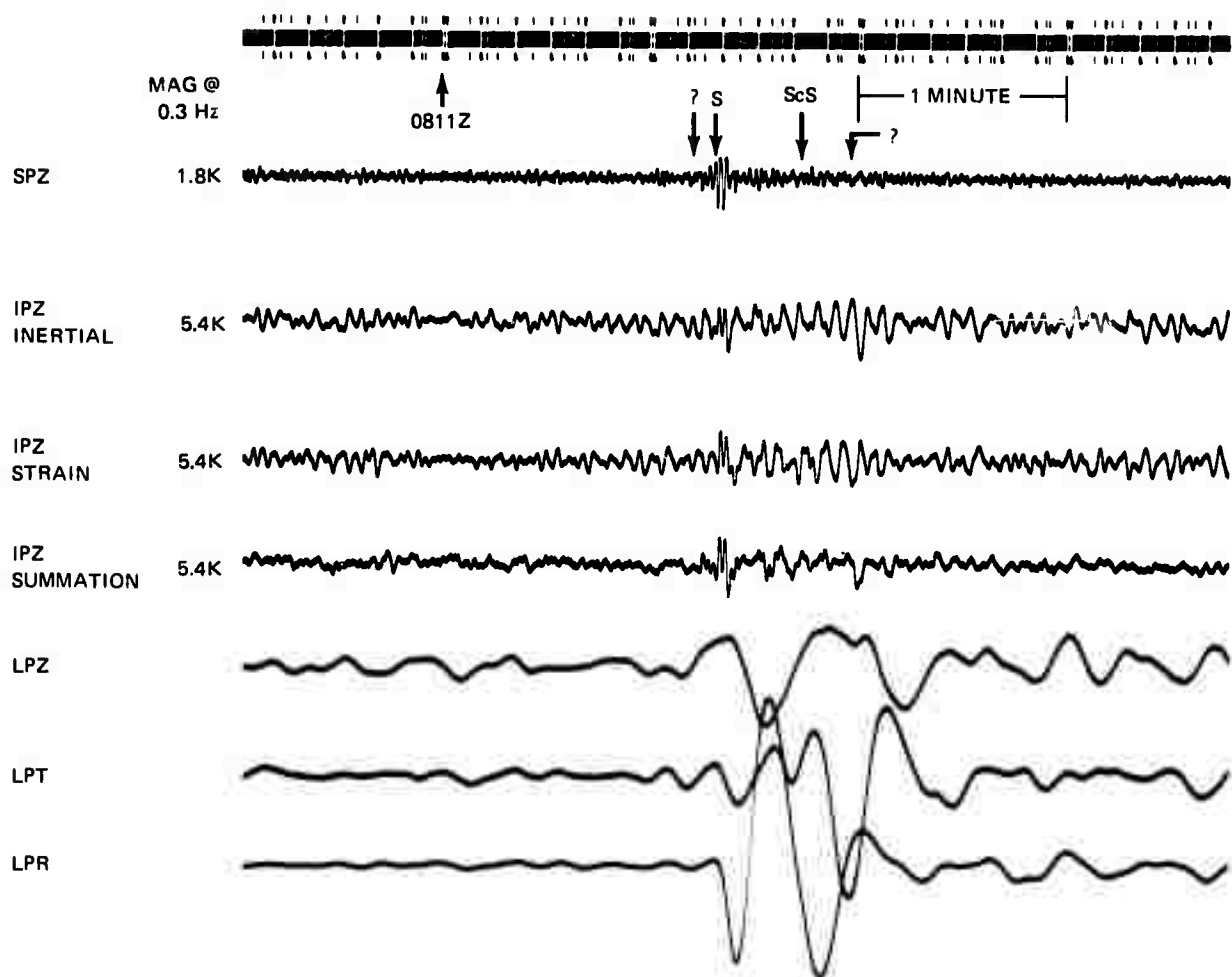


Figure 36. Tape playback of an earthquake recorded at Houlton, Maine on 05 September 1970 showing improved resolution of closely spaced body phases on the IPZ summation trace compared with the SPZ and LPZ traces. Origin 07 52 27.4Z, 52N 15.4E, Sea of Okhotsk,  $\Delta = 76.5^\circ$ ,  $M = 5.7$ ,  $h = 580$  km

G 6225

HNME  
RUN 248  
05 SEPT 1970



HNME  
RUN 248  
05 SEPT 1970

Figure 37. Earthquake from the Sea of Okhotsk showing change in character of the IPZ summation trace and potential discrimination of S phases arriving at closely spaced intervals

G 6226

b. The IP strain system only infrequently contributes to the enhancement of either the short-period or the long-period P wave when both the SPZ and LPZ recordings are available. Furthermore, the IP strain system is inferior to the SP strain system for enhancing short-period P waves. Only when the P wave exceeds a period of 1.0 to 1.5 seconds does the IP strain system become competitive with the SP strain system.

c. The IP strain system recordings have a more varied character than either the SP or LP; therefore, it has a potential advantage in the discrimination of closely spaced body phases.

d. The response of the vertical strain seismometer to shear waves, together with the increased response to periods exceeding 1.0 to 1.5 seconds, provides better detection of short-period S phases on the IPZ recording than on the SPZ.

e. The detailed signal character provided by the IP system increases the potential of the IP system for enhancing depth phases. Additional study of the data is required to support this thesis.

f. The IP strain responds well to Lg; however, the LP seismographs respond with a larger S/N ratio.

g. The IP system suppresses Rayleigh waves effectively, but nevertheless has a poorer S/N ratio than the SPZ for body phases that coincide with the time of arrival of the surface waves. The same is true of coincident phases from two or more earthquakes.

In relation to the instrumentation in the IP strain system, it is concluded that noise in the period range beyond 10 seconds, the source of which has not been determined, reduces the effectiveness of the IP system for enhancing long-period P waves. Some of the data suggests that the noise on the IPZ strain output increases in proportion to the microseismic storm activity. A change in velocity at a given frequency or a change in wave mode could introduce a mismatch in the amplitudes of the IPZ strain and the IPZ inertial outputs.

If the long-period noise problem could be resolved, it would be worthwhile to consider extending the response of the IP strain system to a higher frequency. The response of the inertial component could be extended one octave by using a seismometer with a natural frequency of 1.6 Hz instead of 0.8 Hz. The response of the strain component could be extended one octave by using a narrow-band filter that peaks at 1.6 Hz instead of 0.8 Hz. The response to short-period P waves would be increased while preserving the relative response of intermediate and long-period P waves.

In relation to the ground motion, the energy in the intermediate-period band does not, on an average, exceed the energy in the long-period band an amount sufficient to make use of the ability of the IP strain system to suppress intermediate-period microseisms. This factor, coupled with the noise problem at periods exceeding 10 seconds, limits the usefulness of the IP strain system.

The effort expended on the evaluation of the IP strain system was not sufficient to yield a rigorous, quantitative evaluation. Especially lacking is power spectral density data sufficient to isolate the source of the noise occurring mainly on the strain recordings in the period range 10 to 100 seconds. Also lacking is a sufficiently thorough evaluation of the potential of the IP strain system for enhancing closely spaced phases that merge together on the LP channels. The possibility of enhancing depth phases is also given only a cursory examination. Therefore, it is recommended that the aforementioned potentially useful characteristics of the IP strain system be further evaluated.

## 6.5 DPEP-HOLE, LONG-PERIOD PROJECT

### 6.5.1 Introduction

The purpose of this project was to make an initial investigation of a deep-hole, long-period installation. Planning for the project was based upon the reasonable extension of available deep-hole, short-period facilities and instrumentation. Major objectives of the investigation were to determine instrument capability, record and process signal and noise measurements, and analyze factors involved in installing and operating a long-period transducer in a deep hole.

### 6.5.2 Instrumentation

Sensing systems were realized by combining deep-hole, short-period transducers with long-period amplifiers and special-purpose filters. System responses were matched to the Advanced Long-Period High-Gain or Notched response (ALPN). Use of the short-period transducers ensured compatibility with the deep-hole facility and support equipment, and minimized ponderable instrumentation aspects. The major problems of cable noises, down-hole cable-connector seals, holelocking, suspension stability, and limiting resolution had been dealt with earlier in short-period projects but required further attention for the long-period application.

Three deep-hole, short-period transducers were available: (1) the Model 11167 deep-hole vertical transducer; (2) an experimental Deep-hole Triaxial Transducer, Model 22700; and (3) the Model 23900 deep-hole vertical transducer. Two amplifier types were available for use with these transducers. One was the Model 5240 long-period phototube amplifier (PTA) with a Model 2980 30-second galvanometer and special filter assemblies. The other was a special purpose amplifier and filter assembly utilizing the Model 33330 low-noise preamplifier, a solid-state instrument having a noise figure comparable to that of the PTA.

The system used for final field measurements was comprised of the 23900 transducer modified to have a natural period of about 4 seconds and a down-hole amplifier packaged in a case extension to the 23900. Two matched systems were used for comparative depth measurements.

The construction and testing of preliminary and final systems are discussed further in section 6.5.6 of this report.

### 6.5.3 Field Measurements

Field measurements were conducted at the PI2WY site and recordings (Develocorder and magnetic tape) were made for the deep-hole systems, the advanced long-period three-component vault systems, a long-period microbarograph system, and an anemometer system. Measurements were taken at depths of 130-, 1000-, and 8000-feet while one deep-hole instrument was operated at a depth of 130-feet in a shallow-hole adjacent to the deep-hole and vault instruments.

Comparative depth measurements did not yield enough information to determine the behavior of surface-induced noise with depth. It was found that disturbances due to atmospheric pressure and wind variations were readily detected in the vault systems but were difficult to detect on the deep-hole system at the 130-foot depth. Both the vault and deep-hole systems were operated at typical magnifications of 50K at 25 seconds with the ALPN response. Consequently, disturbances due to the larger pressure and wind variations occurring at PI2WY were near the deep-hole system threshold at a depth of only 130 feet, and measurements at greater depths could not show corresponding attenuations.

Later in the project, pressure seals on the vault installation were improved and disturbances to the vault systems were reduced. Recording and analysis of field data are discussed further in section 6.5.7 of this report.

### 6.5.4 Installation and Operation

Several features of the instrumentation used in this project were evaluated in the course of installation and operation, and are discussed in section 6.5.8 of this report. It is anticipated that a high-resolution, three-component, long-period instrument will be developed for deep-hole installation and such a development must take into account the aspects discussed.

### 6.5.5 Potential Magnification

In the concluding section 6.5.9, background and system noise spectra from low-noise mine installations are used to estimate the limiting threshold of a system that would not interfere with the potential magnification of the deep-hole, long-period installation.

### 6.5.6 Construction and Testing

Three deep-hole, short-period instrument types were available: (1) the Model 11167 deep-hole vertical seismometer; (2) an experimental triaxial seismometer, Model 22700; and (3) the Model 23900 deep-hole vertical seismometer. Seismometer selection from these instruments were based on the following relations.

#### 6.5.6.1 Seismometer Selection

The seismometer is comprised of a motion sensing suspension and a transducer that converts the relative mass-frame motion of the suspension into an electrical signal. Therefore, the transfer sensitivity (S) of the seismometer consists of two factors: (1) the relative mass-frame motion per unit input or earth motion, i.e., the suspension sensitivity ( $S_1$ ) and (2) the electrical output per unit of relative mass-frame motion, i.e., transducer sensitivity ( $S_2$ ).

Mathematically,

$$(e = \text{electrical output}) = S \cdot (a = \text{input acceleration}); S = S_1 S_2$$

and

$$(x = \text{mass-frame displacement}) = S_1 \cdot a$$

$$S_1 = (T_n = \text{natural period of suspension})^2 \cdot (\psi = \text{frequency dependent term})$$

That is, the relative mass-frame displacement per unit input acceleration is proportional to square of the natural period of the suspension.

The available seismometers each employed the coil-magnet or velocity sensing transducer wherein the electrical output is in proportion to the mass-frame velocity or for sinusoidal motion, the product of mass-frame displacement and frequency. A figure of merit (fv) for comparison of velocity transducers can be formed by the ratio

$$fv = \frac{G}{\sqrt{Rc}} \cdot \left( \frac{1}{T} \right)$$

where G is the generator constant in volts per meter/second

Rc is the coil resistance in ohms, and

T is period of input acceleration in seconds.

A composite figure of merit ( $F_s$ ) for the seismometer can be formed by

$$f_s = (T_n)^2 \left( \frac{G}{\sqrt{Rc}} \right) \left( \frac{1}{T} \right)$$

wherein the magnitude of the electrical output per unit input acceleration is proportional to  $f_s$ . For a conventional long-period seismometer such as the Model 7505A, the value of  $f_s$  at a signal period of 25 seconds is about 100. Table 7 shows comparative values for the deep-hole short-period seismometers.

Table 7. Comparative values of  $f_s$  for various seismometers

<u>Model</u>	<u>Mass kg</u>	<u>Natural period</u>	<u><math>\frac{G}{\sqrt{Rc}}</math></u>	<u><math>f_s</math> @ 25 sec</u>
7505A	10	20.0	6.24	100.0
11167	100	1.0	45.0	1.8
22700	5	1.25	10.0	0.63
23900	5	1.25	8.0	0.50
Modified 23900	5	(5.0)	8.0	(8.0)
Modified 23900				(400.0)
Displacement	5	(5.0)	8.0	Displacement

Therefore, relative to the long-period seismometer, the electrical output of the deep-hole, short-period seismometer would be smaller by a factor ranging from about 50 to 200. In present high-frequency, long-period systems the seismometer output is coupled with little or no attenuation to a low-noise, long-period amplifier. Consequently, it was necessary to consider modifications to increase seismometer sensitivity.

Initial testing was started using the Model 11167 without modification while modifications to the Model 23900 were undertaken to gain sensitivity by (1) mechanically extending the natural period, and (2) incorporating a displacement transducer. The overall benefit to be gained from the second modification was dependent upon factors other than resolution, and as the project developed the displacement transducer was only partially completed. Although resolution was to be superior to that of conventional long-period systems, the second modification required the greater effort and did not provide for horizontal measurements.

The Model 22700 would have provided for triaxial measurements. However, the complexity of linkages and flexures in the experimental suspension indicated stability problems that could be prohibitive in long-period measurements. The triaxial instrument would have greater sensitivity than the vertical instrument for tilt measurements versus depth, but the low sensitivity ( $f_x$  value of 0.63) of the 22700 would have required modification for period extension or a displacement transducer which would have compounded the suspension problem. Consequently, the effort anticipated for the 22700 was considered excessive for the initial investigation.

Figure 38 shows comparative calculated noise spectra for the systems considered in terms of equivalent mean square earth displacement per Hz. For equal natural periods, noise spectra for the 22700 system would be approximately the same as that of the 23900 system.

#### 6.5.6.2 Seismometer-Amplifier Configuration

The seismometer-amplifier configuration of the deep-hole, long-period system differed from the conventional in two respects - physical and electrical. The change in physical configuration was brought about by the deep-hole cable, while the change in electrical configuration was brought about by the great range of signal amplitudes produced by the short-period seismometer.

6.5.6.2.1 Downhole Amplifier Package. The decision to package the amplifier with the seismometer was not automatic since this would preclude use of the PTA, and could possibly set up convection currents in the area of the suspension. Observations were made with the 11167 and solid-state amplifier, and with the modified 23900 and the PTA. Cable lengths of 350-, 5,000-, and 10,000-feet were used in the 11167 system and a cable length of 500 feet was used in the 23900-PTA system.

With the shorter cable lengths, 350- and 500-feet, the cable was routed directly from the seismometer at a shallow-depth (less than 200 feet) to the amplifier located in a shelter. Each strand of the deep-hole cable conductors were scraped to achieve copper-to-copper, low-thermal contacts to the amplifier input. Under this condition, cable-noises were not significant at magnifications of less than 50K at 25 seconds with the ALPN response but the arrangement was susceptible to cultural disturbances.

With the greater cable lengths, the winch was required. Signal connections at the drum assembly and at the amplifier input were modified for copper-to-copper low-thermal contacts. Cable leakage presented severe problems and will be discussed further in section 6.5.8 of this report. Measurements with the 11167 system using 5,000-foot and 10,000-foot cable lengths encountered severe noise problems. While there were several noise mechanisms possible, the worst disturbances occurred when leakage resistances of the downhole signal circuits were on the order of  $10^8$  ohms or less.

Considering the magnitudes involved, a potential difference of 1 millivolt acting through an impedance of  $10^8$  ohms will produce a current of 10 pico-amperes. If the current-path encounters the input signal circuit, the potential developed across the signal pairs (about 1.6 nanovolt for the 11167 system) would be greater than the limiting system noise in an octave about 0.02 Hz (50 seconds). It was also found that noise generated at the winch connections increased system noise slightly.

These noise problems had been encountered at a magnification of only about 15K at 25 seconds with the ALPN. Therefore, it was considered imperative that the long-period amplifier be packaged with the seismometer for deep-hole measurements.

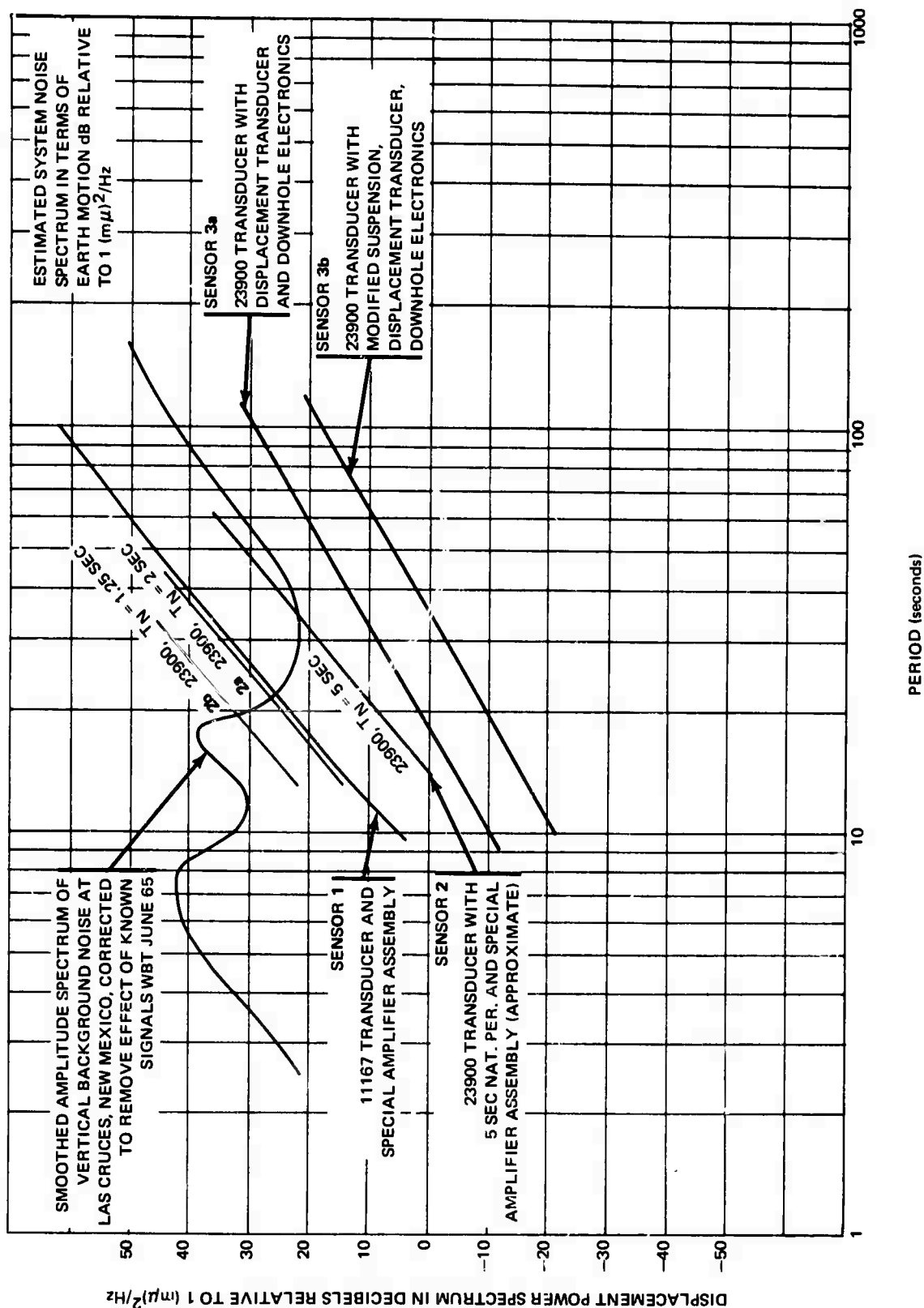


Figure 38. Smoothed amplitude spectrum of vertical background at Las Cruces, New Mexico and estimated system threshold in terms of equivalent displacement spectrum for the modified deep-hole, long-period sensors

6.5.6.2.2 Electrical Configuration. In the conventional long-period PTA system, sensitivity to 6-second microseisms and short-period signals has been restricted by the long-period seismometer and the long-period galvanometer. Although these signals have interfered with long-period measurements, their magnitudes were normally within linear operating ranges through the system. With the extended frequency response of the short-period seismometer and the absence of the galvanometer filtering, the sensitivity at short periods relative to that at long periods has increased by orders of magnitude in the downhole (or solid-state) amplifier system. To reduce short-period sensitivity, feedback was coupled round the input amplifier through a high pass network to provide an effective forward low pass response at the amplifier input. The characteristics of the feedback loop were such that the forward transfer sensitivity was similar to that of a seismometer with a natural period of 80 seconds. This configuration was satisfactory with both downhole and surface amplifier systems.

In the system using the PTA (5240-30) with the 23900 modified for a 3.5 second natural period, the microseismic noise level at the phototubes ranged from one-third to one-half full-scale. To estimate the magnitude of distortion products in the long-period band generated by slight nonlinearity and high-level microseisms, two-frequency distortion tests were made. The PTA was equipped with a standard filter having a 6-second notch and the galvanometer was driven at two frequencies near 6 seconds whose difference was approximately 50 seconds.

This provided for notch attenuation of the fundamental signals while long-period distortion products received maximum amplification. Distortion products (50-second) were not clearly resolved for steady-state drive levels less than about 80 percent of full-scale at the phototube. Slight variations in amplitude, phase, or frequency in the test signals produced large disturbances. Measurement accuracy was limited by generator instability in the long-period range.

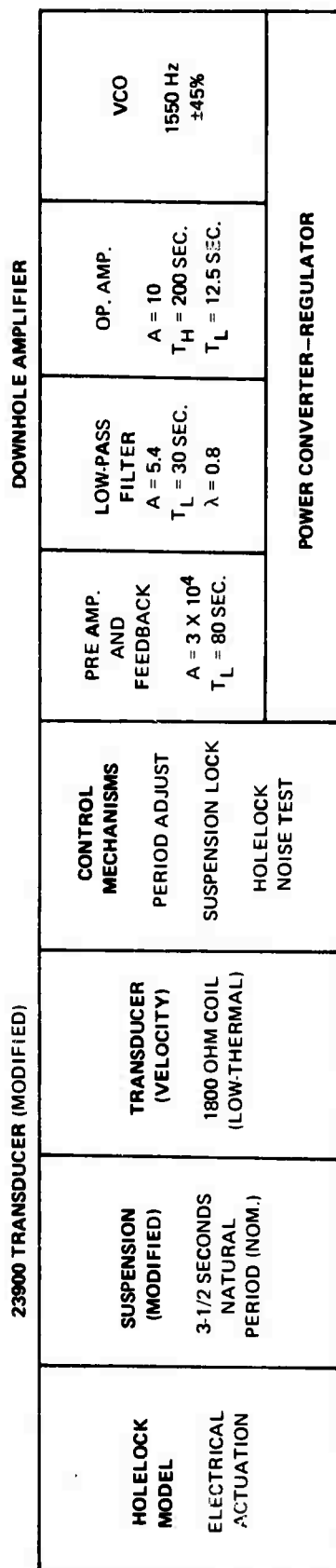
The PTA system was tested in conjunction with the downhole amplifier systems but was not used for field measurements. Block diagrams of the downhole amplifier system and the PTA system are shown in figures 39 and 40, respectively.

### 6.5.6.3 Test Results

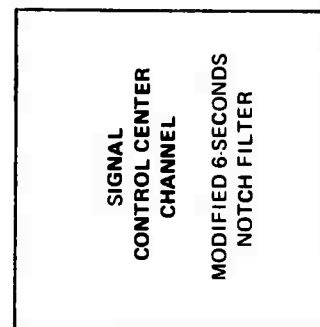
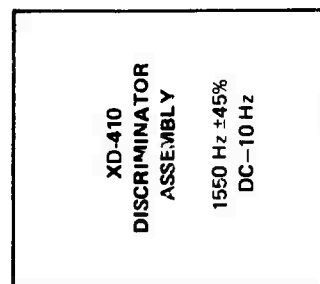
Initial testing of the downhole amplifier systems was conducted at the Garland facility using the 350-foot test hole prior to operation in the deep-hole at PI2WY.

The shallow-hole facility was constructed in 1953 at latitude 42°52'33" N, longitude 96°40'12" W. The hole was drilled to 360 feet in Austin chalk, cased to 350 feet and the casing cemented from the bottom through a float shoe to the surface. Casing specifications are:

- 7-5/8 in. outside diameter,
- 7.025 in. inside diameter,



DOWNHOLE PACKAGE  
12:14 CABLE ASSEMBLY (MODIFIED)



CENTRAL RECORDING EQUIPMENT

Figure 39. Block diagram, downhole amplifier systems - DHA1 and DHA2

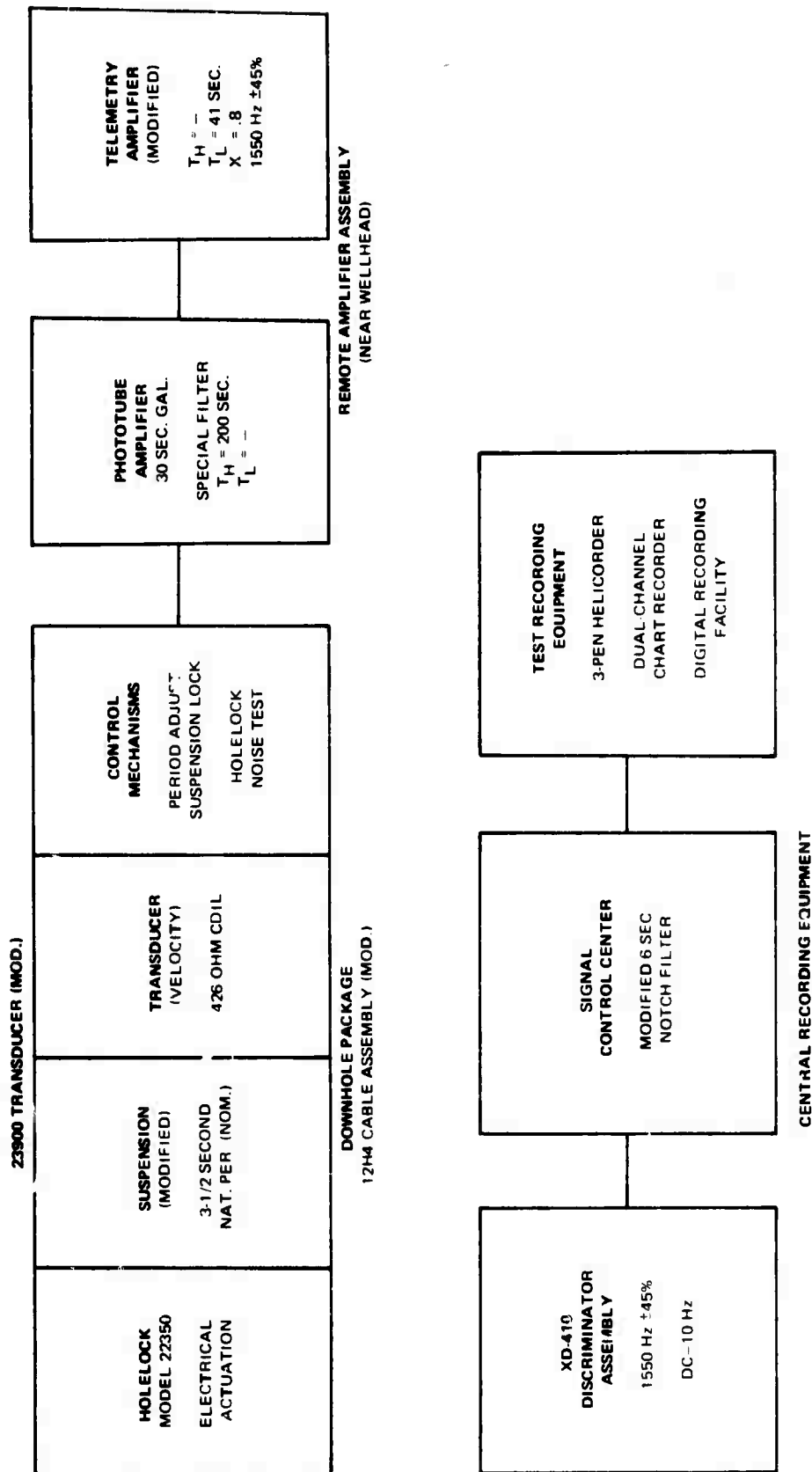


Figure 4u. Block diagram, 23900 (3-1/2 sec)/phototube amplifier (PTA) system

0.300 in. wall thickness,  
24 lb/ft nominal weight,  
Grade H-40 (mill test pressure of 1900 psi),  
Range - 2 lengths, 30-foot nominal  
(25 to 34 feet)

Inclination of the hole as measured with a Sperry-Sun inclinometer in 1958 was 1/2 to 7/8 degree. At present, the hole contains several feet of bottom debris, about 140 feet of water, and about 160 feet of SAE-40 oil.

Tests were conducted with the hole not sealed to the atmosphere.

Systems were tested in their full configuration, i.e., downhole instrument to remote terminal equipment to central terminal equipment. Signals were first recorded on a 3-pen Helicorder and later, by 9 March 1971, a Develocorder was added. Central equipment was located adjacent to the computer facility to allow selected data to be digitally recorded and processed.

6.5.6.3.1 Summary of Developments. Construction of velocity and displacement systems was initiated in December 1970 and operational testing of initial velocity systems began in early January 1971. By mid-January it became apparent that response or coupling complications had been encountered in testing the velocity systems. At this point, effort was concentrated on the velocity systems under test.

To resolve this problem, the first downhole amplifier instrument (DHA1) was modified to include a noise test mechanism, and a second downhole amplifier instrument (DHA2) was constructed to closely match the first. A third system (PTA) using a Model 5240-30 phototube amplifier was maintained and a noise test mechanism was installed in the transducer.

The noise test mechanism consisted of a remotely actuated latching relay that allowed either the velocity transducer coil or a noise test resistor to be connected to the signal terminals. This was important in two respects: (1) the mass-locking mechanism did not generally inhibit all motion; and (2) a stabilization time of 24 hours or more was required after mass-lock operations.

The PTA, DHA1, and DHA2 systems were operated from 12 February to 17 February at respective depths of 65 ft, 85 ft, and 110 ft. Although a stabilizing characteristic could be observed, severe differences endured between systems on background and local disturbances - there was fair correlation on events.

On 17 February, the PTA, DHA1, and DHA2 instruments were lowered 150 ft to 200 ft, 225 ft, and 250 ft, respectively. Agreement between systems was significantly improved even in initial operation. Agreement between DHA1 and DHA2 continued to improve until intermittent operation developed in DHA2 on 20 February. Suspension pulses had been occurring in the PTA system since 12 February and by 20 February almost all signals were obscured.

On 21 February, all instruments were put through a complete locking, unlocking, and adjustment sequence. Signals remained obscured on the PTA system, but intermittent outages on DHA2 were reduced. System DHA1 showed the same background as DHA2 except for an added long-period component (~100 sec) that generally reduced in time. Differences to local disturbances remained large.

On 22 February, all instruments were retrieved for repairs and minor modifications. The PTA transducer suspension was generally reworked, realigned, and tested on the surface. On 1 March, stabilization began with the PTA, DHA2, and DHA1 instruments at respective depths of 200 ft, 225 ft, and 250 ft. About 48 hours later the PTA system became very noisy and subsequent checks showed that a drastic change had occurred in the suspension.

The installation was not disturbed and observations continued with the two downhole amplifier systems DHA1 and DHA2. By 11 March significant data had been collected and a test report covering the period from 1 March to 11 March was prepared. Several conclusions were reached.

- a. The transducer suspension produces a significant noise during stabilization (four or more days), but after stabilization was achieved suspension noise could not be resolved with the velocity systems.
- b. Differences in response to local disturbances were associated with the holelock mechanism. (Discussed in paragraph 6.5.8)
- c. Adjustment procedures were critical for satisfactory stabilization and operation. (Discussed in paragraph 6.5.8)
- d. The velocity systems are capable of operating at a magnification of 50K with a recorded system noise level of 1 to 2 millimeters.

One of the more interesting findings was the variety of long-period signals observed at the test installation. During a normal 24-hour period, there were long intervals of low background during which magnifications of 50K to 100K could be recorded satisfactorily. There was some cultural interference during heavy traffic hours but the major disturbances were those produced by the delivery and switching of railroad cars in the area adjacent to the test hole. These disturbances allowed response differences and directional sensitivities to be clearly observed.

Later in March and April, wind activity and background increased on both the deep-hole systems and nearby vault systems. Several wind gusts were correlated with background signals.

**6.5.6.3.2 Test Data.** During the night of 9 March 1971, a seismic background sample, almost free of local disturbances, was digitized and processed with noise samples from the downhole amplifier systems.

Figure 41 shows response curves for the downhole amplifier systems DHA1, DHA2, and the modified 23900-PTA system, (measured prior to suspension failure on 3 March). The spectra shown in figures 42, 43, and 44 have not been corrected for system response. Figures 42 and 43 compare system noise and seismic background for the DHA1, DHA2 systems, respectively. Figure 44 shows the spectra of the difference trace formed by linear subtraction of DHA2 from DHA1. The difference spectra was not corrected for its noise gain, nominally 3 dB, with respect to individual traces.

#### 6.5.6.4 Threshold Comparison of Several Long-Period Systems

Early on 26 March 1971, reference data from an operating long-period vault system were recorded and processed with data from the downhole amplifier system. These data have not been duplicated here. However, another long-period seismometer (7505A) was on the pier with the reference system and was used to extend the comparison of long-period systems.

Data shown in the attached plots have been processed from signals recorded on 6 April 1971. System noise and response recordings were made with the systems indicated in block form in figure 45. Background spectra have not been presented because of interference by teleseismic signals during the recording period.

The diagram at the top in figure 45 represents the configuration in which three solid-state amplifier systems were operated. These three amplifier systems are denoted by reference suffixes A, B, or C.

6.5.6.4.1 Systems A, B, and C. In the "A-System," the amplifier used was the original portable system amplifier with a conventional preamplifier. Laboratory tests on the amplifier used in the "A-System" showed that it was operating with slightly less noise than that specified for this preamplifier.

In the "B and C-Systems," the solid-state amplifier was replaced with a new low-noise preamplifier. The same amplifier was used for both "B and C-Systems," but in different configurations. In system "B," the transducer was coupled directly to the input of the low-noise preamplifier. In system "C," the transducer was coupled directly to the input of the low-noise preamplifier in conjunction with feedback from the preamplifier output. The feedback transfer characteristic was high pass or differentiating and resulted in a forward low-pass transfer characteristic. The amplifier assembly used in systems "B" and "C" was used earlier with the 11167 transducer in the "C-type" configuration. The same amplifier type and configuration were used in the downhole amplifier systems. Amplifier and filter configurations are indicated in figures 46 and 47, respectively.

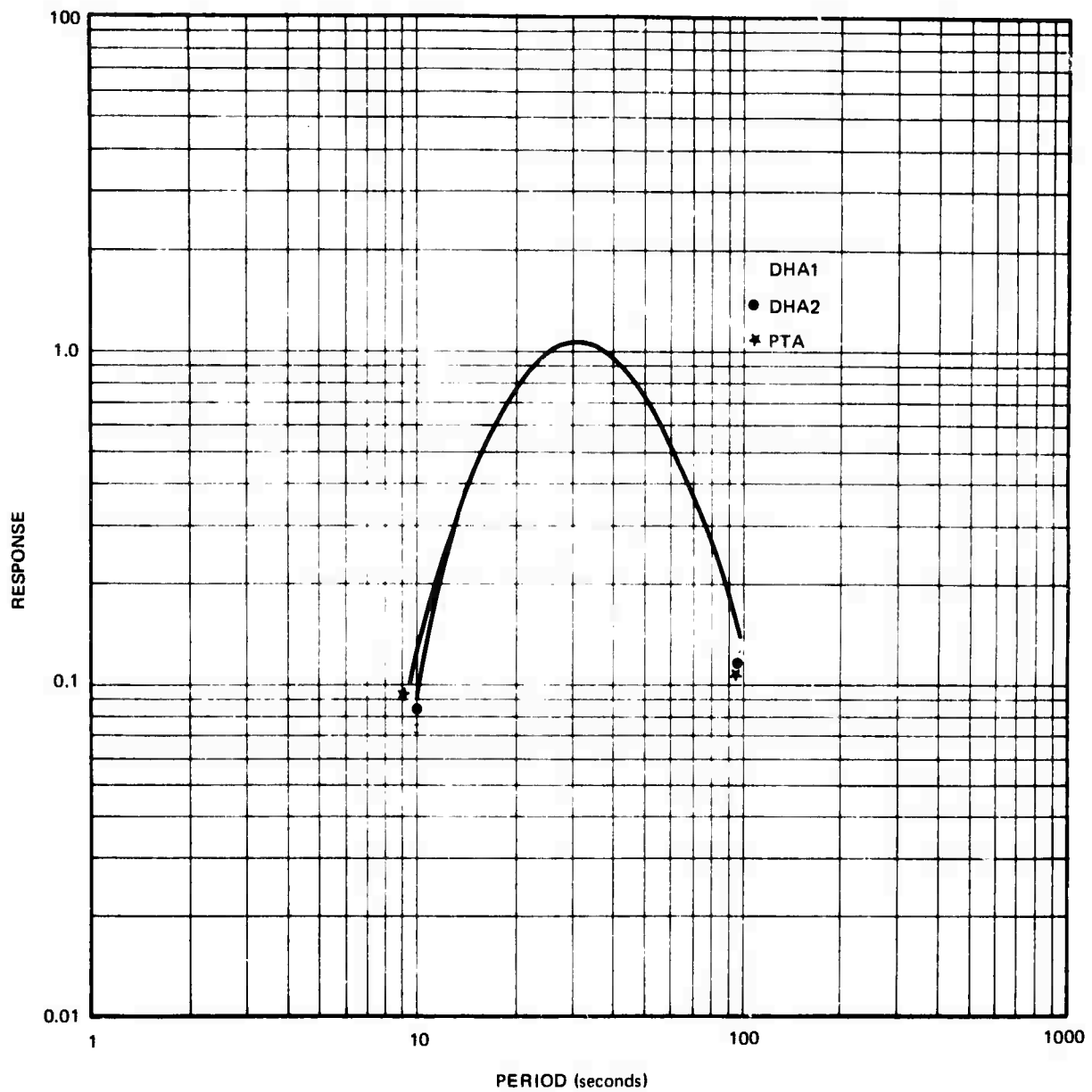


Figure 41. Frequency response of experimental deep-hole, long-period velocity systems

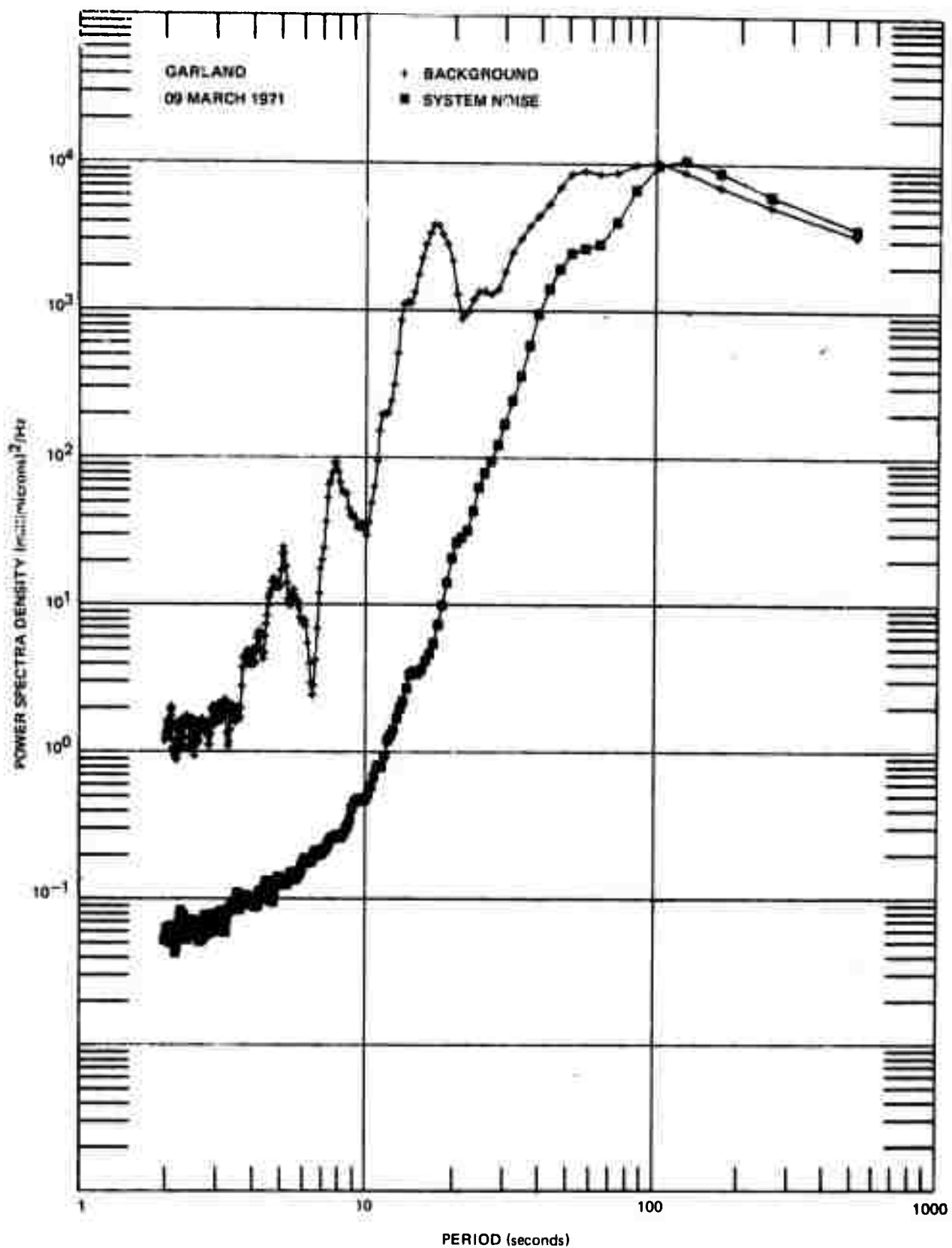


Figure 42. Comparison of background and system noise for downhole amplifier system DHA1

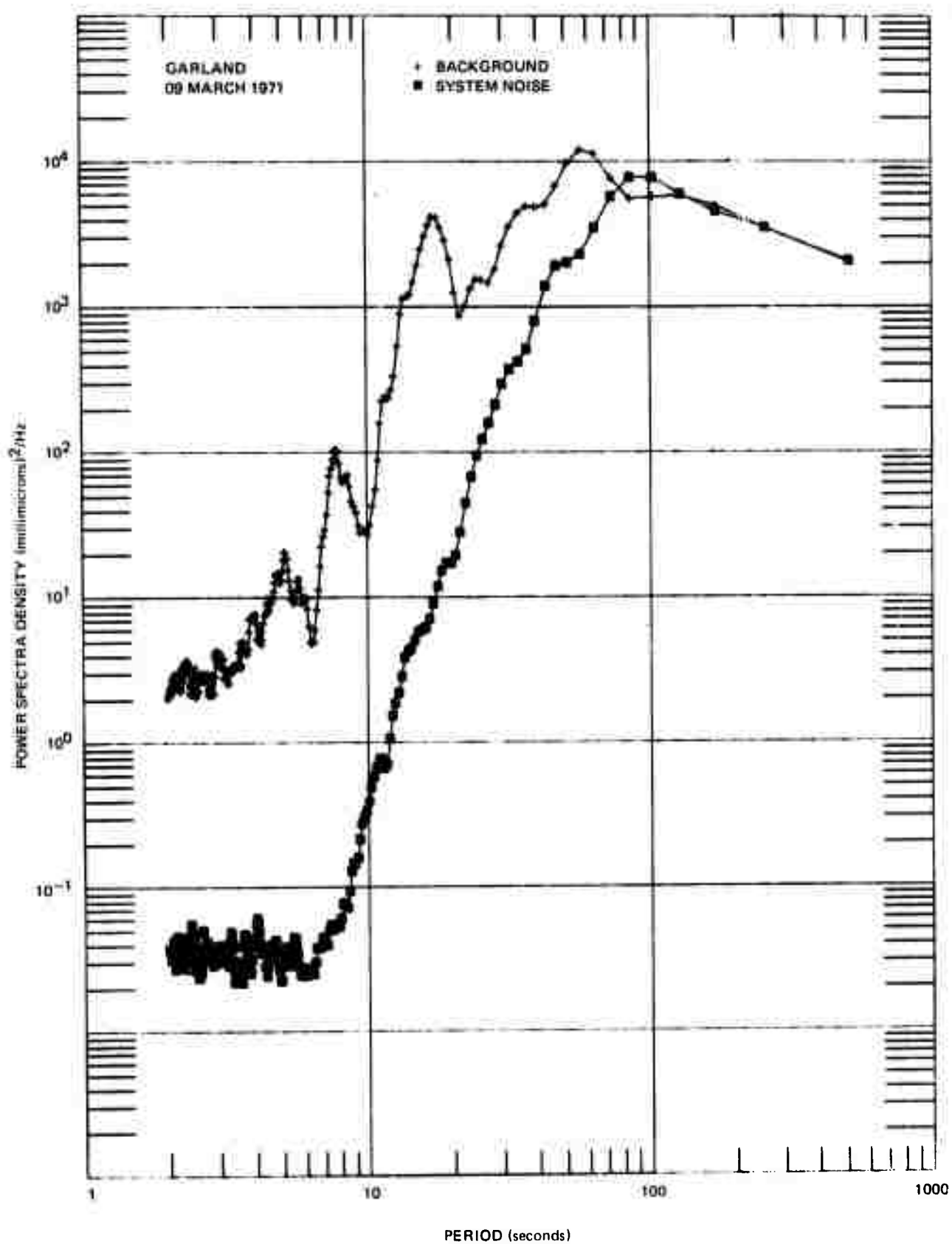


Figure 43. Comparison of background and system noise for downhole amplifier system DIA2

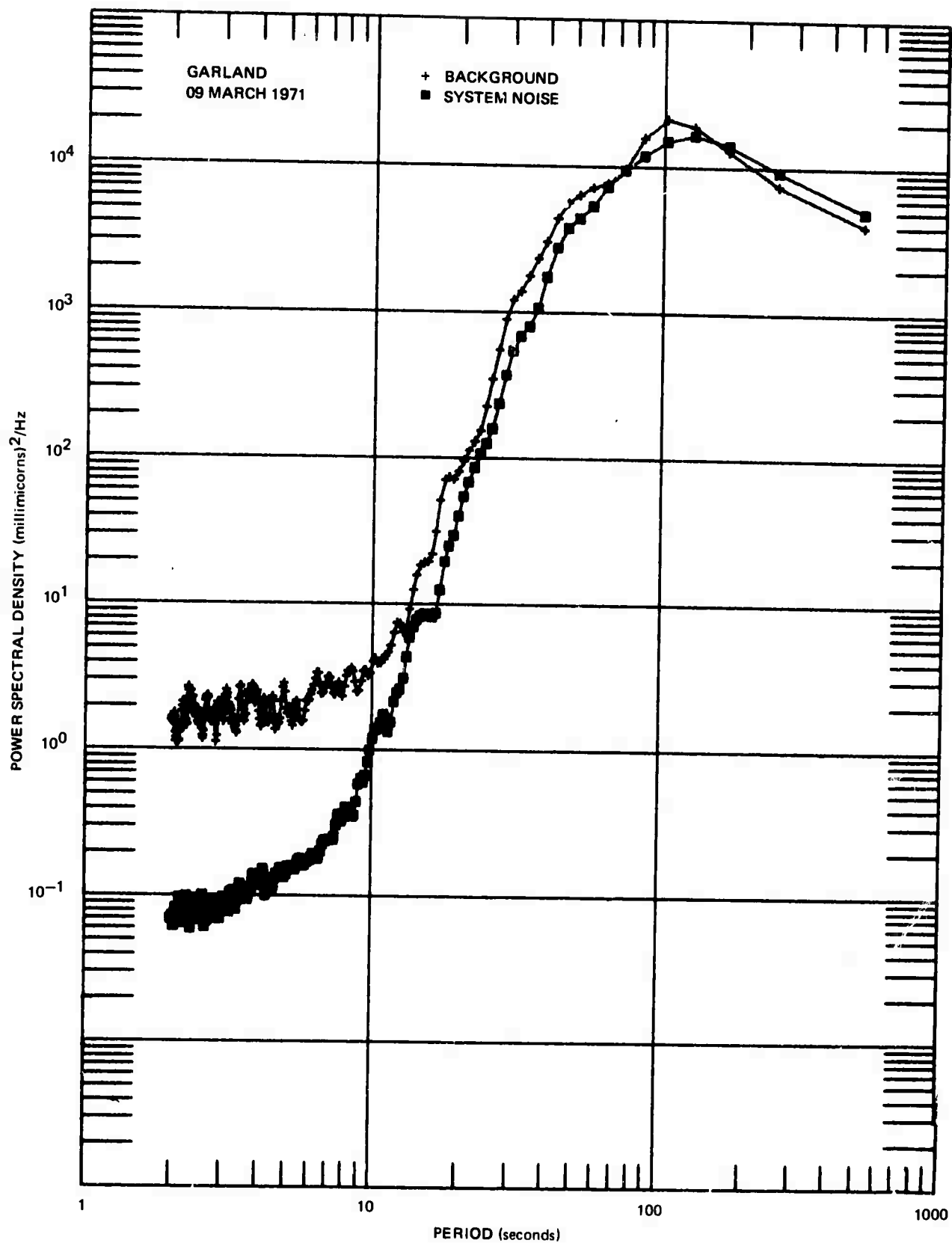


Figure 44. Comparison of background and system noise difference for downhole amplifier systems DHA1 and DHA2

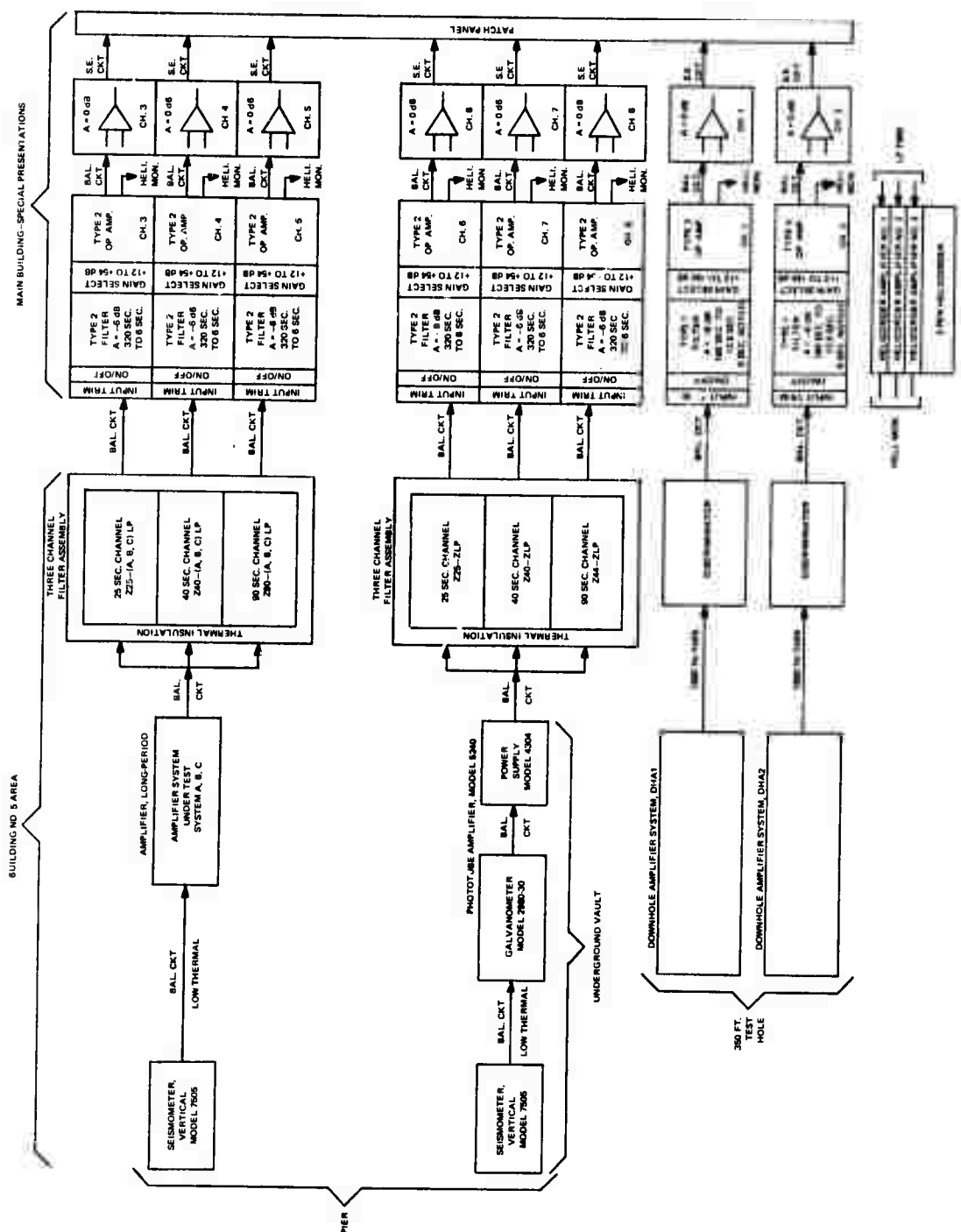


Figure 45. Block diagram, LP systems and filter channels



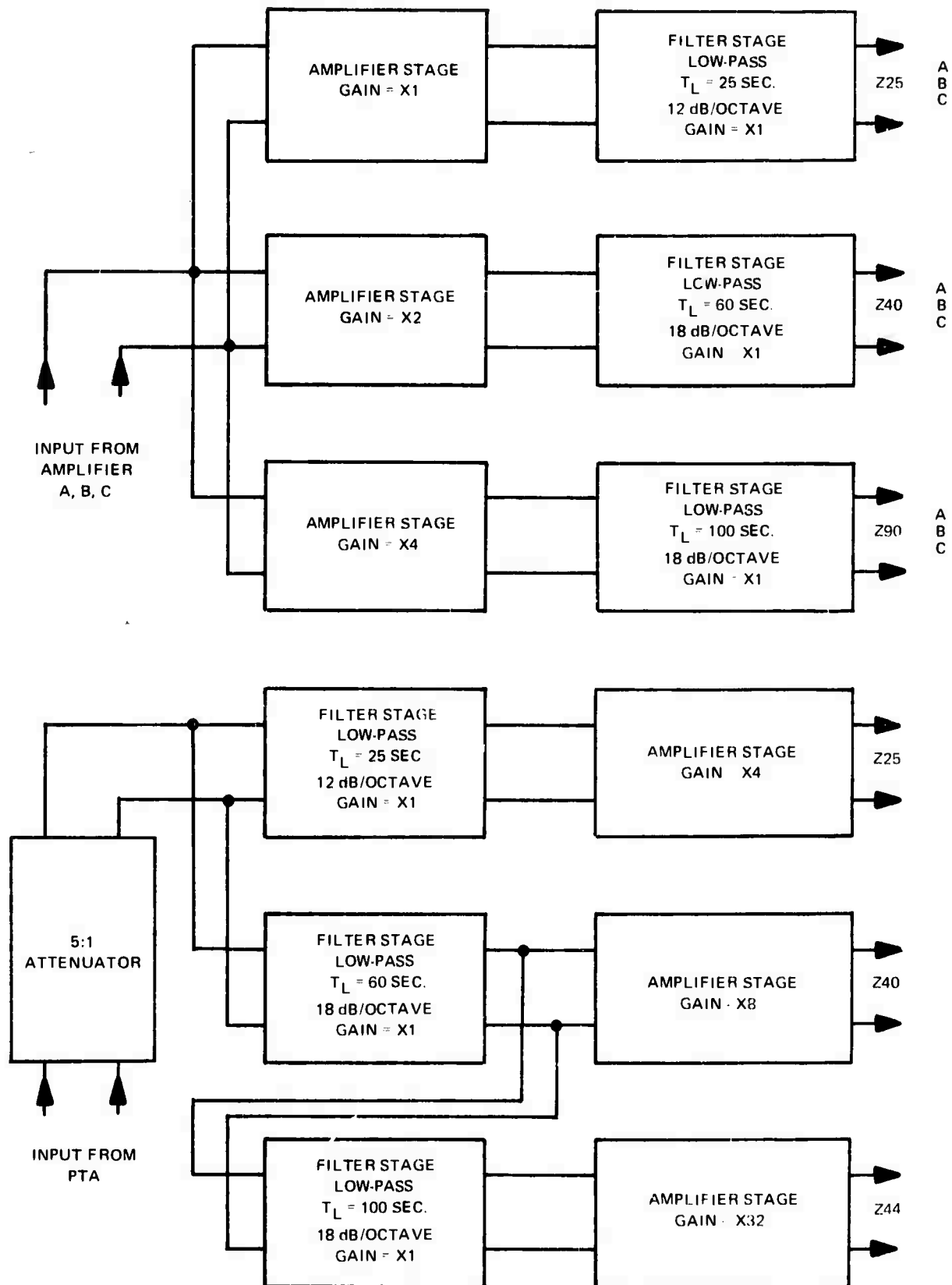


Figure 47. Configuration, three-channel filter assemblies

6.5.6.4.2 Reference System. The Long-Period Phototube Amplifier (PTA), Model 5240, with the Galvanometer, Model 2980-30 (30-second) had been in operation for several months at this location and served as a reference system. It should be noted that this system differs from advanced long-period systems employing the 110-second Harris galvanometer.

Channel Z44 of the PTA system was not operating properly, but was processed to help resolve the problem. Comparison of system noise and background spectra indicate an unusual type of calibration/sensitivity problem. If corrected, the Z44 system noise should be closer to the Z40 and Z25 values at periods greater than about 40 seconds. At shorter periods, depending on channel response, thresholds were limited by the recording system threshold.

6.5.6.4.3. Downhole Amplifier Systems. Thresholds of the deep-hole, long-period systems (DHA1 and DHA2) were limited by the noise levels of the downhole amplifiers. Consequently, an increase in suspension sensitivity directly improved the system threshold. Bench tests on the downhole amplifiers have shown the DHA2 amplifier noise level in the long-period range to be approximately 6 dB less than that of the DHA1 amplifier. (The noise level of the amplifier used in the "B" and "C" configurations was intermediate to the two downhole amplifiers.) The DHA1 suspension has been capable of operating at a greater natural period or sensitivity than the DHA2 suspension. In previous tests the suspension-amplifier combinations produced approximately equal system thresholds. In this test, the transducer-amplifier combinations were the same as before, but the period or sensitivity of DHA1 was less than that of DHA2 and consequently the threshold of DHA1 was greater as shown in figure 48. Amplitude response curves were very nearly the same as shown in figure 41.

6.5.6.4.4 System Noise Conditions and Plots. In each case of system noise tests, the amplifier input was connected to a "low-thermal resistor" equal in value to the nominal coil resistance of the corresponding transducer. A "low-thermal resistor" was one especially constructed to minimize thermal electromotive forces (emf's) in a copper circuit. In addition, input circuits were insulated to minimize temperature gradients. Without such practices, temperature effects can interfere severely with long-period measurements.

The passive or dummy source resistor allows fairly accurate threshold determination except in the region of transducer resonance. Depending on the system type, configuration, and conditions, the observed "dummy source noise" about the transducer natural period can be either too large or too small.

Noise signals were amplified such that average levels were one-fourth to one-half full scale for the 12-bit digitizer. In one case, Z25B, approximately 30 samples exceeded full scale by approximately 10 percent.

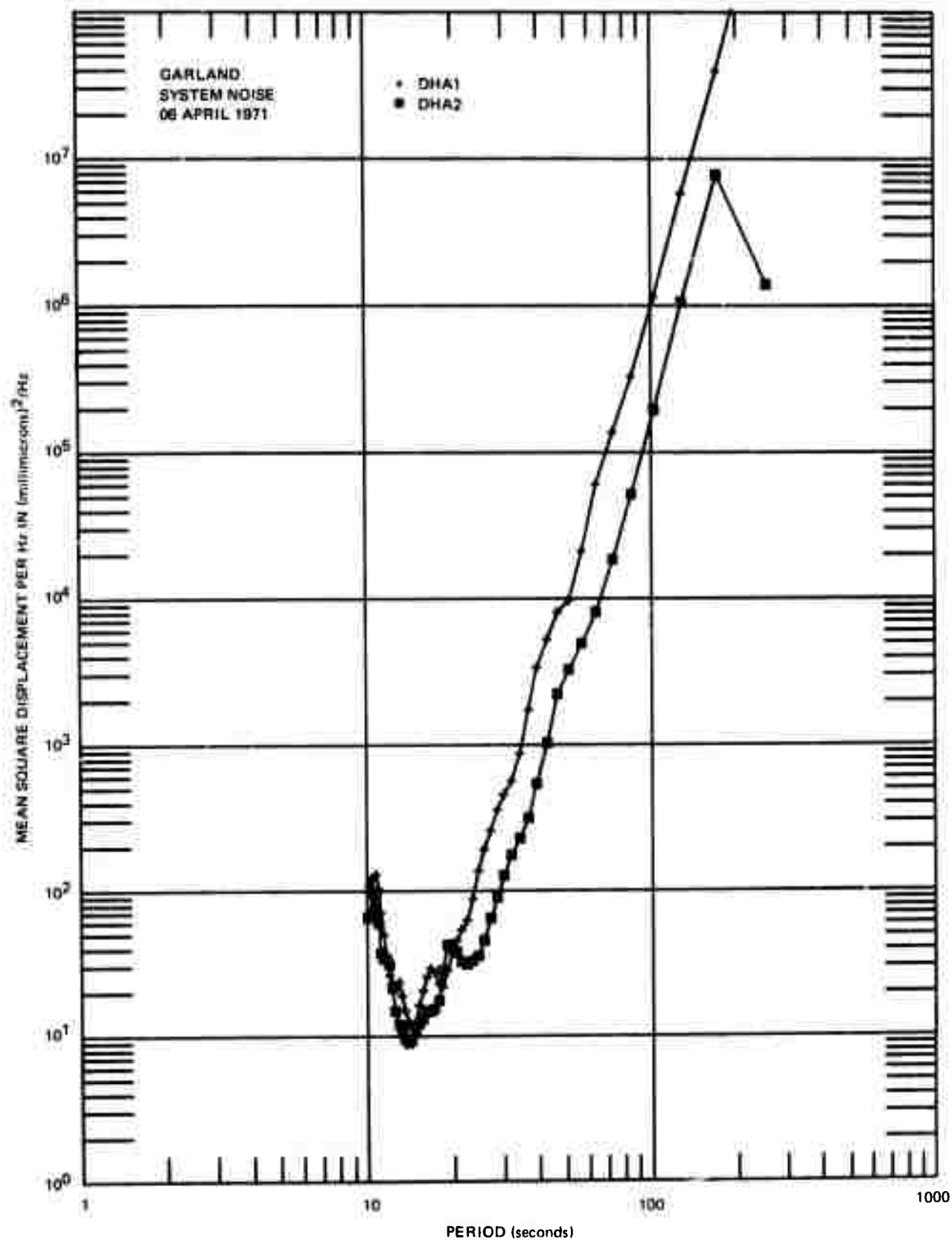


Figure 48. Comparison of system noise for downhole amplifier systems DHA1 and DHA2

In all cases, thresholds at longer periods are determined almost entirely by the dummy source resistance and first amplifier section. Thresholds at shorter periods are determined by channel response and recording system threshold. Post-stage noise power density increases in direct, or greater, proportion to period and can interfere with the input threshold at longer periods even though there may appear to be adequate separation between post- and input-noise levels when observed broad band.

Channels of the "A and B-Systems" were least affected by post-stage noise at longer periods. The input noise of System A also increases with period and System B had the greatest first stage amplification. In the C-System and the downhole amplifier systems, feedback lowered the first-stage amplification relative to that of the B-System.

The separation in the Z25 and Z40 spectra at the longer periods may indicate some interference at long periods by the filter assembly. The attenuator at the filter input has been required to reduce calibration and 6-second microseismic background signals, but could be bypassed for noise tests. However, for data recorded on 26 March 1971, Z25 and Z40 spectra were in better agreement with each other and with the Z25 spectra for 6 April. Therefore, the Z25 spectra (6 April) has been taken to be the best estimate of the 7505/5240/2980-30 PTA system threshold.

All system noise spectra have been plotted on the same grid having a mean square displacement per Hz range of  $1 \times 10^0$  to  $1 \times 10^6$  millimicrons squared per Hz and a period range of 1 to 1000 seconds. Spectra were first computed and then corrected for system (displacement) response over the range of 250 seconds to 10 seconds. System response curves for the PTA system and systems A, B, and C are shown respectively in figures 49, 50, 51, and 52. Corresponding system noise spectra are shown in figures 53, 54, 55, and 56. Background spectra have not been distributed due to interference by teleseismic signals during the recording period. Signal arrival began several hours before the recording period, but long-period signals persisted. The (corrected) spectrum was rather broad with a slight peak in the 70 to 80 second region.

#### 6.5.7 PI2WY Data, May 1971

Sections of data recorded at the PI2WY site during May 1971, have been processed to examine some of the spectral characteristics of barometric effects and system thresholds. During this recording period, the deep-hole (vertical) instruments, DHA1 and DHA2, were operating at depths of 130 feet and 8000 feet, respectively. Vertical, north-south, and east-west surface instruments were located in the vault adjacent to the DHA1 and DHA2 holes.

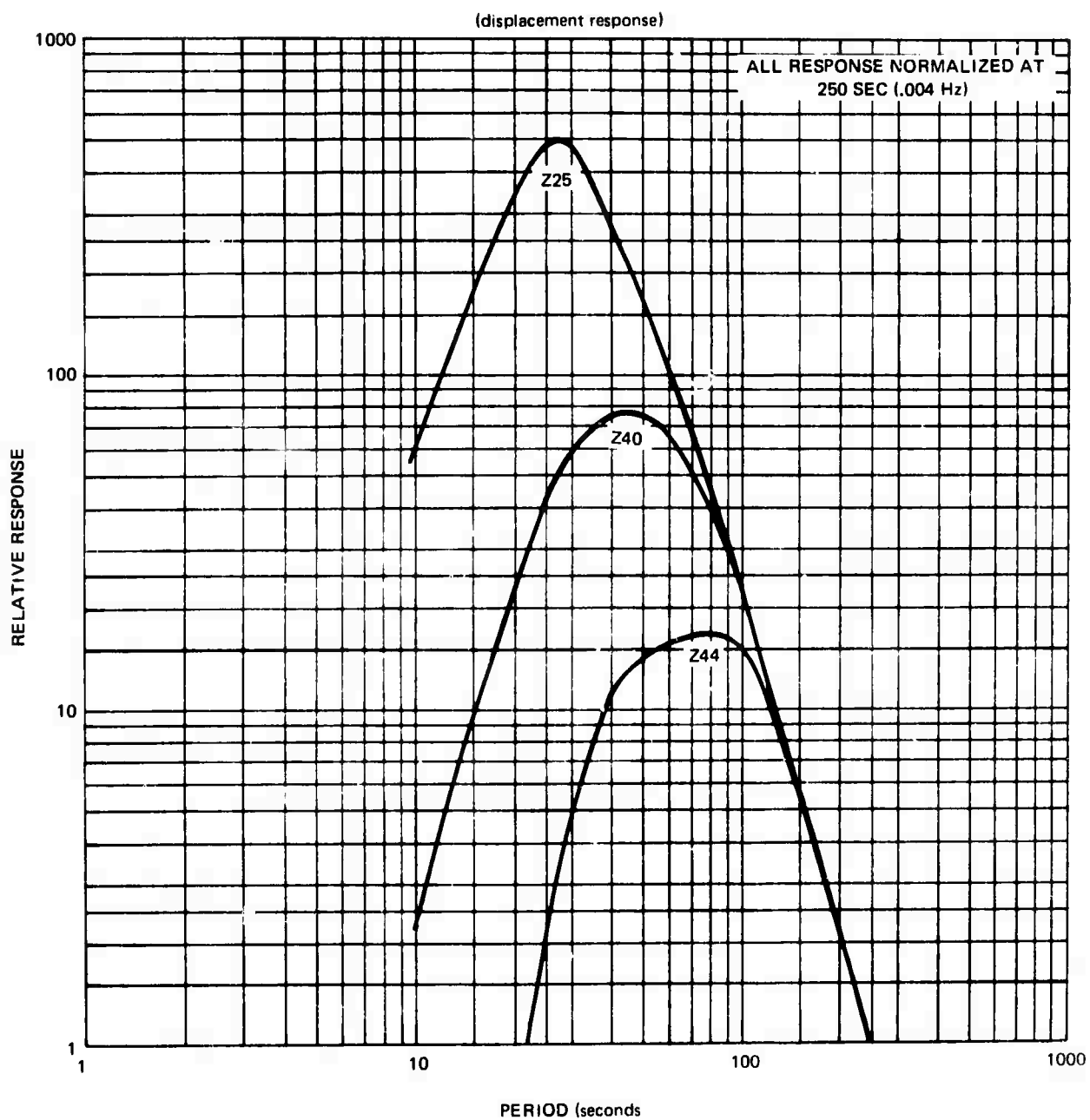


Figure 49. Response curves for PTA system (2980-30/5240)  
channels Z25, Z40, Z44

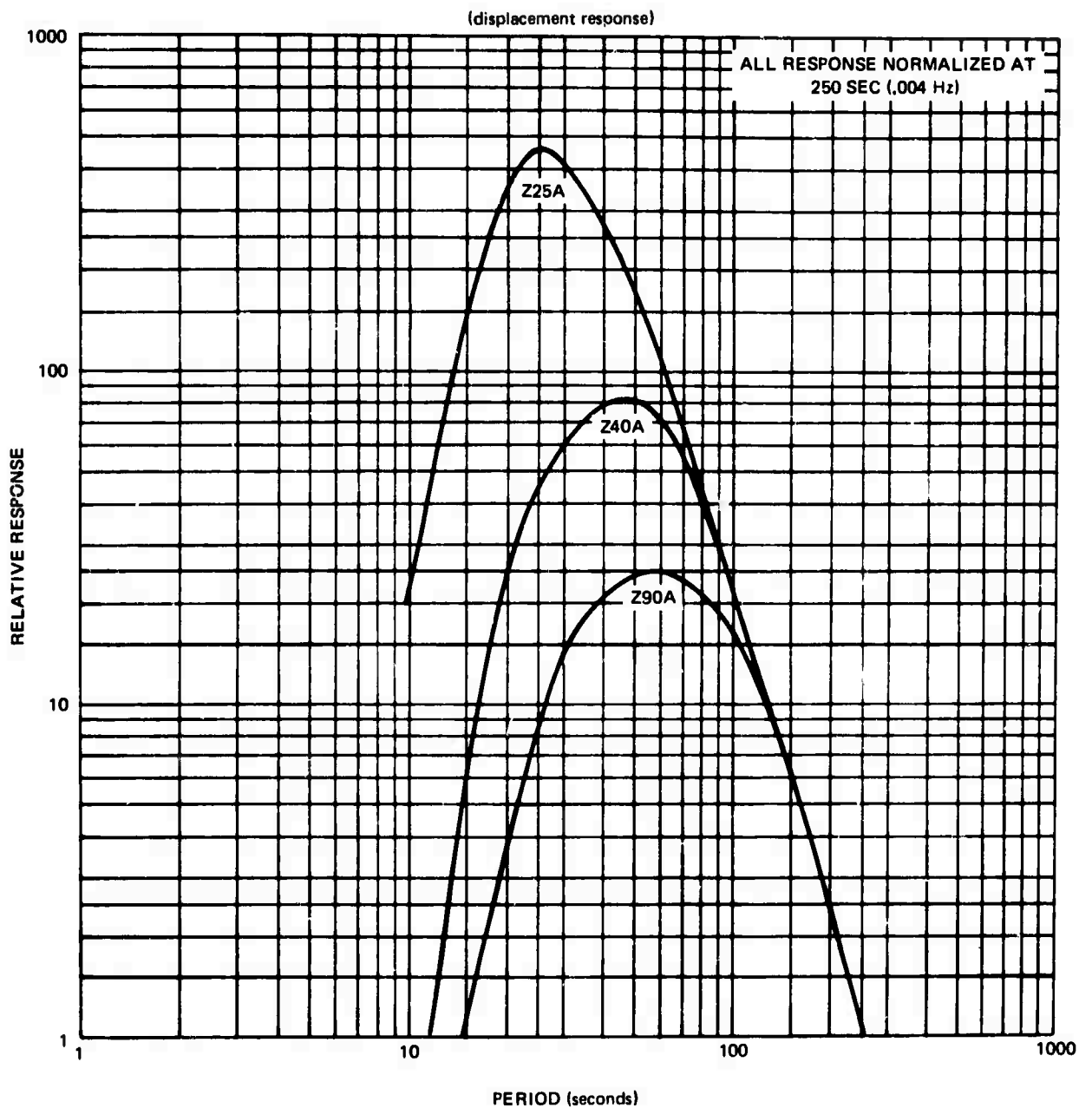


Figure 50. Response curves for amplifier "A" system channels Z25A, Z40A, Z90A

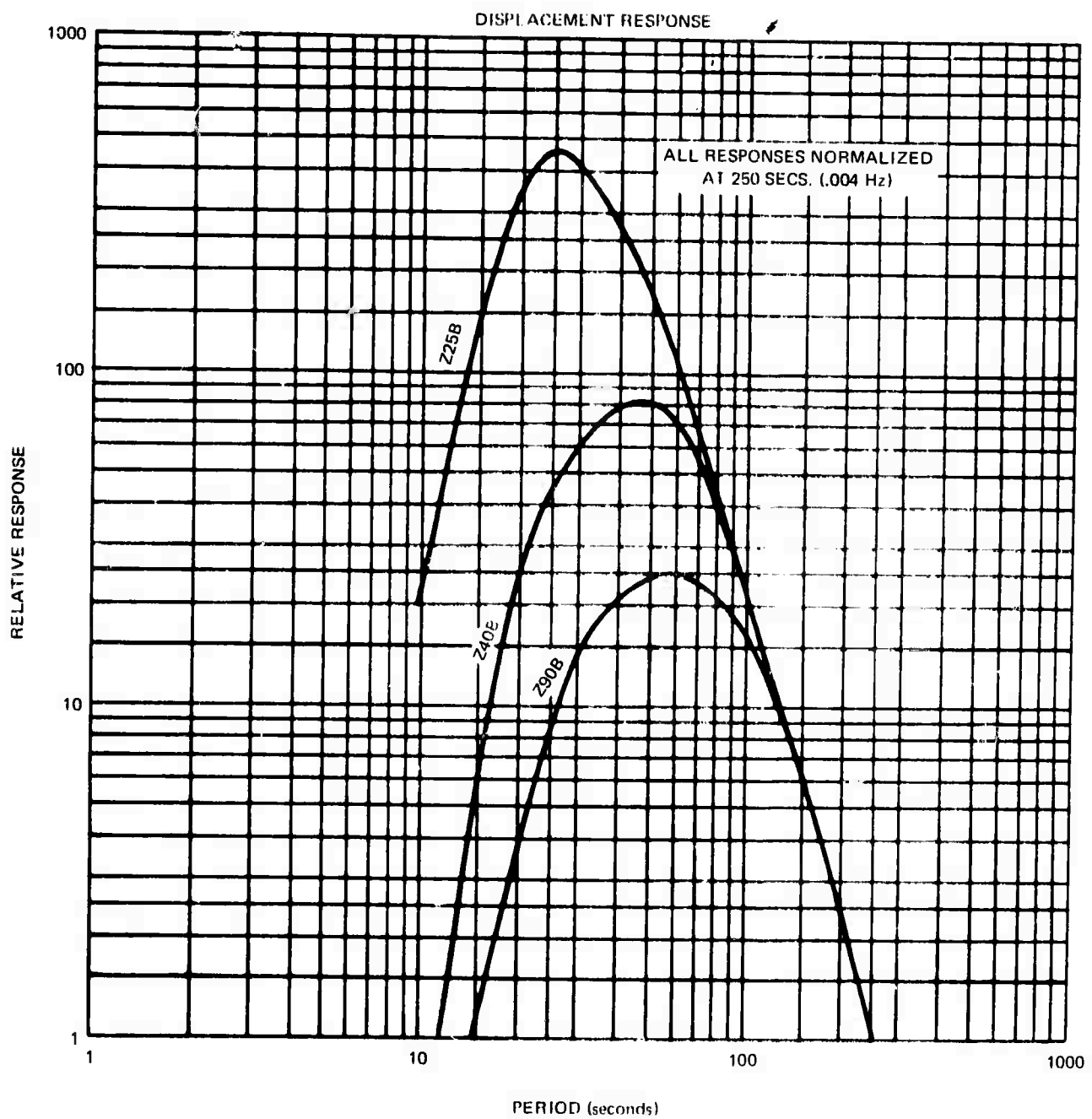


Figure 51. Response curves for amplifier "B" system channels Z25B, Z40B, and Z90B

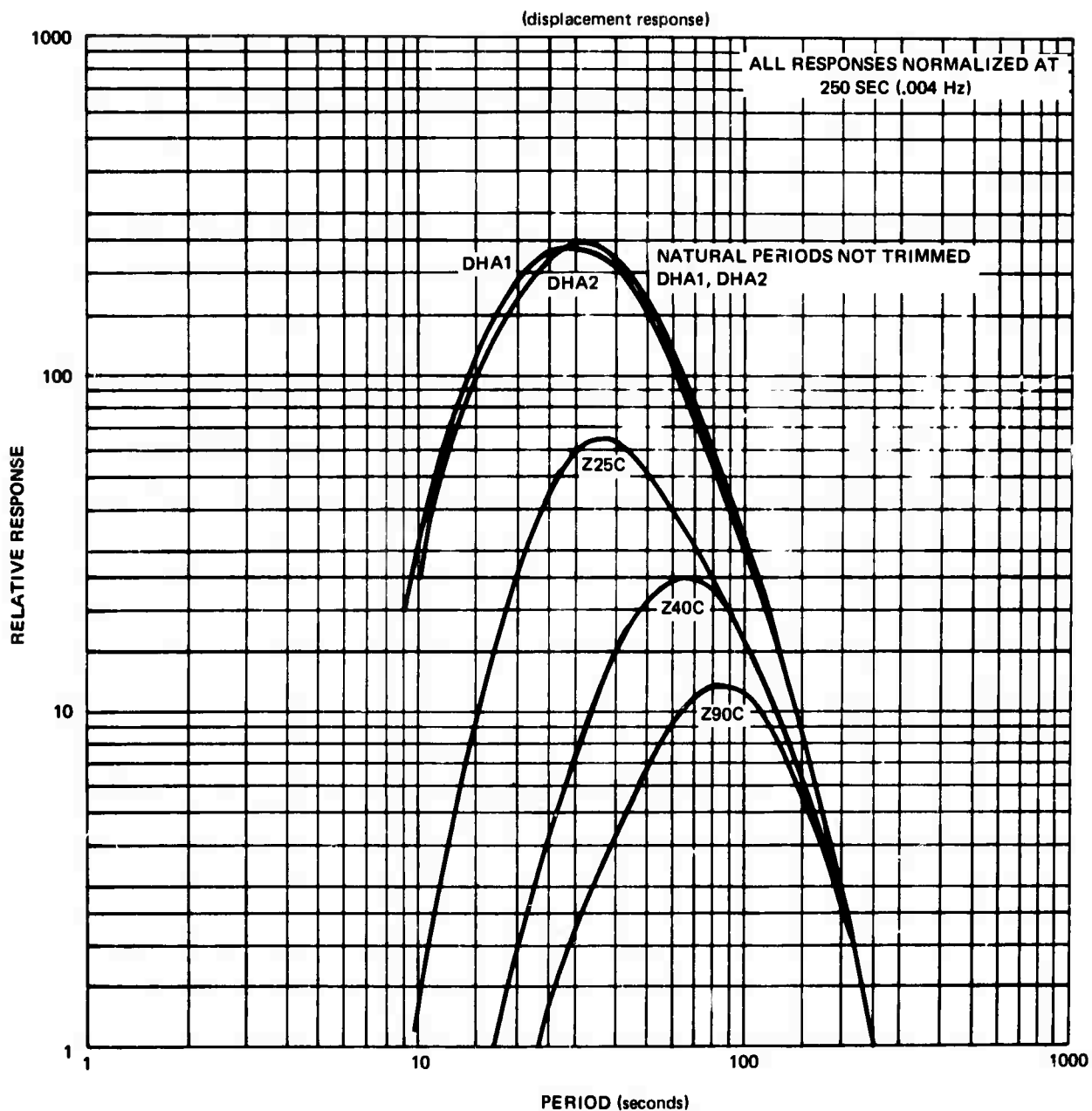


Figure 52. Response curves for amplifier "C" system channels Z25C, Z40C, Z90C and downhole amplifier systems DHA1 and DHA2

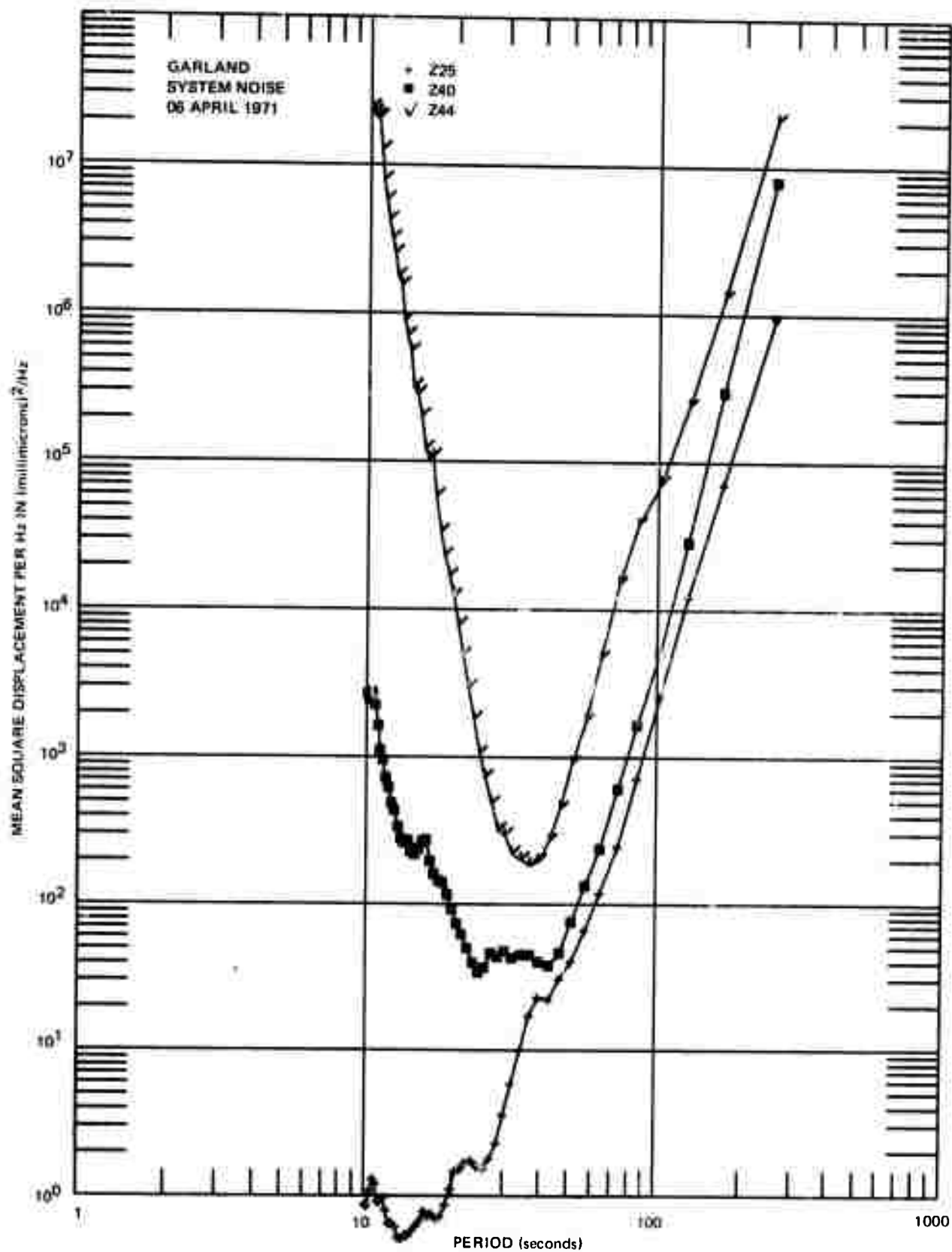


Figure 53. System noise spectra for the PTA system, channels Z25, Z40, Z44

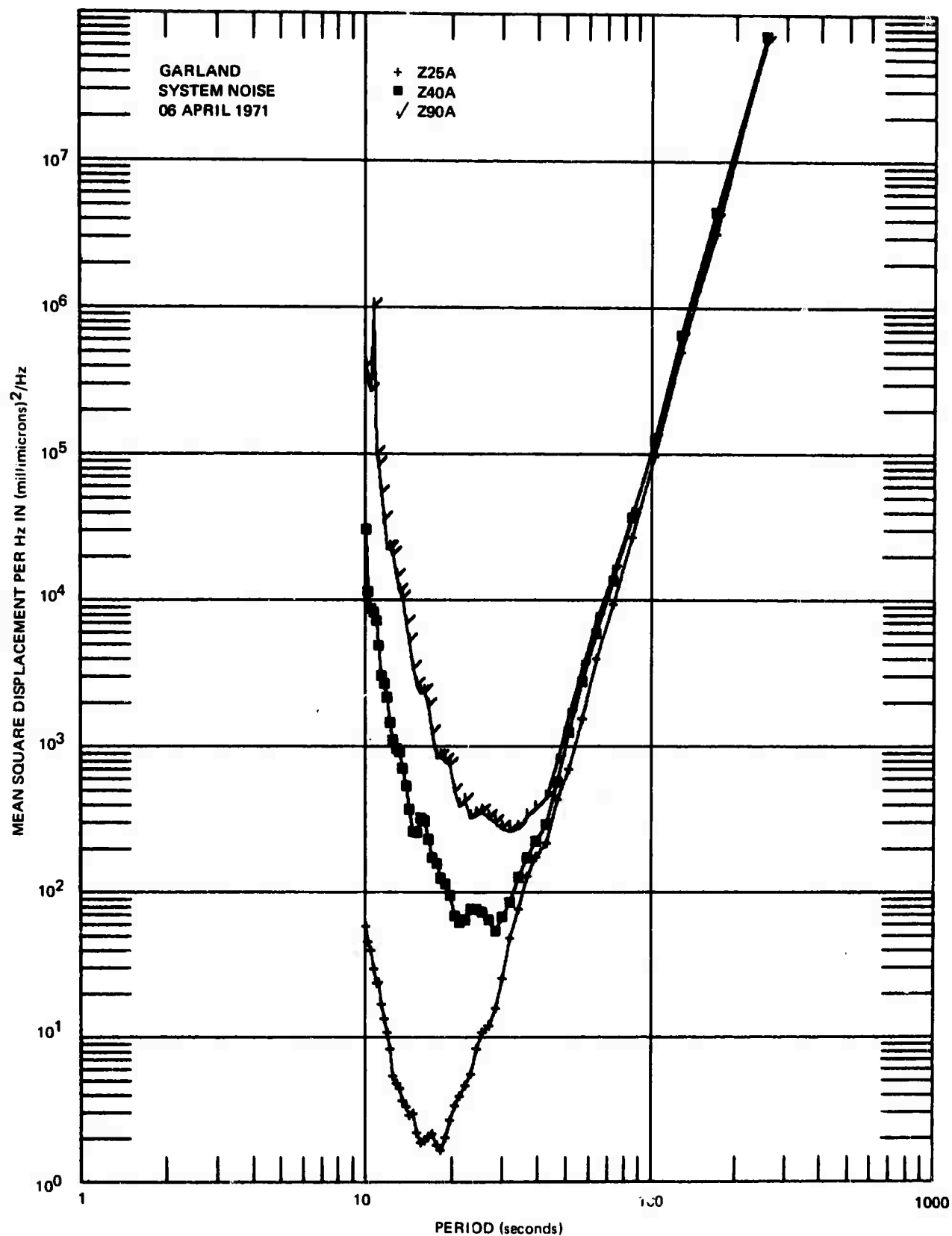


Figure 54. System noise spectra for the "conventional preamplifier" system, channels Z25A, Z40A, Z90A

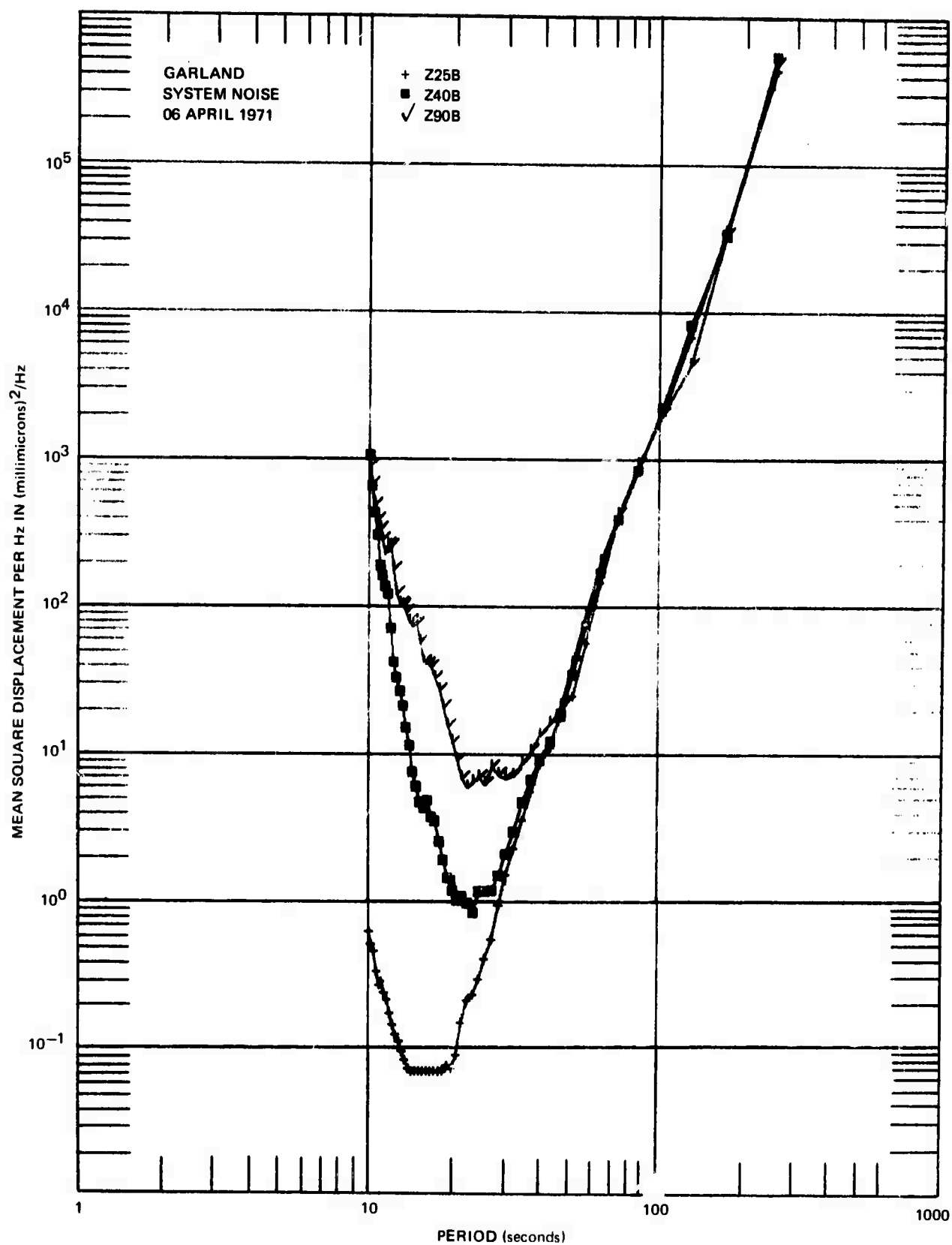


Figure 55. System noise for the "low noise" preamplifier B system, direct coupled

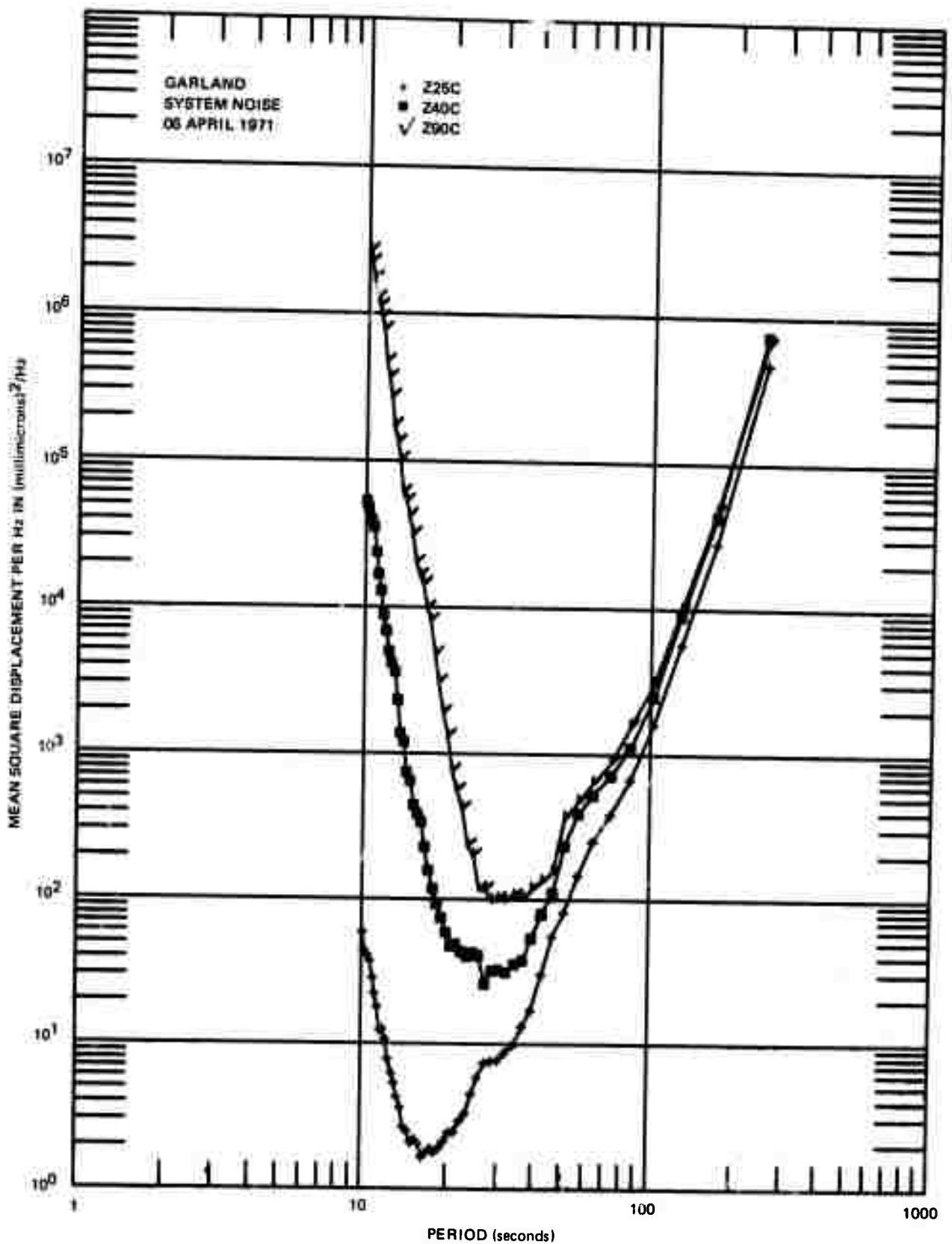


Figure 56. System noise for the "low noise" preamplifier C system, direct coupled with feedback. (Limited at shorter periods by recording system). See figure 65

#### 6.5.7.1 Channel Designations and Response Curves

Wide-band and narrow-band channels were used with each of the instruments. Channel designations and response curves are listed in table 8.

Table 8. PI2WY channel designations

<u>Channel</u>	<u>Instrument</u>	<u>Response curve</u>	<u>Remarks</u>
LZK	Surface, vertical	Fig. 57, A-A	High-gain or notched response
LNK	Surface, N-S	Fig. 58, A-A	"
LEK	Surface, E-W	Fig. 59, A-A	"
DHA1	DH vertical (130 ft)	Fig. 60, A-A	"
DHA2	DH vertical (8000 ft)	Fig. 60, B-B	"
LZ	Surface, vertical	Fig. 57, B-B	Wide-band or unnotched response
LN	Surface, N-S	Fig. 58, B-B	"
LE	Surface, E-W	Fig. 59, B-B	"
DHA1-WB	DH vertical (130 ft)	Fig. 61	"
DHA2-WB	DH vertical (8000 ft)	Fig. 62	"
LZK-SSA	Surface, vertical	Fig. 63	Special test of LZK channel using solid-state amplifier with surface transducer
MB	Microbarograph	Fig. 64 (REF)	Transducer located adjacent to other transducers

#### 6.5.7.2 Effects of Barometric Pressure Variations

Analysis of film records showed that the surface instruments exhibited a significant response to barometric pressure variations. The horizontal instruments exhibited about 10 to 20 dB greater sensitivity than the vertical instrument relative to system displacement sensitivity. At that time, the only effective long-period acoustic time-constant for the surface installation was that of the vertical transducer case.

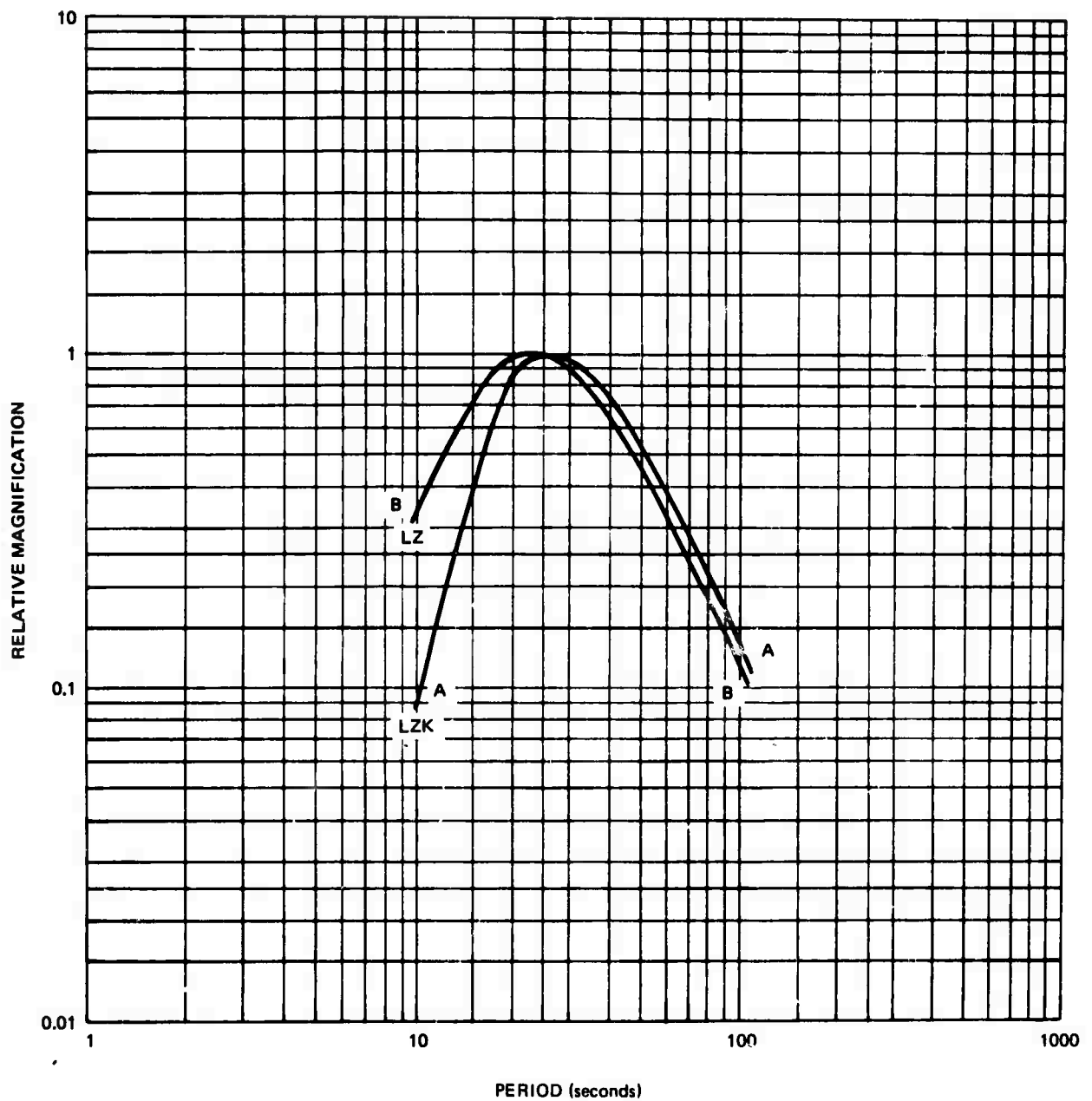


Figure 57. System response, surface vertical LZ - wide-band, LZK - high gain, notched response

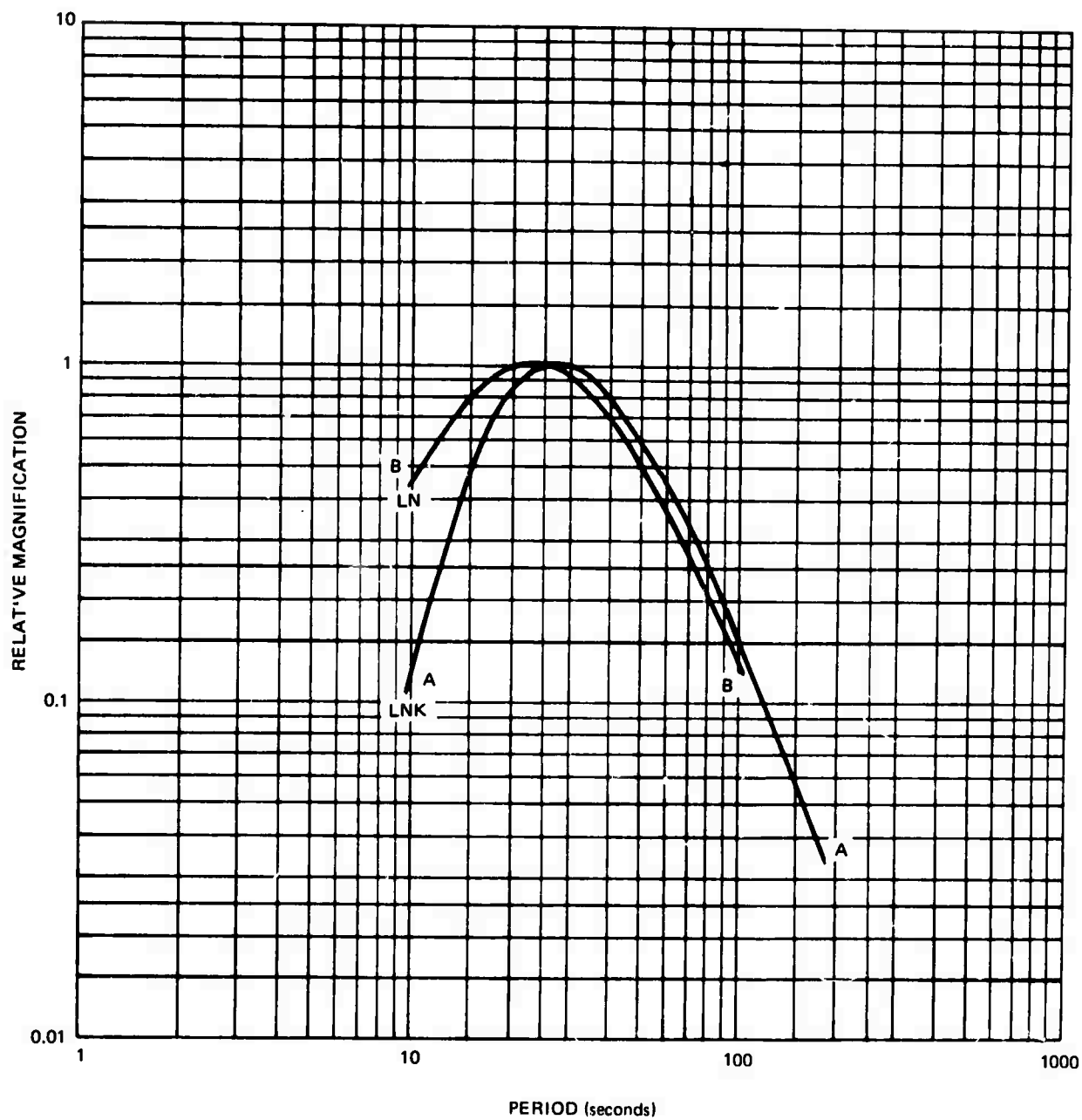


Figure 58. System response, surface north-south LN - wide-band,  
LNK - high gain, notched response

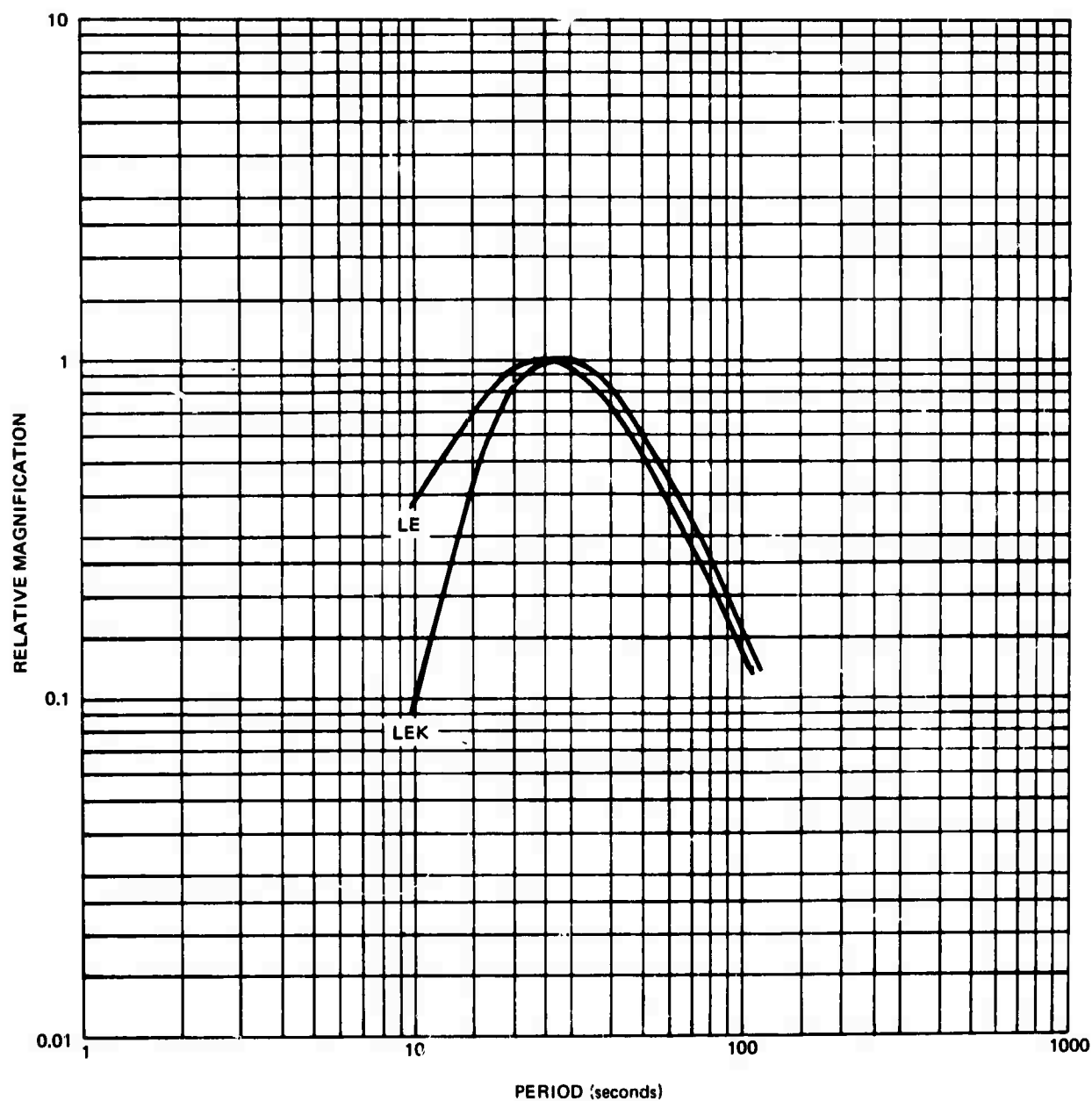


Figure 59. System response, surface east-west LE - wide-band,  
LEK - high gain notched response

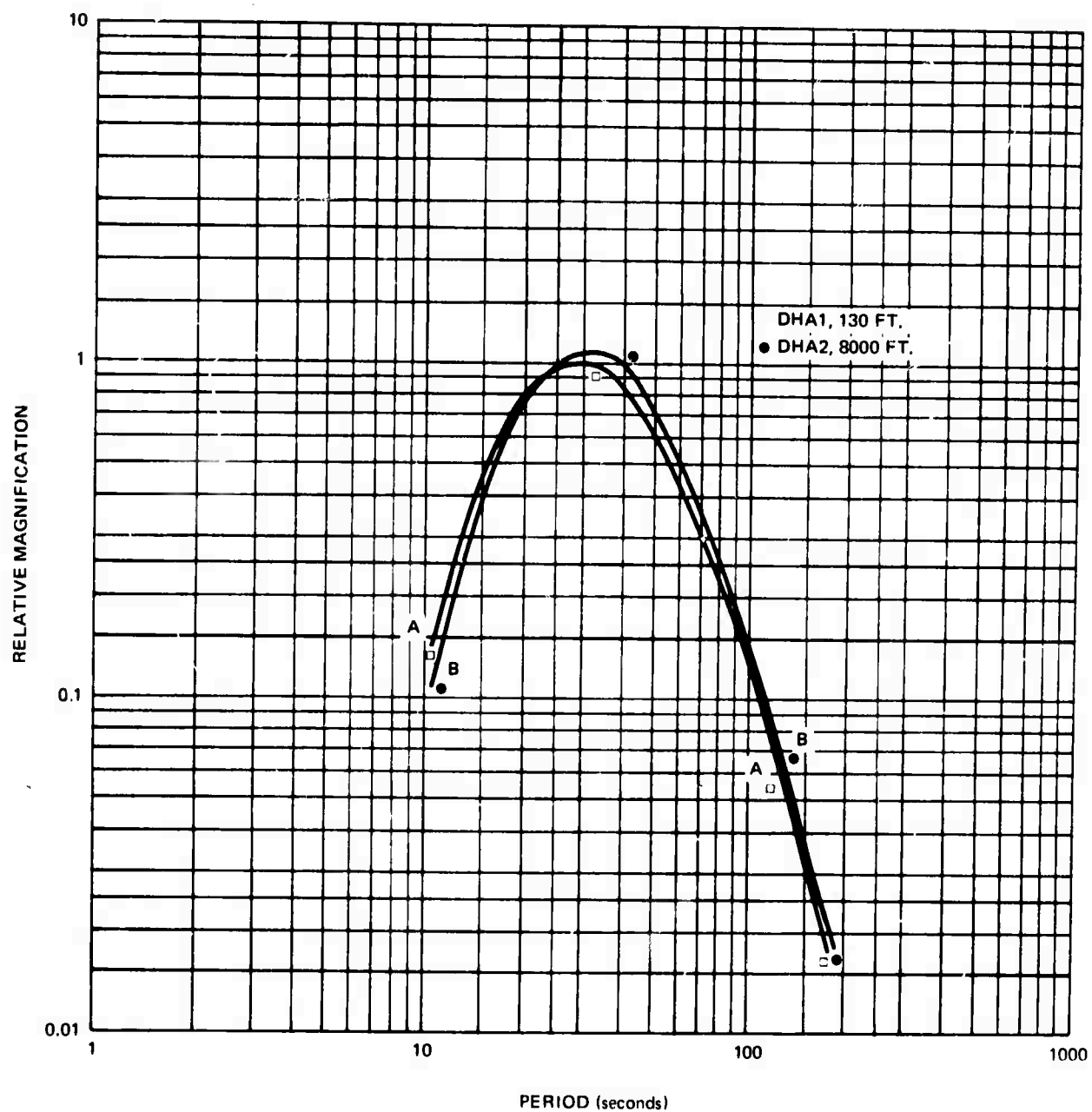


Figure 60. System response, deep-hole systems DHA1 - 130 feet depth, DHA2 - 8000 feet depth

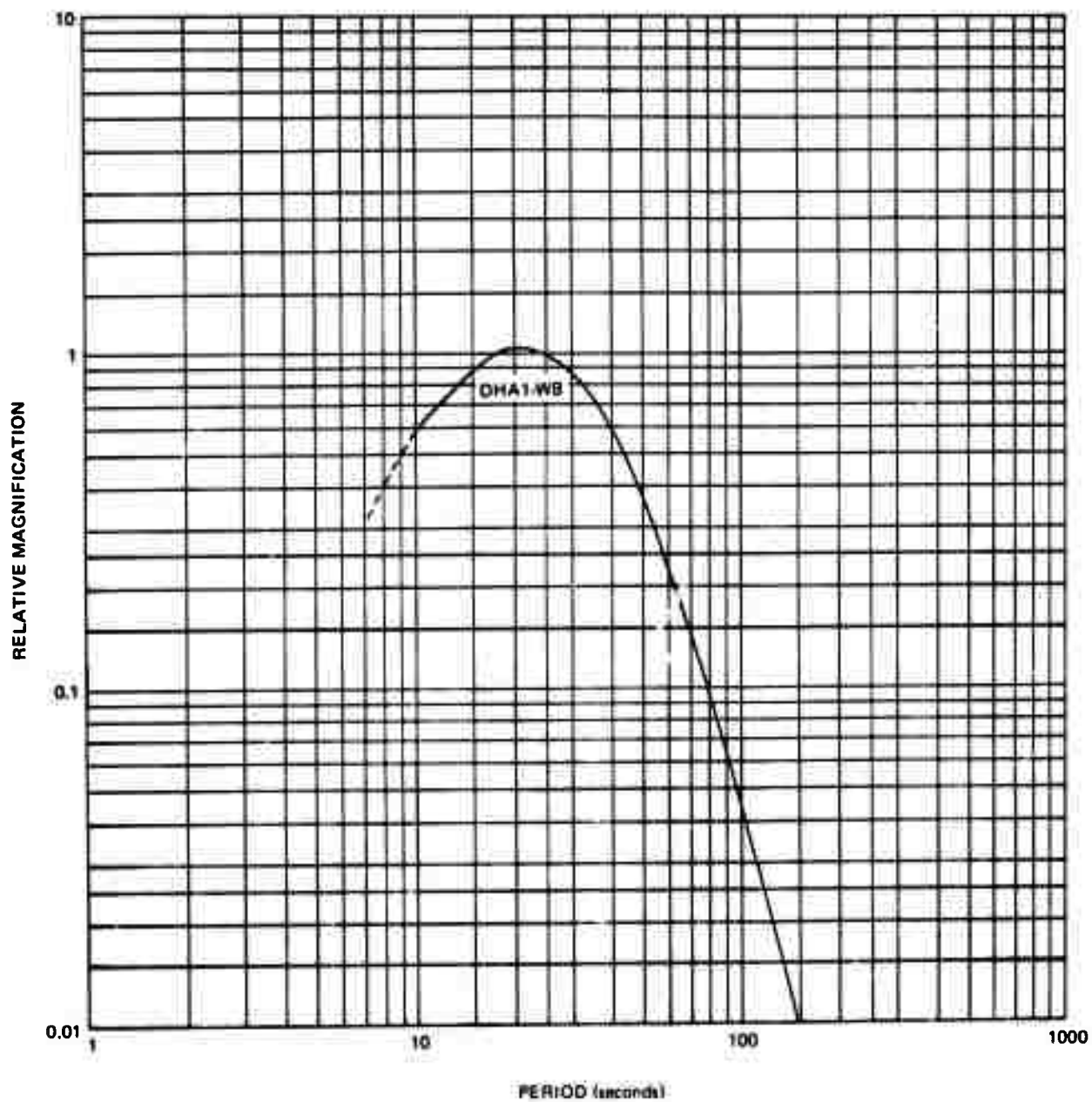


Figure 61. System response DHA1 - wide-band, 130 feet depth

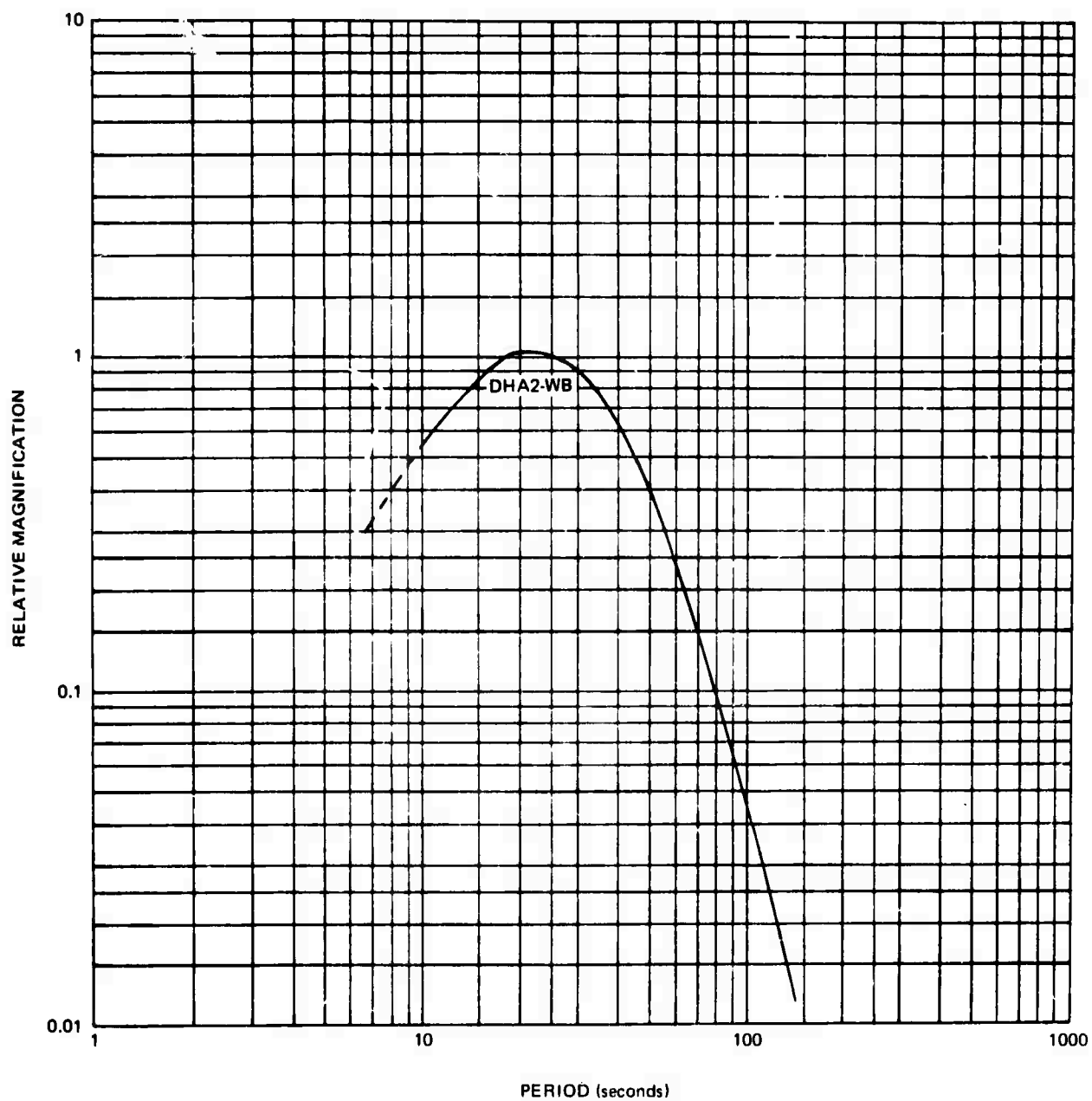


Figure 62. System response DHA2 - wide-band, 8000 feet depth

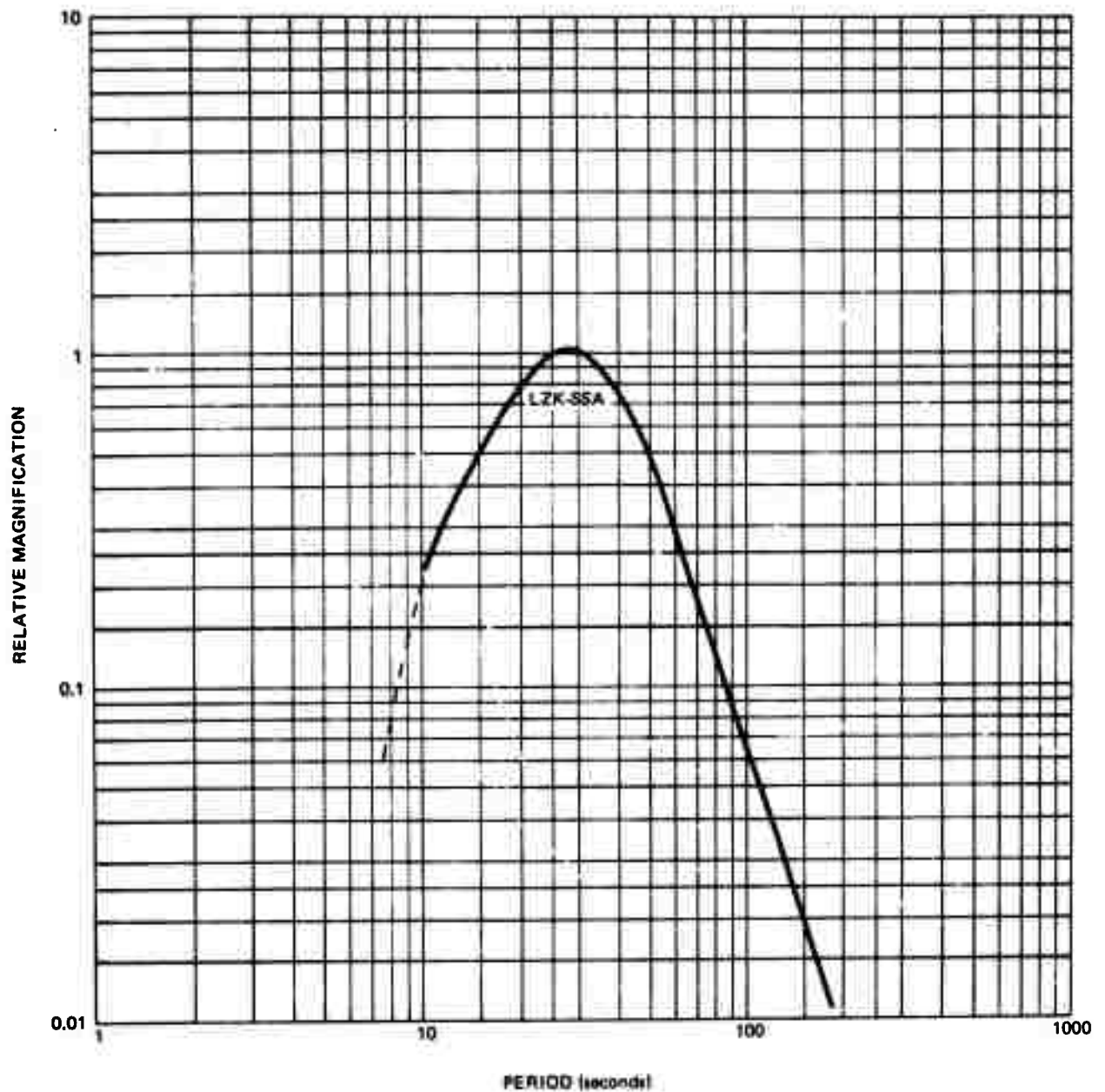


Figure 63. System response LZK/SSA - LZK channel with special solid-state amplifier replacing PTA

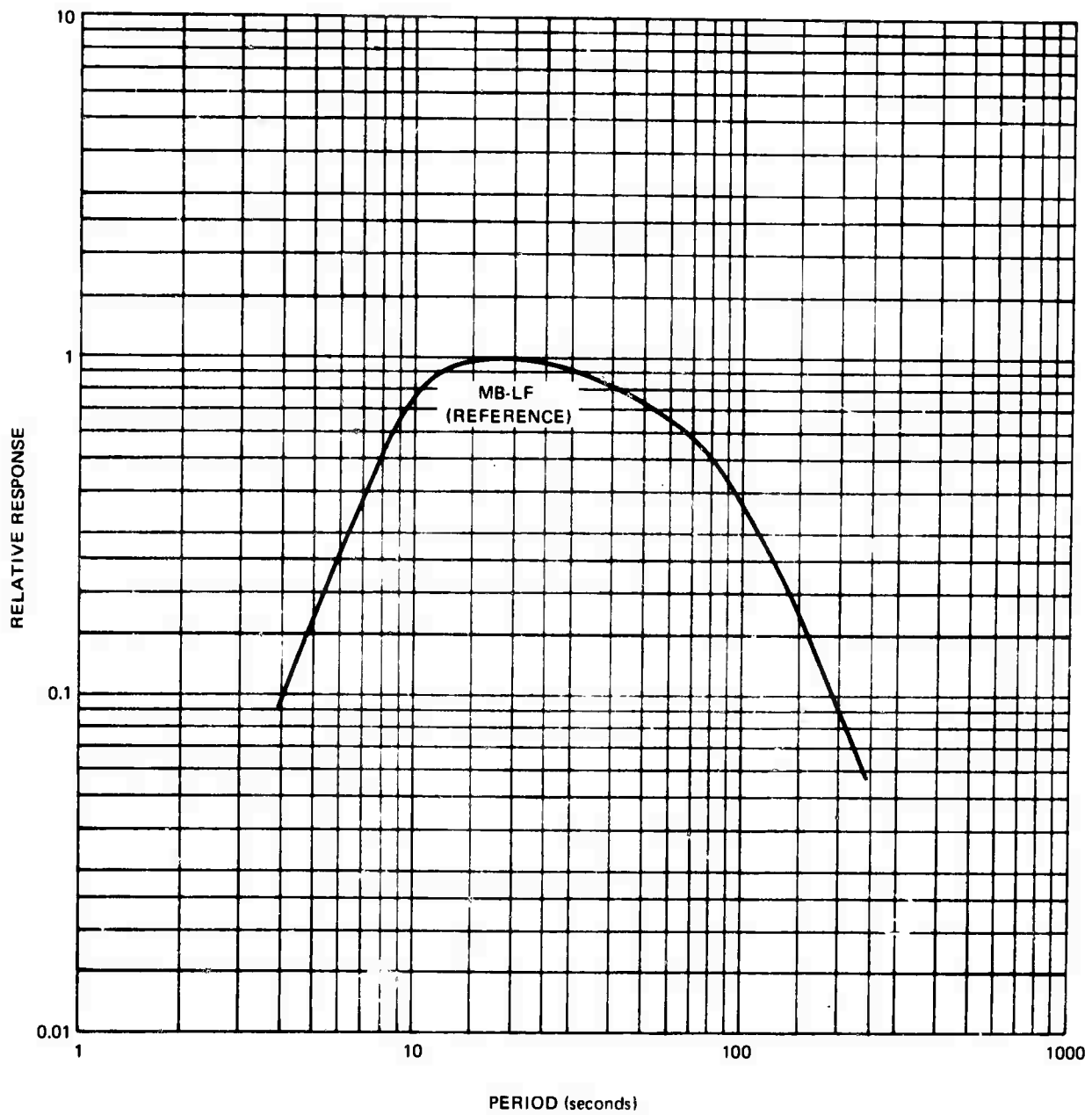


Figure 64. System response for the low frequency microbarograph used at PI2WY (estimated)

One of the objectives of the deep-hole, long-period measurements was to observe the behavior of pressure effects with depth. The limited resolution of the deep-hole (vertical) instrument and the lower sensitivity of the vertical instrument to pressure variations prevented satisfactory observations. However, the measurements did reveal significant information and processing has enhanced several points.

Since direct analysis was restricted most at long periods by system resolution, a time series was selected in which pressure variations were large and fairly wide-band with prominent periods of about 200, 50, and 20 seconds.

The corresponding power spectra of the microbarograph and long-period channels are shown in figure 65. All spectra except that of the microbarograph have been corrected for system response. The coherence plots for the power spectra of figure 65 with that of the microbarograph are shown in figure 66. In figure 67, coherence plots of only the vertical channels are shown. Coherence plots for the vertical channels overlay each other in the 15 to 20 second range. A section of the time series is shown in figure 68.

#### 6.5.7.3 System Noise

It should be noted in the preceding that at periods greater than about 30 seconds, the spectra of the deep-hole channels were largely system noise while that of the surface channels were not. System noise spectra are shown in figure 69.

Noise spectra were recorded at operate settings and at maximum allowable gain. A satisfactory noise sample for the N-S system was not accomplished. At operate levels, surface instrument noise was too near recorder noise, and during the high-gain recording, an offset in the LN channel impaired linearity.

The LZK-SSA was special channel formed by the temporary substitution of a solid-state amplifier for the phototube amplifier in the LZ-LZK system. This substitution was made without changing the transducer coil configuration to avoid disturbing the vertical instrument. This increased LZK-SSA equivalent input noise by approximately 6 dB relative to the preferred series coil configuration.

#### 6.5.8 Problems Encountered in Installation and Operation

Several significant problems were encountered in the installation and operation of the deep-hole systems. Early installations with the 11167 seismometer were made difficult by its mass locking mechanism. The remotely controlled mechanism, inadequate for general transportation, was supplemented with manual blocking which required opening the pressure case at or near the wellhead. This was not only difficult during severe weather, but admitted moisture inside the pressure case. The 23900 instrument was considerably smaller and required only remotely-actuated mass locking.

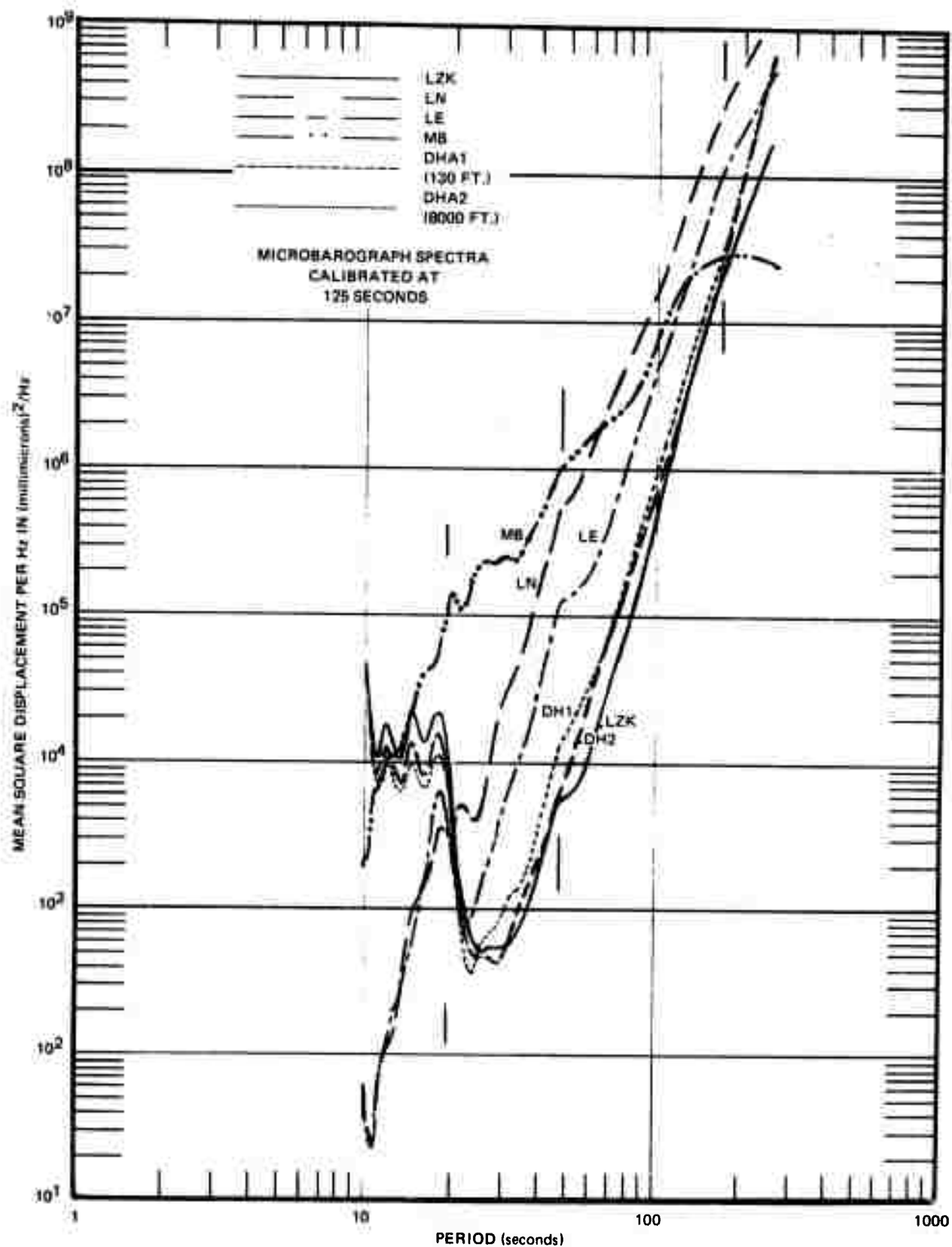


Figure 65. Power density spectra of long-period channels during strong barometric activity, low seismic background

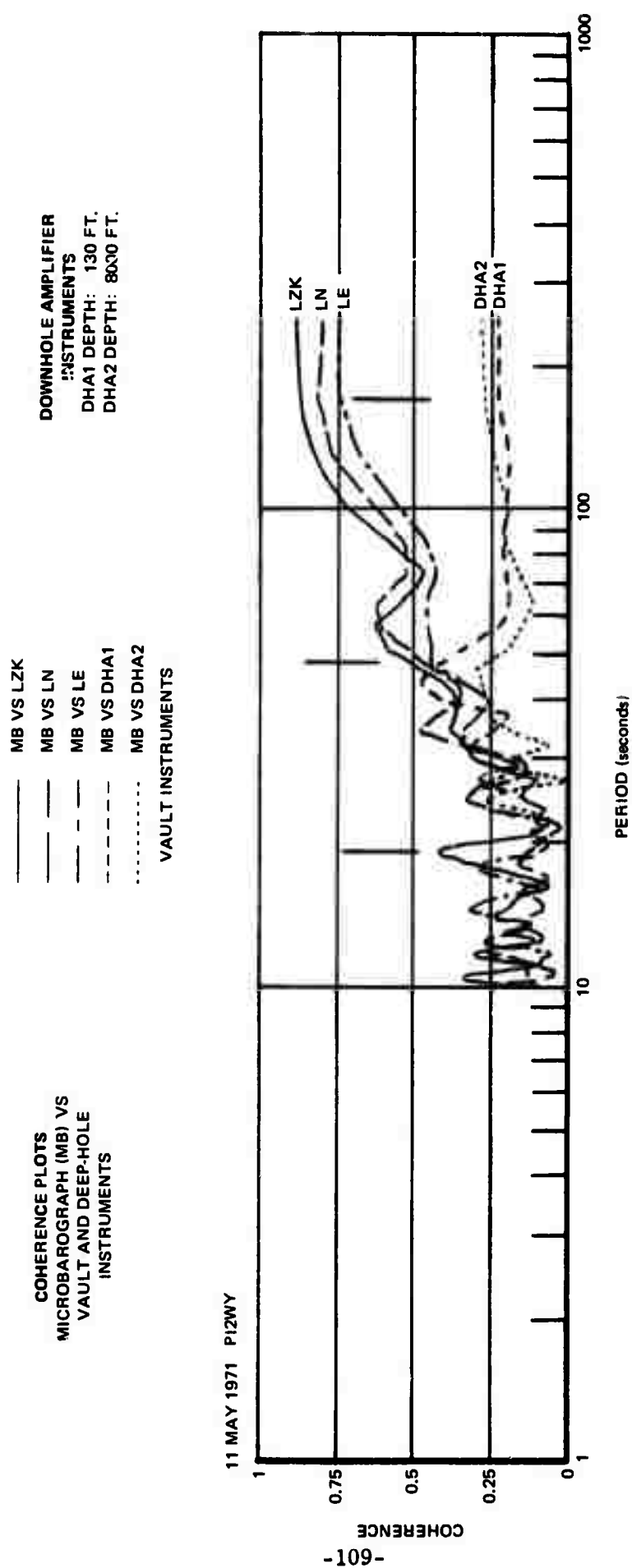
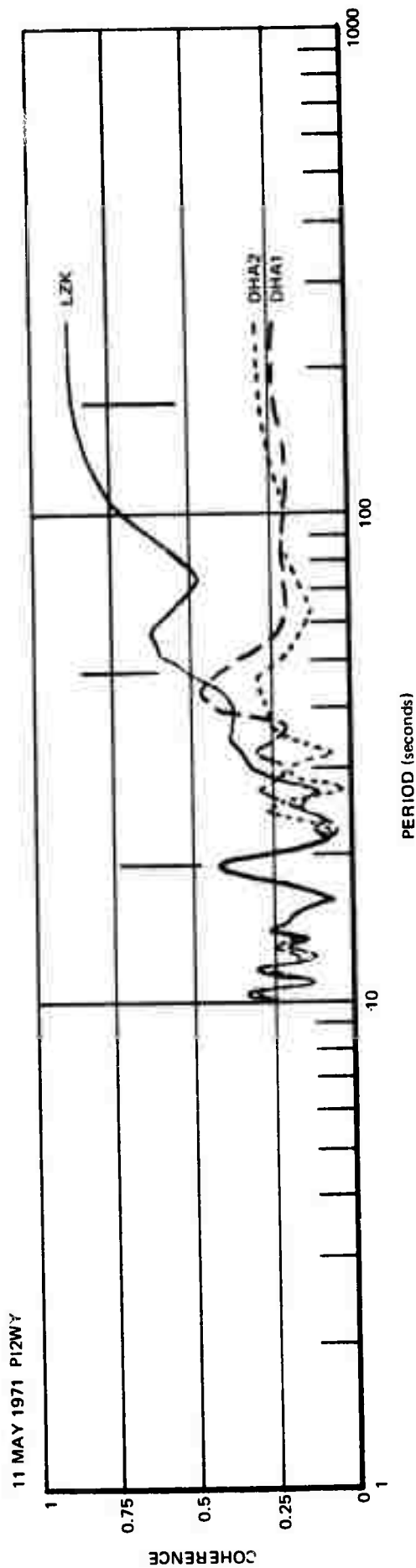


Figure 66. Coherence of long-period channels with respect to microbarograph during strong barometric activity

COHERENCE PLOTS  
 MICROBAROGRAPH (MB) VS  
 VERTICAL INSTRUMENTS

— MB VS LZK  
 - - - MB VS DHA1 ( 130 FT.)  
 . . . . MB VS DHA2 (8000 FT.)



-110-

Figure 67. Coherence of vertical channels with respect to microbarograph during strong barometric activity

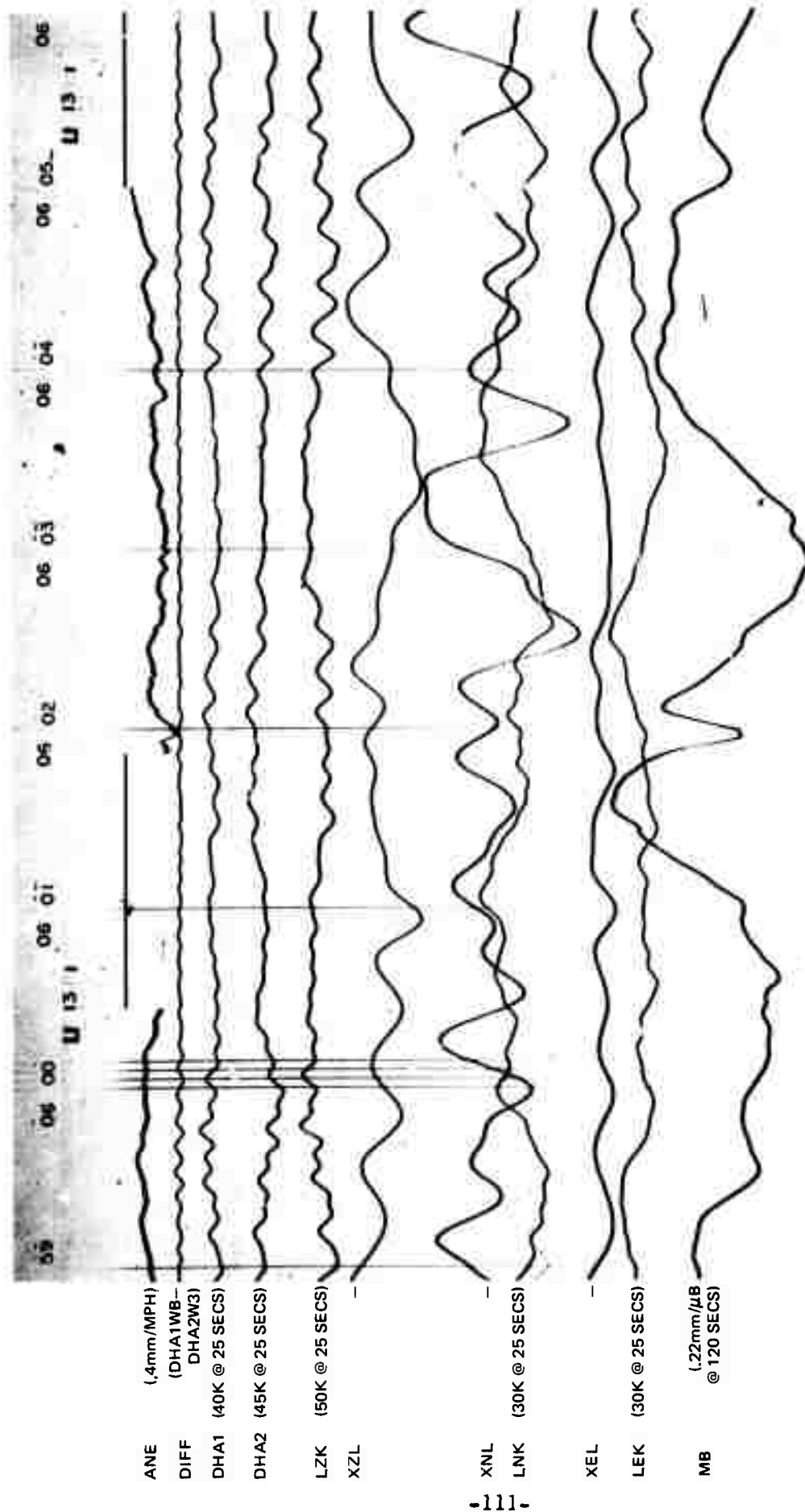


Figure 68. A section of the time series for processed data shown in figures 78, 79, 80 showing effects of atmospheric pressure variation

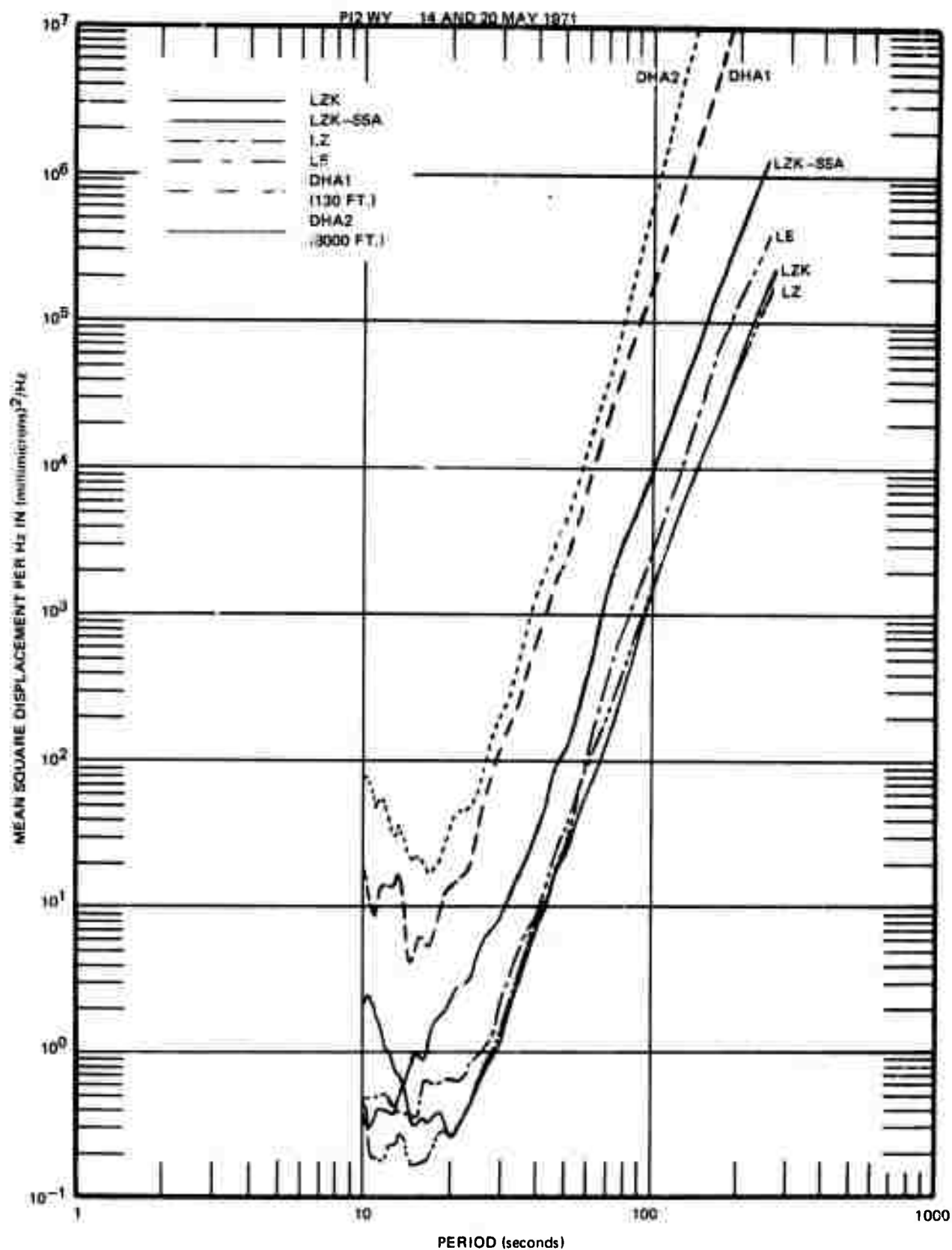


Figure 69. Power density spectra of system noise equivalent mean square displacement density

#### 6.5.8.1 Cable and Cable Header

Since the 23900 instruments were initially dry, leakage resistance measurements could be confidently used to observe leakage in the downhole cable and cable header. Two cable conditions were observed: (1) a cable where water had been forced, between conductor and conductor insulation, several thousand feet up the cable during an earlier deep-hole installation, and (2) an internally dry cable of the same type.

With the "wet-cable" the cable head must seal against external pressure and against water flow down the conductors. Standard and modified cable-head assemblies were used. Over a period of approximately 3 months at a depth of 8,000 feet, leakage resistance eventually dropped to about 1000 ohms on some circuits. This occurred with what was considered the best of the assemblies used.

Only high resistance leakage (about 10 megohms) was encountered with the "dry-cable" at a depth of 4,000 feet for about 1 month. This leakage, if it does not compound, would be satisfactory with downhole electronics and carrier transmission of the amplifier output.

A solution to cable and cable-head leakage will probably require "drying" of the "wet-cable" and an improved cable-head assembly.

#### 6.5.8.2 Holelock Mechanism

The standard holelock used with the Model 23900 transducer used an eccentric, gripping cam and the instrument weight to wedge the instrument against the side of the casing. As depth of operation increased, cable weight increased and the instrument became wedged more firmly in the casing. The "wedging" force developed by the mechanism depended on cam-length and casing diameter, i.e., the "wedge angle." In the 7-1/8 inch casing of the test hole, the force developed with the 5-inch cam was more than four times that developed with the 7-inch cam.

There was evidence that both cable weight and cam length affected the coupling between transducer and casing. One model by which coupling differences could be explained was that the holelock mechanism established a two-point contact with the casing. These points formed an axis about which the instrument could rotate except as constrained by the casing. Since the casing radius was almost twice the radius of the instrument, the constraint allowed significant rotation or instrument tilt. A relaxed cable was almost certain to act on the instrument at some angle about the axis and tilt the instrument.

For small angles and small variations, the sensitivity to tilt signals is proportional to the basic angle. With this model, tilt signals acting along the axis of rotation are tightly coupled to the instrument while signals acting about the axis of rotation are loosely coupled to the instrument. Instruments installed with random orientations should exhibit different directional characteristics. Instruments with the same orientation could still exhibit different sensitivities (and polarities) depending on initial tilt and surface forces acting between the instrument and casing.

Coupling differences were observed in the above at the 350-foot test hole where local conditions caused large surface tilts and cable weight was small. In operation at PI2WY, these differences were not obvious with a magnification of 50K at 25-seconds with the ALPN response, even at the 130-foot depth. However, at magnifications of 100K or greater, coupling differences could be significant with the "two-point" holelock. A "three-point" holelock located between seismometer and cable-head is recommended for future high-resolution systems.

A slippage of some type occurred at a depth of 1000 feet and a cable slack of 24 feet. It was thought that the instrument tilted or slipped in the hole due to excessive cable weight and/or marginal locking at a casing joint. At a subsequent depth of 8000 feet, a cable slack of 8 feet was allowed, and no further slippage occurred.

#### 6.5.8.3 Suspension Instability and Noise

Special attention was given to the 23900 modified suspensions in operational tests at the Garland test hole. Four units were modified and each was significantly different in alignment and behavior. All suspensions were sensitive to temperature variations, but major alignments made in the laboratory underwent very little change after stabilization in the 350-foot test hole. This consistency was not observed during actual field installation at PI2WY and have been partially due to generally lower temperatures on surface and at shallow depths. All suspensions and adjustment mechanisms exhibited large hysteresis, but with refined adjustment procedures, satisfactory but time-consuming, control was achieved.

Three types of suspension instability were observed. The most prominent type began with initial operation and subsided with diminishing rate and amplitude in about 96 hours. This type of instability produced a pulse breaking either up or down, depending on suspension history.

The second type of instability, characteristic of one unit (S/N 236), produced a longer period waveform sometimes difficult to distinguish from long-period background signals. This type of instability could be initiated by period adjustment only and could endure for more than 48 hours.

The third type of instability was observed as a long-term change in natural period. While this instability may have been a continuation of the second type, noise signals of the third type were either below system resolution or outside the system pass band. In operation at PI2WY, this drift did not diminish and adjustment was necessary at about 10-day intervals.

As mentioned earlier, a noise test mechanism was installed in the seismometer because use of the mass-lock mechanism was not rigid at noise level, and because almost a full stabilization cycle was incurred following its operation.

Suspension noise was attributed mainly to the relaxation of members put in high stress in order to extend the period. However, the unmodified suspension could prove to be unstable at the sensitivities required for high-resolution, long-period measurements. In a previous project, tests were conducted with a Model 6480 Johnson-Matheson seismometer equipped with a displacement transducer. External circuits were used to reduce the average spring constant in various degrees. With reduction ratios greater than about 20 to 1, the suspension exhibited severe nonlinearities, i.e., large changes in spring constant versus a small change in mass position - as much as  $\pm 10$  percent over a range of several microns.

These factors begin to show some of the practical, and sometimes hidden, advantages of the long-period suspension over the short period for this application. While small imperfections are difficult to observe, and therefore difficult to remove, in the short-period suspension, the same imperfections can be readily observed in the long period. After mechanical characteristics are improved, electronic circuits can then be used to provide a quasi-static centering force.

#### 6.5.9 Deep-Hole, Long-Period Capability

To estimate the level of background motion that can be anticipated in the deep-hole installation, data taken at several low-background mine installations have been plotted in figure 70. The plots are shown in terms of mean square displacement per Hz versus period on full logarithmic grid. Observed and theoretical system noise spectra are shown for the QC-AZ station.

At a period of approximately 45 seconds, the QC-AZ background plus system noise was only 10 dB greater than system noise alone. This separation decreased to approximately 5 dB at 80 seconds. Thus, for the low-background mine installations, instrument noise interfered with the long-period background at periods greater than about 45 seconds.

The dashed line passing through 100 (millimicron)<sup>2</sup> Hz at 100 seconds with a slope of 40 dB/decade might prove to be a satisfactory instrument noise level for deep-hole installations. This displacement power spectrum is equivalent to an acceleration power spectrum (zero slope) of  $1.56 \times 10^{-21}$  (meter per second<sup>2</sup>)<sup>2</sup>/Hz or  $1.62 \times 10^{-23}$  g<sup>2</sup>/Hz where g is 9.8 meter/second<sup>2</sup>.

Whenever there is a damping force of the form  $-\beta \dot{q}$ , where q is a generalized coordinate of an equilibrium system and  $\dot{q}$  is the time derivative, there will be an associated fluctuating force with power spectrum  $F_n$  of magnitude  $4kT\beta$ , i.e.,

$$F_n \frac{(\text{newton})^2}{\text{Hz}} = 4kT\beta$$

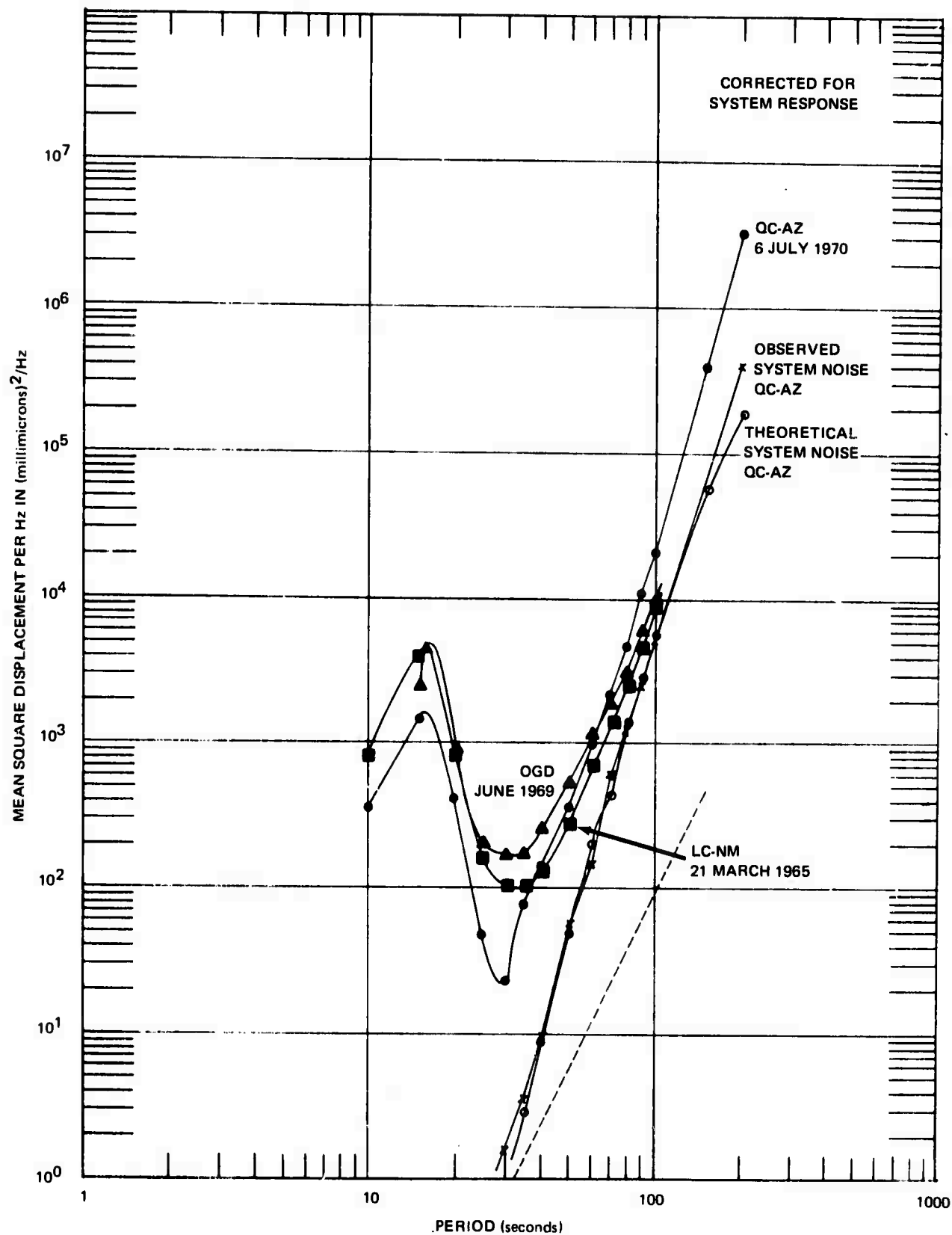


Figure 70. Comparison of backgrounds and system noise observed at mine installations QC-AZ, LC-NM, and OGD

where  $F_n$  is the noise power spectrum in (newton)<sup>2</sup>/Hz;

$k$  is Boltzman's constant,  $1.38 \times 10^{-23}$  joule/°K;

$T$  is the absolute temperature of the equilibrium system in °K (Kelvin),  
300°K here: and

$\beta$  is the coefficient of damping for the equilibrium system in  
newton per meter/second.

For a seismometer in thermodynamic equilibrium, the coefficient of damping  $\beta$  is related to the normalized equilibrium damping ratio  $\lambda$  and quality factor  $Q$  by

$$\lambda = \frac{\beta}{2\omega_0 M} ; \quad Q = \frac{\omega_0 M}{\beta} ; \quad Q = \frac{1}{2\lambda} ; \quad \omega_0 = \frac{2\pi}{P_0} = \sqrt{\frac{K}{M}}$$

where  $M$  is the suspended mass in kilograms,

$\omega_0$  is the natural frequency of the suspension in radians per second,

$P_0$  is the natural period of the suspension in seconds,

$K$  is the force constant of the spring in newton per meter.

An earthquake acceleration power spectrum  $A$  acting on the suspension produces an input force power spectrum  $AM^2$ . This relation can be used to establish an equivalent earth acceleration spectrum.  $A_n$  corresponding to  $F_n$  of the suspensions, i.e.,

$$F_n = 4KT\beta = M^2 A_n = M^2 \omega^2 Y_n$$

where:  $Y_n$  is the displacement power spectrum corresponding to  $A_n$  in  
(meter)<sup>2</sup>/Hz; and

$\omega$  is the angular frequency of displacement in radians per second.

Taking the  $Y_n$  value of 100 (millimicron)<sup>2</sup>/Hz or  $1 \times 10^{-16}$  (meter)<sup>2</sup>/Hz at 100-second period, gives an  $A_n$  value of  $1.56 \times 10^{-2}$  (meter per second<sup>2</sup>)<sup>2</sup>/Hz. By the above expression then, the operating characteristics of a suspension having this noise level must be such that

$$A_n = 1.56 \times 10^{-21} \frac{(\text{meter/second}^2)^2}{\text{Hz}} = \frac{4KT\beta}{M^2} \quad \text{or}$$

$$\frac{\beta}{M^2} = \frac{4\pi\lambda}{MP_0Q} = \frac{2\pi}{MP_0Q} = \frac{1.56 \times 10^{-21}}{1.66 \times 10^{-20}} = .094$$

It should be noted that these relations pertain to a system in thermodynamic equilibrium. System response characteristics associated with these parameters can be altered artificially by non-equilibrium mechanisms. It is the above equilibrium quantities that establish the ultimate resolution attainable with the suspension. The force power spectrum  $4KT\beta$  acting on the suspension and the  $1/2 KT$  equipartition energy of the suspension fluctuations, bear the statistical relation of input spectral density and mean square output, respectively.

Although  $\beta$ ,  $M$  are the independent variables, relations in terms of  $M$ ,  $P_o$ ,  $Q$ , or  $M$ ,  $P_o$ ,  $\lambda$  are sometimes more readily grasped in the following comparisons. Consider the product  $P_oQ$  as a function of  $M$ , i.e.,

$$P_oQ = \frac{2\pi}{M(.094)} = \frac{66.7}{M}$$

so that some of the combinations for the desired noise level are as follows:

<u>M</u> <u>kg</u>	<u>P<sub>o</sub>Q</u> <u>seconds</u>
0.01	6670
0.1	667
1.0	66.7
10.0	6.67
100.0	0.667

The deep-hole instrument must be restricted in outside diameter to approximately 5-inches and must be able to accommodate hole tilts as great as  $5^\circ$  (0.872 radian). Assuming that the suspension must be leveled to within a few seconds, the height  $h$ , and diameter  $d$ , of the suspension are restricted by

$$d \leq 4.50'' - 2(.0872)h.$$

In the following table 9, dimensions corresponding to various suspension heights have been computed along with the parameters of a simple brass pendulum that occupies the total available volume.

While the simple pendulum may not be the optimum suspension for this application, its use here allows an illustration of some of the magnitudes involved in the downhole package and shows that impossible conditions are not imposed on the suspension by the threshold requirement of  $1.62 \times 10^{-23} \text{ g}^2/\text{Hz}$ .

Table 9. Seismometer dimensions corresponding to various suspension heights and parameters of a simple brass pendulum that occupies the total available volume

Height inches	Diameter inches	Volume cubic inches	Mass kg	Period sec	MPo Kg sec	Q required 66.7/MPo	Maximum volume of cylinder	Maximum MPo
3	3.98	37.4	5.34	0.555	2.96	22.5		
6	3.45	56.1	8.00	0.780	6.24	10.7		
8.6	3.00	60.8	8.67	0.934	8.10	8.23		
11.05	2.57	57.4	8.19	1.06	8.66	7.70		
12	2.40	54.2	7.74	1.10	8.51	7.78		
18	1.36	26.2	3.73	1.35	5.04	13.2		
24	0.32	1.93	0.275	1.56	0.429	155		
25.8	0	0	0	-	-	-		

#### 6.5.10 Summary

Existing short-period, deep-hole facilities and instrumentation have been modified for long-period measurements (6.5.6.1, 6.5.6.2), tested (6.5.6.3), compared with other long-period systems (6.5.6.4) and used for field measurements (6.5.7). Magnifications to 50K (vertical, ALPN response) were achieved. Major limitations were imposed by transducer-amplifier resolution, suspension instability, and cable (header) leakage.

Field measurements showed that the response of the deep-hole system to barometric effects was greatly reduced relative to the vault system. However, the reduction observed at a depth of only 130-feet was such that further reduction with depth was overshadowed by system noise - only minor additional reduction was apparent at depths of 1000 feet and 8000 feet.

Problems encountered in installation and operation have been discussed (6.5.8) for reference in future work. It is anticipated that the merit of the long-period, deep-hole or borehole system as a means to improve horizontal and vertical measurements and reduce installation cost will justify further consideration and improved instrumentation.

A value for the desired resolution of a 3-component long-period borehole instrument has been discussed (6.5.9) along with other requirements. The instrument must be capable of long-term operation at a fluid depth of greater than 1000 feet, have an outer diameter no greater than approximately 5 inches, have a leveling mechanism to accommodate hole tilt to 5 degrees, and have a noise level no greater than approximately  $1.6 \times 10^{-23} \text{ g}^2/\text{Hz}$ .

There are two known activities that are of direct interest to this application. One is the development of a small-mass accelerometer<sup>1</sup> by Block and Moore. The other is the development of a 3-component, long-period, borehole instrument actively undertaken by Teledyne Geotech during 1971.

---

<sup>1</sup>Block, B. and R. D. Moore. Tidal to seismic frequency investigations with a quartz accelerometer of new geometry, J. Geophys. Res., 75, No. 8, 1493-1505, March 10, 1970.

## 6.6 LONG-PERIOD STUDIES AT FAIRBANKS, ALASKA

### 6.6.1 Objective

A background noise problem existed during winter conditions at the Alaskan Long-Period Array (ALPA), Project VT/8707. Support effort was required to collect microbarograph and conventional surface long-period reference data to aid in the analysis and evaluation of the ALPA instrumentation system performance. A Long-Range Seismic Measurements (LRSM) mobile observatory (Van No. 219) on standby status in the ALPA area was to be utilized for the effort. Microbarograph data were to be provided to determine if the long-period noise could be correlated with pressure changes. Surface long-period seismograph data were to be provided in order to compare long-period noise at depth with that at the surface. Immediate information of test results was to be provided from analysis of Develocorder data, and data from magnetic-tape recordings were to be available for more extensive analysis. Figure 71 is a block diagram of the seismograph system at station FB2AK.

### 6.6.2 Site Selection and Preparation

ALPA site 3-3 was selected as the location for the LRSM monitor station, primarily because of its usual high winter background noise and access conditions at the site. Also, the LRSM station (Fairbanks, Alaska, FB-AK) at ALPA site 3-4 was not at a typical ALPA installation, since it had a deeper cased borehole, (165 feet working depth).

The LRSM site designation for the new Fairbanks, Alaska, location at ALPA site 3-3 was FB2AK. Neither permafrost nor thick loess/silt is encountered at FB2AK, and previous ALPA construction landscaping at the site had exposed weathered bedrock. The crystalline Birch Creek Schist Formation of Precambrian-Lower Paleozoic age outcrops in this area, and although fractured, the rock is hard and dense at about 1.5 meters (5 ft) depth. Fractures and relict bedding planes in this quartz-mica schist contribute to the inclined formational layering. The working depth inside the borehole casing at the FB2AK (ALPA 3-3) site was 54-1/2 feet from the original wellhead, comparing favorably with the 56-foot average working depth of 18 ALPA sites (without ALPA site 3-4). This FB2AK (ALPA 3-3) site is the southeastern element of the 19-element Alaskan Long-Period Array, and is located north of Chena Hot Springs Road in the SE 1/4 of Section 13, T 1 N, R 1 E, FBBL&M. Geographic coordinates for the site are latitude 64°54'36" N, longitude 147°26'47" W, with an elevation of approximately 343 meters (1125 feet) above mean sea level at the wellhead.

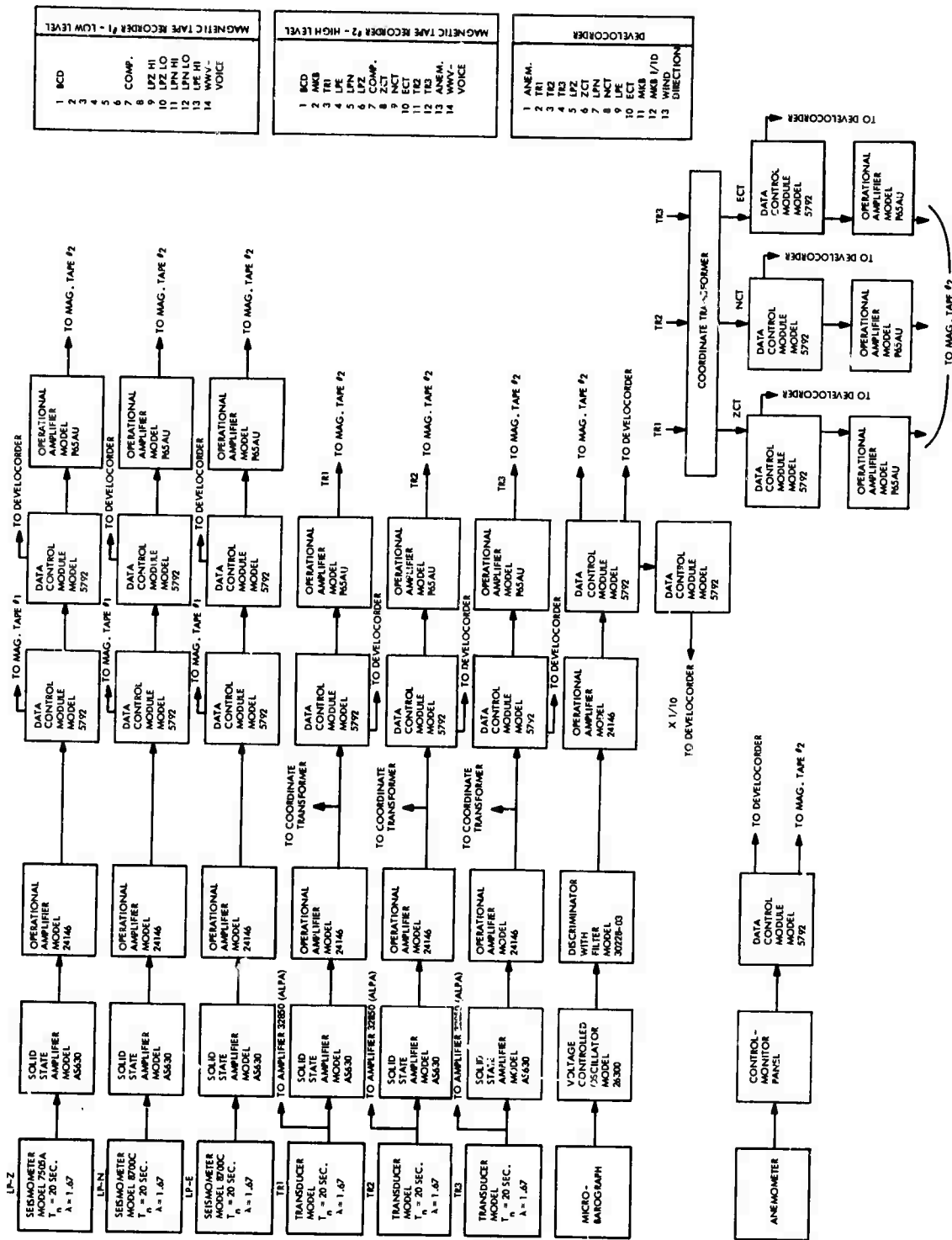


Figure 71. Block diagram of seismograph system at FB2AK

During 1968-69 operations at the old FB-AK (ALPA 3-4) site near Murphy Dome, the wheeled undercarriage assembly had been removed from the van and it was set on cement pads. This van was moved with major portions of the surface equipment to test site FB2AK, Fairbanks, Alaska (ALPA site 3-3), on 01 May 1970. Surface preparations including three Melton-type long-period tank vaults, one half-shell type short-period tank vault, a sheltered concrete pier for possible installation of phototube amplifiers, etc., were finished on 05 May 1970. Load restrictions prevented road aggregate hauling and spreading along the access trail off Chena Hot Springs Road until 19 May 1970. The layout of the FB2AK site is shown in figure 72.

### 6.6.3 Operations and Tests

Team members arrived at the FB2AK site on 12 May 1970. Power generator and site access problems hindered the site installation. Routine recording operations were begun on the following dates:

<u>Recorder</u>	<u>Instruments</u>	<u>Date</u>
Develocorder	Surface Long-Periods Microbarograph Anemometer	7 June 1970
Tape System No. 2 (High seismic back-ground input level)	Surface Long-Periods Microbarograph Triax (raw and transformed) Anemometer	9 June 1970
Tape System No. 1 (Standard LRSM seismic back-ground input level)	Surface Long-Periods at high and low gain	12 June 1970

Because of recurring problems with the 15 kW U.S. Motors power generator at the FB2AK station, a Deutz-Tate 30 kW diesel generator was rented in Fairbanks. The generator was installed in a shelter and routine operations resumed 31 July 1970. A Government-furnished International-Fermount 20 kW diesel generator arrived at the site on 13 August 1970, but trial operations indicated suspect reliability, and this 20 kW unit was never continuously operated at FB2AK. On 3 November 1970, the Deutz-Tate 30 kW rental unit failed, and the U.S. Motors 15 kW generator was placed into intermittent operation. A new Perkins-Kato 30 kW generator was rented and supplied power to the FB2AK station on 13 November 1970. This Perkins-Kato unit provided station power until operations terminated on 14 June 1971.

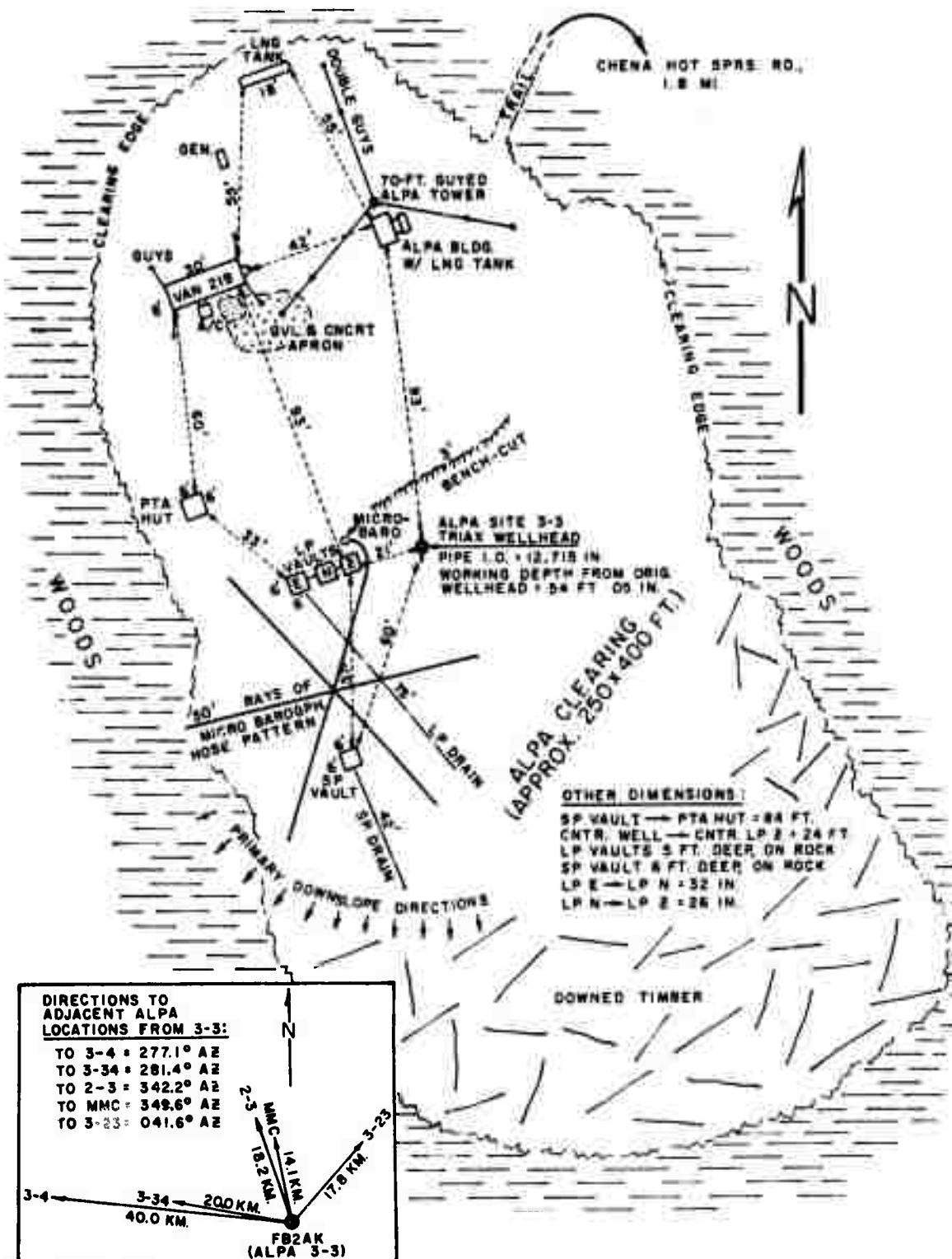


Figure 72. Fairbanks, Alaska (FB2AK) site layout

G 5847

At the end of August 1970, sufficient data had been collected to start evaluating the background noise recorded by the surface long-period seismographs and the borehole long-period triaxial seismographs.

The response of the surface and downhole systems were found to be closely matched by comparing surface waves from large events. Figure 73 shows the long-period frequency response at FB2AK. Figures 74, 75, and 76 show preliminary results of the data analysis with one set of spectra computed and with system noise levels not analyzed. The antialias filter used when digitizing eliminated the 10-second microseismic peak.

Figure 74 shows the long-period noise spectra of the surface vertical and coordinate-transformed downhole vertical. The wind velocity was less than 5 miles per hour during the time this sample was taken; no wind-generated noise was visible on any of the traces. As expected, in the period range where traveling wave energy is present (<25 seconds), the spectra are almost the same. For periods greater than 25 seconds the downhole seismograph noise level is appreciably lower than at the surface. This behavior is in quantitative agreement with visual observation of the 16-mm film recordings; extremely long-period noise can be seen on surface vertical trace at most quiet times, but not on the downhole seismograph. These preliminary observations were made during July and August 1970, prior to the arrival of the winter-associated noise.

Figure 75 shows the spectra of the surface and downhole verticals during a time when the wind was blowing 15-20 miles per hour. The microseismic peak is higher than that shown in figure 74; however, the samples are 2 days apart and the microseismic level is known to change from day to day. The peak at 120 seconds on the surface spectra did not change from the windless sample while the triaxial vertical increased significantly. Conclusions on this phenomenon were withheld until the system noise level spectra were computed. Figure 76 shows the coherences between the vertical surface and downhole long-period seismographs obtained from the same data used to compute the spectra shown in figures 74 and 75. The coherences are high between 10 and 30 seconds, the period range where microseismic activity predominates. For periods greater than 30 seconds, the coherence levels are close to the expected zero level, indicating that there is no linear relationship between the two outputs. Coherences computed between the surface microbarograph and the surface and downhole vertical seismographs recordings for the same times discussed above indicate that there was no significant coherence in the period range under discussion (10-256 seconds). This result was not unexpected as the results obtained during the Grand Saline, Texas (GA-TX and GA3TX) experiment indicated the same type of behavior during most of the recording period. Again, these preliminary observations were made during July and August 1970, prior to the arrival of winter-associated noise.

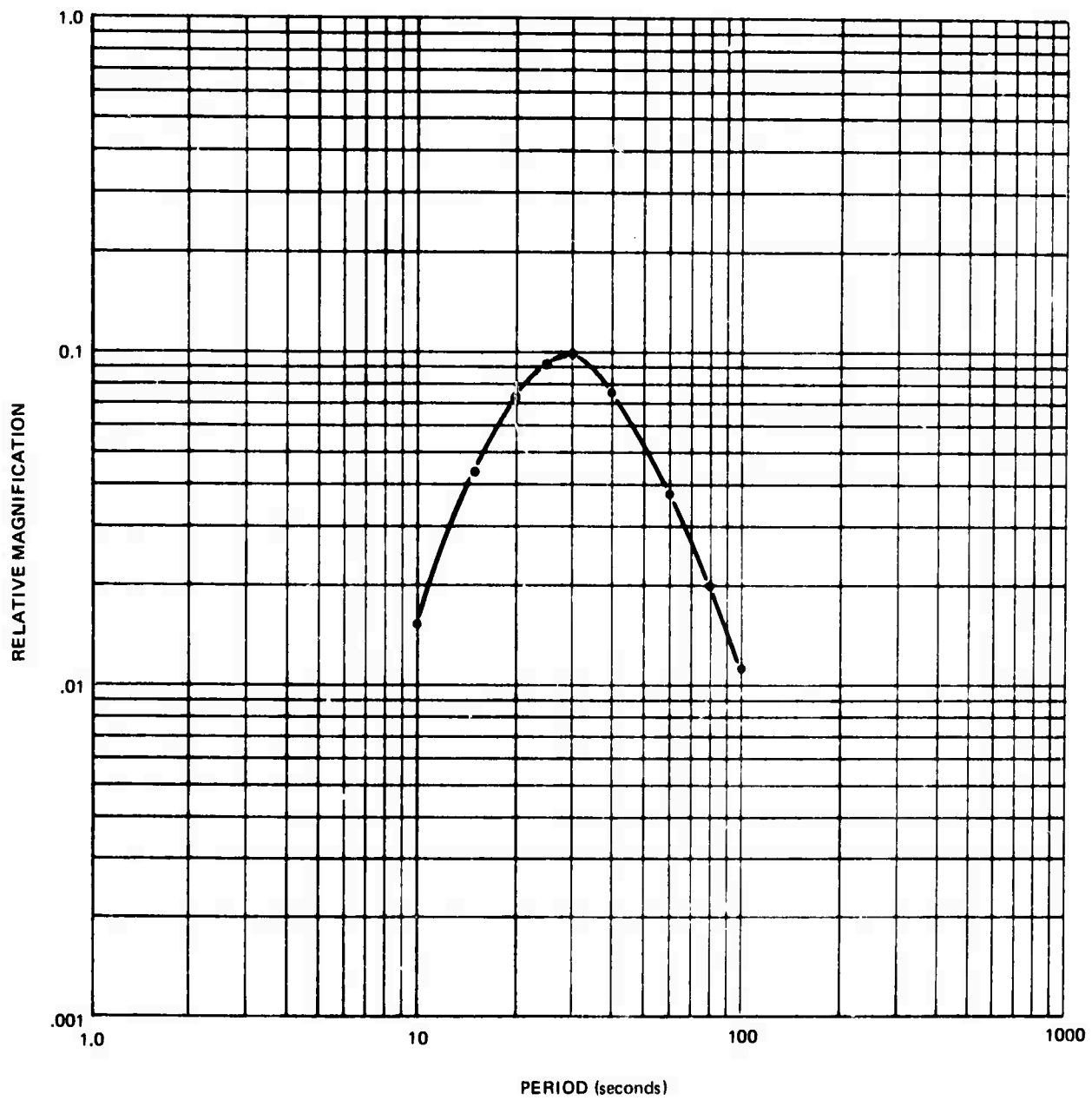


Figure 73. FB2AK long-period frequency response

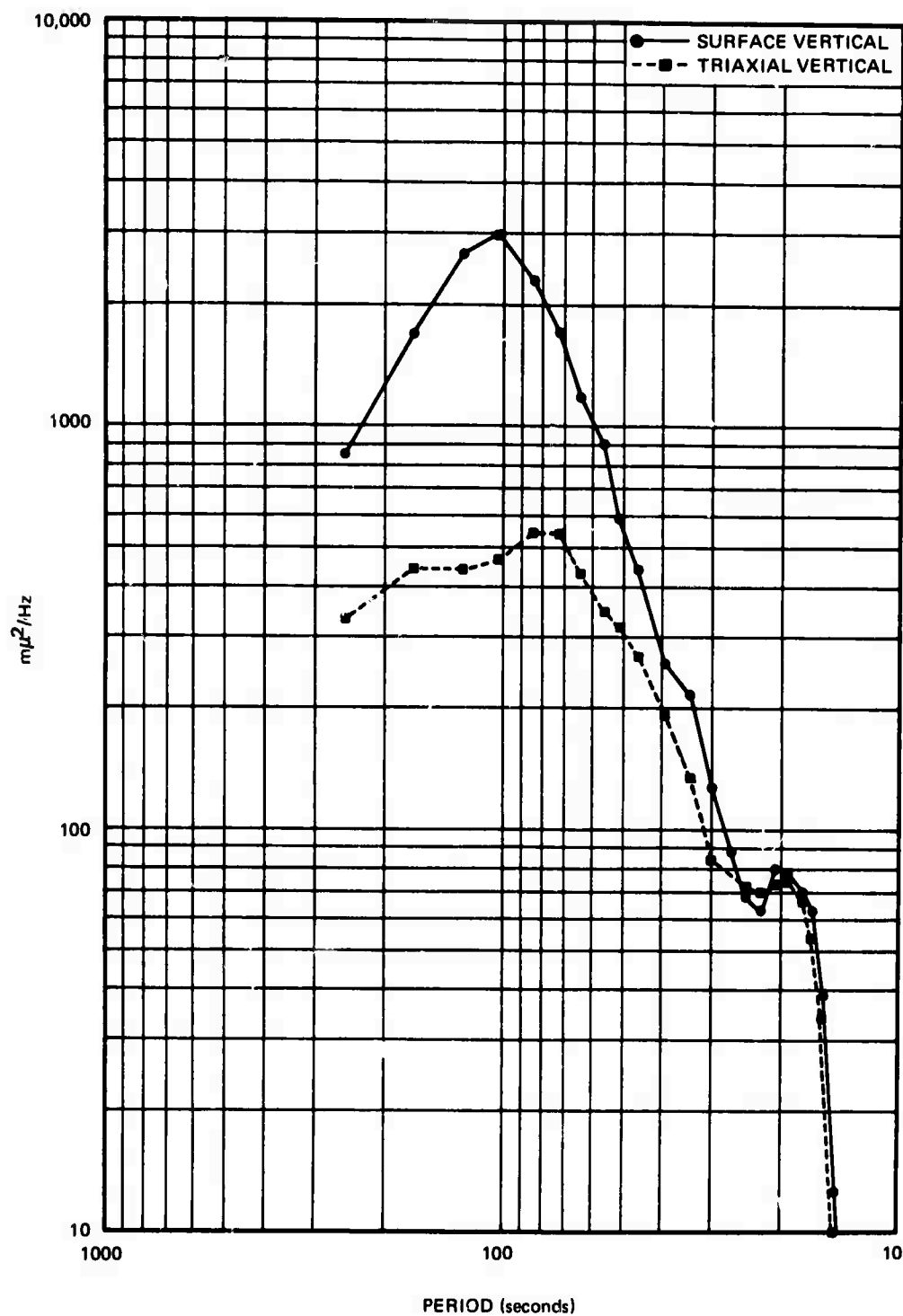


Figure 74. Spectra of the long-period seismograph background noise. Wind velocity 0-5 miles/hr. Not corrected for seismograph response

G 5988

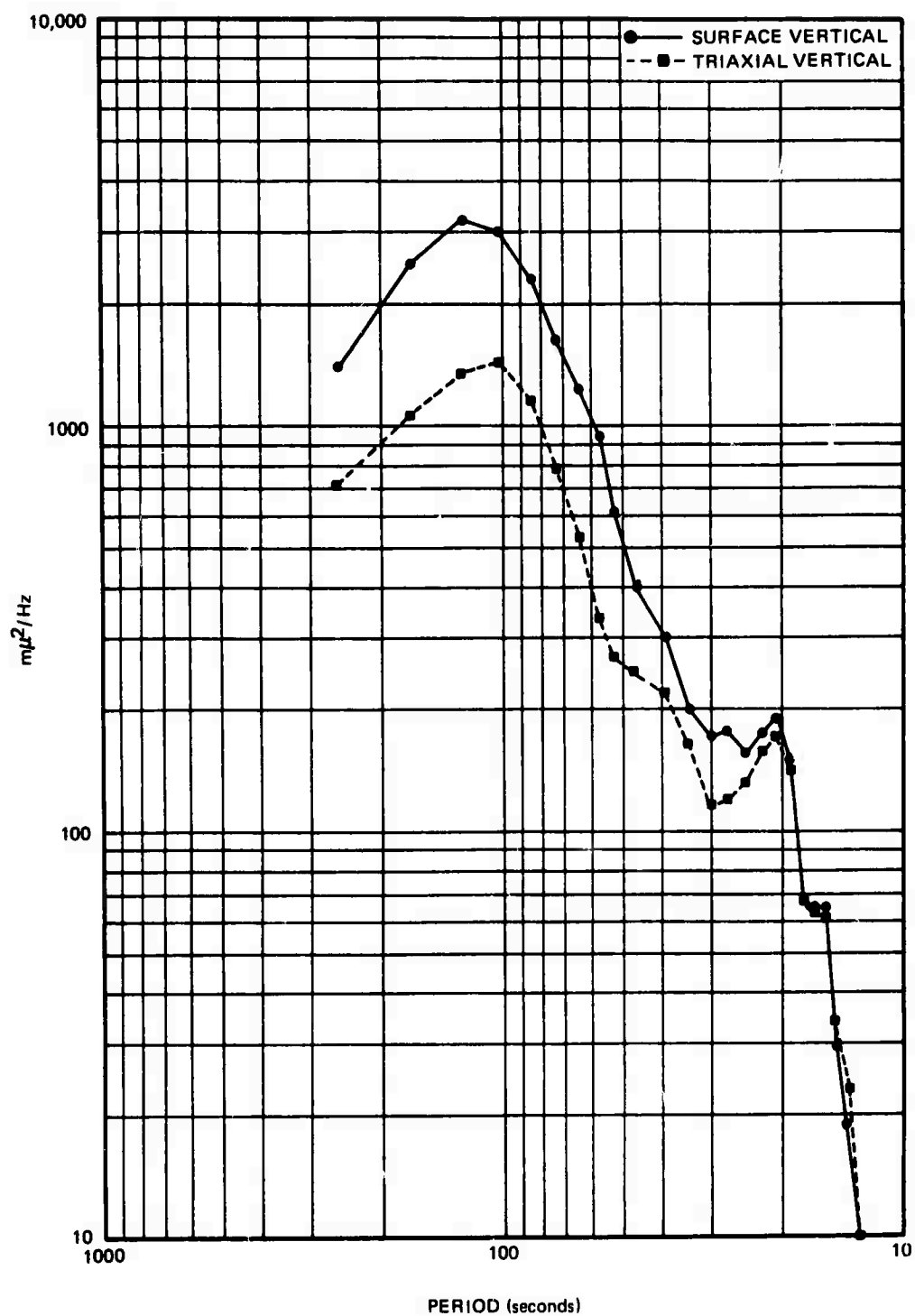
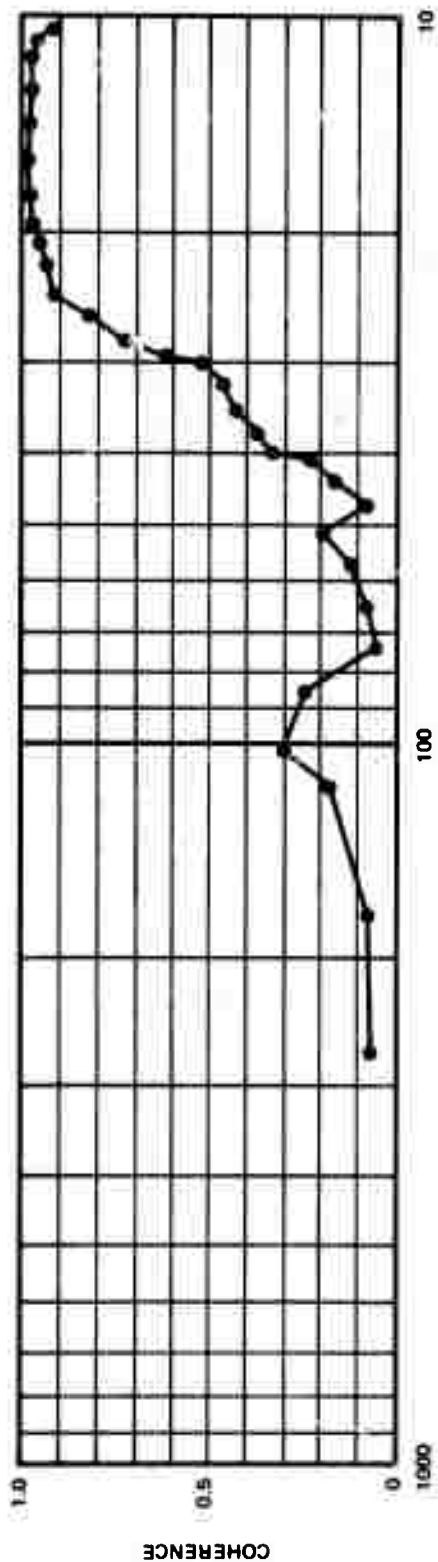
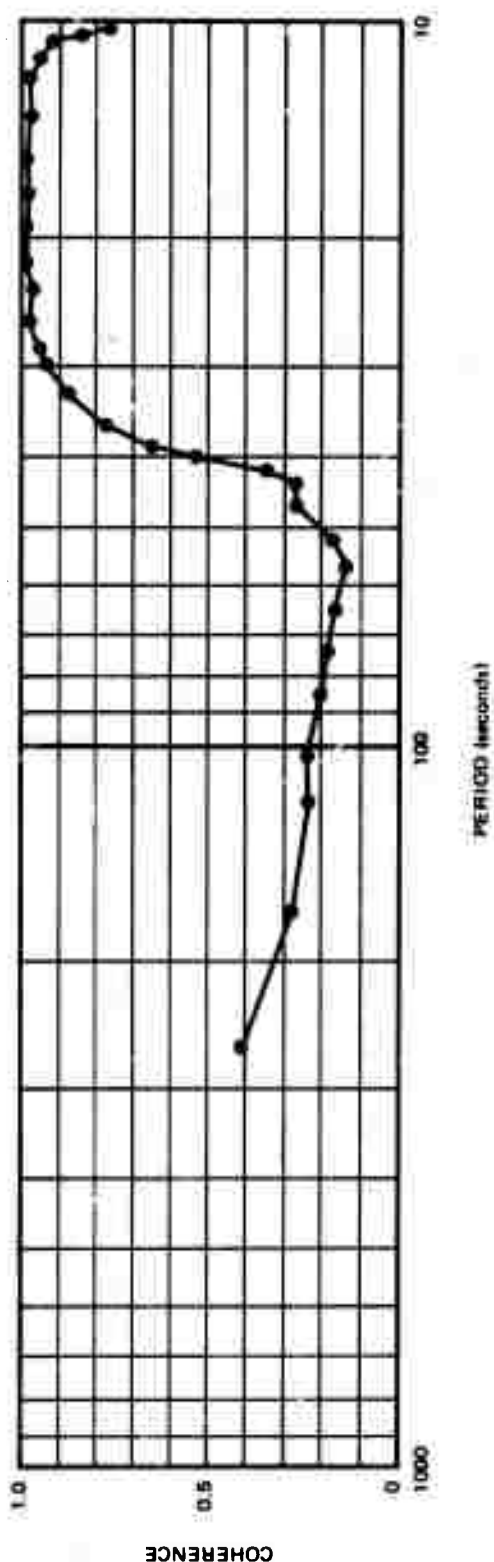


Figure 75. Spectra of the vertical long-period seismograph background noise. Wind velocity 15-20 miles/hr. Not corrected for seismograph response

G 5989



a.



b.

Figure 76. Coherences between long-period vertical seismographs at the surface and at 60 feet:  
a. wind velocity 15-20 miles/hr; b. wind velocity 0-5 miles/hr

Visual examination of the long-period horizontal seismographs shows that, as expected, the surface horizontals were seriously affected by wind-generated tilts. The attenuation of this type noise was quite rapid with depth; the coordinate-transformed triaxial horizontals were much less affected than the surface horizontals. There was a distinct directional effect connected with the wind-generated tilts. The north and east components were out of phase ( $\pm 30$  degrees) almost all the time, regardless of the direction of the wind, indicating a preferential tilt in a northwest-southeast direction. Furthermore, the attenuation with depth of the tilt was considerably larger in the north direction than in the east direction. These preliminary observations were also made during July and August 1970, prior to the arrival of winter-associated noise.

In September 1970, excessive data trace excursions ("spikes") occurred on the surface long-period north system (LPN). This "spiking" problem on the LPN data continued through February 1971. Efforts to correct this situation included heat-cycling the Model 8700C long-period horizontal seismometers, partial suspension and flexure disassembly, actual replacement with a new seismometer, etc. The LPN system was inoperative for considerable periods of time during the winter months of 1970-1971. On 04 March 1971, the LPN system was again placed in operation as a low gain channel, and by mid-March 1971, with the apparent end of below 0°F weather, the LPN noise level was generally comparable to the surface long-period east system (LPE), with only a few spikes. The LPE data had also contained intermittent spikes during the winter months, but not as severe as the LPN. In fact, all three surface long-period seismographs (LPZ, LPN, and LPE) had quieted by mid-March 1971, and were comparable to the borehole long-period triaxial seismograph data during low wind durations. The high noise level on the surface long-period horizontal seismographs during the winter months may have been related to the environment and/or vault-type installation rather than to problems in the seismometers themselves. The spiking noise was not reduced by replacement of the LPN seismometers in January 1971, nor was anything specifically wrong discovered in the seismometers during maintenance.

In October 1970, the noise level at site FB2AK in the period range of 50-70 seconds had increased appreciably. Identification of the source and elimination of the effect of this background noise was the primary objective of the project. The noise was related in some unknown manner to a decrease in daily temperatures, and was not generated by atmospheric pressure changes as recorded by the surface microbarographs. Relationships between the horizontal coordinate-transformed long-period triaxial seismograms remained constant; the two traces were approximately of the same amplitude and in phase, indicating either an apparent displacement or tilt in the northeast-southwest direction. These displacements or tilts did not appear to be present in the earth as the adjacent surface long-period horizontal seismometers did not respond to this motion.

Examination of earthquake signals showed that all the FB2AK seismographs were responding correctly to true earth motion. Also in October 1970, response of the borehole triaxial seismometer package to rapid warming and cooling of the air inside the top of the sealed borehole casing was observed. As a light bulb installed in the top of the borehole casing was turned on and off; the noise level (40-70 second period) decreased a few minutes after the light bulb was turned off and did not increase until 8 hours later. The cause of this noise was thus again related to temperature changes but the manner in which such temperature changes actuated the apparent movement of the triaxial seismometer masses was not evident.

In November 1970, thermistors were installed inside the borehole casing at the top, at the 15-foot depth, and at the 46-foot depth (near the top of the triaxial seismometer package). Circuitry was available for recordings temperature changes detected only by the 15- and 46-foot depth thermistors. A heater adjustable to up to 196 watts output was also installed inside the borehole casing at the 60-foot depth, but was not operated in November 1970. The temperature measured inside the top of the borehole casing was about  $-1^{\circ}\text{C}$ . The interior borehole casing temperature at the 15-foot depth was approximately  $+3^{\circ}\text{C}$ , and varied a few hundredths of a degree. The temperature just above the triaxial seismometer package at the 46-foot depth remained nearly constant at  $+2^{\circ}\text{C}$ , with no recorded temperature variations comparable to those at the 15-foot depth. Although minor changes occurred in these temperature values during late November and early December 1970, the relationship held that air inside the borehole casing at the 15-foot depth was warmer than the air at either the top or at the 46-foot depth, and that air inside the top of the borehole casing was colder than the air near the bottom of the casing at the 46-foot depth. These temperature variations indicated that air convection currents were present inside the borehole casing.

Also in November 1970, surface microbarograph recordings showed an increase in level of atmospheric pressure variations, with continuous 4.0 second period microbaroms which were almost never present at site FB2AK in the summer of 1970. Long-period oscillations with periods greater than 100 seconds were another new feature recorded by the surface microbarograph in November 1970. The origin of these 100-second oscillations was unknown, but they were associated with moderate wind conditions and were recorded by the long-period seismographs.

Excessive snow accumulation in the FB2AK site region during December 1970 hampered station operations. The heater in the borehole casing was operated at the 10-foot depth from 3 to 10 December 1970 at various output settings. No appreciable change was noticed when the heater was operated at wattages up to about 60 watts. Above the 60-watt output, the noise level in the 50- to 60-second period range increased on the triaxial seismograms. When the hole heater was turned off, this noise level decreased, but did not disappear. On 11 and 12 December 1970, a baffle was placed in the borehole casing at the 44-foot depth (2 feet above the triaxial seismometer package). The hole heater was attached to the bottom of the baffle. An insulation combination of crumbled polystyrene aggregate in bags, plastic container-plugs filled

with frothed urethane, and loose crumbled polystyrene aggregate was emplaced in the borehole casing atop the baffle up to the 15-foot depth. On 29 December 1970, additional insulation consisting of loose crumbled polystyrene aggregate was placed in the borehole casing up to the 3-foot depth. A 100-watt light bulb with adjustable output circuitry was also installed at the 2-foot depth in the borehole casing. The triaxial long-period noise amplitude decreased significantly after installation of the baffle and insulation in the borehole casing at site FB2AK (ALPA 3-3), but the noise amplitude over the entire ALPA network had also decreased, and no definite conclusions could be made concerning the effectiveness of these efforts. The hole heater just below the baffle and near the top of the triaxial seismometer package was operated at a 1-watt output on 15 December 1970, and no change in background was noticed either during or after the heater operation. By the end of 1970, insufficient data had been recorded to evaluate hole insulation and hole heater test modifications.

Extremely cold weather in January 1971, made performance of even the most routine maintenance and testing at site FB2AK difficult. Recording of long-period surface and downhole triaxial data was continued. The borehole casing was sealed with an approximate 180-hour time constant, and a replacement long-period surface seismometer was set in the LPN vault. The hole heaters were not operated and no further tests were conducted on the long-period triaxial system in January 1971.

On 30 January 1971, after a power generator failure, the recording van at the FB2AK site suffered fire damage. Approximately 16 square feet of interior wall near the propane wall heater was partially burned, but no other equipment was damaged. Electric heaters were normally used inside the van because propane vaporization problems occurred at the extremely low temperatures during the winter of 1970-71. The propane heater had been started in an attempt to warm the van while the team members were trying to restart the power generator. The automatic fire extinguisher in the van discharged, effectively stopping the fire. The van wall heater was removed and a hand fire extinguisher was used to ensure that the fire was out. On 03 February 1971, operations at FB2AK were resumed after restoring station power and repairing the interior van wall. Power generator problems on 25 February 1971 also resulted in the station being inoperative. The initial generator problem resulted in further equipment malfunctions (voltage fluctuations, batteries freezing, etc.) that required attention before satisfactory operations could be resumed on 03 March 1971.

From February until mid-March 1971, efforts at the FB2AK site were directed toward improvement of the operation of the surface long-period instruments and special wellhead tests on the triaxial system in cooperation with ALPA personnel. These tests were generally concerned with the effect of pressure pulses into the sealed borehole casing and the removal of the baffle and insulation from the casing.

Continued tests on the long-period triaxial seismometer at site FB2AK (ALPA 3-3) were as directed by the Project Office.

In mid-March 1971, a special, accelerated test program was initiated to obtain data necessary to determine the sources of unexplained noise in the long-period range (near 50 seconds period) at the ALPA, and to investigate means to eliminate or reduce the effects of this noise. Sufficient data had been collected to define the nature of the noise problem, but not its cause. The winter season at the ALPA was drawing to a close, and with only a maximum of 6 to 8 weeks of expected winter-associated noise remaining, the need for controlled experimentation became urgent. The special test program was outlined in a Project Office plan received at Geotech on 11 March 1971. The accelerated effort was to be accomplished as part of Project VT/0703 in conjunction with Projects T/1703 and T/1707. The mobile observatory at site FB2AK (ALPA Site 3-3) was to be the principal special test facility. Included in the special test program were specifications for an on-site engineer to supervise and coordinate field tests, additional triaxial seismometer package testing at the ALPA Monitor and Maintenance Center (MMC), pressure pulse tests with triaxial seismometer package rotation, borehole casing air evacuation, triaxial seismometer casing perforation, borehole casing microbarograph and temperature gradient tests, emplacement of a special subsurface vault covering the wellhead at ALPA Site 3-23 (later performed at ALPA Site 2-3), raising and locking the triaxial seismometer package at positions within the borehole casing at ALPA Site 2-3, tests with triaxial seismometer package stiffeners, equipment and supplementary tests at other facilities (Garland and Wills Point, Texas), extension or modifications of these tests to exploit the most promising areas of investigation, etc.

Detailed operations and results obtained in performance of the special test program are presented in a separate report: Technical Report No. 71-22, Alaskan Noise Field Investigation, March through June 1971. Operations and tests from mid-March until the FB2AK station termination on 14 June 1971 will only be summarized here.

By the end of March 1971, and the apparent end of severely cold weather, the winter-associated, long-period, high-amplitude background noise detected by the triaxial seismograph had almost disappeared at site FB2AK. External cooling of the wellhead by the application of dry ice was then used during triaxial seismometer tests to artificially approximate conditions associated with the high noise amplitudes. During the month of April, primary emphasis was placed on various triax seismometer tests at FB2AK, generally following the test plan recommended by the Project Office. Installation of the special subsurface wellhead vault at ALPA Site 2-3 was started on 30 March and completed on 12 April 1971, with provisions for operating a microbarograph isolated from spurious pressure and temperature changes. These pressure and temperature isolation provisions for a microbarograph were also utilized at the FB2AK site (ALPA 3-3), and a microbarograph to sense internal pressure changes within the borehole casing was placed into operation there on 11 April 1971. One noteworthy development during April 1971 indicated that noise-producing pressure changes within the borehole casing were caused by convection cells in the air near the top of the casing that in turn resulted from external cooling of the wellhead. The borehole casing was completely filled with crumbled polystyrene aggregate, capped with expanding urethane froth insulation, and sealed with

the wellhead plate on 13 April 1971. The internal sensing microbarograph and downhole long-period triaxial background data quieted almost immediately after filling the borehole casing.

Various long-period triaxial seismometer tests continued during May 1971, including installation of a stiffener assembly which was positively clamped around the triax package at the FB2AK site. This stiffener assembly consisted of a modified section of 11-3/4 inch OD, 52-1/2 lb/ft oil field casing. The stiffened triax package was operated in the cased borehole in several different operational positions (on-bottom, locked uphole, rotated, etc.). Pressure pulse tests performed for each operational position showed that all three stiffened triaxial modules always responded with a negative trace deflection for a positive pressure change. The stiffener assembly apparently constrained the triaxial package in some way since the polarity of previous pressure pulse responses was for the most part unpredictable without the stiffener. In addition to tests at FB2AK, tests were performed at ALPA Site 3-34 involving borehole casing air evacuation, rotation of the triaxial package, and pressure pulses.

During 29 May to 5 June 1971, the pressure seal of the individual modules in the triaxial package at site FB2AK was checked while the package was out of the cased borehole for sealing the enclosing stiffener assembly. The bottom two modules (TR1 and TR2) did not leak. The top module (TR3) had a slight air pressure leak due to a missing gasket at the lower data cable connector in the triax stabilizer. A gasket was installed and the problem was solved. It is not known what effect, if any, this air leak in TR3 had on previous pressure tests. Sealing compound was placed in the annular space between the triaxial package and the inside of the stiffener assembly case at positions near the top of the top module (TR3) and the bottom of the bottom module (TR1). Holelock and stabilizer functions were unaffected by this sealing. The sealed, stiffened triaxial package was installed in the borehole on 5 June and tests were resumed on 7 June. The tests consisted primarily of pressure pulses into the borehole casing with the sealed and stiffened triaxial package in various positions of operation: on-bottom and on the holelock at both standard and at 120° counterclockwise rotations.

Data for most tests showed that TR1 and TR2 produced a negative deflection for a positive pressure pulse and TR3 was positive. Previous pressure pulses on the triax with the unsealed stiffener had produced negative deflections on all modules. The overall results of this and previous tests at FB2AK indicated that it was not possible to predict the polarity or the amplitude of the pulse on any triaxial module in response to a pressure pulse. Also, there was no evidence that the stiffener assembly, either sealed or unsealed, improved the operation of the long-period triaxial seismometer in any significant manner.

At the end of the recording run on 14 June 1971, operations at FB2AK were terminated as directed by the Project Office. The van and equipment were left in "mothball" status in preparation for expected future operations. All equipment was secured and external cables were disconnected to prevent possible lightning damage. Rental equipment, including the generator, was returned. The Government-furnished 20 kW International-Fermount diesel generator was

returned to Fort Wainwright, at Fairbanks, Alaska. During the removal of the stiffener assembly, the triaxial package fell, and two of the three modules were damaged. Spare modules were obtained from the ALPA facility and the downhole long-period triaxial seismometer was placed in standard operation at FB2AK (ALPA Site 3-3) by 16 June 1971. All LRSM personnel left this Fairbanks, Alaska, site by 21 June 1971.

#### 6.6.4 Results

As previously mentioned, operations and results of the special test program are presented in a separate report: Technical Report No. 71-22, Alaskan Noise Field Investigations, March through June 1971. Preliminary, field results from station FB2AK, for May 1970 through June 1971 under Projects VT/0703 and T/1703 are, however, herewith briefly listed:

- a. Wind-generated earth tilt effects in the summer of 1970 were rapidly attenuated with depth as seen in comparing the surface and downhole long-period seismograms;
- b. A preferential wind-generated earth tilt direction of northwest-southeast was noted regardless of the wind direction (surface long-period seismometers);
- c. For periods greater than 25 seconds the downhole long-period vertical seismograph noise level was appreciably lower than that of the surface long-period vertical in the summer of 1970;
- d. The winter-associated noise in the 50-70 second period range on the downhole long-period triaxial seismograph increased in October 1970, when the minimum daily temperature values approached the freezing point;
- e. This winter-associated noise on the downhole long-period triaxial seismograph was not generated by atmospheric pressure variations or earth tilts/displacements;
- f. Air convection currents within the sealed, but unfilled borehole casing can be excited by natural or artificial cooling of the wellhead exterior;
- g. These convection currents were related to pressure variations inside the sealed borehole casing which correlated with motion of the downhole long-period triaxial seismometers;
- h. Convection currents/pressure variations inside the sealed borehole casing were excited (and thus the LP triax) by cooling the wellhead exterior even when an aggregate of crumbled polystyrene insulation filled the borehole casing up to 3 feet from the top of the casing;

i. Completely filling the borehole casing with insulation aggregate caused the noise levels to dramatically decrease on both the (internal-sensing) microbarograph and downhole long-period triaxial seismograph data;

j. Calculations indicated that the internal pressure variations were not deforming the borehole casing (13-3/8 inches OD, threaded, 48 lb/ft pipe);

k. If these internal pressure changes were acting directly upon the long-period triaxial seismometer package, there was no evidence that the sealed or unsealed stiffener assembly improved the operation of the triaxial seismometer;

l. Trace excursions ("spikes") on the surface long-period horizontal seismograms in the winter months may well have been related to temperature effects on the Model 8700C seismometers and/or the vault type installation;

m. The major source of the troublesome 50-70 second period winter-associated noise was caused by thermally-induced air convection cells which in turn produced pressure variations inside the borehole casing. These pressure variations, by an unknown mechanism, produced noise on the long-period triaxial seismograms, and complete filling of the borehole casing with insulation aggregate substantially retarded this effect.

## 6.7 ATMOSPHERICALLY-GENERATED SEISMIC NOISE PROJECT

### 6.7.1 Wills Point, Texas, LP Triaxial Station

#### 6.7.1.1 Objective

Analyses of the data from the atmospherically generated seismic noise project at Grand Saline, Texas (GA-TX and GA2TX), confirmed that local changes in the atmospheric pressure field on the order of 50 to 100  $\mu$ bars could create motions of the surface of the earth which would contribute significantly to the seismic noise field at periods greater than 20 seconds. Figure 77 shows the typical instrumentation and frequency response. The analyses also supported the theory that the seismic disturbance created by variations in atmospheric pressure should attenuate very rapidly with depth. The primary objective of the Wills Point, Texas, experiment was to measure the variation in the atmospheric component of the long-period seismic noise field as a function of depth. To satisfy this objective, two 3-component long-period seismic systems were required, one system for operation in sealed surface vaults, and another system that could be moved to various depths and operated in a sealed borehole. A microbarograph array was also required.

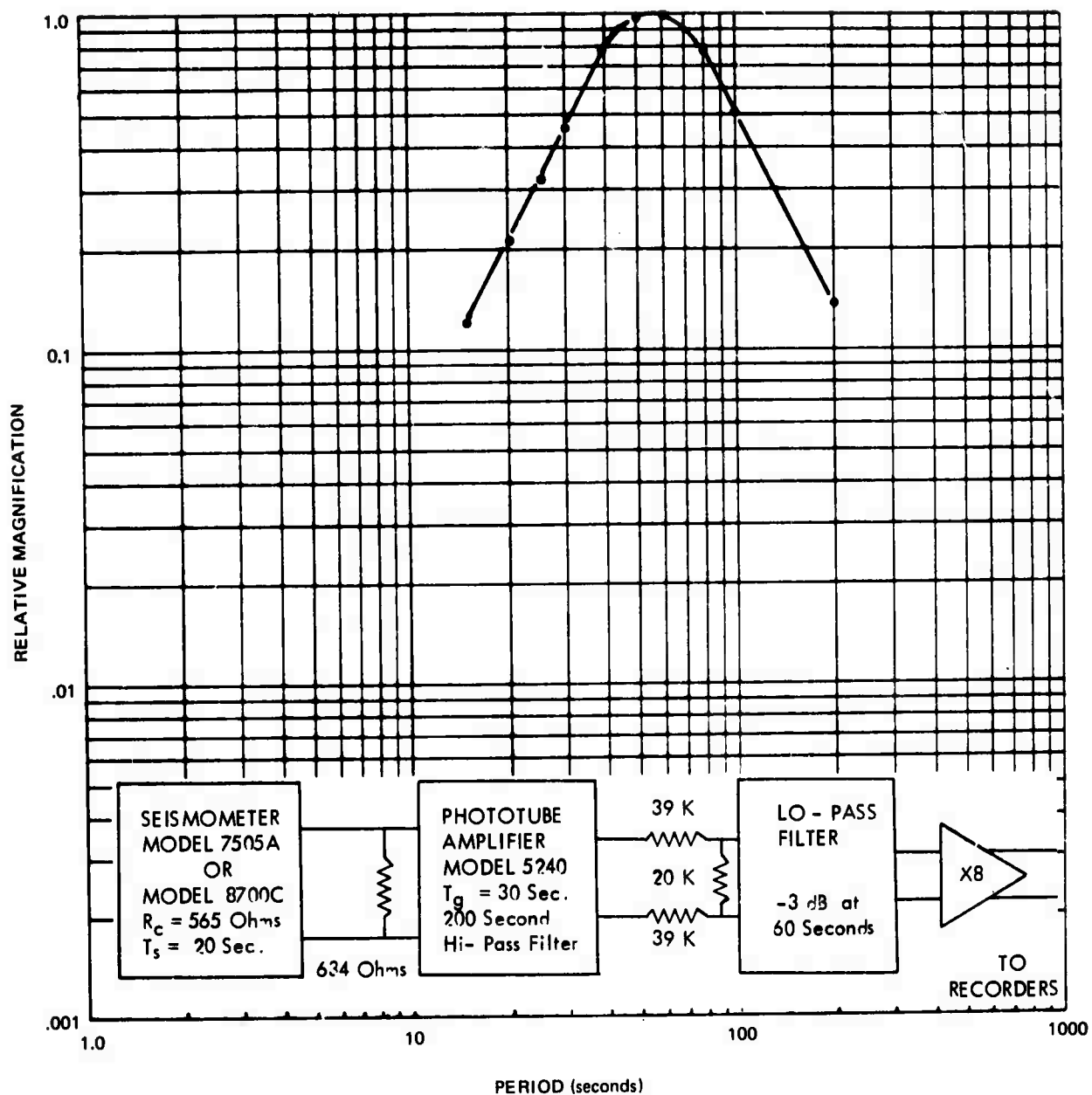


Figure 77. Typical instrumentation and response, atmospherically-generated seismic noise project, Grand Saline, Texas

#### 6.7.1.2 Site Selection

During July and August of 1970, numerous logs and plugging reports on abandoned petroleum prospect holes in southern Oklahoma and northeastern Texas were reviewed. Primary site selection considerations were the depth of re-enterable 13-3/8 in. OD surface casing, area suitability for a microbarograph array, and the economics of using Geotech at Garland, Texas, as an operational base. Field investigations were performed at four locations. These efforts culminated in the selection, acquisition, and re-entry of the Pan American Petroleum Corporation No. 1, J. T. Edwards Gas Unit dry hole in Van Zandt County, Texas. This location is about 55 road miles east of Geotech and was designated as the Wills Point, Texas (WP-TX) site. Figure 78 presents a sketch of the site location and layout.

Originally, the Pan American No. 1 J. T. Edwards Gas Unit was drilled to a depth of about 4262 meters (13,982 feet) as a Jurassic Smackover Formation petroleum test. Depth to the pre-Mesozoic basement rocks is probably about 4650 meters (14,500-16,000 feet). Surface casing is 13-3/8 in. OD, 61 lb/ft, threaded range-2 pipe with a 12.515 in. ID, set to about 484 meters (1587 feet) below the surface. The surface casing depth for this size pipe is unusual in the area, and no internal or lower casing was set in the 8-3/4 in. diameter hole to total depth. The hole was abandoned by Pan American and various cement plugs were set on 25 August 1969.

Surface material near the wellhead consists of unstable, mottled gray/red sandy clays of the Eocene Wilcox Group, and is about 130 meters (425 feet) thick. Clastic sand, clay and shale sequences of Lower Tertiary and Upper Cretaceous age dominate the subsurface section to near casing depth, where the surface pipe was landed at about 485 meters (1587 feet) in thin limestone or chalk beds associated with marls and shales of the Cretaceous Upper Taylor Group. The first really massive, competent bedrock in the subsurface at this site is considered to be the Cretaceous Pecan Gap Chalk Formation, at about 740 meters (2425 feet) depth, with velocities approaching 3-1/2 kilometers per second. The deeper sedimentary section consists of carbonates, shales, marine sands, and evaporite zones. The drilled section with interval velocities is illustrated in figure 79.

Permission to utilize the hole was acquired from Pan American Petroleum Corporation on 18 September 1970. An agreement with the surface owner (J. T. Edwards) was executed on 23 September 1970. Permits for re-entry and maintaining the casing in an open condition were received from the Oil and Gas Division of the Railroad Commission of Texas (regulatory body) on 16 October 1970. The WP-TX site is located 4750 feet from the NW line and 9350 feet from the NE line of the William Sherman Survey, Abstract 761, Van Zandt County, Texas (Lat. 32°36'25" N, Long. 095°53'10" W), and has a surface elevation of 161 meters (529 feet) above mean sea level. In February 1971, assistance was provided to Southern Methodist University Geophysics Department in selecting and permitting microbarograph sites in the vicinity of the WP-TX site.



# TELEDYNE GEOTECH NO.1 J. T. EDWARDS WELL AT SITE WP-TX (RE-ENTRY) (PAN AMERICAN PETROLEUM CORP. NO.1 J.T. EDWARDS GAS UNIT)

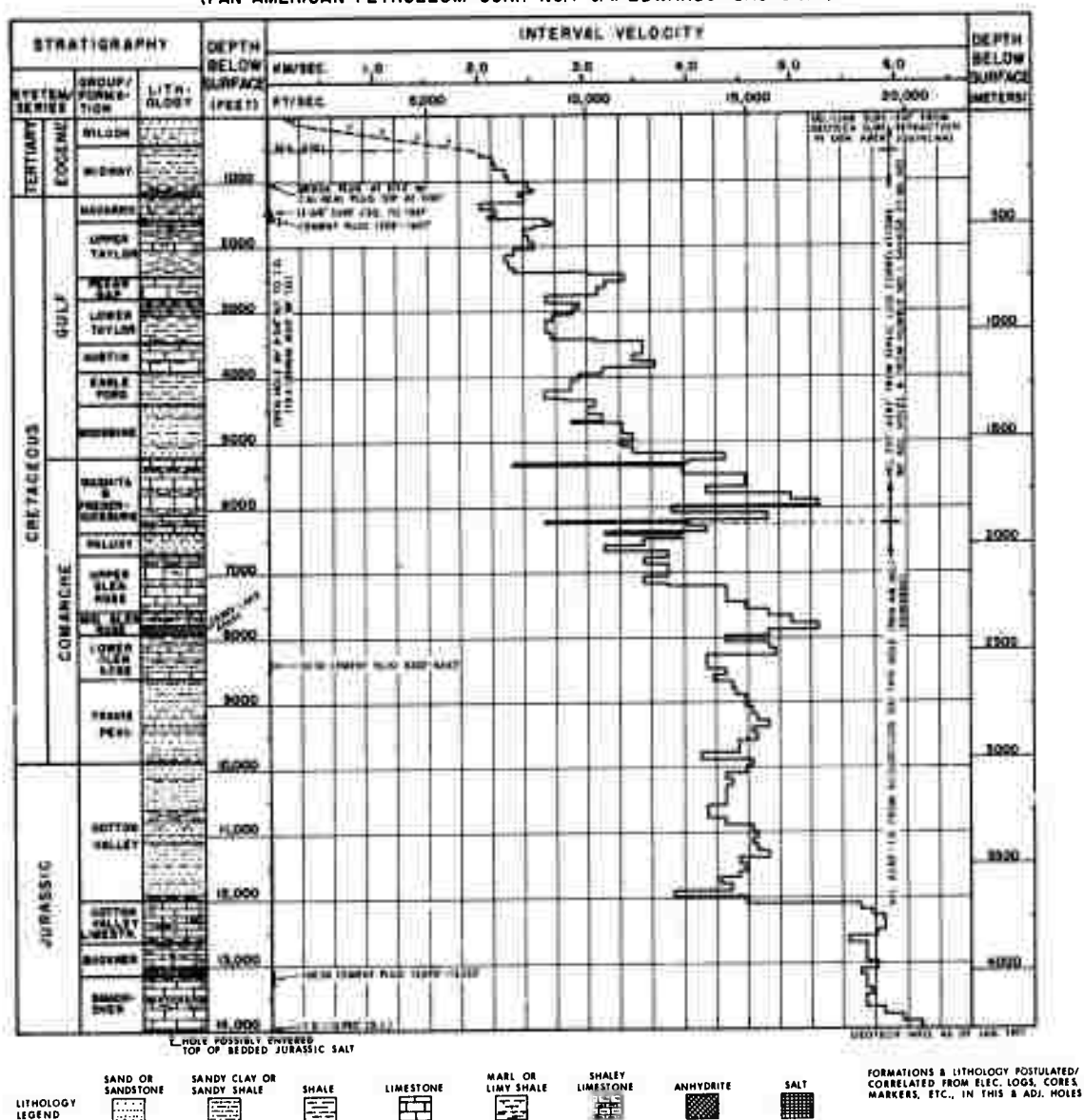


Figure 79. Drilled section with interval velocities

#### 6.7.1.3 Site Preparation

Re-entry of the WP-TX hole was started on 17 November 1970 with a contracted workover rotary drilling rig. Cement plugs were removed and the interior of the casing was cleaned with a rock bit 12-1/4 inches in diameter. On 19 November 1970, drilling was terminated at 1558 feet below ground level in a hard cement plug within the 1587 feet of casing. The plugging report for the hole indicated this plug to extend to 1607-foot depth. More uphole cement was encountered than was indicated in the plugging report. Also, on 19 November 1970, the casing was blown dry. Pressure tests at that time indicated no leaks.

Surface preparations at WP-TX involved installing four surface vaults, isolated amplifier piers, a wellhead slab, two winch foundations, road aggregate spreading, and installation of commercial power. The surface installations were completed on 04 December 1970.

On 03 December 1970, the wellhead cap was removed from the cased hole at WP-TX and clear, slightly salty water was observed below the wellhead collar. This slow leak into the casing involved an inflow volume of about 9,950 gallons of water, which exerted about 710 psi at the 1558-foot clean-out depth. The leak, assuming it was at the bottom, was overcoming this pressure. A 10 psi wellhead pressure was found to hold the water level static. Subsequent tests at the site included sampling the bottom-hole liquid (original drilling fluid), checking inflow rates after removal of various volumes of water by bailing, logging water resistivity versus depth, and logging water temperature versus depth; all in an attempt to determine the location of the leak. Results of these downhole surveys indicated the primary leak was from the bottom, passing the 29 feet of cement plug remaining in the casing from the 1558- to 1587-foot depth when the well was plugged originally. The electronic surveys also indicated an anomalous zone from the 1040- to 1080-foot depth that could relate to water entry through a hole in the casing or a leaking collar joint. A decision was made to set a wire-line bridge plug above the highest suspect leak. This operation did not require a drilling rig to move back onto the location to run tubing downhole.

On 21 December 1970, a drillable, electric-firing, wire-line bridge plug was set at a depth of 1015 feet below the surface between two collar joints in the casing. This plug was a Model N, size 9-AA, manufactured by Baker Oil Tools, Inc. The hole was bailed and sounded in stages with positive water shutoff by the Baker plug indicated. Successive downhole dumps of Cal Seal (expanding hydraulic cement) and common Portland cement were placed on the bottom to provide a 13-1/2 foot protective column of cement above the Baker plug. The result was a dry, open-hole with a working depth of 1001-1/2 feet. On 06 January 1971, the casing was pressured to 30 psi with air. On 11 January 1971, the wellhead gauge read 21.5 psi. The casing pressure tests were then terminated. The compressed air had decayed to 72 percent of original pressure in 114 hours, a loss rate of 0.0746 psi per hour (a portion of which were small air leaks at the wellhead fittings). On 27 January 1971, the WP-TX casing

was again sounded to test for possible water entry, and 1001-1/2 feet of dry hole was verified. Earlier surveys indicated a temperature of approximately 80°F at the 1000-foot depth and an increasing temperature gradient of about 1.9°F per 100 feet of depth when the casing was full of salty formational water. The well at WP-TX was ready for installation of the long-period triaxial seismometer (LP triax).

On 05 August 1971, a Lamont-Doherty seismometer vault was installed at WP-TX in a 5-foot-deep drained excavation that is in unstable, sandy, formational clays of the area. It is 5-1/2 feet northwest of the LP-Z vault. Construction methods and materials used were the same as for all adjacent surface seismometer vaults at the site. On 10 August 1971, the cylindrical lower portion of the special vault was prestressed, the subbase void was filled with mortar and the cylinder was bolted to the pad as per installation instructions in Lamont-Doherty reports.

#### 6.7.1.4 Special Equipment

A coordinate transformer capable of electronically rotating the two horizontal axes of the long-period seismometers was designed, fabricated, tested, and installed in the van at site WP-TX. A prototype LP triax controller originally used at site FB-AK was modified to conform to the Model 32620 LP triax controller for use at WP-TX. A Develocorder was installed in the van. A LP triax holelock was also obtained for the experiment.

To move the LP triax within the well casing, an electric winch was equipped with 1900 feet of 3/8-inch diameter wire rope. The stinger portion of the LP triax stabilizing holelock assembly was modified to provide for attachment of the wire rope. An additional winch was assembled and equipped with about 1800 feet of multiconductor data cable. A connector separated a 1000-foot and an 800-foot segment of the data cable. When lowered in the hole, the data cable is clamped to the wire rope at a spacing of approximately 25 feet for support.

#### 6.7.1.5 Operations and Tests

Initial tests and set-up calibrations of surface LP seismometers data were recorded by SMU personnel using their digital recording van which had been moved on-site in December 1970. The SMU van recorded the microbarograph and LP triax data in digital form for the experiment. Figure 80 shows a block diagram of the seismograph system at WP-TX.

In February 1971, special testing of the LP triax seismometer to be used at WP-TX was performed at the Geotech facility in Garland, Texas. These extensive tests involved operating the unit under pressure and with no pressure, with jack screws set between the faces of the lower flange of each triax module.

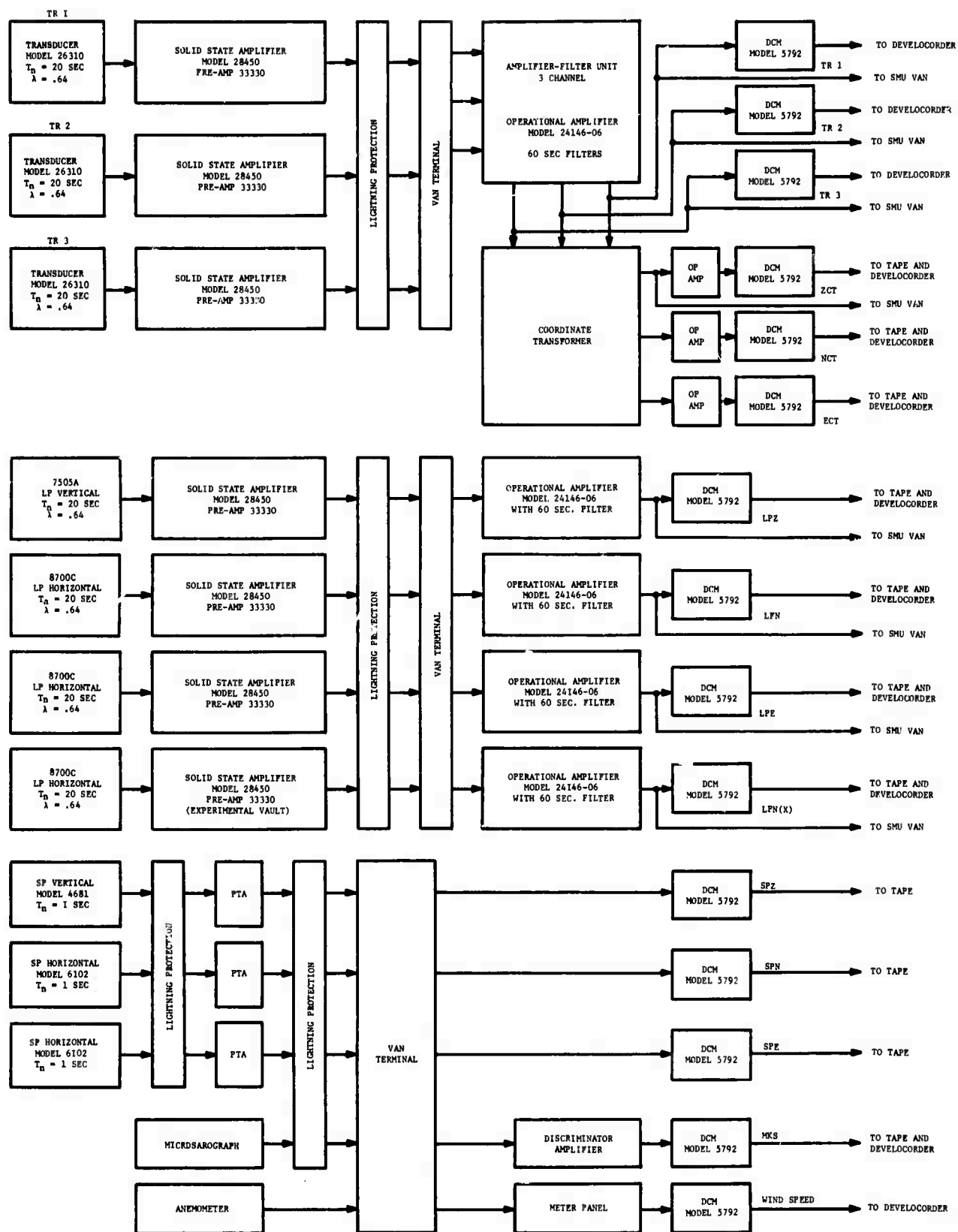


Figure 80. Block diagram of seismograph system at WP-TX

Data recording at WP-TX was started on 18 March 1971, on both magnetic tape and the Develocorder. Data were collected from the three long-period surface seismometers and the three long-period triaxial seismometer modules. Both raw and transformed triax data were recorded. The long-period vertical (LPZ) surface seismometer used was a Model 7505A. The two long-period horizontal surface seismometers were Models 8700C, oriented for positive trace deflection with earth motion toward the north (LPN) and east (LPE).

Initial operation of the triax was near the surface, with the top of the stack 6 feet below the wellhead. Both load bearing and stabilizing holelocks were used. The lower triax module was designated TR1 and was oriented north. The middle triax module was designated TR2, and by the nature of the stack assembly, was oriented 120° counterclockwise from north, or at 240° azimuth. The upper triax module was designated TR3, and by the nature of the stack assembly (with TR1 north), was oriented at 120° azimuth. The wellhead was sealed, insulated, and sandbagged. The wire rope and multiconductor data cable passed through a wellhead cap-plate. Surface vaults were sealed, insulated, and sandbagged, and the tripod atop the wellhead slab was lowered to reduce wind effects.

The recording of short-period vertical (SPZ) data on the Develocorder as a "flag" trace was started on 12 April 1971. A Model 18300 short-period seismometer was used for this recording. Long-period data continued to be recorded by both the LRSM and SMU vans, with the LP triax at 6 feet below the wellhead.

On 21 April 1971, the LP triax was lowered to 50 feet below the wellhead, with the TR1 module oriented north. The TR2 and TR3 modules were necessarily thus oriented at 240° azimuth and 120° azimuth, respectively, as before. Recentering problems developed in the TR1 module which required removal of the stack to return it to the Geotech Garland facility for maintenance. On 30 April 1971, the LP triax was reinstalled at the 50-foot level in the WP-TX well, all masses were recentered, and recording continued. The incompetent surface material at the site allows the long-period horizontal seismometers to respond to tilts caused by one person walking in the general area of the vaults.

Heavy rains in May 1971, contributed to excessive spiking of all surface channels. Although the excavations are sufficiently drained to prevent water from covering the concrete vault-base pads by more than 2 inches, moisture condensation within the steel vaults provided high resistance leakage paths to ground in the calibration circuits. The long-period horizontal systems were also noisy because of vault tilt attributable to rains wetting the plastic clays under the vault foundations. On 17 May 1971, a wellhead microbarograph was installed, and microbarograph data began to be sampled from both inside and outside the well casing. From 19 through 21 May 1971, the surface vaults were opened to dry them out and to perform maintenance upon the instruments. After lowering the LP triax to a depth of approximately 985 feet and setting the holelocks, the full operations were continued on 27 May 1971. The physical orientation of the LP triax at 985 feet depth was not determined because the unit could not be seen from the surface.

Initial observations indicated that the noise levels of the LP triax system at the 985-foot depth were at least 20 dB below those observed at the 50-foot depth. The spectrum of the pressure variations inside the well casing remained relatively constant regardless of external meteorological conditions, but the seismic noise power varied directly with changes in the external atmospheric pressure. The well casing or the data cable were suspected as the medium through which the external pressures were being transmitted to the LP triax. The pressure-related noise recorded by the triaxial seismograph was observed to increase by a factor of 3 or 4 when a syringe needle was placed in the data cable jacket, allowing transfer of atmospheric pressure down the cable to the LP triax. An effort to exclude pressure effects inside the well casing by intermittent vacuum pumping began on 18 June 1971, and was terminated on 09 July 1971. Vacuum attained was only 4.3 inches of mercury and no significant change in the pressure-related noise was observed. However, no significant change was expected until a vacuum of 1-1.5 inches of mercury was reached. Also, during June and July of 1971, the TR1 data line between the van and the amplifier and between the amplifier and the cable reel was replaced to eliminate a high resistance leakage path to ground. The long-period surface vaults were re-entered late in June 1971, to eliminate ground loops caused by moisture condensation in the data, calibration, and mass position monitor circuits.

During August and September 1971, because of suspected transfer of atmospheric pressure changes into the cased borehole, and resulting pressure-related noise in the LP triax system, the connector between the 1000- and 800-foot data cable segments was placed inside the casing. The wellhead was resealed and a plug of room-temperature-vulcanizing rubber was placed in the data cable outside the wellhead. Pressure tests were again conducted on the borehole casing, and 77 hours were required for the pressure to decrease to 1/3 of its initial value (77-hour time constant). In order to completely seal the casing from atmospheric pressure changes, the wire rope was positively clamped inside of the wellhead, cut, and the free-end was let down into the well casing. A sealed bulkhead-type connector for the data cable was also installed in the wellhead plate to block any passage of air through the cable.

A Model 8700C long-period surface horizontal seismometer was also installed in the special Lamont-Doherty vault during August and September 1971. It was oriented north and designated LPXN. Pressure tests were performed on the vault to verify its seal, and recording of this additional long-period channel was begun.

A preliminary comparison of the data recorded from the long-period horizontal seismograph in the adjacent standard "Melton" type vault (LPN) to that recorded from the instrument in the Lamont-Doherty vault (LPXN) indicated no significant difference in the systems noise levels.

A reduction of system noise on the LP triax system at WP-TX was accomplished in October 1971 by relocating the amplifiers and by minimizing the length of the data line and the number of connections. The triax amplifiers were removed from the amplifier hut to an enclosure immediately outside the wellhead on the tripod slab. This change removed approximately 800 feet of multi-conductor cable stored on a reel on the surface from the unamplified data circuit. This resulted in approximately a 2 dB reduction in the noise considered to be related to electronic sources.

The tripod at the wellhead was laid down during October 1971 after being utilized for triax data cable and wire rope modifications. A three-component, short-period system was installed and operated in preparation for an event from the Aleutian Islands. These short-period seismometers were set in the half-shell tank vault prepared in December 1970, and oriented for positive trace deflection with earth motion towards up (SPZ), north (SPN), and east (SPE).

At the end of this report period (31 October 1971), the LP triax remained at the 985-foot depth, and tests were continued under Project T/1703.

#### 6.7.1.6 Preliminary Results

The February 1971, gross pressure tests on the WP-TX LP triax at the Geotech Garland facility revealed that the lower flanges on each module base could be distorted sufficiently to change the free period and recentering characteristics of the modules. Relative pressures to as high as 300 psi exerted on the LP triax stack caused instability of the seismometers that was considerably reduced by placing jack screws between the flanges beneath each stanchion. The seismometer suspension is mounted on tilt tables which are in turn indirectly mounted on the upper face of the lower flange in each module. A force on the top of the transducer can be transmitted the length of the modules through the stanchions to the upper faces of each lower flange. Although the test demonstrated that the LP triaxial seismometer could be made more stable in high pressure environments by the addition of jack screws in the flanges, the LP triax at the WP-TX site was operated without the jack screws.

Vertical earth motion in response to wind-generated pressure changes can be measured by the surface or near-surface long-period systems at WP-TX and the magnitude of the response appears to be 4 to 6 dB greater than that observed at the Grand Saline, Texas, surface site (GA2TX) at periods greater than about 50 seconds. The GA2TX surface site is about 100 meters (327 feet) above the top of a broad salt dome, and about 18 kilometers (11 miles) east-northeast of the WP-TX site.

A substantial fraction of the noise recorded by horizontal seismographs on or near the surface during windy periods was due to earth tilt in response to local atmospheric pressure changes at WP-TX.

Theoretical calculations regarding the buoyant response of a vertical seismograph were verified.

The feasibility of operating a LP triax within a dry, cased, 1000-foot-deep borehole was demonstrated.

Initial analysis indicated that noise levels recorded by the triaxial seismograph when operated at a depth of 985 feet were 20 dB below the levels recorded when the seismometer package was operated at 50 feet. However, a significant fraction of the noise at periods greater than 50 seconds was directly related to atmospheric pressure fluctuations at the surface.

Analysis of microbarograph data recorded both inside and outside of the sealed wellhead showed that outside pressure was not leaking into the casing. Also, the microbarograph data indicated that the noise (at periods greater than 50 seconds) sensed by the LP triax at a depth of 985 feet was not related to pressure changes within the well casing. A possible explanation of the atmospheric, pressure-related sensitivity of the downhole installation that was considered was that pressure fluctuations were being transmitted along and within the data cable to the LP triax. The possibility of pressure transmission along the data cable was excluded (bulkhead/wellhead cable connector), and noise related to the external atmospheric pressure field was still recorded by the LP triaxial seismograph. Tests were continued to identify the source of this noise.

Elimination of the noise (at periods greater than 50 seconds) from the LP triax data was expected to lead to about a 3.6 dB increase in magnification and result in a noise level comparable to that observed on the mine vertical seismograph at Grand Saline, Texas (GA-TX). Previous spectra obtained at Grand Saline did not indicate transmission of wind-generated noise to the 672-foot depth within the salt dome.

Tests and analysis of the data recorded at WP-TX will be continued in an effort to resolve this problem and determine the source of the noise.

#### 6.7.2 Long-Period Noise Experiment at the Morton Salt Company Mine Near Grand Saline, Texas (GA2TX)

##### 6.7.2.1 Introduction

When the wind blows across the surface of the earth, it can cause relatively large perturbations in the local atmospheric pressure field. Since the earth is not a perfectly rigid body, it will deform in response to these pressure changes. Recent calculations (Sorrells and Der, 1970, Sorrells, 1971) indicate that certain relatively common meteorological and geological conditions, the earth's response to wind-generated pressure changes contributes significantly to the long-period noise field recorded at the surface. An experiment to measure the magnitude of this response at the surface and at a shallow depth

was conducted at the Morton Salt Company mine near Grand Saline, Texas. The experiment was supported under Project VT/0703 in a joint effort with Southern Methodist University. A description of the experiment and a discussion of the results are contained in the following paragraphs.

#### 6.7.2.2 Instrumentation

The seismic data were recorded by two, 3-component, sets of long-period seismographs installed at the surface and in the mine. The vertical and horizontal distance between the two installations is shown in figure 81. Also shown in this figure are the relative positions of the microbarographs, the anemometer, and the recording trailer used during this study. Data from the sensing systems were transmitted to a digital acquisition system housed in the trailer. There the data were sampled at 1-second intervals and stored on magnetic tape. Details regarding the digital acquisition system, the microbarographs, and the anemometer are given by Herrin and McDonald (1971). The average frequency response of the microbarographs and seismographs are shown in figure 82.

#### 6.7.2.3. Presentation of Results

The results presented in this section are power spectral density and coherence estimates calculated from data recorded by the mine and surface vertical seismographs and by the base microbarograph. The data samples used in the calculations were chosen to illustrate the noise levels observed during dummy load tests, during calm and turbulent atmospheric conditions, and during the passage of acoustic waves. All samples are free of obvious earthquake signals and are 10,240 seconds (~3 hours) in length except for those recorded during the passage of the acoustic wave which are 7168 seconds (~2 hours) long. The power spectral density estimates shown in the subsequent figures were calculated using a block averaging technique described by Welch (1967) and summarized by McDonald et al (1971). They have been corrected for their respective system responses. Their stability at the 90 percent confidence level is  $\pm 1.4$  dB for the samples which are 10,240 seconds in length and  $\pm 1.8$  dB for the samples which are 7168 seconds in length. Squares of the estimated coherence which exceed 0.06 for 10,240-second samples and which exceed 0.09 for the 7168-second samples are significantly different from zero at the 95 percent confidence level.

6.7.2.3.1 Results of Dummy Load Tests. In figure 83 (a), we compare power spectral density estimates of the noise recorded by the vertical seismograph in the mine during calm and windy periods and during an interval when the seismometer was replaced by an equivalent resistance. This comparison clearly demonstrates that at periods less than about 150-200 seconds, noise sources within the system do not contribute significantly to the observed spectrum.

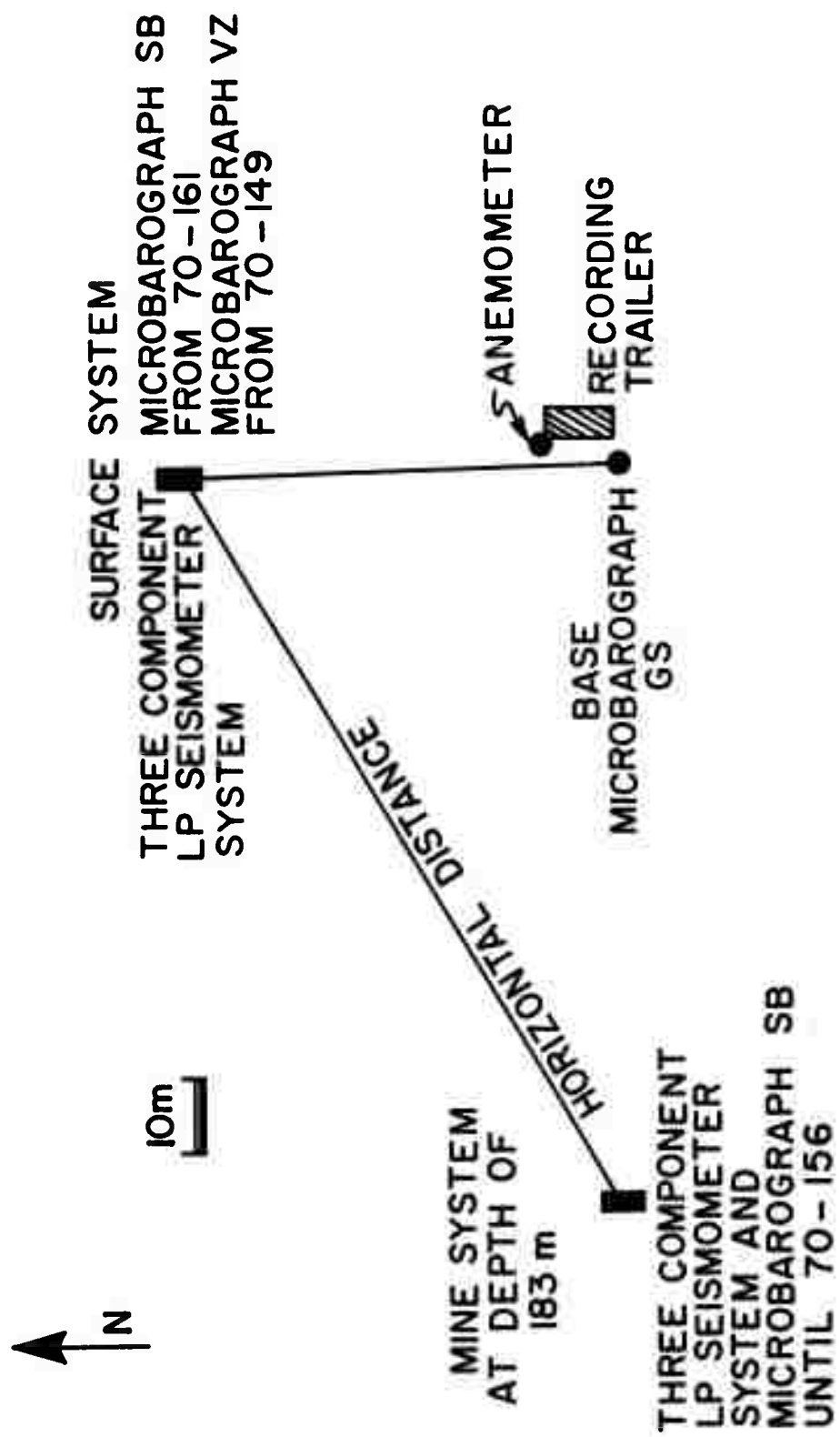


Figure 81. Vertical and horizontal distances between systems

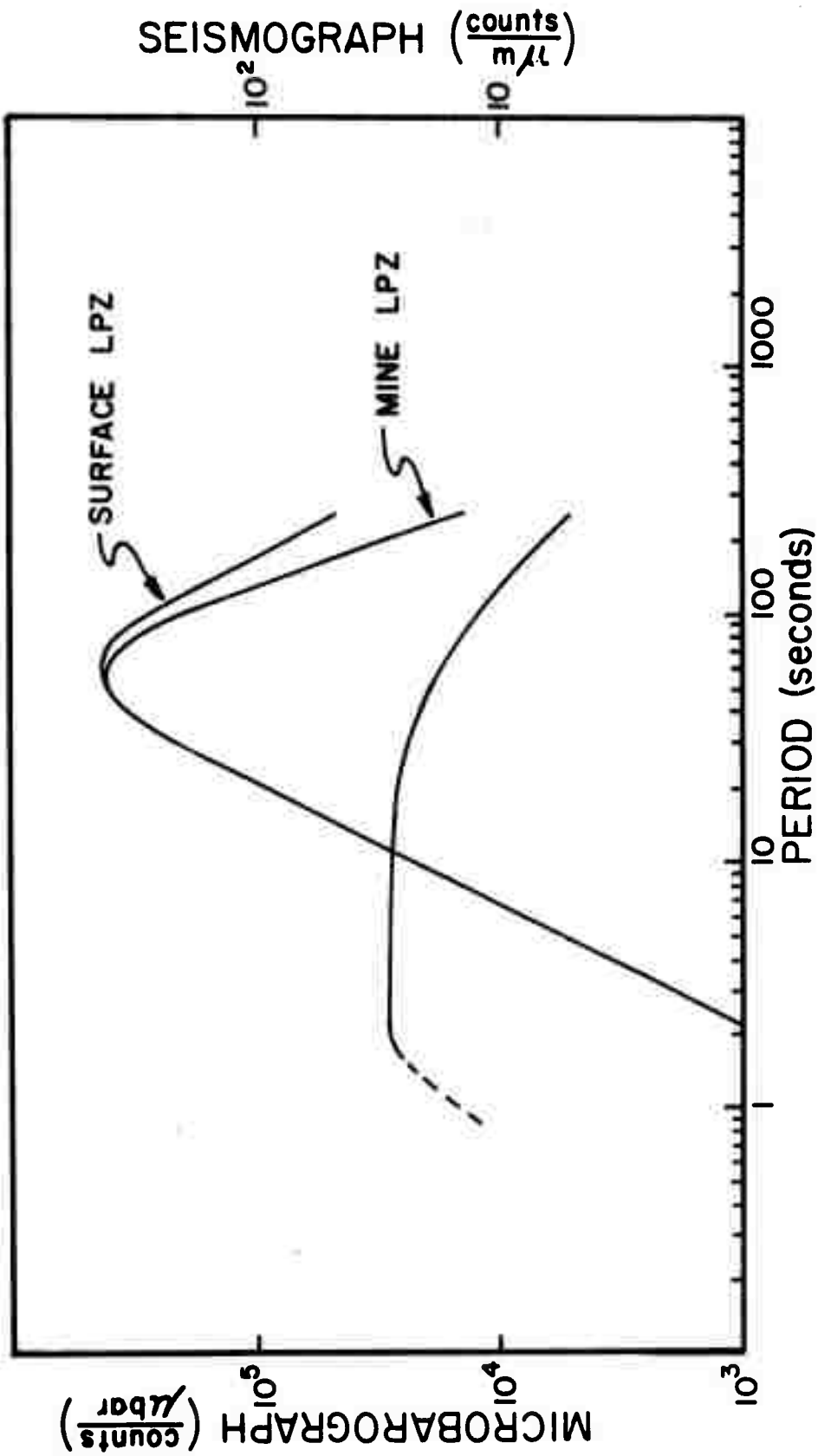


Figure 82. Average frequency response of microbarographs and seismographs

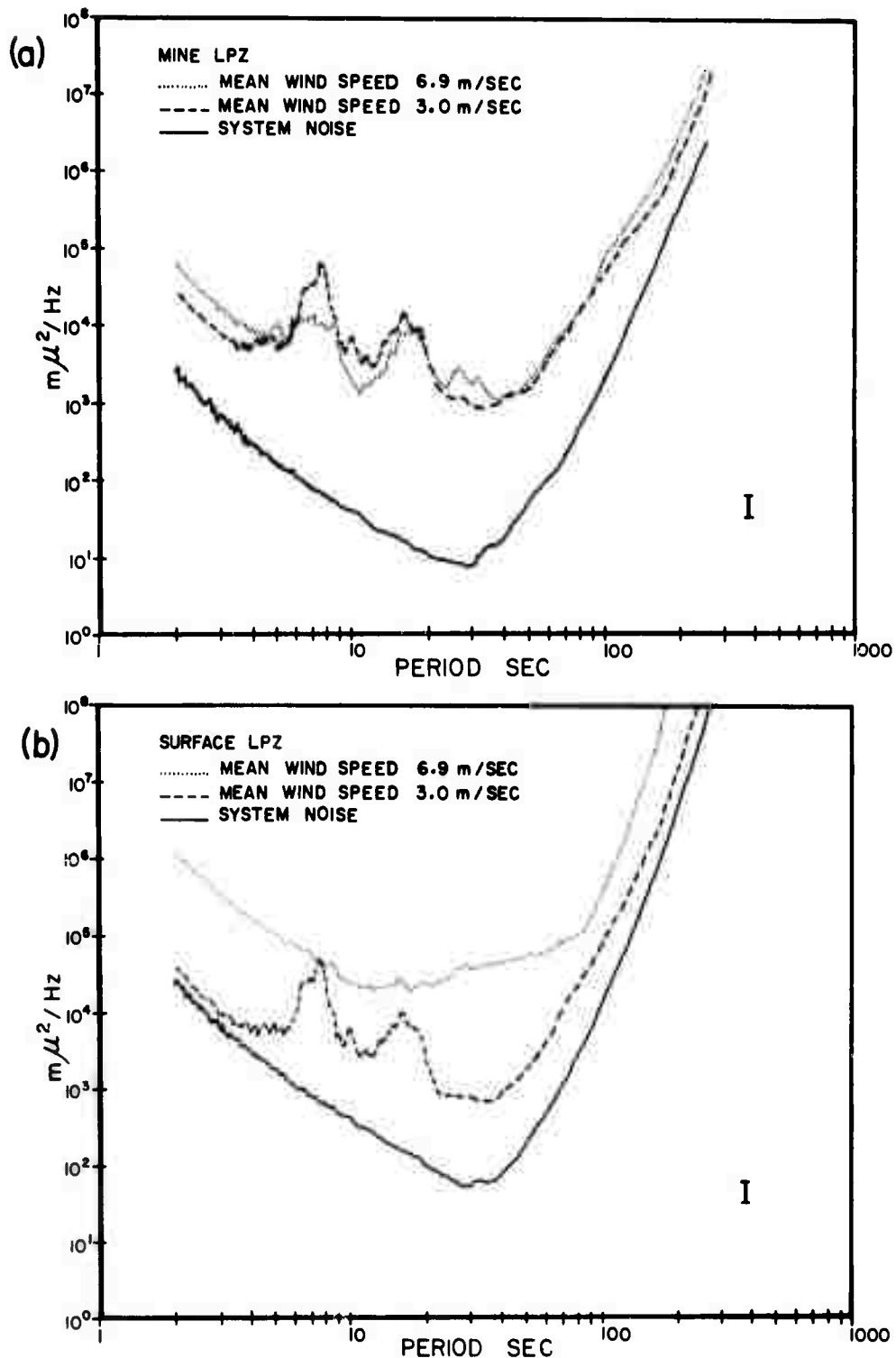


Figure 83. A comparison of the power spectral density estimates calculated from data recorded during calm and windy periods, and during equivalent resistance tests. (a) Data recorded in the mine. (b) Data recorded at the surface. The small vertical bar appearing in the lower right hand corner of these and subsequent figures indicates the expected spread of the estimates at the 90% confidence level

A similar comparison is made for data recorded at the surface in figure 83(b). Observe that the noise of the system at the surface is about 9 dB greater than that observed in the mine. However, despite the higher level, it can be seen that system noise sources make an insignificant contribution to the noise (ground motion) recorded at the surface in the 5-150 second period range.

6.7.2.3.2 Noise Recorded During a Calm Period. The results shown in figures 84(a) through 84(d) were calculated from data recorded during an interval when the mean wind speed was 3.1 meters/sec. As shown by the power spectral density estimate displayed in figure 84(a), the fluctuations in the local atmospheric pressure field are quite low. In the 20-100 second period range, the RMS pressure amplitude is 0.7  $\mu$ bars. The spectral estimates of the noise recorded by the vertical seismographs in the mine and at the surface are compared in figure 84(b). Notice that they are, for all practical purposes, identical. A prominent gap in the spectrum of the noise is observed to occur roughly in the 20 to 100-second period range. Within this pass band, the RMS amplitude of the noise was found to be 17  $m\mu$ . It has been shown by Molnar et al (1969) that the existence of this gap can be potentially important to the solution of the problems associated with the detection and identification of surface waves generated by low-magnitude earthquakes and underground nuclear explosions.

The squares of the estimated coherence between the seismic noise recorded at the surface and in the mine is shown in figure 84(c). The relatively high values between 8 and 16 seconds are not unexpected since most of the noise within this period range is known to consist of fundamental mode Rayleigh waves with wavelengths much greater than the distance between the two seismographs. Notice, however, that the range of significant coherence extends out to periods on the order of 150 seconds. This result demonstrates the important point that presently operating long-period seismographs are not limited by system noise. To illustrate this observation more clearly, we have converted the coherence data shown in figure 84(b) into estimates of the ratio of earth-to-system noise. In order to carry out the conversion, the following assumptions were made.

- a. The earth noise is the same at both locations.
- b. The surface system noise spectra has the same form as that observed in the mine but is 10 dB greater.
- c. The earth noise and the mine and surface systems noise are mutually independent variables.

The estimated earth noise to system noise ratio for the vertical seismograph in the mine are plotted as a function of period in figure 85. Notice that the estimated ratio is greater than 6 dB at all periods less than 128 seconds. Thus, further reduction of the noise level observed on long-period vertical seismograms over that obtained in the mine at Grand Saline depends more on the development of techniques to attenuate earth noise than it does on the development of low-noise instrumentation.

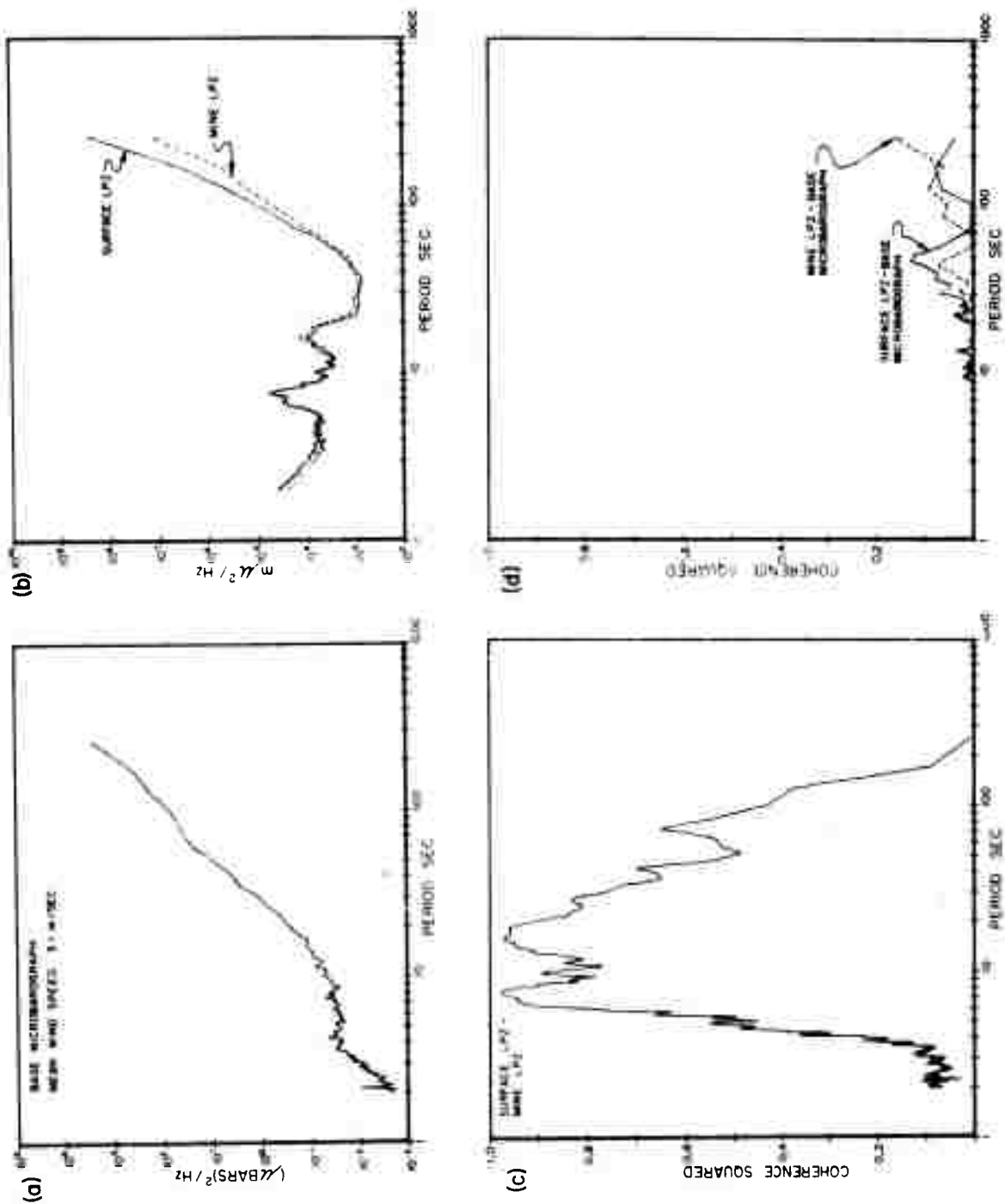


Figure 84. Noise recorded during a calm period

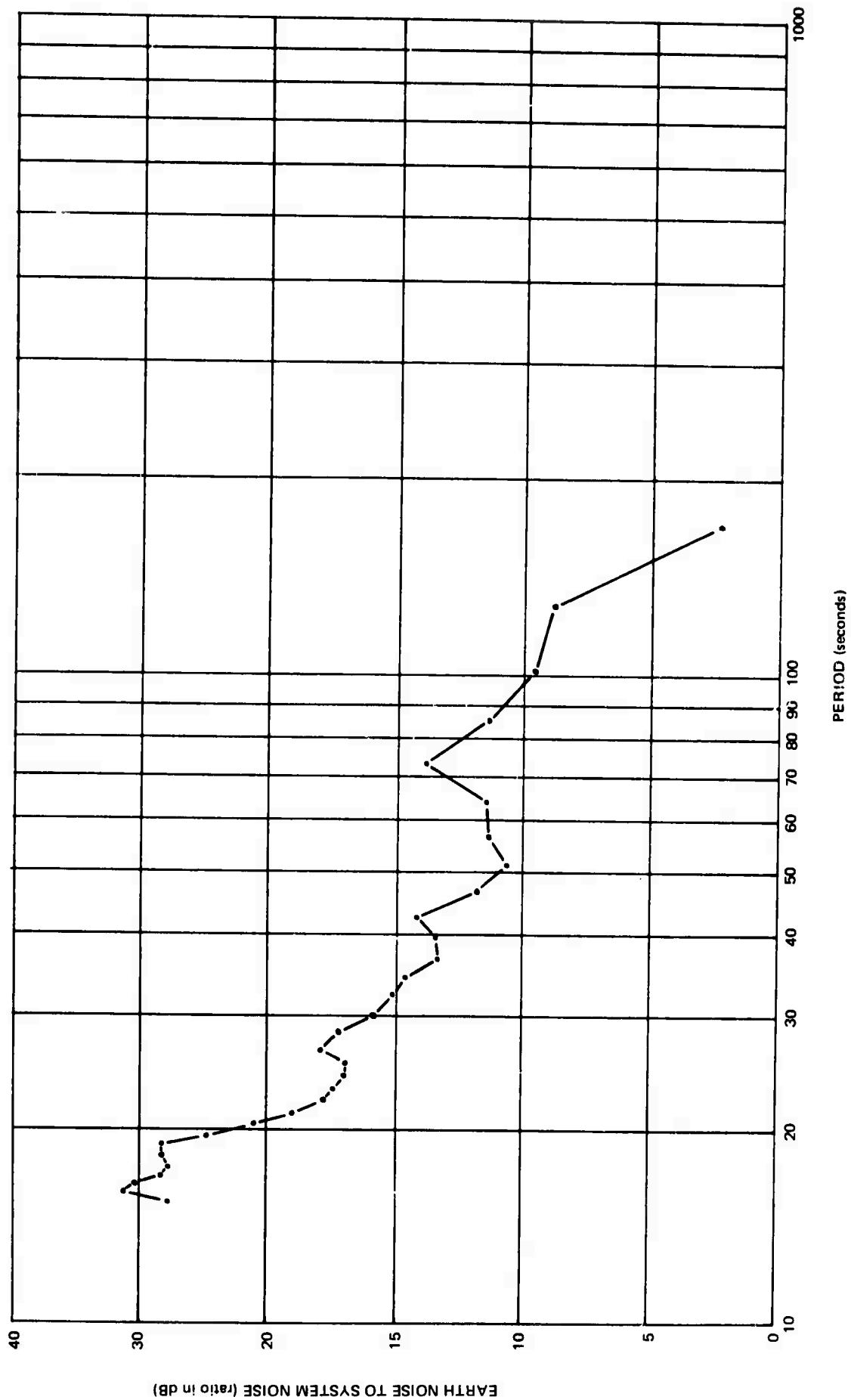


Figure 85. Ratio of earth to system noise for the vertical seismograph located in the mine at Grand Saline, Texas

The source of the earth noise observed during calm intervals in the 20-100 second period range is not clearly understood at the present time, although the coherence calculations shown in figure 84(d) suggest that a small fraction could be related to atmospheric pressure changes in the immediate vicinity of the seismic stations.

6.7.2.3.3 Noise Recorded During a Windy Period. Power spectral density and coherence estimates calculated from data recorded during an interval when the mean wind speed was 7.8 meters/second are present in figures 86(a) through 86(d). Comparison of the spectral estimate shown in figure 86(a) with that shown in figure 84(a) demonstrates that as the velocity of the mean surface wind increases, there is a dramatic increase in the level of local atmospheric pressure fluctuations. In the period range 20-100 seconds, the RMS pressure amplitude was 12  $\mu$ bars during this interval or about 24 dB greater than that observed during a calm period. As shown in figure 86(b), the increase in the amplitude of the pressure changes is accompanied by an increase in the seismic noise recorded at the surface relative to that observed in the mine. The RMS amplitude of the noise recorded at the surface in the 20-100 second period range during this interval increased to 54  $\mu$ m while that observed in the mine remained at 17  $\mu$ m. This amounts to about a 10 dB difference between the noise levels recorded at the two locations. The square of the estimated coherence between the seismic noise recorded at both locations is plotted in figure 86(c). Notice that the coherence is quite low in comparison to similar measurements made during the calm period. The loss of coherence plus the increased noise observed at the surface implies that during windy periods, noise is added to the surface but not to the mine spectrum. As shown by the solid curve in figure 86(d), the principal sources of the added noise in the 20-100 second period range are fluctuations in the local atmospheric pressure field which are caused by the wind. In this pass band, 48 percent of the noise power recorded by the surface vertical seismograph is directly related to local pressure fluctuations and accounts for about 7 dB of the 10 dB difference observed between the surface and mine noise levels. In contrast, as shown by the dashed curve, there is no statistically significant linear relationship between the seismic noise recorded in the mine and local pressure variations at the surface.

6.7.2.3.4 Noise Recorded During the Passage of Acoustic Waves. Spectral density and coherence estimates calculated from data recorded during the passage of an acoustic wave are shown in figures 87(a) through 87(c). As shown in figure 87(a), the fluctuations in the local atmospheric pressure field during this interval are considerably smaller than those observed during the windy interval. In the 20-100 second period range, the RMS pressure amplitude was only 2.4  $\mu$ bars. Despite the relatively small fluctuations in atmospheric pressure, it can be seen from the spectral estimates shown in figure 87(b) that the seismic noise is quite high not only at the surface but in the mine as well. Estimates of the square of the coherence between local atmospheric pressure changes and the seismic noise recorded at both sites are shown in figure 87(c). It can be shown with these data that 35 percent of the surface noise power and 62 percent of the mine noise power are related to local

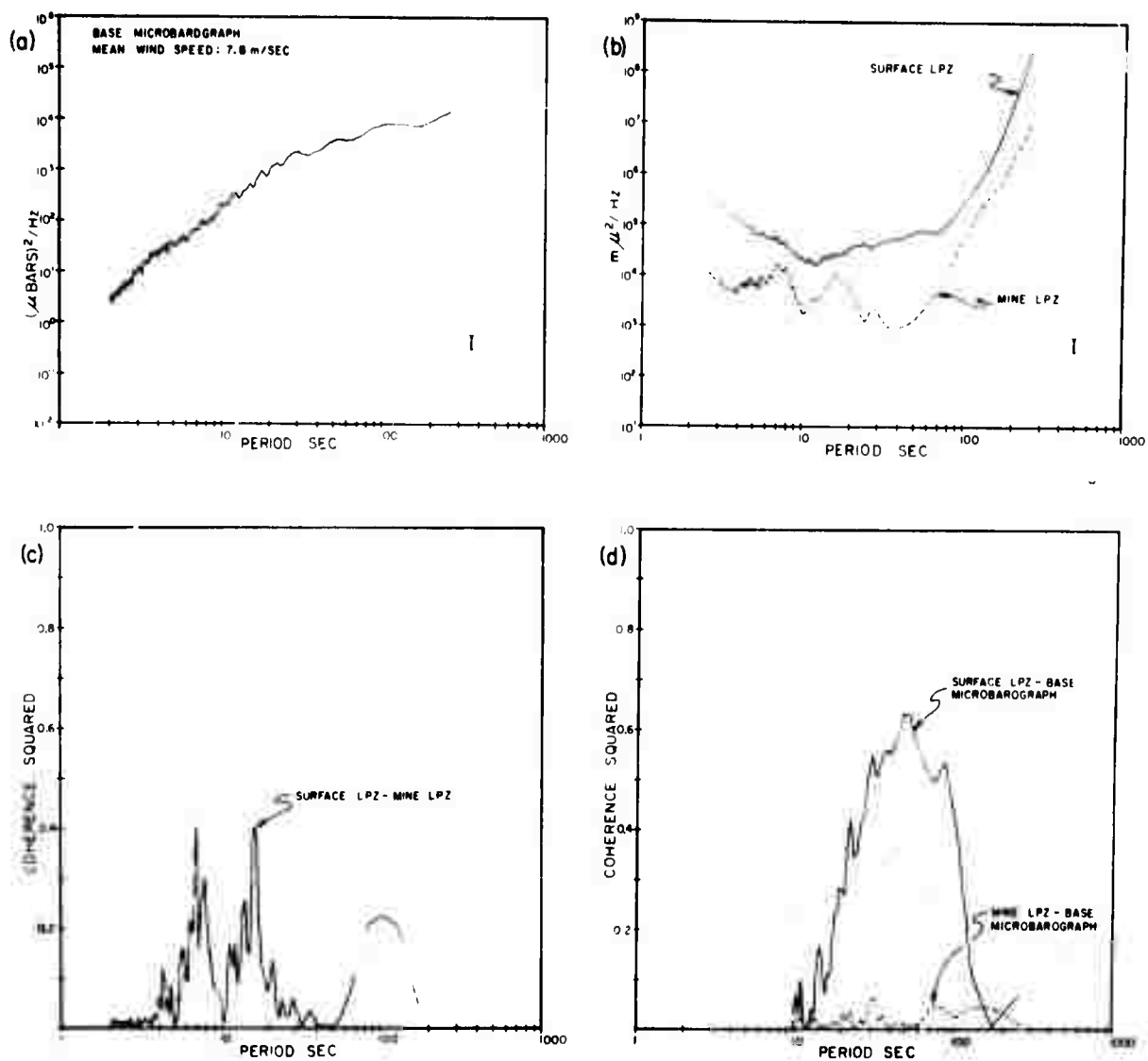


Figure 86. Noise recorded during a windy period

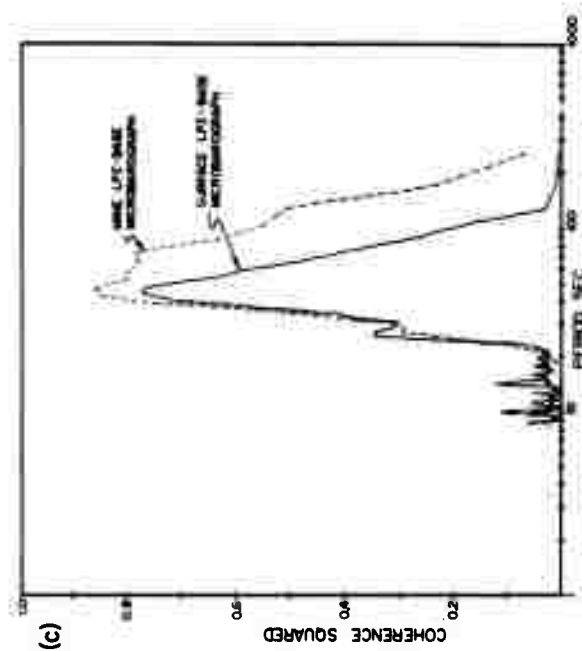
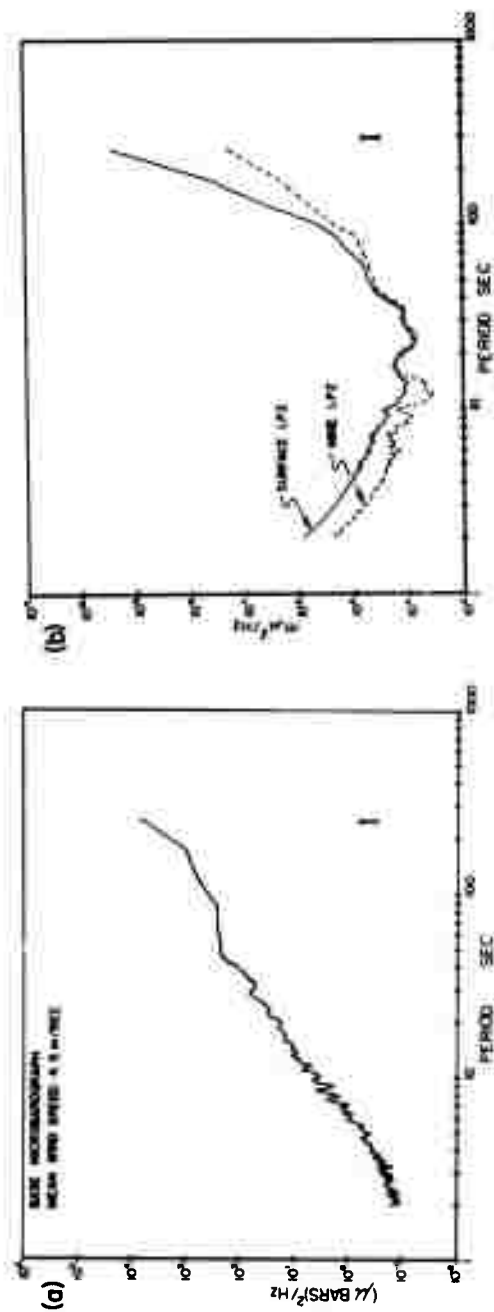


Figure 87. Noise recorded during the passage of acoustic waves

atmospheric pressure fluctuations. Thus, pressure changes associated with the passage of an acoustic wave, despite their relatively small amplitudes, contribute significantly to the seismic noise recorded at both locations, in contrast to wind-generated pressure changes which, as shown previously, contribute to the surface spectrum only.

#### 6.7.2.4 Discussion of Results

It is evident from the results presented in the preceding section that local variations in atmospheric pressure can contribute significantly to the noise observed on vertical seismographs, especially in the 20-100 second period range. The two most likely explanations for this phenomenon are that either the vertical seismometer is responding buoyantly to pressure changes acting directly on the mass, or the earth motion caused by atmospheric pressure changes is large enough to be observed against the background of noise from other sources.

6.7.2.4.1 Buoyancy. It has been known for some time that vertical long-period seismometers are quite sensitive to pressure changes. This effect was described by Cray and Ewing (1952) who showed that the apparent vertical earth displacement,  $W_a$ , caused by a sinusoidal pressure change of amplitude  $\delta p$  and frequency  $\omega$  acting on the mass of the seismometer could be expressed by

$$W_a(\omega) = \frac{\rho_o g \delta p}{\rho_m p_o \omega^2} \quad (1)$$

where  $\rho_o$  is the density of the air,  $p_o$  is the ambient pressure,  $g$  is the local value of gravity and  $\rho_m$  is the density of the seismometer mass. The apparent earth displacement in  $m\mu/\mu\text{bar}$  predicted by (1) were calculated using parameters appropriate to our system then listed in table 10 as a function of period. Notice that in the 20-100 second period range, the apparent displacements increase from about 16 to 300  $m\mu/\mu\text{bar}$ . Thus, unless steps are taken to isolate the vertical seismometer from the atmospheric pressure field, buoyant motion of the mass can be the primary source of noise in this period range.

In order to reduce buoyant effects, the vertical seismometers used in this experiment were placed in rigid steel containers which were then enclosed in sealed steel vaults. The time constant of the acoustic filter formed by the seismometer case according to tests made at the conclusion of the experiment was greater than 15 hours. The minimum time constant measured for the surface vaults was 8 hours. The apparent displacement that an external pressure change would cause in a system consisting of a sealed vault and seismometer case is given by

$$|W_a| = |R_v| |R_c| W_a \quad (2)$$

Table 10. The buoyant response of a vertical seismograph

<u>Period (seconds)</u>	<u>Open system mμ/μbar</u>	<u>*Closed system mμ/μbar</u>
10	3.92	$1.89 \times 10^{-6}$
20	15.68	$3.02 \times 10^{-5}$
30	35.28	$1.53 \times 10^{-4}$
40	62.72	$4.84 \times 10^{-4}$
50	98.00	$1.18 \times 10^{-3}$
60	141.12	$2.45 \times 10^{-3}$
70	192.08	$4.54 \times 10^{-3}$
80	250.88	$7.74 \times 10^{-3}$
90	317.52	$1.24 \times 10^{-2}$
100	392.00	$1.89 \times 10^{-2}$
120	564.48	$3.92 \times 10^{-2}$
140	768.32	$7.26 \times 10^{-2}$
160	1003.52	$1.24 \times 10^{-1}$
180	1270.08	$1.98 \times 10^{-1}$
200	1568.00	$3.02 \times 10^{-1}$

\*The closed system response is calculated under the assumption that the seismometer is enclosed in a sealed case and vault which have time constants of 2 and 8 hours, respectively.

where  $|R_v|$  and  $|R_c|$  are the moduli of the frequency responses of the acoustic filters formed by the vault and case, respectively. Both moduli are of the form

$$|R(\omega)| = \left[ \left( 1 + \frac{\omega\tau}{2\pi} \right)^2 \right]^{-1/2} \quad (3)$$

where  $\tau$  is the time constant of the filter. Equation 2 has been used to obtain a theoretical estimate of the direct contributions that local pressure changes could make to the noise recorded by the surface vertical seismograph. For the purposes of these calculations, the vault time constant was assumed to be 8 hours while the case constant was arbitrarily taken to be 2 hours. The results are listed in the last column of table 10. Observe that despite the low case time constant, the anticipated contribution at 100 seconds would only be about 0.02 mμ/μbar. On the other hand, theoretical studies of the earth's response to the wind-generated pressure field indicate that for rocks similar to those found at Grand Saline, the vertical displacements should be of the order of a mμ/μbar in the 20-100 second period range (Sorrells, 1971). Therefore, if the observed time constants accurately describe the pressure attenuation characteristics of the surface seismometer case and vault, the buoyancy contribution to the long-period noise recorded at the surface should be negligible in comparison to the anticipated earth motion at least at periods less than 100 seconds.

Similar arguments can be used to demonstrate that buoyancy effects are not anticipated to contribute significantly to the noise recorded by the mine vertical seismograph. In this case, the vault time constant was found to be about 24 hours. In addition, the mine itself acts as a low pass filter with respect to surface pressure variations. At periods less than 100 seconds the pressure variations in the mine were found to be more than 20 dB below those observed at the surface.

Thus, it can be expected that buoyancy effects on the mine vertical seismograph will be at least a factor of 30 smaller than those calculated for the surface system and therefore negligible in comparison to noise from other sources.

There is a more direct line of evidence bearing upon the buoyancy question. Suppose  $|H(\omega)|$  is the modulus of the frequency response which links changes in atmospheric pressure to one of the noise inputs of the vertical seismograph and suppose all other inputs are uncorrelated with local pressure changes; then an estimate of the frequency response function of the unknown operator may be obtained from

$$|\hat{H}(\omega)| = \frac{|\hat{R}_m(\omega)| |\hat{G}_{zm}(\omega)|}{|\hat{R}_z(\omega)| \hat{G}_m(\omega)} \quad (4)$$

where  $|\hat{R}_m|$  and  $|\hat{R}_z|$  are respectively the estimated frequency response functions of the microbarograph and the vertical seismograph;  $\hat{G}_{zm}$  is the cross spectral density estimate between the outputs of the two systems and  $\hat{G}_m$  is the power spectral density estimate of the output of the microbarograph. Equation 4 has been used to calculate  $|\hat{H}(\omega)|$  from data recorded by the surface vertical seismograph and the base microbarograph. Examples of the responses calculated from data recorded during a windy period and during the passage of an acoustic wave are listed together with their respective 95 percent confidence limits in tables 11, 12. These results assume no errors in the estimated frequency response functions of the base microbarograph and the surface vertical seismograph. In order to account for errors of this type it is necessary to multiply both the estimated response and its confidence limits by the factor

$$\frac{1 + \epsilon_z}{1 + \epsilon_m} \quad (5)$$

where

$$\epsilon_z = \frac{|\hat{R}_z| - |\hat{R}_z|}{|\hat{R}_z|}$$

and

$$\epsilon_m = \frac{|\hat{R}_m| - |\hat{R}_m|}{|\hat{R}_m|} \quad (6)$$

Now generally speaking in the period range 20 to 100 seconds  $\epsilon_z$  and  $\epsilon_m$  probably do not exceed  $\pm 0.1$ . Thus, the actual values could be as much as 1.23 (+1.8 dB) times greater or 0.823 (-1.8 dB) times less than those listed in tables 11, 12. In figure 88 we compare the experimentally determined functions with the buoyant responses of open and closed systems which were listed in table 10. It can be seen that the open system buoyant response lies well above the upper 95 percent confidence limits of both observed functions. From this, it may be inferred that at least one of the time constants is greatly in excess of 100 seconds. Therefore, if the observed functions are caused by the buoyant response of the vertical seismographs they should be increasing with increasing period at a rate of at least 18 dB/octave throughout the entire range of observation. However, a brief inspection of the experimental data is sufficient to demonstrate that a line with an 18 dB/octave slope cannot be fitted to either observed response and still remain within the 95 percent confidence limits for an appreciable range of values. This result strongly indicates that buoyancy does not contribute significantly to the observed results at periods less than 100 seconds. Finally, it can be seen that the response to atmospheric pressure changes caused by the acoustic wave is significantly greater than the response to pressure changes generated by the wind, at least over the period range from about 30-100 seconds. Even if we

Table 11. Estimated frequency response, windy period data\*

Period (seconds)	Estimated response $m\mu/\mu\text{bar}$	95% confidence interval	
		Upper limit $m\mu/\text{bar}$	Lower limit $m\mu/\text{bar}$
20.5	3.59	4.65	2.56
21.3	3.86	4.89	2.83
22.3	3.56	4.66	2.46
23.3	3.62	4.76	2.48
24.4	3.96	5.00	2.92
25.6	3.48	4.39	2.57
26.9	3.38	4.25	2.51
28.4	3.56	4.41	2.71
30.1	3.66	4.51	2.81
32.0	3.70	4.62	2.78
34.1	4.00	4.88	3.12
36.6	4.18	5.03	3.33
39.4	4.30	5.17	3.43
42.7	4.06	4.83	3.29
46.5	3.70	4.37	3.03
51.2	3.60	4.29	2.91
56.9	3.73	4.39	3.07
64.0	3.78	4.40	3.14
73.1	3.47	4.13	2.81
85.3	3.36	4.05	2.67
102.4	3.34	4.26	2.42

\*The estimated response given above was calculated from 9 hours of data recorded at 3 hour intervals when the mean wind speed was  $8.0 \pm 0.2$  meters/sec. The equivalent degrees of freedom for the calculation are 168.

Table 12. Estimated frequency response, acoustic wave data\*

<u>Period (seconds)</u>	<u>Estimated response <math>m\mu/\mu\text{bar}</math></u>	<u>95% interval</u>	
		<u>Upper limit <math>m\mu/\mu\text{bar}</math></u>	<u>Lower limit <math>m\mu/\mu\text{bar}</math></u>
20.5	0.0 <sup>+</sup>	-	-
2.3	0.0 <sup>+</sup>	-	-
22.3	0.0 <sup>+</sup>	-	-
23.3	0.0 <sup>+</sup>	-	-
24.4	11.0	19.7	2.3
25.6	13.0	20.5	5.5
26.9	11.5	18.2	4.8
28.4	11.0	17.8	4.2
30.1	12.1	19.7	4.5
32.0	13.5	20.6	6.4
34.1	12.7	18.9	6.5
36.6	15.8	21.6	10.0
39.4	19.1	23.4	14.5
42.7	18.6	22.8	14.4
46.5	18.1	22.3	13.9
51.2	18.5	24.0	13.0
56.9	17.5	23.5	11.0
64.0	17.9	25.4	10.4
73.1	20.4	30.8	10.0
85.3	21.1	34.8	7.4
102.4	21.5	39.5	3.5

\*The estimated response given above was calculated from 2 hours of data.  
The equivalent degrees of freedom for the calculation are 39.

<sup>+</sup>Not significantly different from zero at the 95% confidence level.

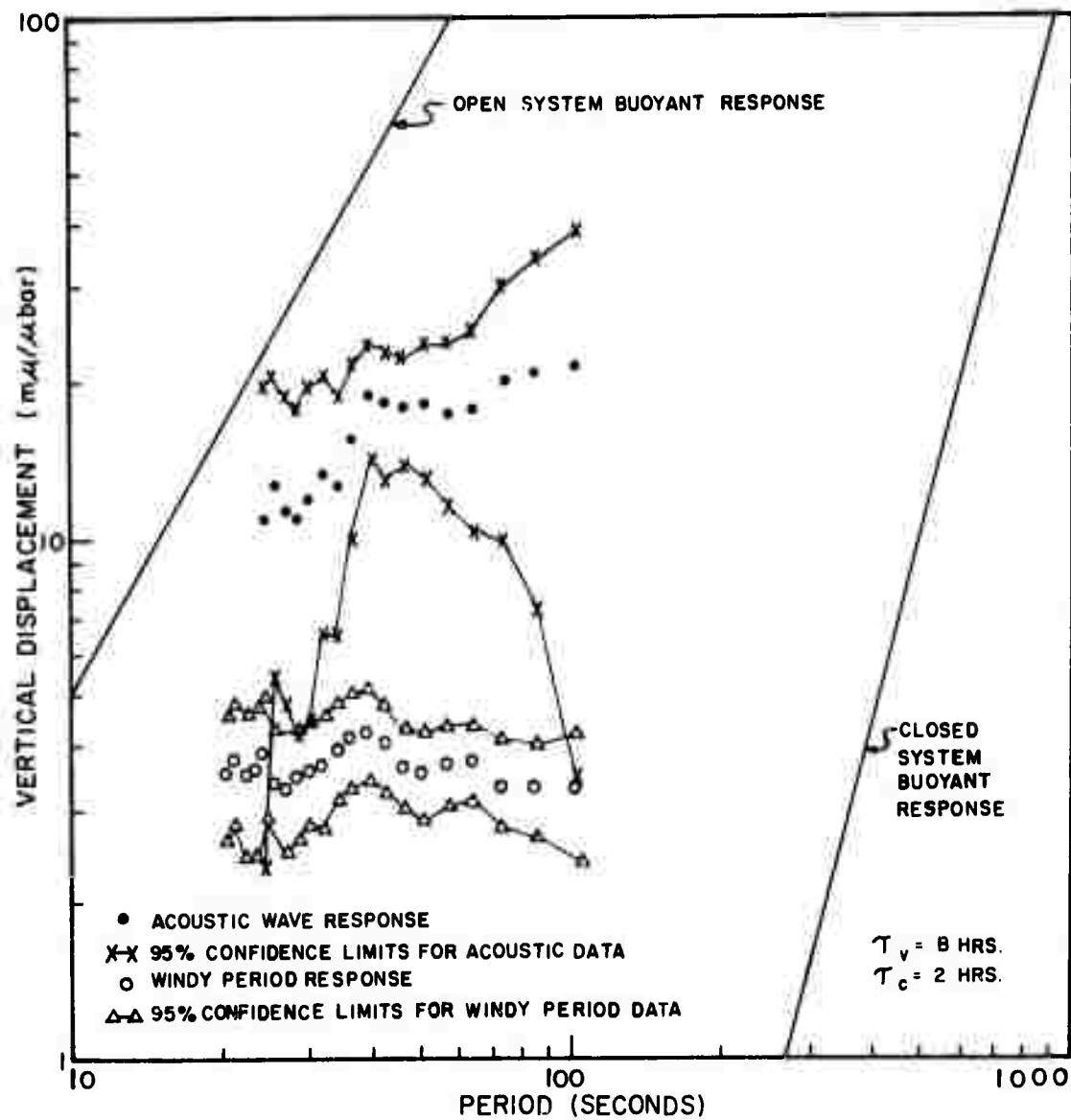


Figure 88. Comparison of observed responses with calculated buoyant responses

assume combined errors in the estimated instrument responses of -1.8 dB for the acoustic data and +1.8 dB for the windy period data there will still be no overlap of their respective 95 percent confidence regions in the period range 40-100 seconds. This observation is completely at odds with the buoyancy hypothesis since the response of a vertical seismometer to a pressure change acting directly on the mass must be the same regardless of the cause of the pressure change. Therefore, on the basis of the results presented in this section, we conclude that the pressure related seismic disturbances observed during windy periods and during the passage of acoustic waves are not caused by the buoyant response of the vertical seismograph.

6.7.2.4.2 Elastic Deformations. There is considerable experimental evidence which indicates that the pressure field caused by the wind is spatially organized and tends to propagate at the mean wind speed. On the strength of this evidence, Sorrells (1971) suggested that to a first approximation, the wind-generated pressure field could be considered to be a plane wave propagating at the speed and in the direction of the mean wind. A computer program has been developed which calculates the displacement frequency response of a layered elastic half space to a slowly moving plane pressure wave (Sorrells and Der, 1970). This program has been used to calculate the responses of two earth models which approximate the structure at and about the Grand Saline Salt dome. Model 1 which approximates the structure at the salt dome is shown in figure 89. The salt dome itself is assumed to be infinitely extended in the horizontal dimension and is represented by the semi-infinite layer in this model. The second layer represents the salt dome cap which is remarkably thin at Grand Saline, while the upper layer represents the poorly consolidated Tertiary sediments overlying the dome. With the exception of the P and S velocities in this upper layer, the properties of this model are reasonably well established. There is, however, a considerable uncertainty associated with the estimates of these quantities. Sonic log data from a nearby well shows the P-wave velocity to be 1.9 km/sec at a depth of 183 meters. We would anticipate the velocity above this level to be somewhat lower. Cores from test holes in the immediate vicinity of the recording site show that the upper layer consists primarily of sandy clay with interbedded sand lenses. Measurements reported by Press (1966) indicate that P-wave velocities could be as low as 900 meters/sec. We have assumed a value of 1.3 km/sec; however, it could be as high as 1.5 km/sec or as low as 1.1 km/sec without substantially changing the calculated response. The shear wave velocity in the upper layer was assumed to be 0.475 km/sec because that value provided a theoretical response which agreed reasonably well with the experimental data at periods less than 30 seconds. As we shall see, however, the velocity could be as low as 0.400 km/sec or as high as 0.550 km/sec.

Since the salt dome is in fact limited in horizontal extent, it is necessary to consider the sediments surrounding the dome as well. Model 2 which is shown in figure 90, approximates the structure in this region. Down to a depth of 88 meters it is the same as that used in Model 1. Below that depth the P-wave velocities and thicknesses were taken from a sonic log which was made approximately 5 miles northwest of the recording site. The S-wave velocities were calculated from P-wave data under the assumption that Poisson's ratio was 0.33. Likewise densities were calculated from the P-wave data assuming a linear relationship between the two quantities.

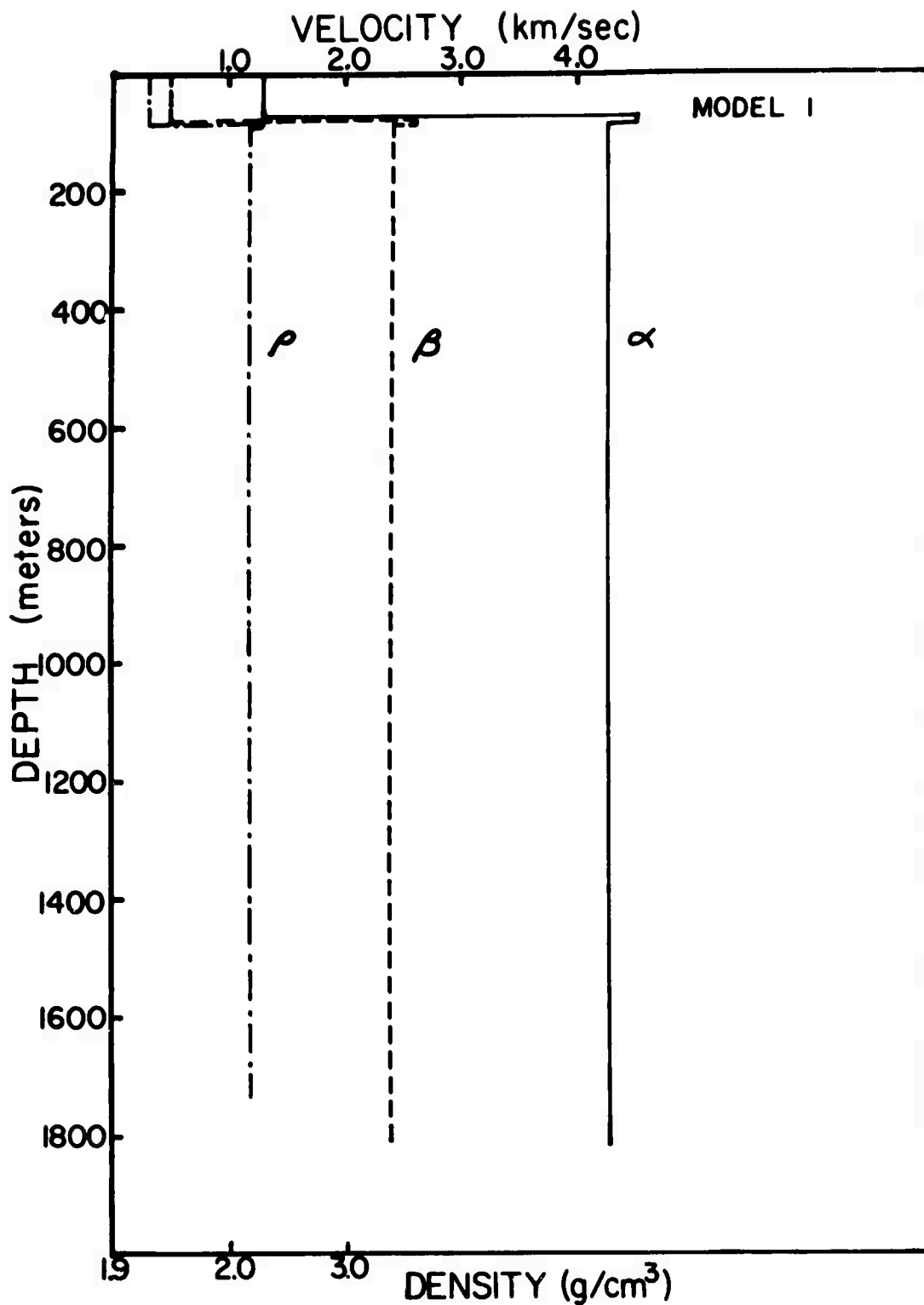


Figure 89. Velocity model of earth structure at the Grand Saline salt dome

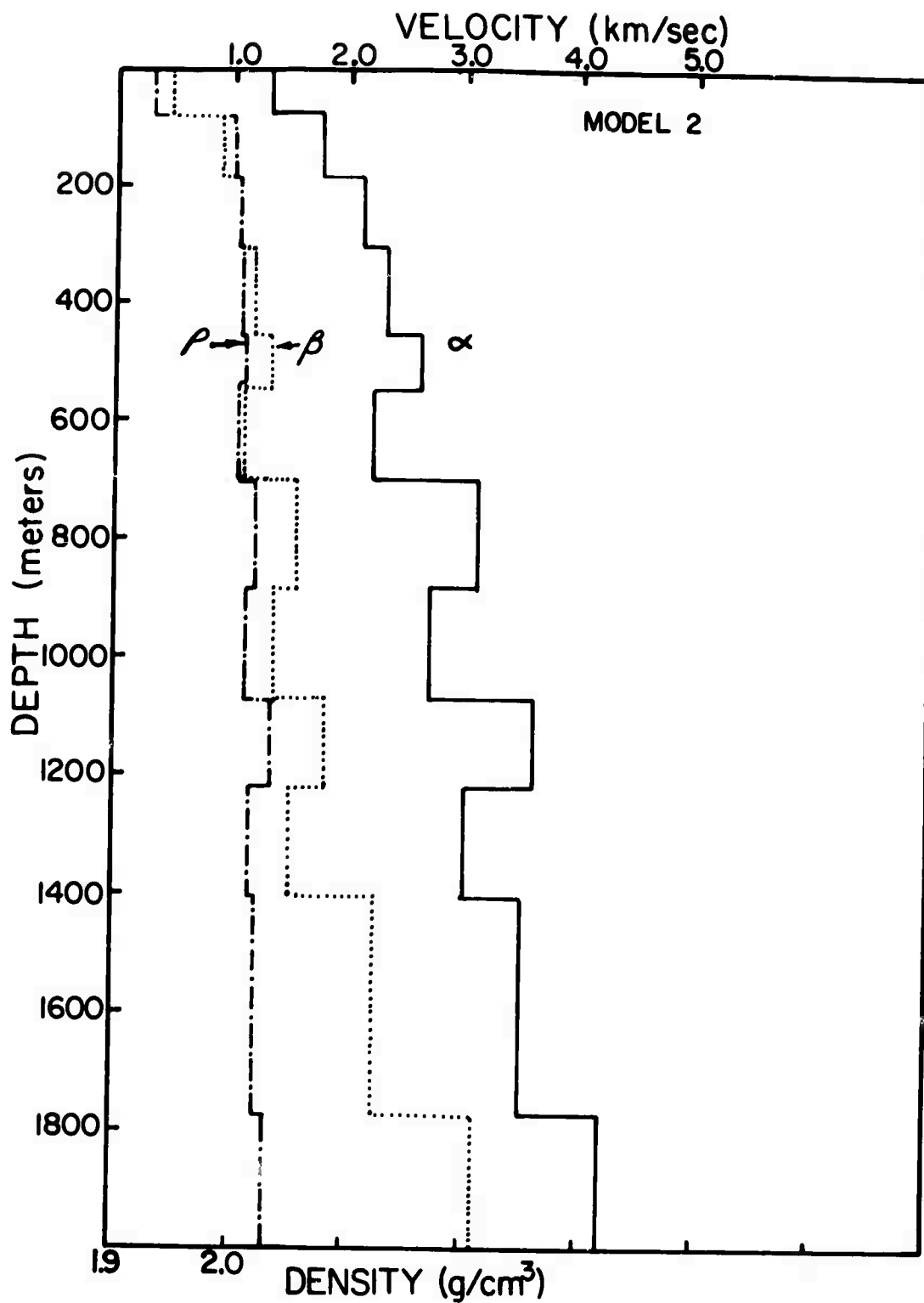


Figure 90. Velocity model of the earth structure surrounding the Grand Saline salt dome

In figure 91, the theoretical responses for Models 1 and 2 are compared to an experimental response calculated using equation 4. The data used in the calculation were recorded by the surface vertical seismograph and the base microbarograph during an interval when the mean wind speed was 9.4 meters/sec. Notice that at periods less than about 30 seconds the response of Models 1 and 2 are virtually identical. While there is considerable scatter in the experimental data in this period range, its basic trend is satisfactorily approximated by the predicted response. The shape of the response curve below 30 seconds is determined largely by the structure in the uppermost 80 meters. The observed scatter suggests that the structure within this zone may be considerably more complex than was assumed in constructing the models. The two dashed curves which form the envelop enclosing the experimental data are the responses obtained from Model 1 when the shear wave velocity in the first layer is changed to 400 meters/sec and 550 meters/sec. These probably represent the limits on the value the shear wave velocity can assume in the upper layer.

Observe that at periods greater than 30 seconds the experimental data favors Model 1. This is encouraging since the recording site is located above the salt dome and the wavelengths involved are less than the diameter of the dome ( $\sim 3$  km). Notice, however, that there is a systematic divergence between the observed data and the Model 1 response at periods greater than about 50 seconds (wavelengths  $\sim 470$  meters). It is felt that this reflects the influence that the sediments surrounding the dome exercise on the observed response. This influence should increase with increasing wavelength until at wavelengths large compared to the diameter of the dome, the observed response should closely resemble the Model 2 response. As shown in the next paragraph the observed acoustic wave data are in good agreement with the response predicted by Model 2. The apparent absence of pressure generated noise in the mine during windy periods can be explained by comparing the responses of Model 1 at the surface and at a depth of 183 meters. It will be observed that at periods less than 100 seconds the calculated responses predict that the amplitudes of the pressure generated noise recorded in the mine should be at least a factor of 7 below that recorded at the surface.

Experimental responses estimated from data recorded by the surface and mine vertical seismographs and by the base microbarograph during the passage of an acoustic wave are compared to the Model 2 response to a plane wave propagating at 330 meters/sec in figure 92. The theoretical responses are seen to provide a relatively good fit to the observed data at periods greater than about 40 seconds.

Notice that the surface experimental response runs consistently lower than its theoretical counterpart, but at periods greater than about 40 seconds the maximum difference is only about 3 dB. This could be caused by errors in the estimated response of the surface vertical seismograph. At periods less than 40 seconds, both observed responses depart systematically from the theoretical prediction. The cause of this phenomena is not presently known.

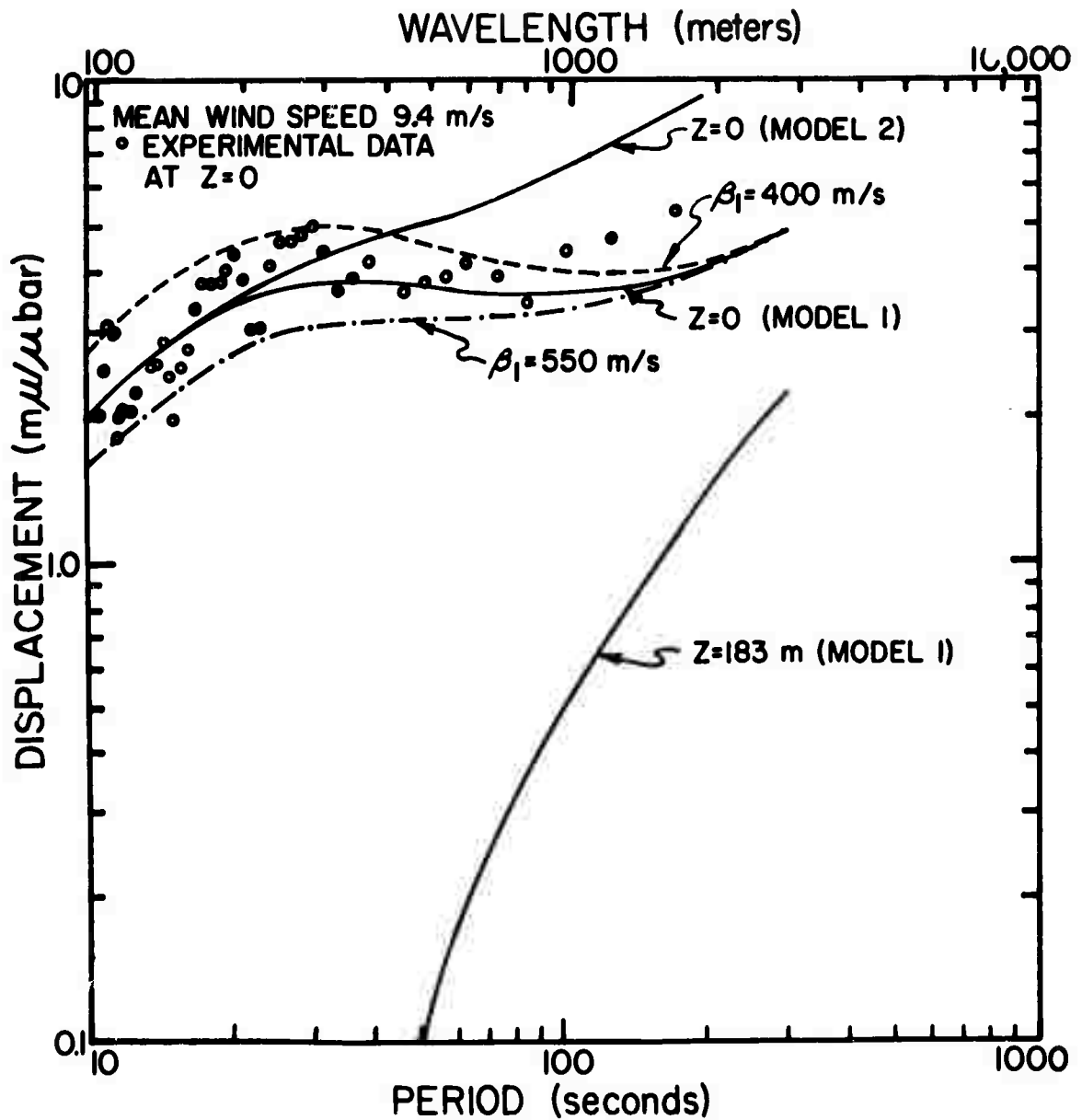


Figure 91. Comparison of the observed and predicted surface vertical displacement responses for windy period data

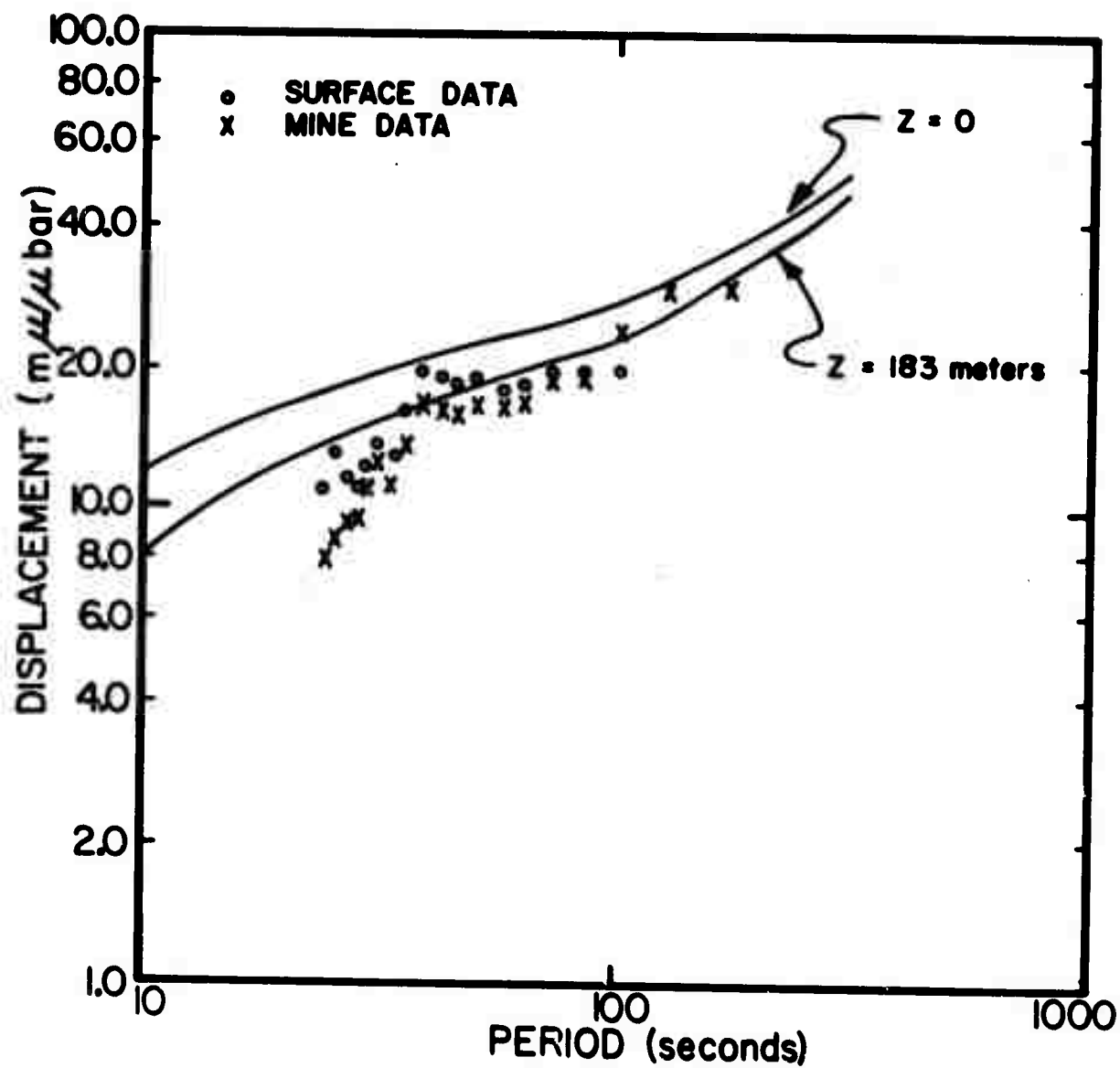


Figure 92. Comparison of observed and predicted vertical displacement responses for acoustic wave data

Overall, however, the agreement between the observed and calculated responses is good for both the windy period and acoustic wave data. This strongly indicates that much of the noise recorded during windy periods and during the passage of acoustic waves at Grand Saline is earth motion generated by local atmospheric pressure fluctuations.

6.7.2.4.3 The Response of Other Geologic Media to the Wind Generated Pressure Field. The relatively good agreement between observed and calculated responses implies we may use the theory developed during this experiment to predict the pressure generated contribution to the long-period noise recorded by a vertical seismograph located in other geologic media. In figure 93 we compare the windy period response obtained at the surface at Grand Saline with theoretical responses calculated for a granitic half space and for a semi-infinite layer of granite overlain by a 2 meter thick section of low-velocity material. The parameters used in the calculations are listed in table 13. These models were selected for examination because they represent the general type of geologic environment that experience has led us to associate with a "quiet" surface seismograph installation. Note that the inclusion of the thin low velocity surface layer has little effect on the granitic response at periods greater than about 20-30 seconds. There is, however, a dramatic difference between the anticipated granitic response and the Grand Saline response. At a period of 100 seconds the hypothetical granitic response is about 20 dB below the Grand Saline response and at a period of 20 seconds the difference is almost 32 dB. Using these results and assuming that the noise unrelated to local pressure variations is the same at Grand Saline and the hypothetical granitic site, it can be shown that the same pressure field which contributed almost 50 percent of the noise power observed at the surface at Grand Saline in the 20-100 second period range would contribute less than 1 percent of the total noise power recorded in the same pass band at the surface of the granite site. Hence, other things being equal, the noise level observed at a surface site with the elastic properties of the rocks listed in table 13 should be consistently comparable to that observed in the mine at Grand Saline. Furthermore, it can be anticipated that the coherence between the seismic data recorded on the granite would be incoherent with data recorded by a nearby microbarograph.

Table 13. Parameters used in the calculation of displacement responses

<u>Model No.</u>	<u>Layer No.</u>	<u>Thickness (meters)</u>	<u>P velocity (km/sec)</u>	<u>S velocity (km/sec)</u>	<u>Density (g/cm<sup>3</sup>)</u>
3	1	$\infty$	5.56	3.15	2.63
4	1	2	1.5	0.5	1.9
	2	$\infty$	5.56	3.15	2.63

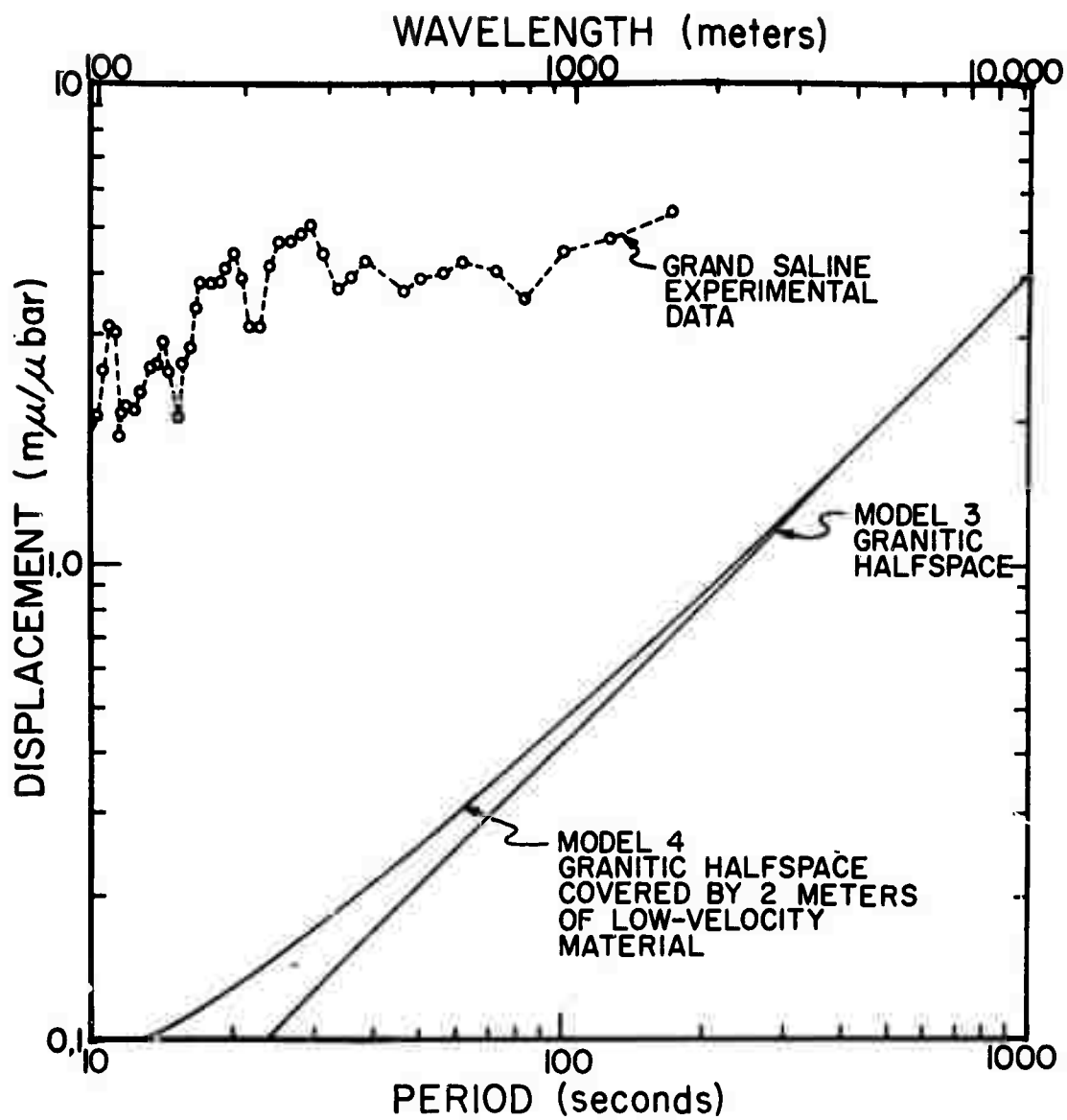


Figure 93. Comparison of the observed Grand Saline vertical displacement response with those predicted for a granitic half space and a thin low-velocity layer overlying a granitic half space

#### 6.7.2.5 Conclusions

The results of the Long-Period Noise Experiment at Grand Saline have demonstrated quite clearly that earth motion in response to the wind-generated pressure field can contribute significantly to the noise recorded at the surface in the 20-100 second period range. Both theory and experiment indicate that this type of noise will be most severe in geologic regimes characterized by a low velocity surficial layer which is more than 50-75 meters thick. In such regimes, however, our results demonstrate that the earth motion caused by wind generated pressure changes can be substantially reduced by placing the detector at a depth of several hundred meters. In regions where high velocity rocks extend to the surface, the theory predicts that this noise will be negligible in comparison to noise from other sources and it can be anticipated that the noise levels observed at the surface in such regions will be comparable to those obtained in mines. These results are consistent with empirical observations gathered over the years which have taught us to seek out "hard rock" geology as sites for seismic observations. Thus, the results of the Grand Saline experiment have provided us with information necessary to eliminate the wind generated pressure field as a major long-period noise source. However, even after elimination of noise from this source, presently operating long-period seismograph systems are still limited by earth rather than system noise. Little is known about the source of this noise other than it appears to be characterized by much longer wavelengths than those found in the wind-generated pressure field. Results by Savino et al (1971) and Haubrich (1970) imply that a substantial fraction may be generated by large scale atmospheric pressure changes. If this is true then methods similar to those used to eliminate wind-generated pressure noise could be applied to reduce its contribution. However, in this regard, it should be recalled that in the case of the acoustic wave, which was the only clear cut example of noise observed during the Grand Saline experiment caused by a large scale pressure disturbance, pressure generated earth motion contributed virtually the same amount of power to the noise recorded at the surface and at a depth of 186 meters. From this we may infer that it will be necessary to locate seismometers at substantially greater depths (probably on the order of a kilometer or so) if this source proves to be a major contributor to the long-period noise spectrum.

#### 6.7.2.6 Recommendations

The results of this experiment clearly demonstrate the importance of the role that local geology plays in determining the noise level recorded by a long-period vertical seismograph. In general, areas characterized by a low velocity surface layer should be avoided. As a rule of thumb, long-period seismograph systems should not be installed at the surface if the average P-wave velocity of the uppermost 50-75 meters is below about 2.0 km/sec. If other circumstances require the installation of a seismograph system in a poor geological environment then they should be placed at depths on the order of several hundred meters.

In the absence of noise caused by the wind-generated pressure field, earth motion is still recorded at a level well above the system noise level at least out to periods on the order of 130 seconds. Any further improvement in surface wave signal-to-noise ratio at a given site over that obtained through the elimination of wind-generated pressure source, will be determined by how successful we are in reducing this noise. In order to design techniques for the elimination of this noise its source or sources must be known. A proposed experimental program dealing with this problem has been submitted to the Project Office.

## 6.8 STUDY, TEST, AND MODIFICATION OF THE LONG-PERIOD TRIAXIAL SEISMOMETER

### 6.8.1 General

Tests conducted on the Triaxial Seismometer, Geotech Model 31300, at various locations have indicated that external pressure variations cause spurious deflections in the output data. Results of these tests and mechanisms which might produce this pressure sensitivity are discussed in the following paragraphs.

The well casings in which triaxial seismometers are installed are normally sealed. It was originally assumed that pressure variations inside the casings would be negligibly small. However, an investigation into the possible causes of noise which appeared at the outputs of the instrument systems during the winter months indicated that pressure changes in the range from 10 to 100 microbars were occurring inside well casings which had been verified to be properly sealed.

Further investigation revealed air turbulence within the casing as the probable mechanism causing the pressure changes. Air warmed within the depth of the casing would rise; air cooled at the casing head would fall. The warm air and cool air, traveling in different directions would generate the turbulence. Under turbulent conditions, the average temperature of the air in contact with the cool casing head would vary with time, giving rise to a time-variable heat flow and therefore a time-variable mean temperature within the casing. With a constant volume of air within the casing the changing temperature would cause a changing pressure. It would appear that the pressure changes caused by this sequence of events would be exceedingly small, and indeed the experienced pressure changes are in the order of a few parts per hundred thousand.

The pressure changes can be eliminated by filling the upper portion of the casing with granular insulation material. This apparently stops the turbulent flow and converts the energy out-flow into a slower, more uniform process. However, it obviously would be desirable to make the triaxial seismometer less sensitive to pressure changes.

There is a question as to what sensitivity (i.e., equivalent input motion versus pressure change) should be considered allowable. This sensitivity produces a spurious output which should be restricted to a level no greater than that allowed for total system electronic noise. This restriction indicates that pressure changes should be allowed to cause an equivalent input motion not greater than about 10 millimicrons peak-to-peak.

Experience has indicated that long-period systems cannot be operated successfully when exposed to the atmosphere where pressure changes of several hundred microbars are common. While no definite information is available to indicate the maximum pressure changes which could be allowed, this value is undoubtedly below 100 microbars. Tentatively, the value of 100 microbars will be selected as a desirable maximum allowable pressure change, with the stipulation that this value may not be attainable in practice.

The statements on pressure sensitivity of the long-period triaxial seismometer may be summarized as follows:

It would be desirable for the output of the seismometer to be less than the equivalent of 10 millimicrons input motion in response to pressure changes as great as 100 microbars.

The frequency band in which this sensitivity should apply will be discussed in another paragraph.

In some of the tests conducted on the triaxial seismometer, trace deflections of approximately 3 millimeters p-p were noted at a magnification of 15K when the unit was subjected to pressure variations of 30 microbars p-p. If 100 microbars p-p had been applied, trace deflections of approximately 10 millimeters would have been recorded and this output would be equivalent to approximately 670 millimicrons p-p. This indicates a sensitivity approximately 67 times greater than the desirable value.

Results of other tests confirmed that the pressure sensitivity indicated in the preceding paragraph was fairly typical; leading to the tentative conclusion that the sensitivity is a function of the design of the triaxial transducer. This conclusion prompted a careful examination of the physical design of the transducer to isolate any design features which might account for the sensitivity to pressure.

The triaxial transducer is shown in figure 94 and an individual module is shown in figure 95. In these figures, the module cases have been removed. The module case for each module does not attach rigidly to the unit, but "floats" on O-rings around the perimeters of the upper flange (upper ring seal and top plate) and the lower flange of the module.

As may be seen in figure 95, the transducer element is attached to the lower flange and the lower flange and upper flange of each module are connected by four stanchions. Figure 94 shows how the stabilizer, modules, and hole-lock are fitted together at the flanges to make up the triaxial seismometer.



Figure 24. Triaxial Transducer, Model 31300

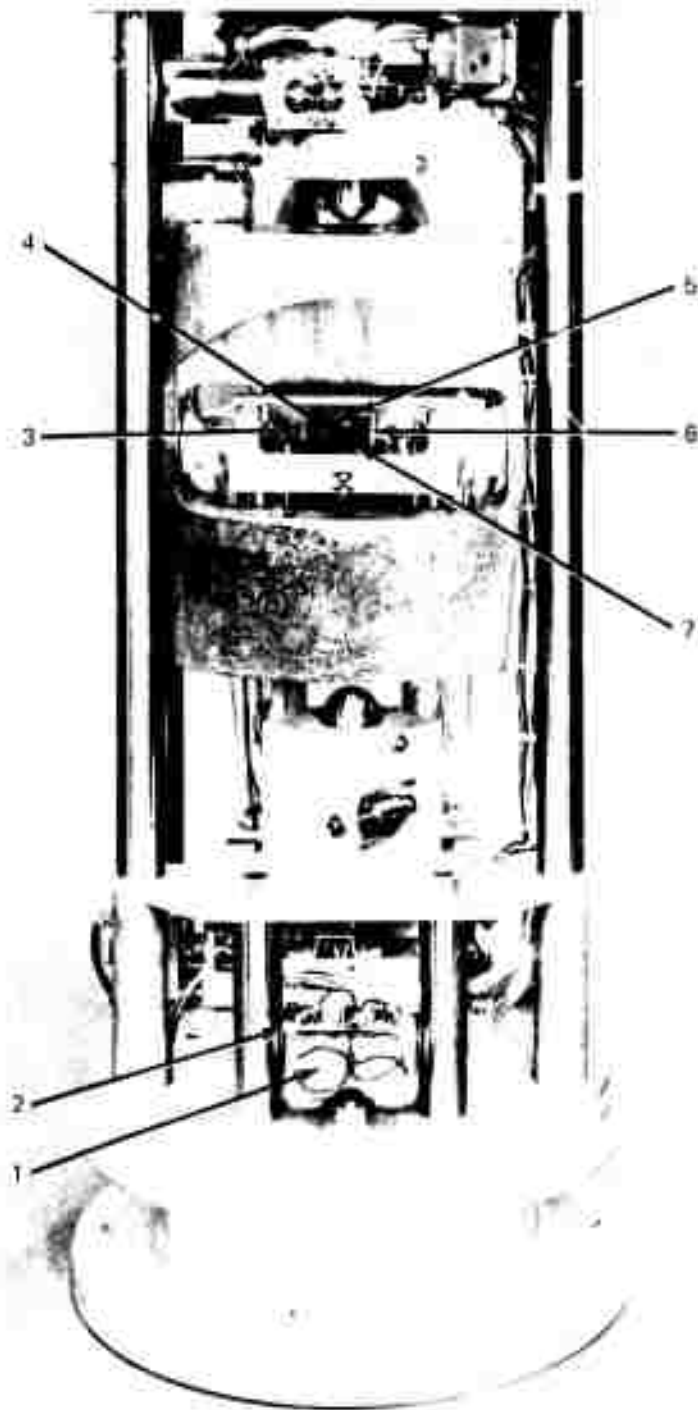


Figure 95. Transducer Module, Model 26310

The effects of an increase in pressure on the transducer may be examined by considering the axial and radial pressure components separately. The axial component of the pressure increase will cause a force to act along the vertical axis of the seismometer. This force will be transmitted through the stanchions and flanges from the stabilizer to the molelock. The stanchions and flanges will be compressed, and the flanges will be deformed because of their physical shape.

Differential variation of the distance between the top flange and bottom flange along the axes of the stanchions may occur because of variations in the firmness of seating of the stanchions against the plates.

The radial component of the pressure increase will cause a force to act on the outer surface of the module cases. These cases will be compressed diametrically, and a small force will be transmitted through the O-rings to "squeeze" the flanges. The surfaces of the flanges open to the pressure increase will also experience a radial "squeeze."

The investigation disclosed two other ways in which an external pressure increase could influence the transducers. The external pressure increase will decrease the volume of the transducer housing by compression causing an increase in the pressure inside the housing. A flexible mechanical coupling connects from the top flange assembly to the base of the transducer mounted on the lower flange. Compression of the stanchions will cause the top flange to move downward with respect to the lower flange and some force can be transmitted through the flexible mechanical coupling. Several flexible electrical wires also form mechanical linkages from the case portion of the transducer module to the sensitive element. These wires exit from a wiring bundle attached to a stanchion and are connected to terminals on the sensitive element. Stanchion compression could cause forces to be transmitted through these wires.

The possible ways in which a pressure increase could act on the sensitive element of the transducer to cause a spurious output are listed below:

- Compression of stanchions
- Axial compression and deformation of flanges
- Differential seating of stanchions
- Radial compression of flanges
- Change in internal pressure
- Force transfer by flexible mechanical coupling
- Force transfer by flexible electrical wiring.

Each of the four stainless steel stanchions which connect the upper and lower flanges of each module is 7/8 inch in diameter and 19 inches long. The active area at the top or bottom of each module is approximately 80 square inches, so that a 100 microbar pressure increase would cause an axial force of 0.12 pound. Each stanchion would experience a force of 0.03 pound and using Young's Modulus as  $30 \times 10^6$  pounds per square inch, each stanchion would be compressed by only 0.8 millimicron - over an order of magnitude below the system threshold.

The stanchion forces caused by the pressure change are transmitted to the top surface of the lower flange - the surface on which the sensitive element of the transducer module is seated. The fact that the stanchions were seated on this critical surface in overhanging positions prompted a careful investigation to determine if the forces transmitted by the stanchions might be causing deformations of sufficient magnitude to cause tilting of the sensitive element. The effects of the stanchion forces on the lower flange are analyzed by approximation methods in appendix 1 and the effect of tilt on horizontal long-period transducers are analyzed in appendix 2.

These data indicate that a 100 microbar pressure change would induce local tilts in the surface on which the sensitive element is seated several hundred times greater than the maximum allowable value. The pattern of these tilts would have some symmetry; however, second order effects approximately an order of magnitude below the amplitude of the local tilts could be expected. Thus, the expected second order tilting would essentially explain the results of pressure sensitivity tests discussed in a previous paragraph.

It is possible that differential seating of the stanchions in one module could cause tilting of the modules mounted above it. Differences in the firmness of the connections between the stanchions and the flanges could cause the effective stanchion length to vary under the influence of pressure changes even though the stanchions were compressed identically. Calculations based on the information given in appendix 2 indicates that the maximum allowable difference in effective stanchion compression is only 0.001 millimicron.

Rough estimates indicated that radial compression of flanges probably would produce less than 1/10 of the effect of axial compression and that changes in internal pressure and force transfer by flexible coupling and wiring probably are negligible.

#### 6.8.2 Work Progress

The work set forth in Engineering Change Proposal No. 1 was begun during August 1971. The test procedures, instrumentation configurations, and results of the tests conducted at ALPA from March to June 1971, were received while preparations were being made to conduct field tests on standard and modified triaxial modules in a quiet location. The studies indicated that the pressure sensitivities of modules assembled in a standard stack varied over a range of approximately plus 9 to minus 9 microns per millibar, where pressure sensitivity is defined as the equivalent earth motion in microns at a 25-second period required to produce the same output as the applied pressure change in millibars. The pressure sensitivity of modules in the standard stack varied within this range when the stack was positioned in different orientations, and also when the stack was removed and reinstalled. Module pressure sensitivities showed much less dependence upon orientation, and little dependence upon method of module support (with or without holelock and/or stabilizer)

when the stack was mounted inside a stiffener that supported both ends of each module. These data indicate that module pressure sensitivities are strongly affected by strains in the module. The results of tilt tests at Garland also were studied, and plans were made to repeat these tests under closely controlled conditions, as the early test results indicated a relationship between module pressure sensitivity and tilt.

Two experimental module flanges were built. The first was simply webbed to strengthen it and prevent its distortion by axial forces applied through the stanchions. The second was both webbed for strength and counterbored to accept long stanchions which transmit axial module forces to the bottom of the flange without distorting the top surface to which the boom assembly is fastened. Figure 96 shows a photograph of the webbed flange, and figure 97 shows a photograph of the extended stanchion flange.

Two modules, each equipped with one of the experimental flanges, and one standard module were mounted on a triangular baseplate made from 1-inch-thick aluminum jig-plate. The baseplate, equipped with a remotely-controlled tilt mechanism, was placed on the floor of a sealed tank vault installed in the Kleer (salt) mine at Grand Saline, Texas. The tank vault, shown in figure 98, is located at  $32^{\circ}39'55''$  N latitude,  $95^{\circ}42'13''$  W longitude, at an elevation 94 meters (308 feet) below mean sea level. The earth's surface above the vault has an elevation of 119 meters (390 feet) above sea level. A reciprocating pump was connected to the vault and was used to generate very-nearly sinusoidal pressure variations of approximately 0.4 millibar peak-to-peak at periods of 20 and 60 seconds. Figure 99 shows a frequency response of the triaxial channels tested in the mine.

Equipment installation was completed late in September, and testing was begun immediately thereafter. Table 14 presents the results of these tests.

The disagreement in module responses shown by the data taken during September suggested that the seals of one or more modules might be defective, and that pressure variations might be acting directly upon the masses of these modules. Accordingly, the module sealing covers were drilled, tapped, equipped with pipe fittings, and reinstalled on the modules from which they were removed. Module time constants of 91.5, 643, and 89 hours were measured for modules TR1, TR2, and TR3, respectively.

On 4 October, module pressure responses were measured with the holes in the module covers left open. Note that pressure response amplitudes increased, but that the polarities did not change. TR1 and TR3 produced negative responses, while TR2 produced a positive response. However, after the modules were resealed, TR1 and TR2 both produced positive responses while TR3 produced unreadable small responses. During subsequent tests from 6 through 13 October, TR1 and TR2 continued to produce positive responses, and TR3 produced small, variable, negative responses. On 7 October, it was established that banging the masses against their stops by passing current from an ohmmeter through their data coils did not significantly change the module pressure responses.



Figure 96. Modified flange with retained metal webbing

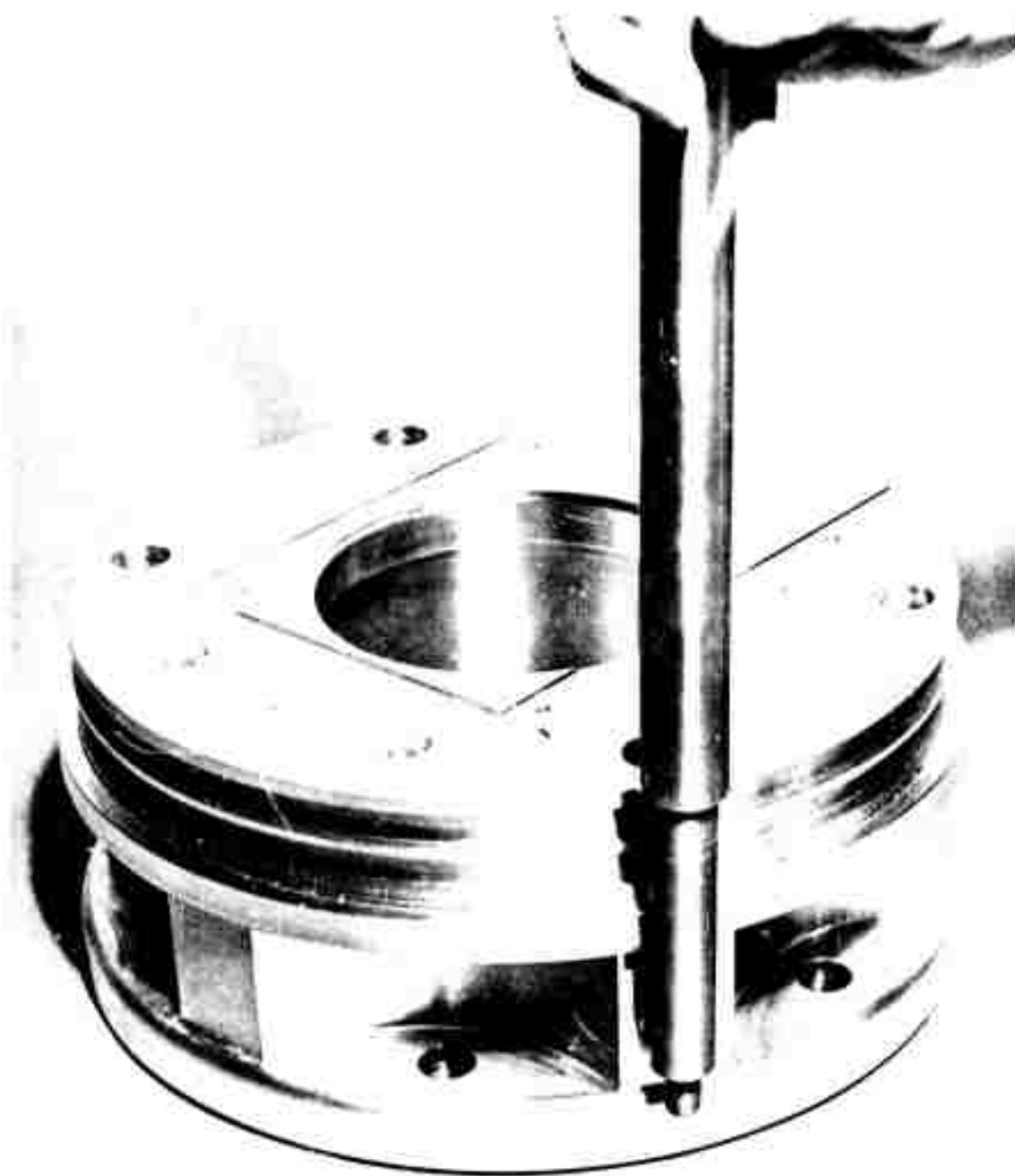


Figure 97. Modified flange with recessed stanchion sockets



Figure 98. Completed vault installation in Kleer Mine,  
Grand Saline, Texas (GA3TX)

G 6506

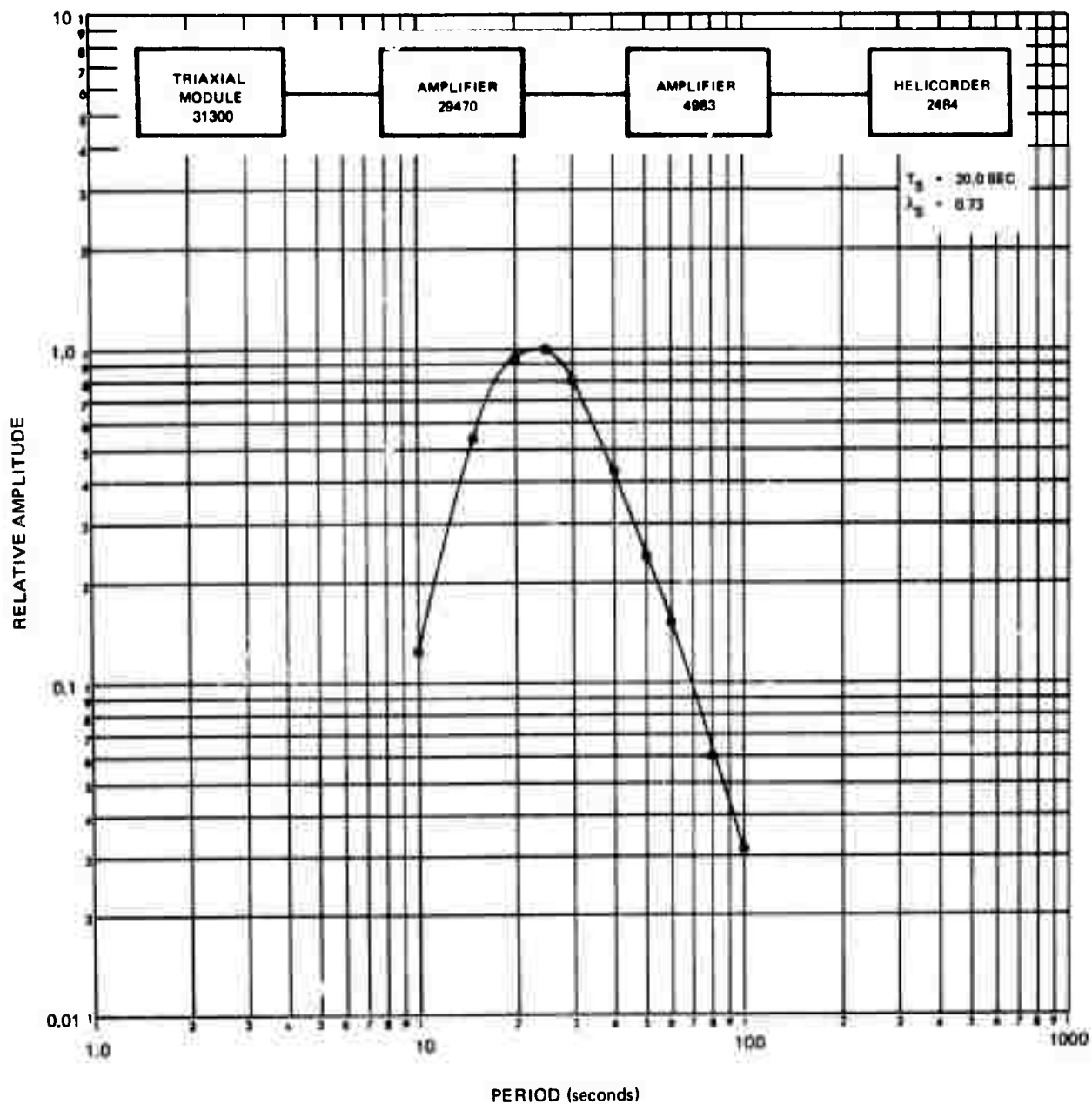


Figure 99. Frequency response of triaxial seismograph channels tested at Grand Saline

Table 14. Pressure sensitivities of triaxial modules measured under various test conditions in salt mine at Grand Saline, Texas. The TR1 module has a standard flange, the TR2 module has webbed flange, and the TR3 module has recessed stanchion sockets.

Equivalent ground motion in microns p-p (no freq corr), with positive deflection equivalent to ground motion up												
Date	TR1		TR2		TR3		Plate tilt	Pump stroke	Module sealing			
	20 sec	60 sec	20 sec	60 sec	20 sec	60 sec						
24 Sep	-2.46		7.48		-4.91		0°	full	sealed			
27 Sep	-0.94	-2.08	6.83	8.32	-2.62	-5.24	0°	full	sealed			
27 Sep	-0.52	-1.04	3.73	4.91	-1.31	-2.62	0°	half	sealed			
29 Sep	-1.84	-3.67	9.00	17.8	-3.20	-6.10	+1°	full	sealed			
29 Sep	-0.92	-1.94	5.20	10.4	-1.66	-3.10	+1°	half	sealed			
30 Sep	-1.71	-3.12	8.69	16.9	-3.80	-6.98	0°	full	sealed			
04 Oct	-3.33	-9.10	10.2	18.3	-4.00	-11.6	0°	full	unsealed			
04 Oct	1.92 (time constant = 91.5 hours)	3.33	17.5	31.6	small (time constant = 89 hours)	small	0°	full	sealed			
06 Oct	1.67	3.33	17.6 (time constant = 643 hours)	32.8	-0.58	-0.78	0°	full	sealed			
07 Oct	1.77	3.33	17.2	23.6	-0.52	-0.93	0°	full	sealed			
07 Oct	bumped masses against stops with ohmmeter											
07 Oct	1.62	3.24	16.7	25.3	-0.51	-0.82	0°	full	sealed			
12 Oct	1.21	2.62	14.2	17.3	inop	inop	-1°	full	sealed			
12 Oct	1.21	2.42	16.2	17.3	inop	inop	-1°	full	sealed			
13 Oct	1.84	3.67	14.7	22.0	-0.18	small	-1°	full	sealed			

Table 14 (Continued)

Date	Equivalent ground motion in microns p-p (no freq corr), with positive deflection equivalent to ground motion up						Plate tilt	Pump stroke	Module sealing
	TR1		TR2		TR3				
	20 sec	60 sec	20 sec	60 sec	20 sec	60 sec			
14 Oct	TR2 module disturbed while valut open								
15 Oct	1.04	2.09	1.37	1.74	0.48	0.71	-1°	full	sealed
18 Oct	1.29	2.78	1.69	2.07	0.40	1.10	-1°	full	sealed
	(TR1 amplifier inop; used TR2 amplifier for both TR1 and TR2 measurements)								
20 Oct	1.19	2.76	1.59	1.99	0.40	1.01	-1°	full	sealed
20 Oct	vibrated all modules with tank open								
20 Oct	1.15	2.93	1.59	2.17	0.42	0.74	-1°	full	sealed
20 Oct	removed and replaced all module cases								
21 Oct	1.45	3.12	1.49	2.12	0.41	0.62	-1°	full	sealed
21 Oct	vibrated all modules with tank open								
21 Oct	1.59	3.57	1.63	2.17	0.62	1.14	-1°	full	sealed
21 Oct	-5.40	-9.28	-5.78	-3.92	-5.85	-3.70	-1°	full	unsealed
25 Oct	1.20	2.40	0.40	0.66	-	-	-1°	full	sealed
	(TR2 = 17.5 second period; TR3 out of vault)								
25 Oct	1.33	2.70	0.64	0.95	-	-	-1°	full	sealed
	(TR2 = 20.0 second period)								
26 Oct	1.20	2.78	1.05	1.46	-	-	-1°	full	sealed
	(TR3 back in vault, but inoperative)								
29 Oct	1.30	1.96	1.09	1.30	0.68	1.16	-1°	full	sealed
	(TR1 amplifier inop; used TR2 amplifier for both TR1 and TR2 measurements)								

On 14 October, while the vault lid was removed, a force of approximately 200 pounds was accidentally applied to the top of the TR2 module. It was removed immediately, but a test on 15 October indicated that the disturbance changed the pressure response characteristics of modules. After a repeat test on 18 October confirmed these results, other tests were made to determine if other major disturbances would further alter pressure response characteristics or if the 200-pound force had released a strain in the module and it had become stable. On 20 October, a standard pressure test was conducted, the tank was opened, and the modules were vibrated severely using an orbital sander. The felt pad of the sander was held in contact with each module top, and the sander speed was varied slowly from zero to maximum and back to zero. After being vibrated, the modules were retested, and their cases were removed and replaced. The next day they were tested, vibrated, and retested. The relatively small scatter in data taken during these days was noted, and the modules were retested with their pressure sealing plugs removed. Note that the ratio between amplitudes of the 20- and 60-second data for TR1 agree well with the similar ratio for TR3, but that the ratio for TR2 has a considerably different value. No explanation for this disagreement has been determined, as the frequency response characteristics of the three channels were measured and found to match closely.

Beginning on 20 October, the TR3 module period started to shorten and could not be adjusted to 20 seconds. Pressure test data were taken on 20 October with a TR3 period of 17.2 seconds. After the last test on that day, the TR3 module was removed from the baseplate and brought to Garland for repairs. On 25 October, module pressure responses were tested with only the TR1 and TR2 modules on the baseplate. On 26 October, the TR3 module, again fully operational, was reinstalled on the baseplate.

Most of the effort expended at Grand Saline during this report period was directed towards debugging the installation, establishing repeatability of data, and determining how mechanical disturbances affected module pressure sensitivity. It was found that the module pressure sensitivities can be changed greatly by stressing the module assemblies, and that pressure sensitivity of the TR3 module is slightly lower than the other two modules.

It is recommended that these tests be continued to establish the relationship between module pressure sensitivity and tilt and to evaluate the effectiveness of the experimental flanges in reducing module pressure sensitivities.

## 7. REFERENCES

- Crary, A. P. and M. Ewing, 1952, On a barometric disturbance recorded on a long-period seismograph: Trans. A.G.U., vol. 33, p. 499-502
- Haubrich, R. A., 1970, The origin and characteristics of microseisms at frequencies below 140 cycles/hr: Mono de L'UGGI (in press)
- Herrin, Eugene and John MacDonald, 1971, A digital system for the acquisition and processing of geoacoustic data: Geophysical Jour. Royal Astro. Soc. (in press)
- Molnar, P., J. Savino, L. Sykes, R. Liebermann, G. Hade and P. Pomeroy, 1969, Small earthquakes and explosions in western North America recorded by new high-gain, long-period seismographs: Nature, vol. 224, p. 1268-1273
- Press, F., 1966, Seismic velocities: in Handbook of physical constants, Geol. Soc. Am. Memoir 97, p. 195-218
- Savion, J., K. McCamy and G. Hade, 1971, Structures in earth noise beyond 20 seconds. A window for earthquakes: (submitted to Bulletin Seis. Soc. Am.)
- Sorrells, G. G., 1971, A preliminary investigation into the relationship between long-period seismic noise and local atmospheric pressure fluctuations: Geophys. Jour. Royal Astro. Soc. (in press)
- Sorrells, G. G. and Z. A. Der, 1970, Long-period seismic noise and atmospheric pressure variations: Geotech Tech. Rpt. 70-12, , 26 p.

APPENDIX 1 to TECHNICAL REPORT NO. 71-24

DEFORMATION OF THE LOWER FLANGES IN THE TRIAXIAL SEISMOMETER

## DEFORMATION OF THE LOWER FLANGES IN THE TRIAXIAL SEISMOMETER

In an investigation of the effects of pressure changes on the triaxial seismometer, deformation of the lower flange in each module was isolated as a possible mechanism by which pressure changes could cause spurious signals at the transducer outputs. The upper surface of this flange is the mechanical interface between the sensitive element of the transducer and the case structure. Because of the extreme sensitivity of the transducer element to tilt motion, this surface is of critical importance; any distortion or deformation of the surface could tilt the sensitive element and cause it to produce a spurious output.

A top view and cross section of the lower flange is shown in figure 1. The points at which the stanchions bear on the top surface are indicated by four small circles in the top view. As may be seen, these bearing points overhang the cylindrical web between the top plate and lower plate sections of the flange. Thus, forces applied at the stanchion bearing points will tend to deflect portions of the outer edge of the upper plate section inducing tilts in the upper surface of the flange. The complexity of the geometry of the flange does not allow a straightforward calculation of the magnitude of the deflections and associated tilts, but through a series of approximate transformations shown in figures 2, 3, and 4. A geometry is derived which can be analyzed through the use of beam bending formulas.

Calculations based on a 100 microbar pressure increase, which would cause a 0.03 pound force at each stanchion bearing point are given in figure 5. These calculations indicate that tilts of approximately  $5.4 \times 10^{-9}$  radians would be induced.

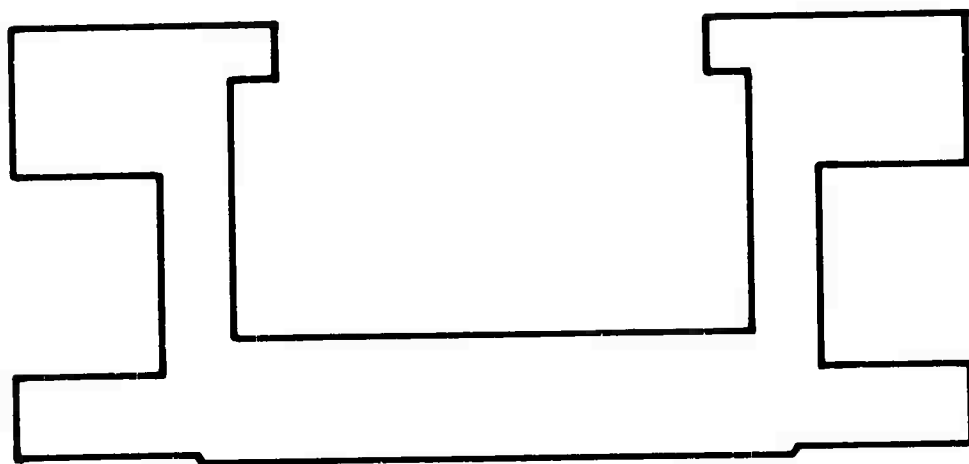
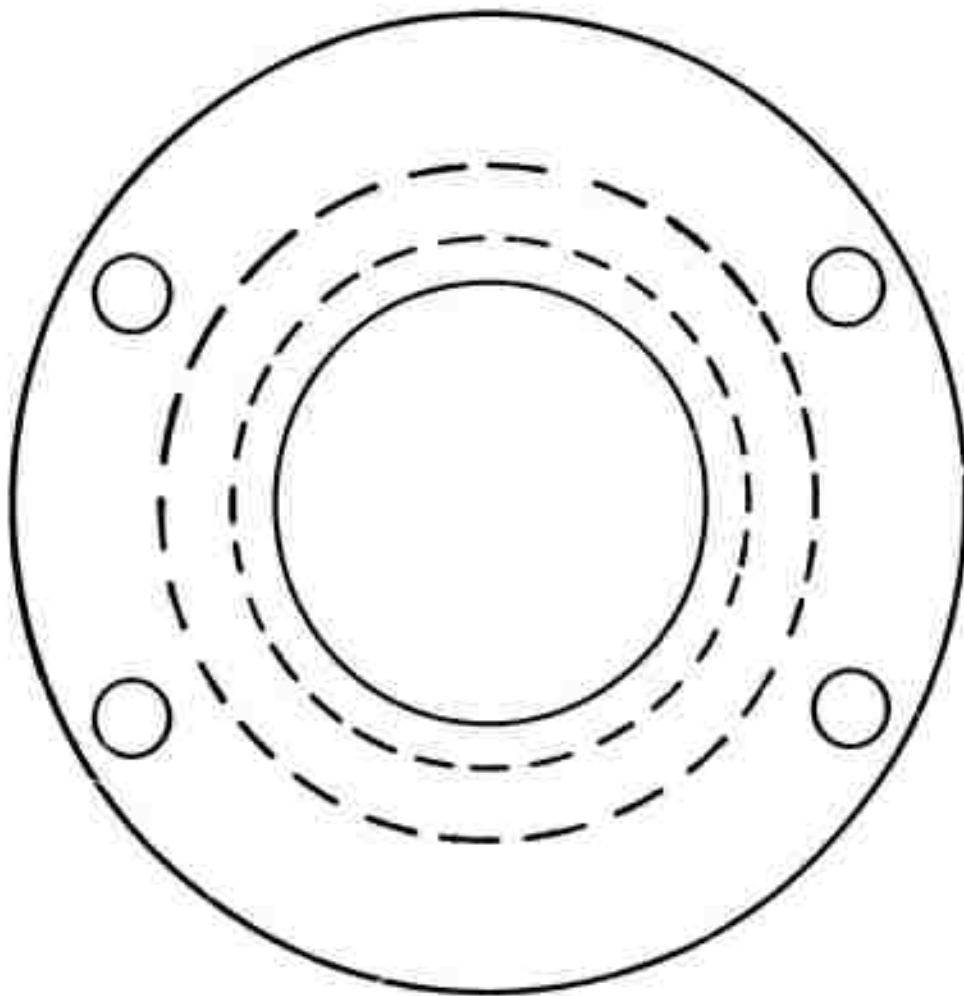


Figure 1. Top view and cross section of lower flange of triaxial seismometer

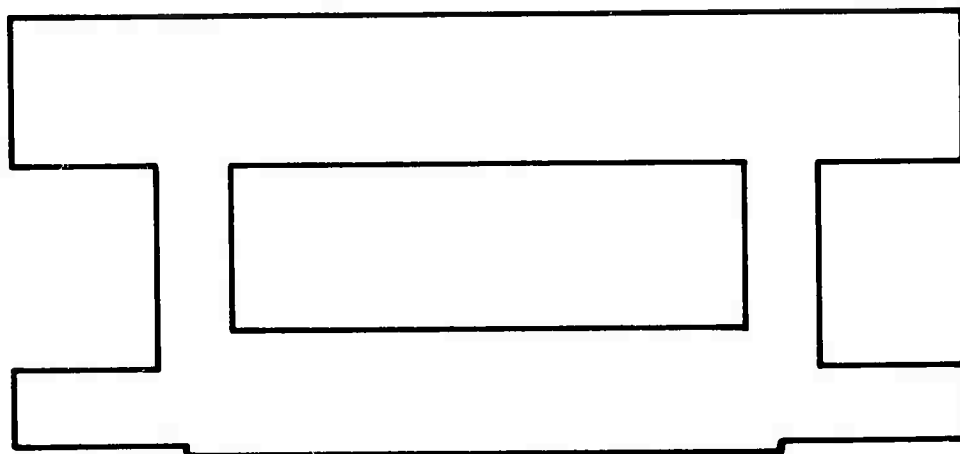
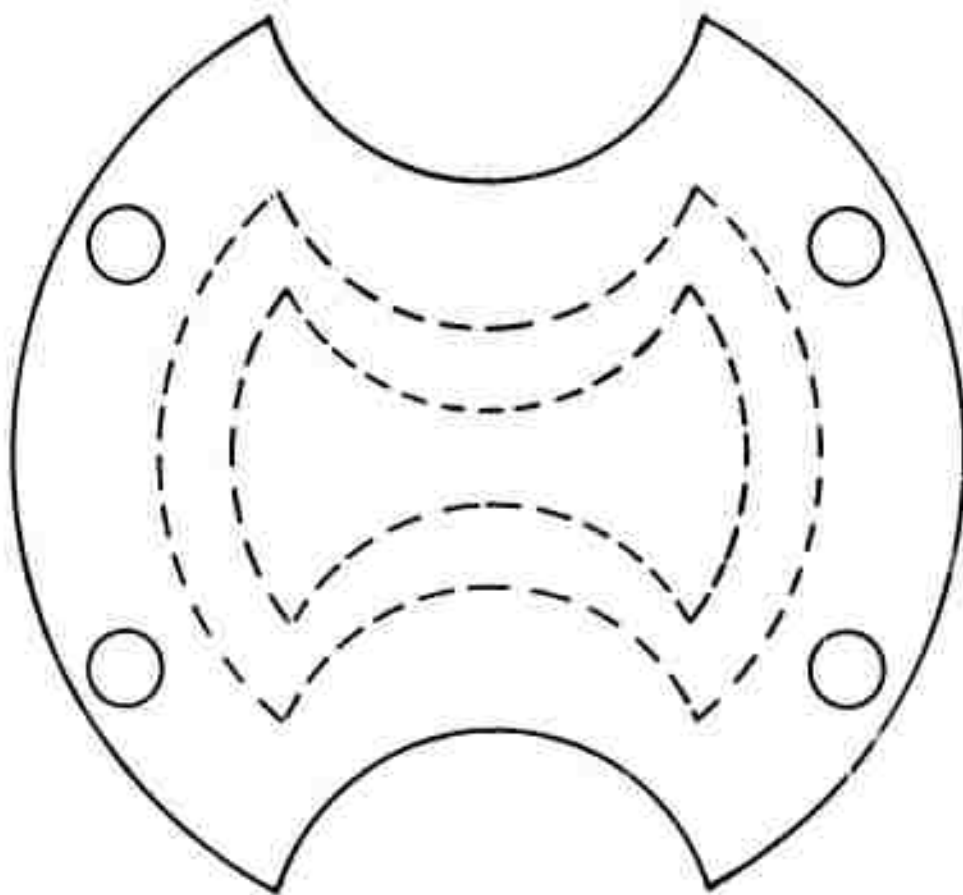


Figure 2. First approximate transformation of lower flange geometry

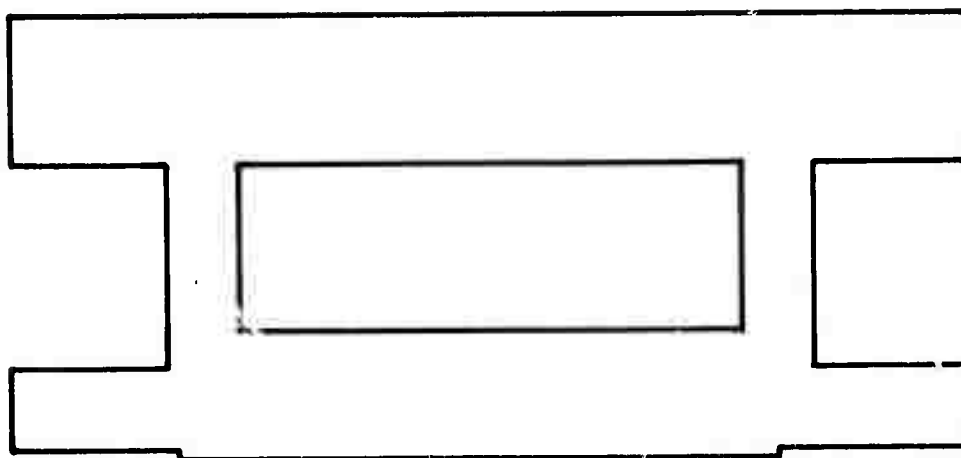
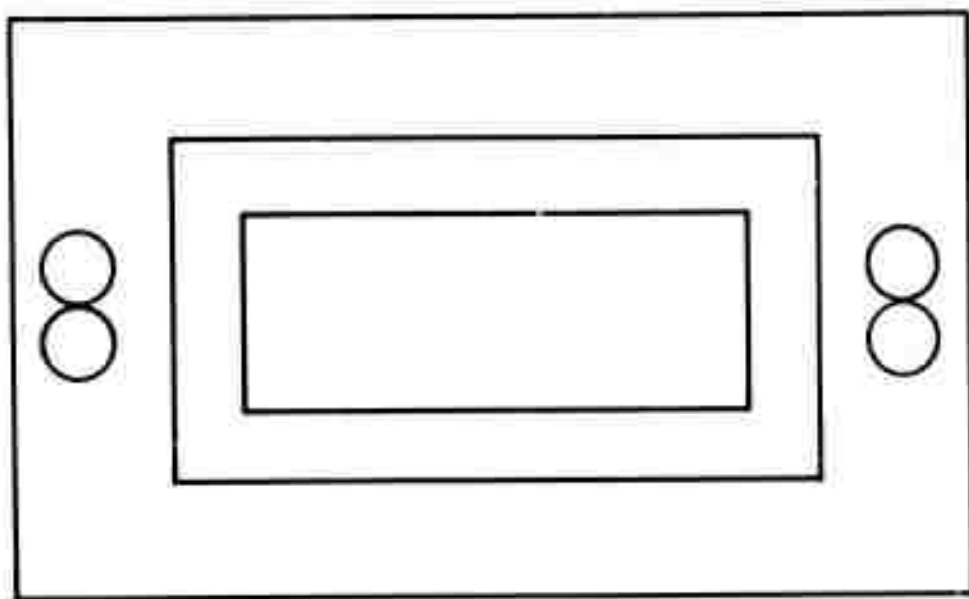


Figure 3. Second approximate transformation of lower flange geometry

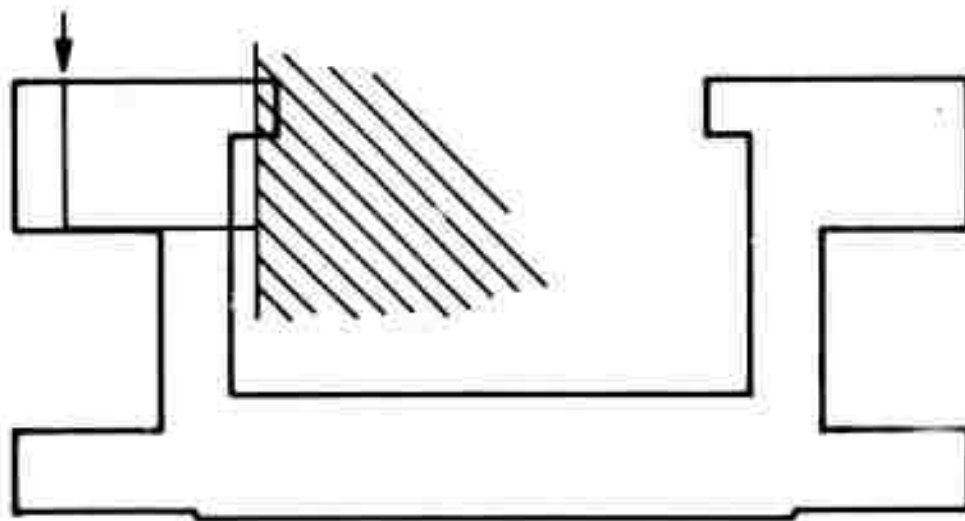
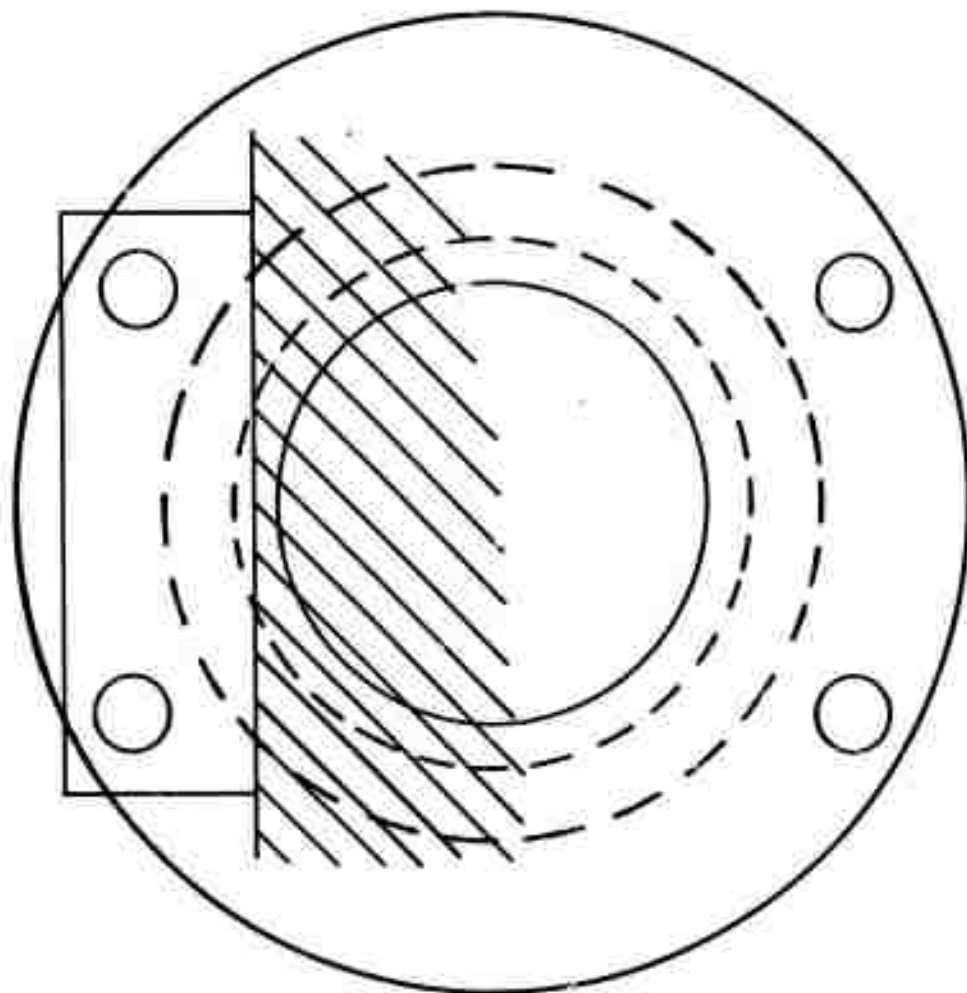
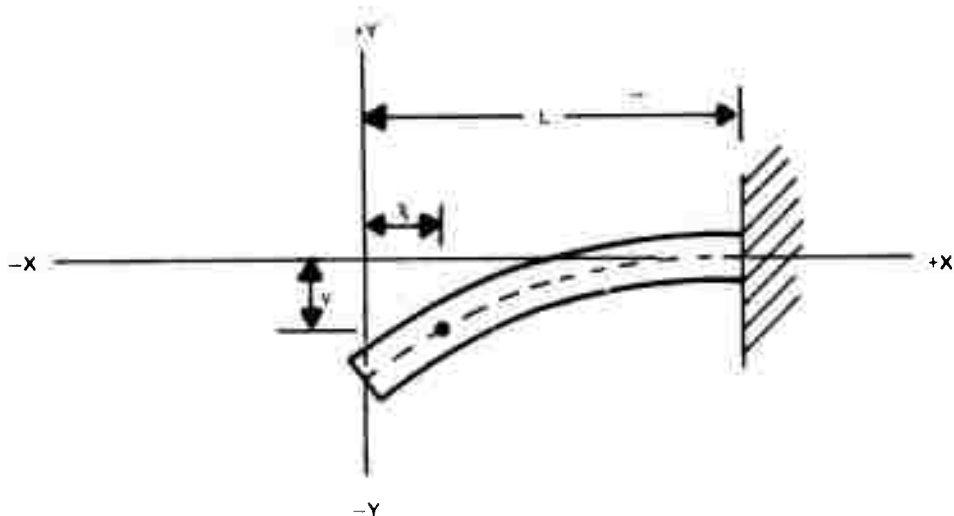


Figure 4. Third approximate transformation of lower flange geometry



$$y = \frac{-P}{6EI} (2L^3 - 3L^2x + x^3)$$

$$y_{\text{end}} = \frac{-PL^3}{3EI} \qquad y_{\text{midpoint}} = \frac{-5PL^3}{48EI}$$

$$\theta_{\text{end}} = \frac{+PL^2}{2EI} \qquad \theta_{\text{midpoint}} = \frac{+9PL^2}{24EI}$$

L = FREE LENGTH OF BEAM (2 INCHES)

I = MOMENT OF INERTIA OF BEAM SECTION

$$= 1/12 (\text{WIDTH})(\text{HEIGHT})^3 = 1/12 (6 \text{ INCHES})(1.5 \text{ INCHES})^3 \\ = 1.69 \text{ INCHES}^4$$

E = MODULUS ( $10^7$  POUNDS/INCH<sup>2</sup> FOR ALUMINUM)

P = DEFLECTING FORCE IN POUNDS

$$\theta_{\text{midpoint}} = \frac{+(9)(.06)(2 \times 2)}{(24)(10^7)(1.69)} = 5.4 \times 10^{-9} \text{ RADIAN}$$

Figure 5. Calculation of tilt induced in transformed lower flange

APPENDIX 2 to TECHNICAL REPORT NO. 71-24

TILT SENSITIVITY OF HORIZONTAL TRANSDUCERS

## TILT SENSITIVITY OF HORIZONTAL TRANSDUCERS

Moving-mass transducers designed for detecting horizontal translational motion are known to be sensitive to tilting motion and serious problems resulting from tilt have been observed in systems operating in the long-period range from 10 to 100 seconds. The effect of tilt on horizontal long-period transducers is analyzed in the following paragraphs.

A simplified diagram of a horizontal transducer is shown in figure 1. From this figure, the force on the mass caused by a sinusoidal tilt with peak-to-peak amplitude  $\alpha$  and a period T is given by:

$$F_{\text{tilt}} = Mg \sin \frac{\alpha}{2} \sin \frac{2\pi t}{T} \doteq Mg \frac{\alpha}{2} \sin \frac{2\pi t}{T}$$

From the seismometer equation, the force on the mass caused by a sinusoidal translation with a peak-to-peak amplitude A, and a period T is given by:

$$F_{\text{tran}} = M \frac{A}{2} \left( \frac{2\pi}{T} \right)^2 \sin \frac{2\pi t}{T}$$

In the two equations above:

$F_{\text{tilt}}$  = force on mass due to tilt (newtons)

$F_{\text{tran}}$  = force on mass due to translation (Newtons)

M = mass of transducer (kilograms)

$\alpha$  = peak-to-peak tilt angle (radians)

A = peak-to-peak translation (meters)

g = gravitational constant  $\left( 9.8 \frac{\text{meters}}{\text{second}^2} \right)$

T = period of applied motion (seconds)

t = base time (seconds)

A comparison of these equations indicates that the tilt which will cause a transducer output equivalent to that caused by a specified translation is given by:

$$a = \left( \frac{4\pi^2}{gT^2} \right) A$$

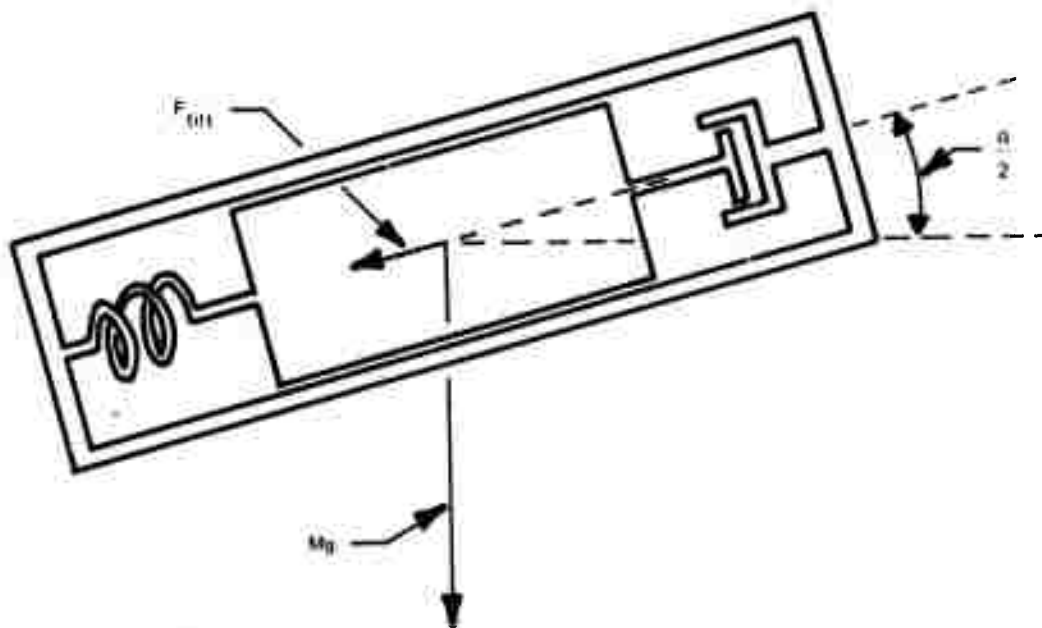


Figure 1. Simplified diagram of a horizontal moving-mass transducer showing the force on the mass caused by tilting

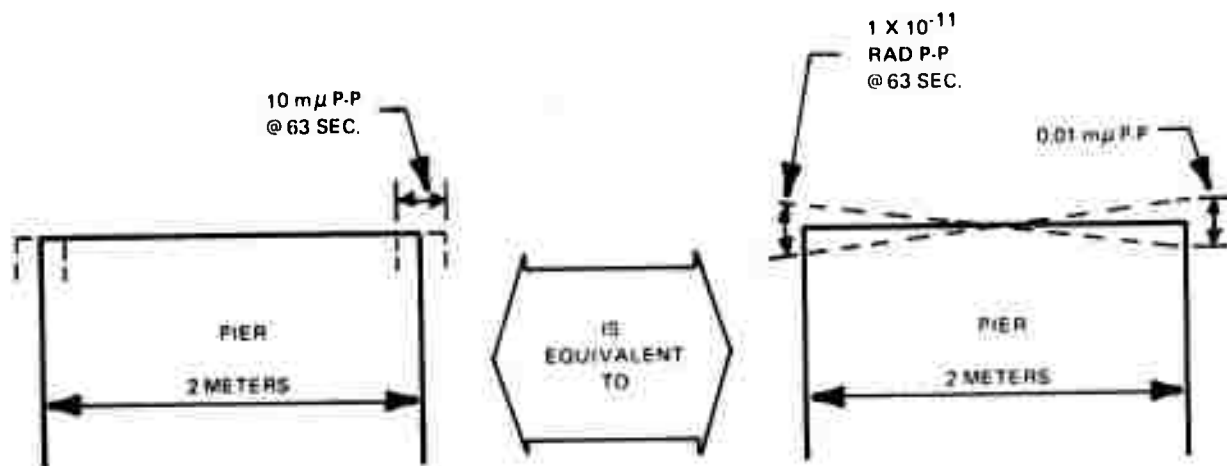


Figure 2. Simplified representation of two instrument piers, one being translated and the other being tilted so as to produce identical outputs from identical horizontal transducers on each

It will be noted that no instrument parameter appears in this equation, indicating that the equivalence between tilt and translation depends only on the nature of the two types of motion and on the fact that the moving-mass transducer is operated in a gravitational field. This equation was used to compute the tilts equivalent to translations at various periods as given in the following table.

Table 1. Tilts equivalent to translations at various periods

<u>Tilt amplitude (radians p-p)</u>	<u>Motion period (seconds)</u>	<u>Translation amplitude (millimicrons p-p)</u>
$4 \times 10^{-10}$	10	10
$1 \times 10^{-10}$	20	10
$4 \times 10^{-11}$	31.5	10
$1 \times 10^{-11}$	63	10
$4 \times 10^{-12}$	100	10

One of the listed cases of tilt and equivalent translation is illustrated in figure 2. This illustration shows two instrument piers, one being translated and the other being tilted so as to produce identical outputs from identical transducers on each pier.

Long-period systems usually have system noise levels equivalent to input motions in the range from 10 to 20 millimicrons peak-to-peak. In terms of the actual motion to be measured by these systems, output signals caused by tilt are spurious and should be minimized. The equivalent translation level of 10 millimicrons peak-to-peak indicated in the list above is considered to be the highest level which will not degrade system performance. It may be shown that the tilt within the earth actually associated with a translational signal is over two orders of magnitude below the equivalent tilt indicated in the table above.

An example will illustrate the minuteness of the maximum allowable tilt angle, if the rays of the  $1 \times 10^{-11}$  radian angle shown in figure 2 were extended to the surface of the moon, they would intersect the surface only 0.16 inch apart.